DEVELOPMENT OF A SPECIALIZED ZEBRAFISH XENOTRANSPLANTATION DATABASE AND ESTABLISHMENT OF ALU-BASED TUMOR DNA QUANTIFICATION METHOD IN ZEBRAFISH: FOCUS ON MODELS OF OVEREXPRESSION AND MICROENVIRONMENT

A DISSERTATION SUBMITTED TO
THE GRADUATE SCHOOL OF ENGINEERING AND SCIENCE OF
BILKENT UNIVERSITY
IN PARTIAL FULFILLMENT OF THE REQUIREMENTS FOR
THE DEGREE OF DOCTOR OF PHILOSOPHY
IN
MOLECULAR BIOLOGY AND GENETICS

BY SENİYE TARGEN

SEPTEMBER 2020

DEVELOPMENT OF A SPECIALIZED ZEBRAFISH XENOTRANSPLANTATION DATABASE AND ESTABLISHMENT OF ALU-BASED TUMOR DNA QUANTIFICATION METHOD IN ZEBRAFISH: FOCUS ON MODELS OF OVEREXPRESSION AND MICROENVIRONMENT

By Seniye Targen

September 2020

We certify that we have read this dissertation and that in our opinion it is fully adequate, in scope and in quality, as a thesis for the degree of Doctor of Philosophy.

_____

Özlen Konu Karakayalı (Advisor)

_____

Michelle Marie Adams

_____

Murat Alper Cevher

_____

Sreeparna Banerjee

_____

Ceren Sucularlı

Approved for the Graduate School of Engineering and Science:

_____

Ezhan Karaşan

Director of the Graduate School

ABSTRACT

DEVELOPMENT OF A SPECIALIZED ZEBRAFISH XENOTRANSPLANTATION DATABASE AND ESTABLISHMENT OF ALU-BASED TUMOR DNA QUANTIFICATION METHOD IN ZEBRAFISH: FOCUS ON MODELS OF OVEREXPRESSION AND MICROENVIRONMENT

Seniye Targen

Ph.D. in Molecular Biology and Genetics

Supervisor: Özlen Konu Karakayalı

September 2020

Successful xenotransplantation of human cancer cells into zebrafish host marked a new era in cancer research enabling high throughput *in vivo* screens. Zebrafish xenotransplantation literature continues to rapidly accumulate, and this necessitates the development of an interactive database for accommodating the collective data for fined-tune search, visualization and statistical representation purposes. Herein, I have introduced an interactive database, ZenoFishDb v1.1 (https://konulab.shinyapps.io/zenofishdb), housing manually curated details on molecularly-modified cell transplantations, PDXs, stem cell and cancer stem cell transplantation studies as well as transplantation studies bearing modified host details. The database projects collected data in a table format via various attributes and provides graphical representation of the curated details as well as statistical analyses yielding information on incorporated numbers and frequencies of selected attributes; hence can be used for reviews and designing new experiments. Zebrafish PDX studies are separately conceptualized and displayed through ZenoFishDb v1.1. Development of the ZenoFishDb v1.1 leads to a better understanding of tumor analysis methods such as assessment of proliferation and/or tumor growth in xenotransplantation studies and further marks the need for development of novel methods for precise quantification of tumor size. In the light of these findings, I have helped establish a novel qRT-PCR-based proliferation assessment method for xenografts in zebrafish, adapted from previous mouse xenotransplantation studies. Herein, the use and precision of ALU

repeat-based quantification of transplanted liver cancer cells in genotyped zebrafish *ache* mutants and wildtype siblings was shown exemplifying microenvironment as an important factor for tumor growth. I further demonstrated the power of ALU repeat-based quantification in Mineralocorticoid Receptor (MR) overexpressing breast cancer cells (MCF7) injected to the transparent *casper* zebrafish as a case study. First, I demonstrated that MR expression and signaling was important in breast cancer biology and prognosis based on *in silico* TCGA and custom RNA sequencing as well as other *in vitro* and *ex vivo* assays. I further showed that results obtained from ALU repeat-based quantification of tumor growth in MR-overexpressing MCF7 cells paralleled fluorescent image-based intensity measurements while the former being relatively less time-consuming and more high-throughput. In this study, accurate quantification of MR overexpression in xenografts was also successfully performed by a cDNA-specific primer pair; and the rate of tumor growth based on image analysis, did not correlate with the amount of MR DNA in *casper* fish xenografts. However, MCF7 cells overexpressing MR exhibited lower cell viability *in vitro* although some of these effects were due to empty vector (EV) integration. Accordingly, tumor size in xenografts of naïve, EV- and MR-transfected MCF7 cells injected into pigmented AB larvae were quantified for ALU-repeats yet no significant difference was observed due to high within-group variability *in vivo*. Future studies are needed to assess the role of varying the volume and placement of injected cells along with the amount of *MR* gene transfected on tumor growth *in vivo*.

Key words: Zebrafish, Xenograft, Database, ALU repeat, Tumor quantification, Microenvironment, Molecular Modification, Mineralocorticoid Receptor.

ÖZET

ZEBRA BALIĞI KSENOTRANSPLANTASYON ÇALIŞMALARINI BARINDIRAN VERİ TABANI GELİŞTİRİLMESİ VE ALU-DAYANAKLI TÜMÖR DNA ÖLÇÜMÜNÜN OVEREKSPRESYON VE MİKROÇEVRE ÖRNEKLENDİRİLMELERİ İLE ZEBRA BALIĞI KSENOGRAFT MODELLERİNDE UYGULANMASI

Seniye Targen
Moleküler Biyoloji ve Genetik Doktora Programı
Tez Danışmanı: Özlen Konu Karakayalı
Eylül 2020

Literatürde zebra balığına uyarlanan hücre ve doku transplantasyon çalışmaları gün geçtikçe artmakta ve buna bağlı olarak bu çalışmaların kolektif olarak, görüntülenebilir ve güncellenebilir bir şekilde aktarılması gereklilik arz etmektedir. Buna istinaden, zebra balığı üzerinde uygulanan moleküler modifikasyona uğramış hücre hatları transplantasyonlarının, hasta dokusu ve primer kültür transplantasyonlarının, kök hücre ve kanser kök hücresi transplantasyonu çalışmalarının, farklı zebra balığı modellerine uygulanmış transplantasyonları barındıran çalışmalarının ve detaylarının veri tablosu halinde, grafikler halinde ve istatistiksel bulgularının da tablo halinde yansıtıldığı, ZenoFishDb v1.1 (https://konulab.shinyapps.io/zenofishdb) isimli bir veri tabanı geliştirilmiştir. Bu veri tabanında primer hüre kültürü ve ksenograft çalışmalarına ayrıcalıklı olarak yer verilmiş ve de farklı veri tablo ve grafik öğeleriyle gösterilmeleri sağlanmıştır. Bu veri tabanının geliştirilmesi ile alandaki eksikler fark edilip, örneğin tümör büyüme çalışmalarındaki uygulamalar incelenip, tümör büyümesi ölçümü için daha hassas ve etkili yeni bir yöntem geliştirilmiştir. Bu metot kantitatif PCR (qRT-PCR) kullanılarak tümör hücresi enjekte edilmiş zebra balığı DNA çıkarımı sonrası insanda bulunan ALU dizilerinin niteliksel olarak değerlendirmesine dayalıdır ve daha önce fare ksenograft çalışmalarında denenmiş bir uygulamadır. Burada, ALU dizisi dayanaklı kantitatif PCR metodunun hassasiyetini ve etkinliğini, karaciğer kanseri hücresi nakledilmiş *ache* mutantı ve normal zebra balıklarından elde edilen DNA üzerinde test

ederek ölçtük. Başka bir örnek uygulamayı ise gen modifikasyonuna maruz kalmış meme kanser hücresi (MCF7) enjekte edilmiş zebra balıklarında test ettik. Öncelikle, modifikasyona uğrayan genin, mineralokortikoid reseptörünün (MR), meme kanserindeki önemi *in silico*, *in vitro* ve *ex vivo* bulgularımızla saptanmıştır. Sonraki çalışmamız ise, ALU dizisi bazlı kantitatif PCR çalışmaları sonucu ile floresan imaj bazlı ölçümleri kıyaslamak olmuştur ve ALU dizisi bazlı tümör DNA nitelendirme tekniğinin çok daha az zaman alan ve çok daha hassas bir yöntem olduğu MR ifadesi artırılmış MCF7 hücresi enjekte edilmiş *casper* balıkları üzerinde test edilip, saptanmıştır. MR transfekte edilmiş hücre barındıran balıklarda MR DNA ifadesinin ölçümü MR cDNA spesifik primer çifti ile başarı ile test edilmiştir. Floresan bazlı tümör oranı ile MR DNA miktarının korelasyonu test edilmiş fakat aralarındaki fark istatistiksel olarak anlamlı bulunmamıştır. Bu deneyler paralelinde, in *vitro* çalışmalarda, MR ifadesi artırılmış MCF7 hücrelerinin hücre kültüründe kontrol vektörü enjekte edilmiş (EV) hücrelere göre daha az çoğaldığı saptanmıştır fakat bu etkinin bir kısmı da EV vektörü entegrasyonundan kaynaklanmaktadır. Son olarak, ALU dizisi bazlı qRT-PCR yöntemi ile tümör çoğalması ölçülen naif, EV barındıran ve MR barındıran hücre enjekte edilmiş pigmentli AB tipi zebra balık grupları arasında var olan yüksek varyasyon sebebinden ötürü, istatistiksel olarak anlamlı bir değişim kaydedilmemiştir. Bu çalışmaların devamında, farklı hacim/sayı ve lokasyonlara yapılacak enjeksiyonların gruplarının ve de farklı dozlarda *MR* transfekte edilmiş hücrelerin enjekte edildiği grupların tümör büyümesi üzerindeki etkilerinin test esilmesi elzemdir.

Anahtar sözcükler: Zebra balığı, Ksenograft, Veri tabanı, ALU dizisi, Tümör ölçümü, Mikroçevre, Moleküler modifikasyon, Mineralokortikoid reseptörü.

ACKNOWLEDGEMENTS

First of all, I would like to express my utmost gratitude towards my PhD supervisor, Ozlen Konu. Although, not possible to fit all six years in two short lines of sentences, she has opened the doors of her laboratories, assigned me with my project and put her trust in me. On top of this, she has been very understanding, encouraging and supportive mentor during this journey.

I also would like to thank Dr. Sreeparna Banerjee and Dr. Murat Cevher for being part of my TIK comittee for all these years and for sharing their most valuable experiences and constructive comments towards my project. I would also like to thank Dr. Michelle Adams and Dr. Ceren Sucularlı for kindly accepting my invitation and sparing their time for evaluating my thesis and being part of my thesis defense committee.

I would like to thank Tuğberk Kaya for R programming in creating the database and Damla Güneş, Ender Avcı and Ayşe Gökçe Keşküş, for their contribution to the manual curation for the database. I would like to thank Bircan Çoban for providing protein expression of MR in breast cancer cell lines and Olivier Staub for helpful discussions and Nourdine Faresse and Onno C. Meijer for hosting me in their laboratories and introducing me to mineralocorticoid receptor and aldosterone signaling in the context of COST BM1301 ADMIRE. I would like to thank Ayşe Gökçe Keşküş for her collaboration in establishing the ALU-based DNA quantification method in zebrafish. I would like to thank EMBL Gene Core Facility at Heidelberg Germany and Vladimir Benes and his team for conducting the RNAseq experiments, and Fatma Betül Dinçaslan, Ayse Gökce Keşküş and Ronaldo Leka analyzing the raw RNAseq data and their help with the PCA analysis. I would like to thank Bilkent University Zebrafish Facility technician Tülay Arayıcı for technical help and Dr. Gulcin Cakan (IBG, Izmir) for contributions to the development of our zebrafish stocks in the facility.

I would like to thank to former and present Konu lab members namely, Murat Yaman, Basak Özgürsoy, Bircan Coban, Ayşe Gökçe Keşküş, Damla Güneş, Şahika Çıngır Köker, Melike Tombaz, Said Rafet Tiryaki, Ronaldo Leka, Burçin İrem Arıcı as well

as each and every one of the Bilkent MBG members who were always there for me and for they have become my family in Ankara.

I would like to thank my family, my father Tözüm Targen, my mother Bilge Targen, my sister Neşe Targen for their unconditional love and support by all means. I thank to my very dear friends; Şebnem Kuter, Pelin Makas, Hürkan Karas and Hazal Özaktan for always trying to keep me positive and literally forcing me to cheer up during the challenging times of my studies. I thank to Onat Şahdalaman for caring for me in difficult moments and sharing beautiful moments with me during my journey in Ankara.

I would like to thank to Bilkent MBG department for providing us a nice and well-equipped laboratory to pursue our experiments. In vitro and ex-vivo Mineralocorticoid Receptor (MR) signaling experiments were supported by a research grant (to Ozlen Konu) from TUBITAK 114S226 and cost action BM1301. I have received PhD scholarship from TUBITAK 114S226 and was funded by COST for attending conferences and workshops.

Table of Contents

List of Figures

List of Tables

CHAPTER 1

INTRODUCTION

1.1. Xenotransplantation applications in zebrafish model organism

Cancer has been the disease of the 21st century due to increased rates of diagnosis and its therapy presents challenges and heterogeneity. Precision medicine is only possible if tumor material from patients are tested for series of drugs to find the one tailored for that patient. Today, tumor xenograft models are central for better understanding and evaluation of cancer biology research. In addition, they have become an important part of precision medicine. For decades, mouse models have been the gold-standard for executing xenograft studies. With the successful xenotransplantation of the human cells into zebrafish embryos in the beginning of this millennia (Lee et al., 2005; Nicoli et al., 2007; Nicoli & Presta, 2007) a whole new era has risen for xenotransplantation applications in cancer research. An example representation of a standard zebrafish xenotransplantation into embryos and adult fish is shown in **Figure 1. 1** .

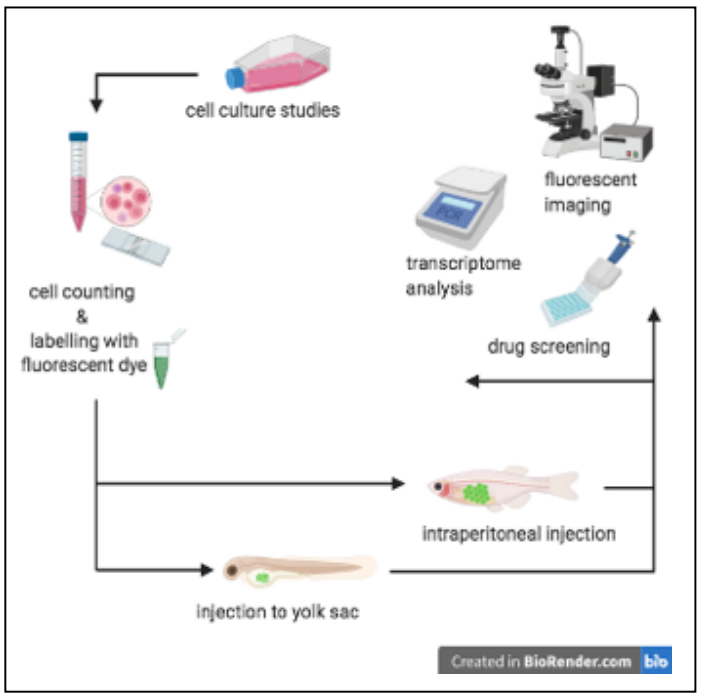

Figure 1. 1 Schematic representation of a standard zebrafish xenotransplantation procedure applied on zebrafish embryos and adult fish.

(This image was created by using BioRender.com).

Zebrafish embryo renders an ideal host model organism for xenotransplantation studies due to several reasons, i.e., external fertilization, high fecundity, optic clarity of the larvae, short generation periods, yet most importantly lack of fully functional adaptive immune system development until 4-6 post week fertilization (Lam et al., 2004; Sullivan & Kim, 2008). Use of zebrafish embryos as xenograft hosts, therefore, could be a preferable alternative model for xenograft studies. Furthermore, humanization of zebrafish for generating immunocompromised strains has led to better assessment of xenotransplantation studies eliminating possible immune-rejection of the host organism. The immunodeficient strains of zebrafish used for xenotransplantation studies are as follows; recombination activation gene 2 (*rag2*) mutants (Q. Tang et al., 2014; Tenente et al., 2014), DNA-dependent protein kinase gene (*pkrdc*) mutants (I. H. Jung et al., 2016) and janus kinase 3 (*jak3*) gene (Moore et al., 2016) mutants. *rag1* and *rag2* are required for B and T lymphocyte differentiation (Willett et al., 1997) serve as adaptive immunity markers in zebrafish. *rag2* mutant line (*rag2*(^{E450fs})), lacks mature T cells and possesses reduced numbers of functional B cells and is currently optimized for xenotransplantation studies in adult fish (Q. Tang et al., 2014; Tenente et al., 2014). Furthermore, *pkrdc*-null SCID zebrafish line functional B and T lymphocytes (I. H. Jung et al., 2016) has been established for adult fish xenotransplantation studies. In addition to *rag2* and *pkrdc* mutant lines, *jak3* mutant line (*jak3*^{P369fs}) lacking both T lymphocytes and Natural Killer (NK) cell immunity has been also generated for better mimicking of immune-deficiency in fish studies (Moore et al., 2016). Additionally, application of immunosuppressants such as dexamethasone (Eden et al., 2015; Stoletov et al., 2007) and Busulfan (Khan et al., 2019) have been also used to surpass any immunogenic response to engrafted cells or tissues. Although availability of these lines and drug exposure methods offer a broad range of immune-deficiency, still more research is required for fine-tuning both innate and adaptive immune systems for minimizing all kind of immune response to engrafted cells and/or tissues.

Use of zebrafish hosts for xenotransplantation studies could also overcome some disadvantages of mouse xenograft models specially by the terms of timing and cost efficiency. For decades, humanized mouse models have been used to prevent immune rejection of the grafted tumor tissue/cells and ongoing research focuses on fine-tuning on humanizing the host by also manipulating the tumor microenvironment, to mimic

the real scenario of tumor-microenvironment interactions as in human physiology. Athymic nude mice lacking thymus (Flanagan, 1966; Pantelouris, 1968), SCID mice (G. C. Bosma et al., 1983; M. J. Bosma & Carroll, 1991), NOD-SCID mice (Prochazka et al., 1992), *Rag2* knockout mice (Shinkai et al., 1992) are well-established immunocompromised host models. Although zebrafish and mouse models share equivalent immune-compromised models by the means of gene mutations, several other parameters such as cost, timing and possible tumor-microenvironment interactions are to be considered for the experimental design. Accordingly, most xenografting is performed in embryonic/larval zebrafish providing a platform relatively cost- and time-efficient.

Overall, the above-mentioned characteristics of the zebrafish organism with the feasibility of the current technologies for applying tumor cell injections and generation of 'humanized' fish strains paves the way for standardizing the use of zebrafish xenograft models in cancer research more efficiently.

1.1.1. The nature of existing zebrafish xenograft models

1.1.1.1. Immortalized cell line injections

First ever zebrafish xenograft study was performed by Lee and colleagues in 2005 where they had transplanted human metastatic melanoma cells (C8161) into blastula-stage zebrafish embryos and showed successful survival, division and migration of cancer cells (Lee et al., 2005). Herein, survival and motility of primary melanocytes and normal fibroblasts have also been investigated and these cells survived in zebrafish embryos yet exhibited less migratory effects (Lee et al., 2005). Engraftment of immortalized cell lines to zebrafish host model has been carried out since, and to date, cell line engraftments of different human cancer types including breast cancer cell lines; MDA-MB-231 (Qiong Wu et al., 2018; B. Yang et al., 2019; X. Zhao et al., 2019), MCF7 (Mercatali et al., 2016; Sun et al., 2015), T47D (Vazquez Rodriguez et al., 2018), ZR-75-1 (Rodriguez et al., 2017); glioma cell lines, U-87MG (Fan et al., 2019) and U-251MG (Gamble et al., 2018); leukemia cell lines, K562 (Dale P. Corkery et al., 2011); prostate cancer cell lines, PC3, DU-145 and LNCap cells (Bansal et al., 2014) and many other cell lines. In addition to immortalized cell-lines derived from

humans, murine (Weijts et al., 2018), rat (Sandquist et al., 2018), zebrafish (Mizgirev & Revskoy, 2010), dog (Timmermans-Sprang et al., 2019) cell line injections are also present.

Zebrafish, enabling successful transplantation of immortalized cell lines of numerous types derived from numerous organisms, serves as an ideal model for xenotransplantation studies by allowing feasible, efficient, cheap and high-throughput research in the cancer research community.

1.1.1.2. PDXs of zebrafish

Successful patient-derived xenograft engraftment to zebrafish host performed by two individual studies of Bagowski group, i.e., pancreas, ampulla vateri tissue engraftment (Weiss et al., 2009) and pancreas, colon, and stomach tissue engraftment (Marques et al., 2009), had opened a new era for easy application and evaluation of PDXs in zebrafish embryos for research community. Majority of studies using zebrafish PDXs (zPDXs) possesses glioblastoma (Banasavadi-Siddegowda et al., 2018), liver cancer (Lin et al., 2019) and colorectal cancer (Fior et al., 2017)-derived primary cell cultures and/or tissue engraftments. In addition to these cancer types, a broad range of zPDXs exist in the literature and gastric cancer (J. Q. Wu et al., 2017), prostate cancer (Bansal et al., 2014), pancreatic ductal adenocarcinoma (L. Wang et al., 2019), melanoma (Yan et al., 2019), adrenocortical carcinoma (Gianoncelli et al., 2019), breast cancer (Yan et al., 2019) and acute myeloid leukemia (Gacha-Garay et al., 2019) are among many. Most of the zPDX studies have established patient tissue derived primary cell line injections yet several studies exemplified direct tissue transplantation into the zebrafish yolk (Marques et al., 2009; Weiss et al., 2009). In addition to patient derived xenografts, primary cell lines derived from healthy donors have been also used as controls or as test subjects to assess different biological hypotheses raised by the research community. Overall, successful implementation of patient-derived tissue to zebrafish hosts idealizes standardized use of zPDXs in cancer research overcoming the disadvantages of mice model PDXs i.e. longer time-period for tumor establishment and assessment in mice models (J. Jung et al., 2018).

1.1.1.3. Stem cell and cancer stem cell injections

Zebrafish model has been also a useful and preferable model organism for studying stem-cell associated events through xenotransplantation of stem cells and cancer stem cell injections (Banasavadi-Siddegowda et al., 2018; Li et al., 2015; Orlova et al., 2014). One of the pioneer studies of stem-like cell population xenotransplantation in zebrafish embryos have been established by Eugiera and colleagues in 2011 wherein they tested tumorigenic and migratory capacity of the monolayer culture-derived control cell- and mammosphere culture-derived breast cancer cell- xenografts in zebrafish model organism (Eguiara et al., 2011). Herein, both tumor mass and tail migration capacity have significantly increased in mammosphere-derived cell injections when compared to monolayer-derived cell injections when the fish were incubated at 34°C. Additionally, a dietary polyphenol, curcumin, previously shown to modulate self-renewal of breast stem cells of normal and malignant origin, were applied to parental monolayer culture prior to injection and hereby a significant decline were detected in the tail migration and tumor mass in comparison to mock treated control bearing xenografts (Eguiara et al., 2011). This platform, hence, is ideal for pursuing rapid, feasible and inexpensive approach for testing novel drugs on self-renewal capacity of cancer stem cells. A similar approach has been also taken for studying different cancer stem cells such as glioma (X. jun Yang et al., 2013), glioblastoma (Lai et al., 2017; Welker et al., 2017), leukemia (Gacha-Garay et al., 2019; B. Zhang et al., 2015; B. Zhang, Shimada, Kuroyanagi, Umemoto, et al., 2014) and prostate (Nouri et al., 2017) as well as many other cell types.

Studies harboring injection of multiple cell lines are also present in the literature, study presented by Zhang and colleagues, for instance, highlights the use of leukemia and solid tumor-derived stem cell xenografts for high-throughput drug screening. Herein, K562-KOr cell line-derived leukemia stem cells (LSCs), DU-145-KOr cell line-derived prostate cancer stem cells (CSCs), HepG2-KOr cell line-derived liver cancer stem cells had been engrafted to both zebrafish embryos and adult-stage fish for cancer stem cell characterization and high-throughput therapy screening. In line with this hypothesis, cells sorted according to their aldehyde dehydrogenase (ALDH) expression, ALDH positive representing the cancer stem cell characteristic, ALDH+ and ALDH- cells had been transplanted to both zebrafish embryos and 20Gy-irradiated

adult fish. As a result, for K562-KOr-ALDH+(LSCs) and K562-KOr-ALDH-(Non-LSCs injected adult fish experimental groups; 7/10 LCS-injected group whereas 4/10 of Non-LSCs had established tumor in their trunks after 35 dpi.

Injection of prostate cancer stem cells and non-cancer stem cells, DU145-KOr-ALDH+ (CSCs) and DU145-KOr-ALDH-, respectively has been another experimental group of this study. Herein, tumor proliferation in irradiated adult fish have been assessed on 0dpi, 7dpi and 14dpi and DU145-KOr-ALDH+ (CSCs) had proliferated more significantly when compared to non-CSCs. Yet, another experimental group of this study has been transplantation of HepG2-KOr-ALDH+ and HepG2-KOr-ALDH- cells into irradiated fish and herein, tumor formation had been observed in both groups at 28 dpi with metastasis formation in HepG2-KOr-ALDH+ transplanted fish. Zebrafish embryo injection of DU145-KOr-ALDH+ and K562-BFP-ALDH+ and- ALDH- experimental groups into yolk sac of 48hpf fish; 1dpi images of fish have been captured and fish were exposed to drug treatment for additional 48 hours and before final images were captured. Docetaxel treated-DU145-KOr-ALDH+-injected zebrafish embryo proliferation were found to be significantly diminished when compared with untreated-DU145-KOr-ALDH+-injected fish. K562-BFP zebrafish xenograft model high-throughput drug screening for one chemical library has revealed the LSC-selective compound, B647, which later were used carry out its effect on the proliferation of K562-BFP-ALDH+ and K562-BFP-ALDH+ injected zebrafish embryos. LSCs have been shown to exhibit significantly increased proliferation compared to Non-LSCs and B647 treatment has been shown to reduce proliferation of LCSs when compared to control treated fish (B. Zhang, Shimada, Kuroyanagi, Nishimura, et al., 2014). This study demonstrates well that stem cell xenografting in zebrafish can lead to new drug discovery through high-throughput screening.

To summarize, successful zebrafish xenograft models of cancer stem cell applications, hematopoietic stem cells (Hamilton et al., 2018), mesenchymal stem cell (Han & Hsu, 2016; Patel et al., 2012) and induced pluripotent stem cell xenotransplantation (Chan et al., 2015) are also present and stem-cell zebrafish xenograft studies are now in rise.

1.1.2. Molecularly-modified cell injections

Zebrafish xenograft model organism also allows evaluation of immortalized cell lines, patient-derived primary cell lines or primary cell lines of any kind of tissue of origin which has been targeted to any kind of molecular/genetic modification. Thorough screening of the literature has facilitated identification of different kinds of molecularly-modified cell transplantation to zebrafish embryos including cells modified with tag-expression vectors for cell tracking purposes (Banasavadi-Siddegowda et al., 2018; Marranci et al., 2019), overexpression vectors (Jerónimo et al., 2017; Naber et al., 2013; von Mässenhausen et al., 2016), interfering RNAs (RNAi) (D. P. Corkery et al., 2018; Halasz et al., 2013; Leung et al., 2017), morpholinos (Topczewska et al., 2006; Weiss et al., 2009) as well as cells modified with Cre-LoxP (Karkampouna et al., 2018; Weijts et al., 2018) and Cripsr/Cas9 (Gaytan-Cervantes et al., 2017) technologies. Use of zebrafish xenograft models, therefore, enables testing gene specific-derived hypothesis employing different technologies altering gene expression levels and/or gene structures of interest of the cell lines to be injected.

1.1.2.1. Tag expression vectors

One of the earliest studies harboring such molecular modifications is performed by Topczewska and colleagues where they have injected aggressive melanoma cells tagged with GFP expression vector (C8161-GFP), a tag expression vector, and treated with anti-Nodal morpholinos (or scramble morpholinos) where they have been injected to blastula-stage zebrafish embryos in order to investigate the interactions among cancer cells and embryogenic progenitors and C8161 cells have been shown to form ectopic gene expression and had Nodal expression; and this phenotype had been reversed by the anti-Nodal morpholino treated C8161 injection in zebrafish embryos. In parallel, tumorgenicity of the anti-Nodal morpholino (or scramble morpholino)-treated C8161 cells had been examined on subcutaneously injected 5-week-old nude mice at different time intervals (day 3, 7, 14 and 17) and Nodal inhibition had diminished tumor volume significantly at these specified time intervals. This study therefore exemplifies an application of the same cell line transplantation both in zebrafish and mice models and bearing comparative results hence, solid evidence for compatible use of both xenograft models for a given hypothesis (Lee et

al., 2005). This study also highlights the use of GFP tag expression vector for visualizing cell behavior *in vivo*.

Use of tag expression vectors such as GFP (Lee et al., 2005) and mCherry (Marranci et al., 2019) are often preferred as cell tracking sources in fish and use of fluorescent protein tag enables assessment of tumor growth, migration, metastasis, dissemination and other fluorescence-based quantification assessments performed on fish.

1.1.2.2. Overexpression models

Another earliest example of the use of molecularly modified cell xenografts has been established by Nicoli and colleagues where they have developed a zebrafish xenograft angiogenesis model in which they have successfully examined the angiogenic capacity of tumorigenic *FGF2*-overexpressing mouse aortic endothelial cells (FGF2-T-MAE) (Nicoli et al., 2007). Applications of molecularly-modified cell line injections are not solely peculiar to immortalized cell lines, patient derived primary cell lines subjected to modifications have been also successfully engrafted into zebrafish embryos (Banasavadi-Siddegowda et al., 2018; L. Wang et al., 2019). Wang and colleagues have pursued zebrafish xenograft models of PDAC tissue derived primary cancer cells and fibroblasts which have been genetically modified to express anti-apoptotic *BCL2L1* and, fluorescent proteins, eGFP and mKate2, respectively (L. Wang et al., 2019). Herein, modified PDAC primary cells subjected to fibroblast inhibitor treatment and modified fibroblasts have been injected to zebrafish embryo yolk sacs and have been treated with gemcitabine chemotherapy agent in the presence or absence of *BCL2L1* inhibitor, Navitoclax. As a consequence, the gemcitabine treated cancer cells and fibroblasts without *BCL2L1* inhibitor treatment showed significant fall in fluorescent intensity when compared to cancer cells and fibroblasts without *BCL2L1* inhibitor and chemotherapeutic agent treatment, respectively. On the contrary, gemcitabine and *BCL2L1* inhibitor-treated cancer cells and fibroblasts had not shown any significant alterations with counterparts that had only received gemcitabine treatment. This approach has enabled the examination of fluorescent intensity among differential groups aiming to reflect information on tumor viability upon genetic modifications and chemotherapeutic agent treatments while also tumor-microenvironment interaction had been also taken into consideration by co-injection

approach/strategy (L. Wang et al., 2019). However, it might be important to estimate the gene copy number of cells xenografted into the host and for this an accurate quantification method remains to be developed and tested.

1.1.2.3. RNA interference applications

RNA interference applications have been also widely used for generating molecularly-modified cell xenografts and assessments of gene-specifically driven physiological differences in tumor itself or the surrounding microenvironment. Silencing RNA (siRNA) treated cell transplantation to zebrafish embryos are of common use for cell proliferation, metastases, angiogenesis and drug sensitivity assessments in fish model. Wang and colleagues, for instance, had studied the association of *COL3A1* mRNA and protein expression in colorectal cancer prognosis and further tested the functionality of the gene by *in vitro* and *in vivo* viability and proliferation assays, respectively. In fact, *COL3A1*-silenced colorectal cancer cells exhibited reduced growth *in vitro* (shRNA-treated) and xenografted *COL3A1*-silenced cells (siRNA-treated) exhibited decreased tumor proliferation on second day post injection when compared to initial injection time point (X. Q. Wang et al., 2016). Studies harboring several cell-line injections with different molecular modifications are also present and this way, comprehensive research could be performed to decipher the raised scientific question. For instance, a study led by Mukhopadhyay group studied the mechanistic model of extravasation and its association with neurophilin-2 (*NRP-2*), a semaphorin and vascular endothelial growth factor receptor, in clear cell renal carcinoma (RCC) and pancreatic adenocarcinoma (PDAC). Herein, *NRP-2* overexpressing 786-O (an aggressive RCC cell line) and corresponding control cells were transplanted into pericardium of 72 hpf zebrafish embryo for examining extravasation. *NRP-2* overexpressing 786-O cells has been shown to be extravasating from intersegmental vessels (ISVs) whereas controls had remained in the circulation after 24 hours. With a similar experimental approach, a highly metastatic cell line pancreatic cell line with high NRP-2- expression levels, ASPC-1, had been treated with short hairpin RNA (shRNA) targeting NRP-2 and ASPC-1 with reduced NRP-2 levels had been shown to reduce extravasation in zebrafish models (Y. Cao et al., 2013). Herein, different cell lines with different level of gene expression and modified with different molecular

modifications were used to comprehensively study of gene functionality *in vivo* using zebrafish models.

1.1.2.4. Mutations

In addition to gene expression reducing or overexpressing models of unmodified genes, expression of genes with mutations, has been also studied in zebrafish xenograft models. One of the few studies investigating effect of gene mutations in zebrafish xenograft model has aimed to identify metastatis associated events, i.e., invasion raised by differential phosphorylation of Na^+/H^+ exchanger regulatory factor 1, NHERF1, a scaffold protein, in breast cancer (Greco et al., 2019). An unidentified phosphorylated NHERF1 had been previously identified to be involved in B1 integrin-dependent invadopodia formation (Antelmi et al., 2013). In the study by Greco et al., non-phosphorylable form of S279 (S279A), S301(S301A) residues solely as well as S279A/S301A together as double mutants have been introduced to cells as well as corresponding controls, i.e., wild type-NHER1 and expression vector, and invasive behavior of these experimental groups were tested in zebrafish model. In fact, number of metastatic foci and invasiveness percentage were high in wild-type-*NHERF1* over-expressing cells when compared to all of the mutation-introduced cell line xenografts (Greco et al., 2019). This shows that zebrafish host is amenable to test mutant form of proteins in tumor assessment, such as degree of invasiveness.

1.1.2.5. Gene editing tools

Application of Cre-LoxP system induced overexpression and/or knockout cell line zebrafish xenograft models are also present in the most up-to-date literature search for molecularly-modified cell line engraftment studies in zebrafish. One example is the use of CRIPTO-overexpressing HepG2 hepatocellular carcinoma cell line that has been generated using a lentiviral red-to-green pTOMO-CRIPTO construct wherein CRE recombinase activity leads to excision of the floxed RFP cassette, resulting in CRIPTO and GFP expression (Karkampouna et al., 2018). As CRIPTO expression had been associated with poor prognosis in HCC and behaved as a proto-oncogene in various cancer types, the migratory and metastatic capacity of the *CRIPTO*-overexpressing cells were tested in zebrafish xenograft model and increased tumor-foci formation was detected in *CRIPTO*-overexpression model when compared to

control model (Karkampouna et al., 2018). Another application of Cre-LoxP induced molecularly-modified cell xenotransplantation to zebrafish embryos is the engraftment of Cre/LoxP mediated EF7/EF8 double knockout mouse embryonic fibroblasts (MEFs) cell engraftment to zebrafish embryos. Herein, Myc/Ras transformed EF7/EF8 double knockout MEFs and Myc/Ras transformed control cells have been injected to perivitelline space to examine metastatic and angiogenic capacity of these cells. Myc/Ras transformed EF7/EF8 double knockout MEFs have been shown to be metastasizing in the trunk region as well as promoting the intra-tumoral blood vessel branching (Weijts et al., 2018). Molecular modifications introduced by Crispr/Cas9 technology are of common use in molecular cell biology, and zebrafish xenograft studies harboring Crispr/Cas9-modified cells are also present in the current literature (Gaytan-Cervantes et al., 2017). Gaytan-Cervantes and colleagues have studied the role of cis elements and trans factors which is involved in the formation of an anti-apoptotic survivin gene isoform which lacks exon 3, DEx3, whose expression is upregulated when compared to other survivin isoforms in different cancer types (Gaytan-Cervantes et al., 2017). Herein, zebrafish xenograft model has been used to examine the tumorgenicity of endogenous survivin exon 3 mutated-HeLa cells introduced by Cripspr/Cas9 system. Introduced mutation had aimed to affect the binding of Sam68 regulator protein (trans-acting) to examine its role in the alternative splicing of the surviving *in vitro,* and hence allowed to better reflect its physiological effects *in vivo* by assessing tumorgenicity in zebrafish xenograft models. In return, decreased DEx3 survivin through impaired Sam68 binding and hence alternative splicing, the mutant cell injections have exhibited increased tumor formation *in vivo* (Gaytan-Cervantes et al., 2017).

Overall, feasibility of immortalized cell line, stem cell and cancer stem cell injections, PDX-derived primary cell line injections as well as solid tissue engraftments with modifications into zebrafish embryos as well as adult fish encourages the standardization of zebrafish model organism for the use of transplantation studies and hence, reveals an alternative xenograft model organism to rodent studies.

1.1.3. Zebrafish xenograft host modifications

Zebrafish xenograft studies focusing on tumor growth, proliferation, apoptosis, tumor viability and similar assessments which is based on evaluation of tumor volume and/or, tumor cell numbers, dispersion in the fish embryo mostly uses *casper* mutant fish, compound *roy-/-:nacre-/-* homozygous double mutant, which is transparent and named after the friendly ghost *casper* (White et al., 2008). Alternatively, achieving transparency in wild-type fish is also available through PTU administration. In addition to *casper* mutants, transgenic fish possessing fluorescently labelled fish are also commonly used for assessing metastasis and/or angiogenesis. In fact, use of the transgenic fish, Tg(*fli1*:EGFP) (Lawson & Weinstein, 2002), that expresses GFP under the early-endothelial marker, *fli1*, is often preferred in zebrafish xenotransplantation studies. Similarly, another transgenic fish, Tg(*flk1:*EGFP)^{s843}, which also drives GFP expression under another endothelial marker, *flk1* (Jin et al., 2005) is also used for again assessing metastatic capacity and angiogenesis.

In addition to above-mentioned fish which is applicable for more-generalized use fish with desired features are also selected for specific assessment performed in xenograft models. One of the examples, is the use of *ache* mutants and effect of the tumor microenvironment in tumor development (Avci et al., 2018); this study i also a part of this thesis. Herein, homozygous recessive *ache* mutants led to excess accumulation of acetylcholine in fish and its effect on liver cancer was further tested. Another assessment-specific use of fish was the use of *cloche* mutants lacking functional circulation and vasculature and hence, screens the necessity of intact vasculature in tumorigenesis and metastasis (Marques et al., 2009; C. Zhao et al., 2016). Recently, a 'humanized' zebrafish transgenic strain has been also constructed to express human hematopoietic cytokines and has been used to as a host for human stem cell transplantation (Rajan et al., 2019).

In adult fish xenotransplantation studies hosts in use are often modified to lack functional immune system. Herein, immunosuppressant-induced, i.e., Busulphan induced immunosuppressed *casper* mutants (Khan et al., 2019), *prkdc* null mutant SCID fish lacking functional T and B cells (I. H. Jung et al., 2016), fish manipulated to possess cancer-specific immunotolerance without immunosuppression (B. Zhang et

al., 2016), *nacre/rose/fli1:egfp* zebrafish fish subjected to 20-Gy ionizing radiation 2 days prior to engraftment for immune suppression (B. Zhang, Shimada, Kuroyanagi, Nishimura, et al., 2014) are among adult fish used for tumorigenesis, proliferation and tumor growth assessments.

1.1.4. Biological assessment and validation methods in zebrafish xenografts

Utilizing zebrafish model organism for transplantation studies has enabled assessment of numerous tumor-biology associated events. Tumor growth, proliferation, apoptosis, invasion, migration, metastasis, extravasation and angiogenesis are among many assessments which could be pursued using current zebrafish xenograft models. However, there is not a database existing in which this information is searchable. Availability of transgenic and/or mutant zebrafish lines of special features are the main reason for feasibility of biological assessments. Hence, host modifications, biological assessments and validation methods are crucial for establishing right zebrafish xenotransplantation model for desired experimentation. Evaluation of biological assessment together with the use of assessment-targeted modified host is therefore explained in detailed titles, namely, tumor growth, proliferation and apoptosis; invasion extravasation, dissemination and metastasis; angiogenesis.

.

1.1.4.1. Tumor growth, proliferation and apoptosis

Zebrafish xenograft models of tumorigenesis, tumor formation, viability, growth and/or proliferation have been applied to many tumor types including acute myeloid leukemia, hepatocellular carcinoma, melanoma, esophageal squamous cell carcinoma, mouse ovarian surface epithelial cells, colorectal carcinoma, hematopoietic stem and progenitor cells and to numerous cancer types along with other assessments run in parallel. Herein, studies or part of the studies only focusing on tumor growth and/or proliferation will be further exemplified and explained in detail to better portrait the picture of host modifications used, injection sites preferred and/or type of methods applied in order to quantify tumor growth, proliferation and apoptosis.

Assessment of proliferation in embryos and/or adult fish could be performed through several routes which have been extensively applied in majority of zebrafish xenograft

studies. Overall, fluorescence intensity, cell mass area, mean fluorescent area (Marranci et al., 2019) (Liu et al., 2019), fluorescent integrated density (Mazumder et al., 2018; X. Q. Wang et al., 2016; Z. Xie et al., 2018), tumor area (μm^2) (Avci et al., 2018), tumor growth ratio and cell spread (Martinez-Ordoñez et al., 2018) and number of fluorescent cells counted (D. P. Corkery et al., 2018; Dale P. Corkery et al., 2011) were used for assessing proliferation and tumor growth. However, there is a need for more high-throughput methods as used in mouse (Prigent et al., 2015) (please see section **1.1.4.1.1.**). In addition, biochemical measurements on human cells xenografted are possible (see below).

In adult fish, for instance, fluorescently-labelled tumor cell injected *prkdc*-null SCID zebrafish have been assayed for proliferation markers, PCNA and Ki67, employing immunohistochemistry (IHC) on xenografted tissue for evaluating the proliferative activity of tumor cells in adult fish (I. H. Jung et al., 2016). Similarly, optically-clear *prkdc* and *il2rga* compound mutant fish, lacking both B, T and NK cells, xenografted with various type of cancer cells have been assessed for the presence of Ki67 staining by IHC and TUNEL for reflecting proliferation and apoptosis rates, respectively (Yan et al., 2019).

In addition to above-mentioned applications for proliferation assessment, several zebrafish-specific tools reflecting tumor burden have been developed. One of such tools is an open-source software tool, ZF-Mapper and it assesses tumor proliferation by quantifying fluorescence intensity of each pixel in zebrafish images for estimating/quantifying the implanted cell numbers (Yamamoto et al., 2019). ZF-tool offers another methodology that uses the number of GFP pixels and GFP intensity medium value in order to compare two different time points and compute proliferation index (Cabezas-Sainz et al., 2018).

Although majority of the studies used fluorescence-based tumor quantification methods, quantitative-PCR based tumor DNA quantification method was also initially used by our group for precise definition of tumor proliferation in xenograft models (Avci et al., 2018).

Availability of different techniques and tools, when applied in parallel, could help deliver high-precision data on proliferation and tumor growth assessments performed both in zebrafish embryos and adult fish. Moreover, development of novel tools or modifications of those already applied for mouse studies are still needed.

1.1.4.1.1. ALU-based tumor quantification studies

Quantitative detection of ALU repeats of human DNA employing qRT-PCR are in use for quantifying xenografted human cells in mouse models (McBride et al., 2003; Zijlstra et al., 2002) and chick embryo chorioallantoic membrane (Mira et al., 2002) since the early 2000s. Zijlstra and colleagues have established ALU-based detection method for identifying presence of human cancer cell DNA in metastatic organs of mouse xenografted with different cancer cell lines bearing different metastatic capacity. Employing this approach, the sensitivity of the method was approved as 1 human cell per 1.000.000 murine could be detected. The ALU-repeat quantification at the metastatic sites were correlative with histological markers and cells with higher metastatic capacity were projecting intensified ALU-repeat signals. Human cell transplanted xenografts when treated with anti-metastatic the ALU-repeat quantification declined (Zijlstra et al., 2002). Overall, this was an initial method to reflect the precision and quality of ALU-based DNA quantification in tumor quantification in different metastatic sites *in vivo.*

In 2009, study lead by Nehmann and collogues performed a comparative analysis among ALU-based quantification and fluorescent image-based analysis performed by laser scanning cytometry (Nehmann et al., 2010). Herein, they have performed human cancer cell detection by analyzing blood samples derived from immunodeficient mice (100 micromols) which was mixed with different number of colon cancer cells ranging from (1 cell to 10.000 cells) as treatment groups. Detection of presence of single cell has become possible employing either one of the techniques however, overall, ALU-based detection system was shown to be much more sensitive when compared to image based detection method laser scanning cytometry (Nehmann et al., 2010) (**Figure 1. 2**, Error! Reference source not found.**).**

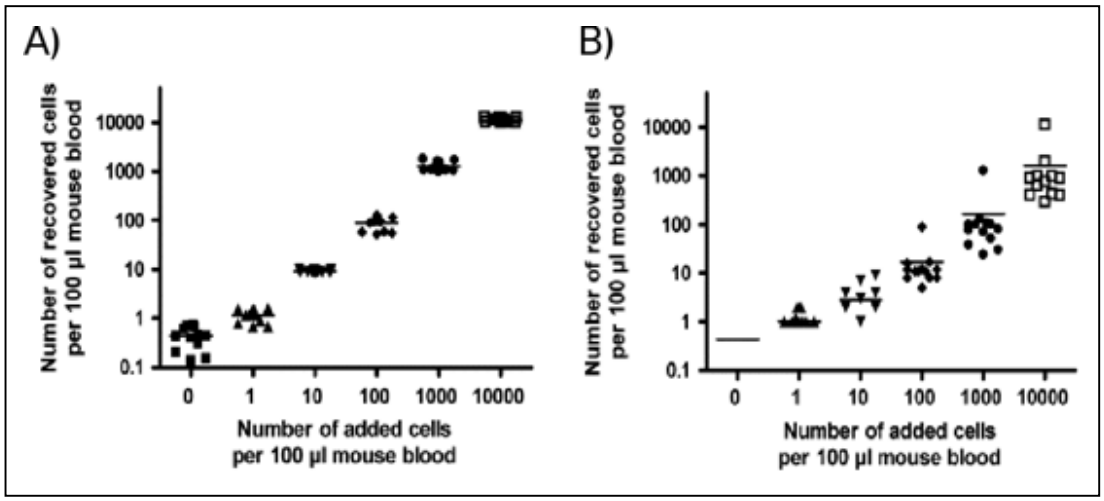

Figure 1. 2 Comparison of ALU-based detection system and laser scanning cytometry system reflecting the number of cells present in colon cancer cell-spiked immune deficient mice blood. A) ALU-based detection system is determined by comparing cell-added groups in 100µl mouse blood with calibration curve formed by known colon cancer tumor DNA concentration. **B)** Laser scanning cytometry-based system establishment by comparing cell-added groups in 100µl mouse blood with calibration curve formed by known colon cancer tumor DNA concentration.

(The image was reproduced by copy right permission and obtained from N ehmann, N., Wicklein, D., Schumacher, U., & Müller, R. (2010). Comparison of two techniques for the screening of human tumor cells in mouse blood: Quantitative real-time polymerase chain reaction (qRT-PCR) versus laser scanning cytometry (LSC). *Acta Histochemica*. https://doi.org/10.1016/j.acthis.2009.05.004)

Table 1. 1 Numerical representation and statistical analysis of recovered cells of ALU-based detection system and laser scanning cytometry method-based detection.

	qRT-PCR vs. LSC cells added per 100 µl mouse blood											
Detected cells	0 cell		1 cell		10 cells		100 cells		1000 cells		10 000 cells	
	qRT-PCR	LSC	qRT-PCR	LSC	qRT-PCR	LSC	qRT-PCR	LSC	qRT-PCR	LSC	qRT-PCR	LSC
Minimum	0.14	0.0	0.69	0.0	8.33	0.0	55.0	5.0	1001.0	24.0	10 050.0	291.0
Median±SD	0.44±0.06	0.0	1.17±0.09	1.0±0.74	9.15±0.13	2.0±2.22	89.25±6.98	11.0±3.40	1260.71±76.94	78.5±33.35	11 153.17±237.4	746.0±438.1
Maximum	0.72	0.0	1.60	2.0	9.90	7.0	127.25	17.0	1767.0	130.0	12 575.0	955.0

(The table was reproduced by copy right permission and obtained from N ehmann, N., Wicklein, D., Schumacher, U., & Müller, R. (2010). Comparison of two techniques for the screening of human tumor cells in mouse blood: Quantitative real-time polymerase chain reaction (qRT-PCR) versus laser scanning cytometry (LSC). *Acta Histochemica*. https://doi.org/10.1016/j.acthis.2009.05.004).

Another lead study of the field was established by Prigent and colleagues wherein they have studied ALU-based quantification method from a different perspective, instead of using the number of cells as base line they have optimized the technique by initially extracting the tumor cell DNA, quantifying it, performing dilutions, mixing them with a constant amount of mouse or rat DNA and measuring their Ct with ALU primers. This technique was shown to be very sensitive and precise as small as 0.01 pg human DNA could be detected in 100g of mouse DNA and 200g of rat DNA mix (**Figure 1. 3**). ALU-based detection system therefore enables precise detection of human DNA when also considered by the terms of added DNA quantity.

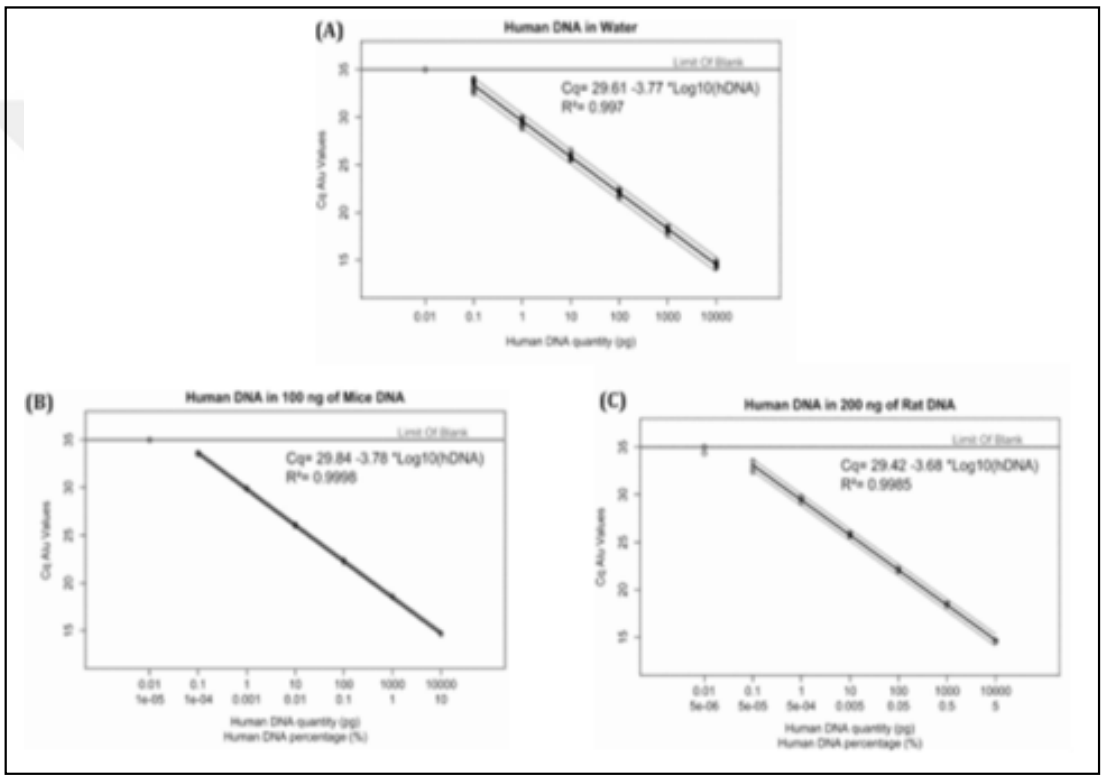

Figure 1. 3 Linear regression analysis of ALU-based detection method (AluYb8) performed across different species. A) Human DNA detection in water**. B)** Human DNA detection in 100ng mice DNA **C)** Human DNA detection in 200ng rat DNA.

(The copy right permission was taken and this imae was taken from Prigent, J., Herrero, A., Ambroise, J., Smets, F., Deblandre, G. A., & Sokal, E. M. (2015). Human progenitor cell quantification after xenotransplantation in rat and mouse models by a sensitive qPCR assay. *Cell Transplantation*, *24*(8), 1639–1652. https://doi.org/10.3727/096368914X681955).

1.1.4.2. Invasion, extravasation, dissemination and metastasis

Zebrafish xenograft models also revolutionized assessment of metastasis-related events *in vivo*. In fact, vast number of studies assesses presence of metastatic foci and/or micrometastasic foci in cancer cell-transplanted fish in parallel with evaluating presence of migration, invasion, dissemination and extravasation in these fish. A generalized approach has been adopted in most of these studies focusing on metastasis-related events assays wherein micrometastatic/metastatic foci forming at different sites, i.e., head, trunk, back, tail fin, are stated (Lara et al., 2011; Spender et al., 2016; C. Thomas et al., 2012). In several studies, step-wise approaches also have been adopted to demonstrate dissemination, extravasation and tissue invasion at one cell-resolution eventually demonstrating micrometastasis at distant foci (Shuning He et al., 2012).

Automated tools are also available for assessing metastasis-related events such as dissemination (Ghotra et al., 2012) and organ-specific distant foci formation (Annila et al., 2013). Ghotra and colleagues developed an automated whole animal bioimaging system for evaluating disseminating cells in zebrafish xenograft models. Herein, multiple parameters, i.e., total tumor cell foci, mean distance, mean intensity, mean area and cumulative distance of tumor burden, are initially evaluated for each embryo. Van der Ent and colleagues exemplify the use of this tool (Ghotra et al., 2012), where they performed automated quantitative image analysis of proliferation and migration. For tumor burden, number of tumor foci detected by its fluorescent emission were multiplied with the mean area of all fluorescence cell clusters. For migratory cells, the distance between site of injection and individual cell clusters are measured and averaged for calculating migration mean value or individual added up for reflecting cumulative/total migration value for each embryo (van der Ent et al., 2015). Similarly, Tan and colleagues used a method wherein metastatic tumor cell foci were initially identified by discarding single migrator cells by minimum area filtering criteria then, cumulative distance (CD) of metastatic tumor cell foci was calculated by summing up all identified tumor foci distances from the transplantation site in each embryo followed by use of a migration index (Tan et al., 2014). These studies show that quantification of migrating cells is important as quantifying the tumor size and volume.

A metastasis-quantifying image analysis tool, ZebIAT, was established and it provides a platform for automated cancer metastasis analyses per organ(Annila et al., 2013). The tool works with fish aging between 2dpf and 5dpf enabling registry of all major organs and upon injection, the mean fraction area of organs harboring cancer cells are examined to reflect the site/organ of metastasis (Annila et al., 2013)

Numerous methods and automated tools exist for assessing metastasis-related events in zebrafish xenograft models and extensive number of studies will give birth to novel assessment methods in time. However, there is still a need for a database through which differences in methodologies can be extracted systematically and over time.

1.1.4.3. Angiogenesis

One of the key and early studies to show successful cell transplantation to zebrafish involved establishing zebrafish xenograft angiogenesis model that was performed by Nicoli and colleagues in the beginning of 2000s where they assessed the angiogenic capacity of tumorigenic FGF2-overexpressing mouse aortic endothelial (FGF2-MAE) cells by performing three independent assays: i. alkaline phosphatase staining; ii. Whole mount in situ RNA hybridization of early endothelial markers including VE-cadherin, Fli-1 and VEGFR2/KDR; and iii. Employing fluorescence-based assessment of neovessels formation from subintestinal vessels migrating and infiltrating the FGF2-MAE cells in VEGFR2:G-RCFP zebrafish embryos (Nicoli et al., 2007). Similarly, majority of the study employed alkaline phosphatase staining for angiogenic assessment (Leali et al., 2010; Moshal et al., 2011) or fluorescence-based assessment of neo vessel formation stemming from the subintestinal vessel and/or intersegmental vessel formation in fluorescently-labelled endothelial marker expressing transgenic fish (Cheng et al., 2011; Hollenbach et al., 2013; Moshal et al., 2011; S. Zhang et al., 2011).

To conclude this section, zebrafish xenograft model provides a feasible platform for application of angiogenesis assessment and aid investigate the angiogenic capacity of xenografted cell lines and PDXs in fish. Nevertheless, there is not an online structured format by which researchers can extract knowledge in table format or visualize the

diversity of approaches. Since zebrafish xenograft field continue to evolve and expand this has now become a necessity as it has been established for mouse models earlier.

1.1.5. Technical perspectives of engraftment procedure in zebrafish model organism

Technical perspectives of zebrafish xenograft applications are of great importance. In fact, successful experimental design for testing one's hypothesis requires detailed-evaluation of technical aspects that are to be considered for zebrafish xenograft models. Herein, the number of injected cells, choice of cell line, the site of injection, cell tracking sources, optimal temperatures for xenograft-bearing fish accommodation should be carefully considered for the type of biological assessment to be performed.

1.1.5.1. Site of injection

The correct choice of site of injection is detrimental for the type of assessment to be performed in the fish, for instance, many studies focusing on proliferation, tumor growth and/or tumorigenic capacity chose to perform the transplantation into the yolk sac (Cabezas-Sainz et al., 2018; B. Zhang et al., 2015). Injection to the duct of Cuvier, on the other hand, allows analysis of metastatic events as it opens to the sinus venous of the heart and aids circulating cell analysis as performed in the majority of studies assessing metastasis (Liekens et al., 2015; Tulotta et al., 2019) and associated events including migration (Olszewski et al., 2019) and invasion (Spender et al., 2016). Another, common route for injection in fish studies is the perivitelline space. Nicoli and colleagues has initially identified successful angiogenic activity upon FGF2-overexpressing MAE cells in the fish by identifying neovessel formation from SIV basket with migratory capacity towards grafted cell area upon cell injection into the perivitelline space 48 hpf old zebrafish (Nicoli et al., 2007). Many groups followed and perivitelline space injections are now commonly used for assessing angiogenesis in zebrafish xenograft models (Britto et al., 2018; Weijts et al., 2018). The possible routes for zebrafish embryo transplantation sites are shown in **Figure 1. 4**.

Therefore, injection site preferences are based upon the type of assessment to be pursued for each research question.

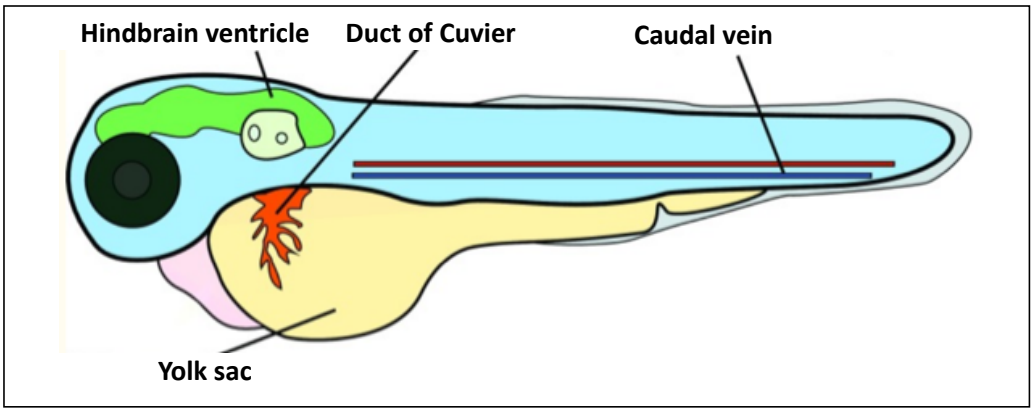

Figure 1. 4 Schematic representation of different injection sites for xenotransplantation studies in 48hpf fish.

(No copy right permission was required for this figure and the figure was was obtained from (Veinotte et al., 2014); Veinotte, C. J., Dellaire, G., & Berman, J. N. (2014). Hooking the big one: The potential of zebrafish xenotransplantation to reform cancer drug screening in the genomic era. In *DMM Disease Models and Mechanisms*.)

1.1.5.2. Injected cell numbers

Cell numbers to be injected are considered as another technical aspect to be evaluated carefully when stating a hypothesis in zebrafish xenograft studies. If to be reviewed, diverse number of cells of different cancer types have been injected to fish and different type of analyses have been performed yet some studies harboring the comparison of these assessments exist and depict the influence of the choice of cell number for the assessment to be taken. For instance, a study led by Gaytan-Cervantes and colleagues used CRISPR-modified HeLa cells for testing tumorigenic capacity of injections performed with different number of cells. CRISPR-modified and control cells were injected as 75 cells, 125 cells or 250 cells as three independent experimental groups to study the tumorigenic capacity in groups of approximately 15 embryos. Monitoring for 4 days post injection revealed control injected cells had 0/15 (0%), 2/13(15%), 3/14(21%) tumor development whereas CRISPR-modified cells had 3/15(20%), 4/13(31%) and 6/15(40%) tumorigenic capacity 75 cell-, 125 cell- and 250 cell-injected fish, respectively. This outcome clearly reflects the importance of choice of cell number in experimental design (Gaytan-Cervantes et al., 2017). Another study also intensifies the need for optimal use of cells in numbers for xenotransplantation studies in zebrafish by illustrating both the influence of injected cell numbers and location on embryo survival for optimization purposes. Herein, 20, 50, 100, 200 and 500 cells were injected to embryonic mass (n:50), subintestinal veins (n:100) and yolk

sac (n:100) and higher survival rates were detected in fish injected to yolk with 200 cells, 500 cells leading to significantly reduced survival rates (X. J. Yang et al., 2013).

As exemplified above, optimization of the injected cell number is essential for delivering the right outcome of the designed experimental set-up per study. Collection and projection of data on the injected cell lines and numbers are essential for canalizing the researchers into most-optimized experimental setups for zebrafish xenotransplantation studies.

1.1.5.3. Cell tracking sources

Zebrafish as a xenograft host provides a feasible route for cell tracking due to its transparency which is either established through using pigment mutants, i.e., *casper* strain or transgenic fish with *casper* backgrou*nd* or through PTU administration for pigment removal. Cell tracking sources are of several options one of which is the tag expression vectors (TV) yielding expression of fluorescent proteins and the others include use of lipophilic membrane dyes, amino-reactive molecules etc. (Jensen, 2012). Prior to transplantation, cells are either transfected or transduced with fluorescent protein expressing vectors i.e. green fluorescent protein (GFP) (C. W. Wong et al., 2019), mCherry (Marranci et al., 2019), DsRed (Liekens et al., 2015; Tulotta et al., 2019), mTurquise (De Boeck et al., 2016) or stained with lipophilic dyes such as CM-DiI (Gianoncelli et al., 2019), DiO (Shi et al., 2019), PKH26 (Xia et al., 2014) or stained with aminoreactive molecules such as CFSE (Xia et al., 2014). Hence, these options reflect the abundance of choice for the cell tracking sources and ease-of-use in zebrafish xenotransplantation studies.

1.1.6. Review of xenograft databases of fish and murine models present in the literature

Rodents are in use for xenotransplantation studies over a century. Collective data presentation on rodent xenograft studies are available through databases and/or tools which are designed to deliver precise information on the experimental design and clinical information to the scientific research community.

1.1.6.1. Mouse Models of Human Cancer Database

Mouse Models of Human Cancer Database (MMHCdb), formerly named as Mouse tumor biology (MTB), database serves as an open-source encyclopedia of mouse models for human cancer since 1999 (Bult et al., 1999, 2015; Krupke et al., 2008) (**Figure 1. 5**). The current version of the database is accessible through http://tumor.informatics.jax.org/mtbwi/index.do. MMHCdb database focuses on three main aspects of mouse studies one of which is the spontaneous and induced tumors in mice, mouse models of cancer including mutant, inbred, hybrid, and genetically engineered strains, and lastly patient-derived xenograft models (Bult et al., 2015).

This database has a user-friendly interface and provides easy access to information through cancer-specific links listed through its main page as well as through 'Advanced search' button by providing search through several attributes including primary site, tumor type, site of metastasis, tumor inducing agent type, genes and alleles, strain, strain type, tumor frequency, study size, reference, additional information and human tissue. Additionally, it provides information through the MTB database-embedded 'Search/Tools' tab such as 'Tumor Frequency Grid (inbred strains), 'Patient Derived Xenograft (PDX) Search, 'PDX Like Me' tools as well as providing links to another independent platforms such as 'PDX Finder' (Conte et al., 2018).

Overall, this database serves as an important platform for projecting data on human cancer mouse models as well as PDX models providing useful information for cancer research community.

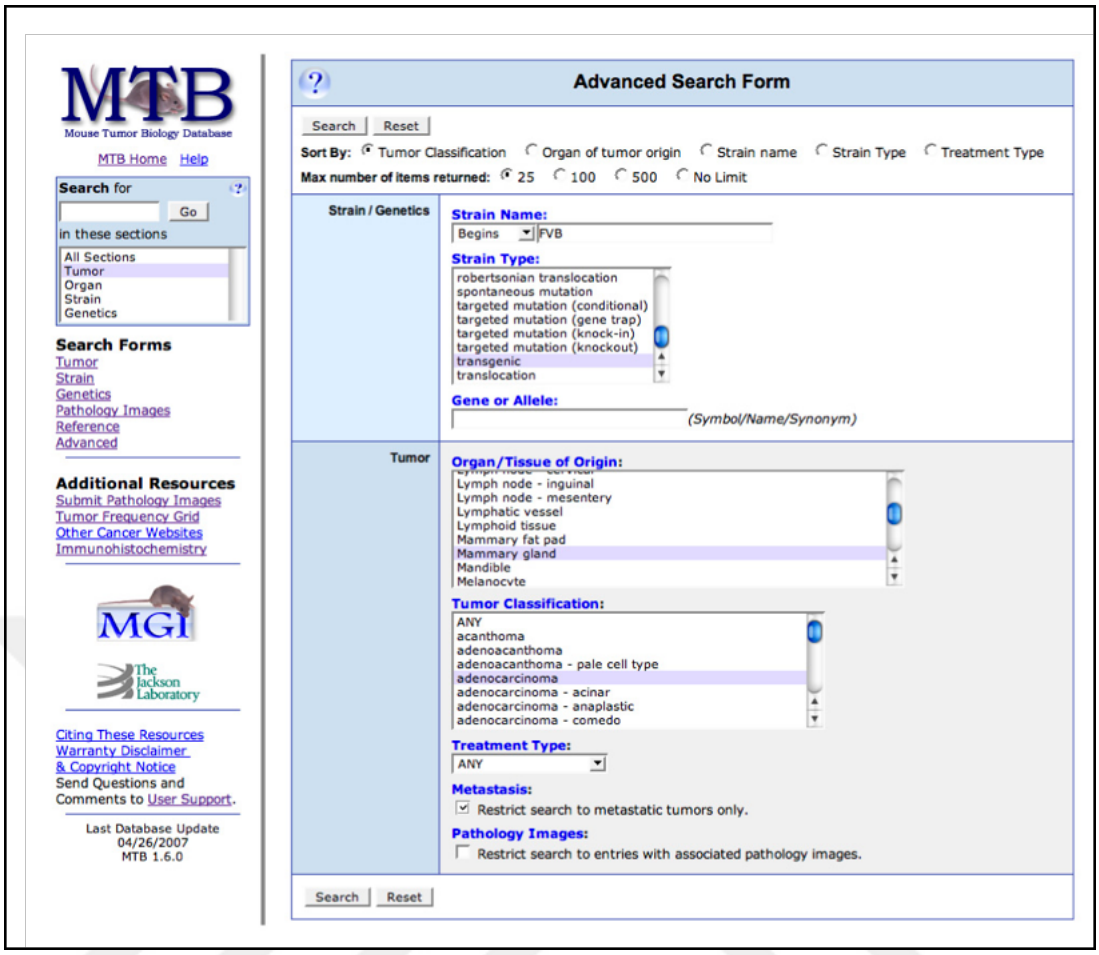

Figure 1. 5 Screenshot of Mouse Tumor Biology database advanced search page.

(This image was retrieved from Krupke, D. M., Begley, D. A., Sundberg, J. P., Bult, C. J., & Eppig, J. T. (2008). The mouse tumor biology database. In *Nature Reviews Cancer*. https://doi.org/10.1038/nrc2390).

1.1.6.2. PDX Finder

PDX Finder is a joint project of EMBL-EBI and The Jackson Laboratory that houses repository of PDX models and associated data (Conte et al., 2018). The PDX finder is originally based on the PDX models minimal information standard (PDX-MI) project (Meehan et al., 2017) that gathers the data and projects them through four modules; clinical (/patient and /tumor), model creation, model quality assurance and model study/associated metadata. The four modules have further sub-modules to be fulfilled as essential or desirable information and are as follows.

Clinical module accommodates detailed query on patient-associated and tumor-associated information to be fulfilled and some of these data are marked as essential

where some are only marked as desirable on the recommendation list. The patient-association data, for instance requires fulfillment of attributes such as submitter patient ID, age, gender, diagnosis, consent to share data as essential query and attributes such as ethnicity/race, current treatment drug, current treatment protocol (dose; details), prior treatment protocol, response to prior treatment and virology status as desirable query to be fulfilled. Tumor-associated data has essential query on submitter tumor ID, primary tumor tissue of origin, primary/metastasis/recurrence, specimen tumor tissue, tissue histology, tissue grade, disease stage and specific markers (diagnostic linked). Desirable attributes such as 'original tumor sample type' and 'tumor from an existing PDX model? ID? Why, sub-line?' are included.

Model creation module requires information about the mouse model used for PDX transplantation. Herein, attributes include 'Submiter PDX ID', 'mouse strain (and source), 'Strain immune system humanized?', 'Type of humanisation', 'Tumor preparation', 'Injection type and site', 'Mouse treatment for engraftment', 'Engraftment rate', 'Engraftment time'.

Model quality assurance module collects information on 'Tumor Characterization Technology', 'Tumor confirmed not to be of mouse/EBV origin', 'Response to Standard of Care (Pharmacological positive control)', 'Animal health status', 'Passage AQ performed'

Model study module consists of 'Treatment, passage', 'Treatment protocol (dose; details), 'Treatment Response', 'Tumor OMICS: sample id; sample site; purity (mouse vs human); technology; passage' 'Development of metastases in strain (Y/N, site); passage' and 'Lag time/doubling time of tumor'.

Associated metadata module accommodates information on 'PDX model availability?', 'governance restriction for distribution' and 'ID for associated publication, image, archived data (URL, PMID, DOI)'.

PDX finder webpage is designed to display this collective information through several routes: e.g., through the Find search engine which is run for cancer diagnosis of interest located on the welcome page. Explore engine is designed to categorize data and aid

data search through ‘frequently mutated gene’, ‘drug dosing’, ‘anatomical systems’ and ‘provider’ links. Yet, the ‘Search’ tab located on the home page diverts the user into more sophisticated search platform wherein PDX model, molecular data, treatment/drug dosing, patient/tumor details are provided through these modules and a fine-tuned search can be performed through this platform easily (**Figure 1. 6**).

As default, with no specified query, PDX finder provides the information of mouse model, histology details, primary tumor information, collection site, type of status i.e. metastatic/primary and other available data about the tumor sample.

PDX Finder, hence, serves as the main encyclopedia of patient-derived xenotransplantation studies performed in rodents. Its user-friendly interface as well as easy-to-follow-up web-site design allows easy access and interpretation of the incorporated data and guides the researchers for collecting data of their interest and review current PDX models of rodents. Furthermore, the possibility direct data submission from the researches also makes it an interactive web base providing most novel applications of PDXs in rodents. Databases such as PDX Finder are in great demand and are of great use for cancer research community.

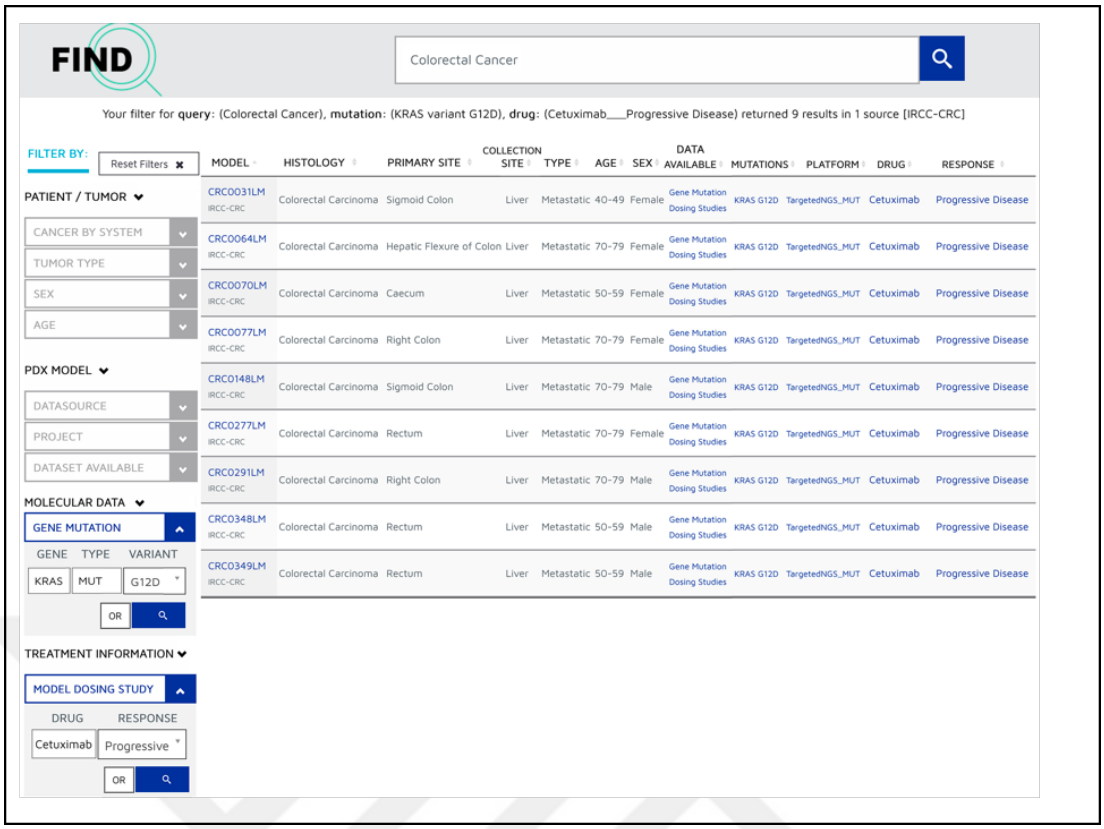

Figure 1. 6 Screenshots of PDX Finder search page. An example search performed by searching colorectal cancer, KRAS gene mutation and Cetuximab drug treatment keywords.

(This image was retrieved from Conte, N., Mason, J., Halmagyi, C., Neuhauser, S. B., Mosaku, A., Begley, D. A., Krupke, D. M., Parkinson, H., Meehan, T., & Bult, C. J. (2018). PDX Finder: A Portal for Patient-Derived tumor Xenograft Model Discovery. *BioRxiv*. https://doi.org/10.1101/291443)

1.1.6.3. Patient-Derived Models Repository Database

National Cancer Institute Patient-Derived Models Repository (NCI-PDMR), accessible through https://pdmr.cancer.gov/, has been established to deposit patient-derived xenografts, *in vitro* patient-derived tumor cell cultures, cancer associated fibroblasts and patent derived organoids for scientific research purposes mainly aiming improvement of preclinical studies for delivering effective therapeutics in clinics. Herein, the PDMR Database is organized to display the information through 8 tabs which are namely 'Home', 'Patient', 'Patient Specimen', 'Sample (PDX or In Vitro Culture)', 'Distribution Lots', 'Genomic Analysis', 'Reports' and 'Search'.

Patient tab is where Patient ID and information such as gender, disease description, disease body location, diagnosis/subtype and STR profile are displayed for informing

the users. Patient specimen further highlights the users about the tissue type, presence of PDX growth curve in mouse model, metastasis model in NSG mouse, provided tissue origin and etc.

Sample (PDX or In Vitro Culture) tab permits the user access to Patient-Derived Xenograft Samples that permits user to check relevant information including Specimen ID and informs about the availability of pathology, OncoKB Cancer Gene Panel, Whole Exome Sequence and RNA-Seq reports. By clicking to specimen ID a report page displaying specimen and engraftment details as well as PDX growth curve is present. In vitro culture option, on the other hand, lists the samples based on patient ID and also presents specimen ID and sample ID details. Additionally, the type of culture such as CAF culture/PDC:Mixed tumor culture/Organoid culture is also present as well as required media for growing conditions are also displayed through this page. Disease-associated details such as disease description, disease body location as well as assessment-specific details such as information on tumorigenic capacity in NSG mice, in vitro image availability, OncoKB cancer gene panel data availability, whole exome sequence data availability, RNA-Seq availability and culture origin are also displayed for delivering all essential information for the users.

Genomic analysis tab diverts the users into the page of OncoKB Gene Panel whereas genomic information about the derived material type stated with patient ID, specimen ID, sample ID, disease-associated information. Herein, genetic alterations such as mutations, altered protein sequences, variant allele frequencies, variant classes, i.e. mutation type, oncogenicity and mutation effect, are stated. Whole exome sequence and RNA-Seq tabs are also present under the genomic analysis tab and through these tabs one can access FastQ files and download the sequences for their interest.

Report tab is another tab that provides access to pathology page which in turn reports the tumor grade, tumor content in percentage, necrosis in percentage, stromal in percentage and inflammatory cell grading as well as pathology notes. Additionally, report tab provides links to deliver information about the ethnicity/race and ancestry as well as treatment history.

Finally, *Search tab* provides a detailed platform for mining data according to the patients and specimens that has known metastatic disease, MSI-high models, metastatic models, at least one sample that has image data, at least one sample that has whole exome sequence data, at least one sample that has RNA-Seq data, germ line sequence by checking one or more than one options for a shared profile. Additionally, search choosing single/and or multiple entries from Patient ID, gender, self-reported race, disease body location, PDM type, disease code, grade/stage tissue type, therapy regimen, Hugo gene symbols are also available for a fine-tuned search through PDMR database.

Distribution lots tab is another feature that informs the user specifically about the availability of cryovials for PDX generation, PDX DNA vials, PDX RNA vials and PDX-Flash frozen vials. Therefore, enables the distribution of the selected PDX to be used in the lab settings.

Overall, PDMR serves as a platform for researchers to search for PDX model of their interest in rodents based on different filtering systems covering patient data, PDX model data and tumor data including genomic analysis and pathology reports. Additionally, it also provides distribution information for delivering research materials of PDX models of interest for direct use in laboratories. Availability of this platform is a great help for those currently performing or planning to pursue rodent PDX models.

1.1.6.4. PDXliver

PDXliver is a database that implements mouse PDX models of liver cancer aiming to provide a global server for developing anticancer therapeutics personalized medicine for liver cancer patients (Sheng He et al., 2018).

The database houses a total number of 116 patient data which are reflected through seven different modules; 'Data Set' '#Patient' implying number of patients, 'Transcriptome', 'Genome', 'Drug', 'Resource' and 'Reference' on the homepage of the database. The transcriptomic data is divided into three datasets, namely, the DataSet1 Affymetrix Human Genome U133 Plus 2.0 Array (gpl570) (raw data: GSE90563) (Registered patient number:46, Registered PDX model:40), the DataSet2 Affymetrix Human Gene Expression Array (GPL15207) (Registered patient number:65, Registered PDX model:43) and thirdly the DataSet3 RNA-Sequencing data (GPL15207) (Registered patient number:5, Registered PDX model:5). The associated genomic data for DataSet1 is derived from both Affymetrix Genome-Wide Human SNP 6.0 Array (raw data: GSE9065) (Registered PDX model:40) and Exome sequencing (Registered PDX model:40) platforms. These two platforms introduce the type of transcriptome data as well as the genomic data that was integrated to this database.

Mining through this database could be established through the *'Browse'* page which displays and enable sorting based on for liver cancer subtypes, viral status, TNM stage, grade, datasets presented on the homepage, germline variants, somatic mutations and copy number alterations (**Figure 1. 7**).

Well-designed architecture as well as data categorization of PDXliver database, hence, allows mining different attributes on mouse liver PDXs including hepatocellular carcinoma, cholagiocarcinoma, hepatoid adenocarcinoma, gastric hepatoid cancer and mixed cancers. The database emphasizes the importance of data delivery on organ-specific xenograft models and aids search of liver PDXs for the use of cancer researchers.

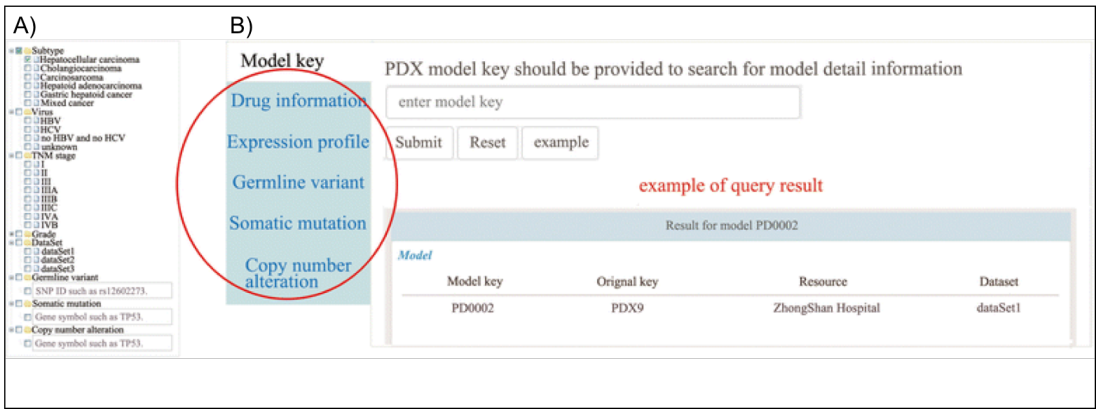

Figure 1. 7 Screenshot of PDXliver browse and search page. A) PDXliver browse page allows data sorting based on page based on liver cancer subtypes, viral status, TNM stage, and grade **B)** PDX search page enables search through the highlighted (in red circle) attributes and example of query result is shown.

(These images were adapted/retrieved from He, Sheng, Hu, B., Li, C., Lin, P., Tang, W. G., Sun, Y. F., Feng, F. Y. M., Guo, W., Li, J., Xu, Y., Yao, Q. L., Zhang, X., Qiu, S. J., Zhou, J., Fan, J., Li, Y. X., Li, H., & Yang, X. R. (2018). PDXliver: A database of liver cancer patient derived xenograft mouse models. *BMC Cancer*. https://doi.org/10.1186/s12885-018-4459-6).

1.2. Mineralocorticoid receptor (MR) signaling and cancer

1.2.1. MR signaling at a glance

Mineralocorticoid receptor (MR/NR3C2) is a member of nuclear receptor steroid receptor subfamily which also houses glucocorticoid receptor (GR), estrogen receptor (ER), progesterone receptor (PR), and androgen receptor (AR) (Helsen & Claessens, 2014; Robinson-Rechavi et al., 2003). MR was primarily identified as an aldosterone binging receptor in rat kidney tissue (Funder et al., 1972; Rousseau et al., 1972); and it is mainly involved in body electrolyte homeostasis and sodium reabsorption. In addition to its presence in epithelial tissues including sweat glands (Kenouch et al., 1994; H. Sasano et al., 1992) and colon (Pressley & Funder, 1975) it is also expressed non-epithelial tissues such as vasculature and brain (Agarwal et al., 1993; Lombès et al., 1992).

MR can bind to mineralocorticoids (aldosterone, deoxycorticosterone), glucocorticoids (cortisol) (Rupprecht et al., 1993; Sutanto & de Kloet, 1991) and progesterone (Myles & Funder, 1996). Although aldosterone is considered the primary physiological ligand of MR, cortisol, which is found more abundantly (100-1000 times more than aldosterone) in bloodstream can bind to MR with high/similar affinity (Bledsoe et al., 2005). Presence of hydroxy beta dehydrogenase enzymes confers specificity for MR ligand binding. HSD11B2 and HSD11B1 enzymes are the two isozymes working as regulators of corticosteroid production and selective affinity to mineralocorticoid and glucocorticoid receptors. HSD11B1 is a reductase enzyme that predominantly converts inert cortisone (Compound E) into active cortisol (Compound F) in human tissues whereas HSD11B2 converts active cortisol (Compound F) to inactive cortisone (Compound E) (Edwards et al., 1988, Funder et al., 1988). HSD11B1 and HSD11B2 expressions vary among different tissues; HSD11B1 is abundantly expressed in liver, adipose and adult brain as well as vasculature, ovary, testis, uterus, placenta, immune and inflammatory cells, skeletal muscle and heart and fetus (late gestation) (Chapman et al., 2013). HSD11B2, on the other hand, is mostly expressed in mineralocorticoid (aldosterone) responsive tissues such as distal nephron, sweat glands, salivary glands, colon as well as exocrine pancreas, adrenal cortex, skin and lung epithelia, vascular endothelium and fetus (early to mid-gestation) (Chapman et al., 2013). Hence tissue specificity and availability of the HSDs play a role

determining the affinity of the corticoids to MR and GR receptors. Therefore, presence of HSD11B2 in epithelial cells thus ensures aldosterone-selective MR activity mechanistically eliminating cortisol induced MR activity.

MR/NR3C2, in the absence of its ligands, resides in cytoplasm and held by its chaperone proteins heat shock protein 90 (hsp90) and FK506-binding protein 51 (FKBP51) (J. Yang & Fuller, 2012). In the presence of its ligand, aldosterone, it binds to the MR-chaperone complex which in turn causes conformational change and leads to replacement of FKBP51 with FKBP52 causing nuclear localization of the ligand-receptor-chaperone complex. Ultimately chaperone proteins disassociate from this complex, and ligand-bound MR form homodimers and bind to hormone-response element (HRE)s. With the recruitment of the co-activator complex, then, MR transactivation takes place (J. Yang & Fuller, 2012) (**Figure 1. 8**). The aforementioned mechanism of action reflects the classical genomic actions of aldosterone-mediated mineralocorticoid receptor signaling.

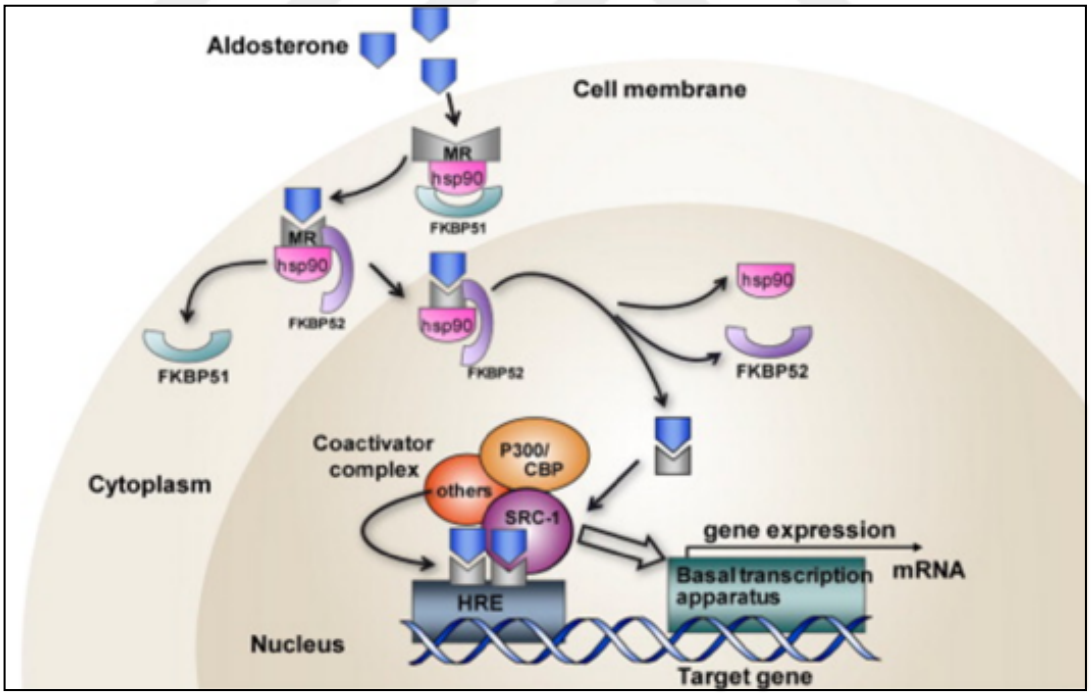

Figure 1. 8 Aldosterone-mediated transactivation of mineralocorticoid receptor.

(This figure was reproduced by copy right permission and was obtained from Yang, J., & Fuller, P. J. (2012). Interactions of the mineralocorticoid receptor - Within and without. In *Molecular and Cellular Endocrinology*. https://doi.org/10.1016/j.mce.2011.07.001 and its use is permitted with copy right permission from Elsevier Publications).

Actions of aldosterone is not only mediated through classical genomic MR binding to HRE. HRE-independent mechanisms, i.e. indirect interaction with other transcription factors should be also considered as possible routes for mediating exert genomic effects of aldosterone through MR binding as it was shown for NFKB p65 subunit mediated repression of MR transactivation (Kolla & Litwack, 2000).

Non-genomic actions of membrane-associated MR also exists; Grossman and colleagues have shown co-localization of MR and EGFR to the plasma membrane that is independent of short-term aldosterone exposure (≤ 1hour) and long-term aldosterone exposure (24 hours) resulted in nuclear translocation of MR and loss of MR-EGFR co-localization at the plasma membrane (Grossmann et al., 2010). MR, similarly to other steroid receptors, exerts its downstream effects through genomic and non-genomic signaling. However, the data on mechanism of action or its modulation of expression or expression heterogeneity of MR remains less studied in epithelial cancers with few studies in literature.

1.2.2. Aldosterone and MR signaling in epithelial tissues

Mineralocorticoid receptor is vital for maintaining water balance and electrolyte homeostasis in human physiology. Its mechanism action has been long studied to better understand human physiology and pathology both at physiologic and gene-level. Genomic actions of aldosterone-driven MR signaling in an epithelial tissue, e.g., a renal polarized epithelial cell, portraits a sophisticated picture of the regulation of downstream effectors of this signaling pathway by mirroring the roles of key effectors in maintaining sodium and water balance under physiological conditions (**Figure 1. 9**).

Aldosterone-driven MR transactivation in an aldosterone-responsive epithelial cell turns on a cascade of events that ultimately leads to expression of two key effector proteins; the apical amiloride-sensitive Epithelial Na^+ channel (ENaC) and the basolateral Na+K+ -ATPase for mediating sodium and water homeostasis taking place principally in the distal nephron and the distal colon (Fuller & Young, 2005). Once MR becomes transactivated, it controls ENaC expression and function through multiple actions. Aldosterone-mediated MR transactivation leads to serum glucocorticoid kinase 1 (SGK1) transcription, which in turn results in ENaC

translocation in the apical membrane (Brennan & Fuller, 2000; Chen et al., 1999; Loffing et al., 2001). Once the SGK1 is transcribed and activated, it phosphorylates Nedd4-2 ubiquitin-protein ligase (Debonneville et al., 2001). Phosphorylated Nedd4-2 can no longer lead to ubiquitination and degradation of ENaC, therefore increasing its expression on the apical membrane (Arroyo et al., 2011).

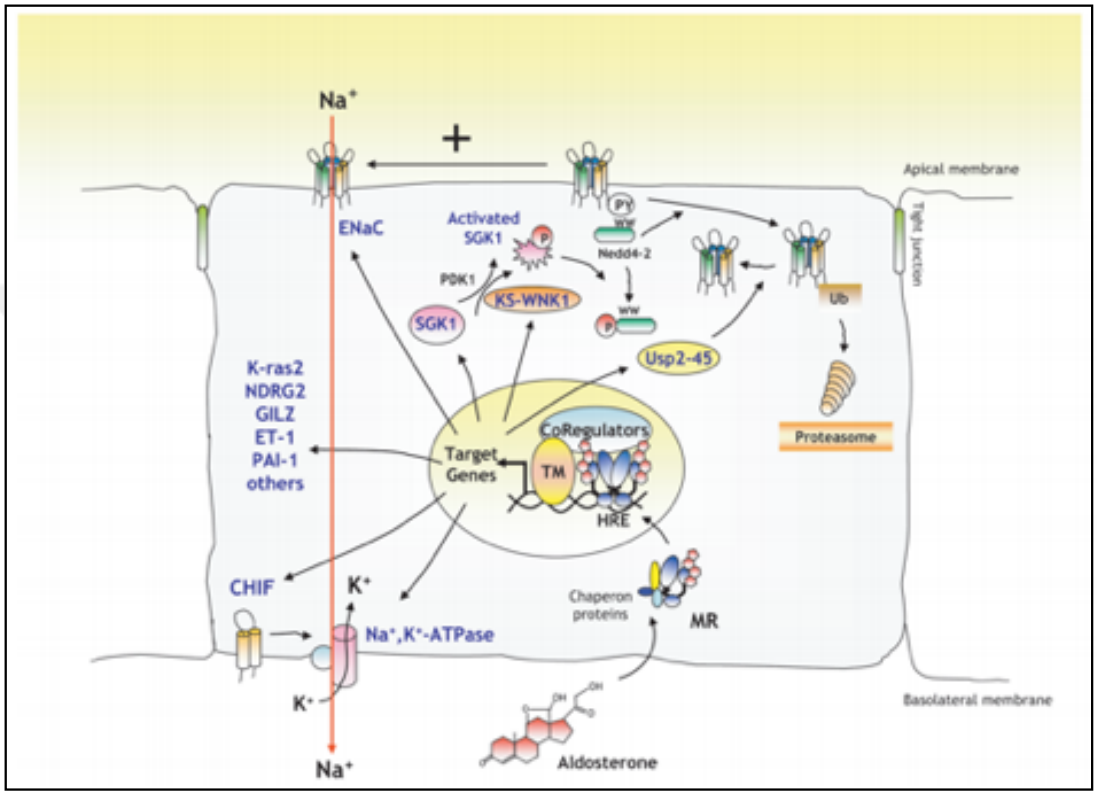

Figure 1. 9 Aldosterone and mineralocorticoid signaling in a polarized renal cell.

(This image was reproducible without the need of copy right permission and required citation and it was obtained from Viengchareun, S., Le Menuet, D., Martinerie, L., Munier, M., Pascual-Le Tallec, L., & Lombes, M. (2007). The mineralocorticoid receptor: insights into its molecular and (patho)physiological biology. *Nucl Recept Signal*, *5*, e012. https://doi.org/10.1621/nrs.05012 .)

1.2.3. Mineralocorticoid receptor and aldosterone signaling in epithelial cancers

Research on deciphering possible tumorigenic or antitumorigenic activity of MR and aldosterone signaling only begun in 2000s. Previous studies regarding to MR and cancer conceptualized studies have remained very limited to immunohistochemistry research where normal tissue and diseased tissue of various origins were screened were presence of MR (Fukushima et al., 1994; Hironobu Sasano et al., 1997; Suzuki et al., 2000). To date aldosterone and/or mineralocorticoid receptor signaling has been studied in several epithelial cancers including cancers of lung, colon, liver, breast and kidney (See below and **section 1.2.4**)

1.2.3.1. Lung cancer

Presence of MR expression in lung cancer tissue was initially identified by Suzuki and colleagues in 2000 (Suzuki et al., 2000). About ten years later, another discovery on MR expression and lung cancer spilled out as Jeong and colleagues were aiming to identify nuclear receptor expression signatures in non-small-cell lung cancers (NSCLCs) and corresponding normal tissues. Herein, only in the corresponding normal tissues, high MR expression was shown to be good prognosis predictor for survival and disease recurrence (Jeong et al., 2010). In another context, Bar and colleagues studied association of sodium regulators, one of which was aldosterone, in NSCLC disease outcome prediction. Elevation in the aldosterone levels with the treatment was shown to be better associated with longer overall survival (OS) in the NSCLC patient group treated with the VEGF inhibitor, Cediranib, when compared with the placebo treated controls (Bar et al., 2015). Aldosterone and MR signaling were mostly studied in NSCLCs. Accordingly, presence of aldosterone and/or expression of MR was shown to be a better indicator of disease prognosis in NSCLCs. Yet, aldosterone and MR signaling remains to be elucidated in other types of lung cancers e.g., small cell carcinoma, squamous cell carcinoma and large cell carcinoma.

1.2.3.2. Colon cancer

Identification of MR expression in gut mucosa dates back to 1975 (Pressley & Funder, 1975). Expression of MR, in cancer tissue, however, was shown on ileum mucosa of patients went under colectomy after 20 years of initial MR expression in gut

(Fukushima et al., 1994). Di Fabio and colleagues, then, studied MR expression in colon cancer wherein, association among MR, and VEGFR, expression was studied in order to investigate any possible association of MR and angiogenesis in colon cancer. MR was shown to be downregulated in colon cancer tissue when compared with the matched normal tissue mucosa whereas VEGFR, was shown to be regulated in the opposite direction, exhibiting an increased expression in tumor tissue when compared to normal mucosa. Underexpression of MR as well as the presence of inverse correlation among MR and well-defined angiogenesis marker, VEGFR, in colon cancer tissues was suggesting tumor suppressive role of MR in colon tumorigenesis (Di Fabio et al., 2007). Further studies towards MR signaling in colon cancer tissues also revealed an inverse correlation among MR and a microvessel density marker (CD34) in colon cancer tissues. Survival analysis performed for association among colon cancer patients stratified by high or low CD34 as well as MR expression also revealed a similar trend wherein low CD34 and low MR expression to be significantly associated with better and worsened overall survival outcomes, respectively (Tiberio et al., 2013). Herein, aldosterone modulated MR signaling on colon cancer cells were additionally tested *in vitro* and VEGFA expression and VEGFRR-2 (mRNA) was shown to be downregulated upon aldosterone administration on transiently MR-overexpressing colon cancer cells (Tiberio et al., 2013).

Another survival analysis by our group using GEPIA tool has also identified an association among high MR expression and better overall survival in colon adenocarcinoma patients (Konu & Targen, 2019). In addition, analysis of impact of MR mutations impacts by Mutation assessor revealed presence of a high impact mutation of MR in colorectal adenocarcinoma patients (Konu & Targen, 2019).

Overall, aldosterone and MR signaling seems to be an important factor in colon tumorigenesis, a part of it at least through its association with the regulation of angiogenetic factors. More studies deciphering role of aldosterone modulated MR-signaling across different biological pathways will also help illustrate a more-complete picture of its role in colon cancer.

1.2.3.3. Renal Cancer

MR has been long studied in renal physiology and pathology (Fuller & Funder, 1976; Matulich et al., 1976). Yet, its connection with cancer had been first studied through identification of its expression together with its counterpart, HSD11B2, in normal renal tissue as well as renal cancer tissue of different origin as well as normal renal tissue in 2000s (Yakirevich et al., 2008). Herein, co-expression of both receptors was identified in normal distal nephron, oncocytoma stemming from distal nephron and chromophobe renal cell carcinoma (chRCC) (Yakirevich et al., 2008). King et al., has also showed co-expression of MR and HSD11B2 in clear cell renal carcinoma tissues (King et al., 2014). Furthermore, the proliferative capacity of aldosterone modulated MR signaling was also assessed in this study. In fact, MR antagonist spironolactone administration was shown to downregulate K-RAS expression and decreased cell proliferation in mutant VHL-expressing and normal VHL-expressing renal cell carcinoma cells in the presence of basal cell culture conditions. Additionally, K-RAS4A was shown to be exerting its proliferative actions through Raf and Akt pathways through knockdown studies (King et al., 2014). On the contrary, aldosterone was shown to be promoting DNA synthesis and migration of murine renal cortical adenocarcinoma via G-protein coupled estrogen receptor (Feldman et al., 2016).

These findings highlight the presence of MR and its counterpart HSD11B2, in diseased kidney tissue along with the normal kidney tissue suggesting a possible role and/or dysregulation in different cancer types of kidney origin. Furthermore, cell type specific actions of aldosterone and/or spironolactone highlights cell-type dependent regulation of MR signaling in cancer development in kidney.

1.2.3.4. Liver Cancer

In liver cancer tissue, particularly of hepatocellular carcinoma (HCC), mineralocorticoid receptor was shown to be underexpressed when compared to corresponding normal liver tissue controls (Nie et al., 2015). Herein, MR silencing and overexpression models were established to study effects of MR alone as well as in the presence of aldosterone/spironolactone on liver tumorigenesis. Presence of MR, by overexpression model establishment, was shown to be decreasing cell viability and increasing apoptotic rate in liver cells in vitro. Furthermore, MR was shown to be

inhibiting colony formation of HCC cells in vitro and tumor formation/growth in vivo. Furthermore, when presence of MR overexpression was coupled with aldosterone cell viability and colony formation were down regulated and this effect by reversed by presence of spironolactone. In the same study, MR was shown to be inhibiting Warburg effect and also, tumor proliferation through the miR-338-3p/PKLR axis in this model (Nie et al., 2015).

Another study also showed involvement of MR in hepatocellular cancer regulation, herein, another miRNA, miR-766 was shown to be directly targeting MR in HCC cells which was in turn, mediating proliferative and metastatic capacity of HCC cells *in vitro* (C. Yang et al., 2019). In fact, MR-overexpression model was rescuing the effects of miR-766 by diminishing cell proliferation, colony formation and metastasis of HCC cells. Furthermore, miR-766 targeting of MR was involved in the regulation of Beta catenin pathway activation wherein miR-766 was activating B-catenin which was reversed by the presence of MR (C. Yang et al., 2019).

Survival analysis performed for MR expression association and liver hepatocellular cancer (LIHC) disease prognosis revealed that high expression of MR was significantly associated with better overall survival and MR was shown to be harboring deleterious high-impact mutation in hepatocellular carcinoma patients assessed by the Mutation assessor (Konu & Targen, 2019).

Overall, classical aldosterone and MR signaling as well as MR subjected to post-transcriptional modifications play an important role in liver carcinogenesis and these implications are important for developing new research questions and better evaluation of MR in liver carcinogenesis as well as in cancer, in general.

1.2.4. Mineralocorticoid and glucocorticoid receptors and breast cancer

Initial identification of mineralocorticoid receptor expression in normal breast tissue along with the diseased breast tissue dates back to late nineties. Herein, expression of mineralocorticoid receptor together with its epithelial tissue counterpart, HSD11B2, expression was studied by immunohistochemistry. Both proteins appeared to be

predominantly co-localizing in the duct epithelia and exhibiting higher expression patterns in invasive ductal carcinoma when compared to invasive lobular carcinoma. (Hironobu Sasano et al., 1997).

Another study by an independent group, later on, showed cytoplasmic MR expression in all breast tissue regardless of any disease status (benign disease of breast, carcinoma *in situ* infiltrative ductal carcinoma and infiltrative lobular carcinoma). GR expression was also studied in parallel, yet its expression exhibited a different expression pattern than of MR, GR expression was all nuclear in benign breast disease tissues and were exhibiting both cytoplasmic and nuclear expression in carcinoma *in situ*- infiltrative ductal carcinoma- and infiltrative lobular carcinoma-derived tissues (Conde et al., 2008).

Very recently, a Finnish group also studied MR, AR and GR-β expression in HER2- breast cancer samples (n=152) out of which approximately 60% were TNBC samples (n=96) (Jääskeläinen et al., 2019). AR expression was found in both cytoplasm and nucleus yet was predominately-nuclear; MR expression were found both in cytoplasm and nucleus, yet it was more frequently cytoplasmic; GR-β, on the other hand, were only cytoplasmic and no traces of nuclear stains were found. A positive correlation was found between nuclear AR expression and cytoplasmic GR-β expression when all samples were considered. Further on, association among AR, MR, GR-β and clinicopathologic parameters were also studied. Herein, nuclear AR was significantly associated with smaller tumor size and better differentiation. Cytoplasmic MR and cytoplasmic GR-β were associated with node-negative status and decreased tumor proliferation, respectively. Furthermore, EMT markers and association of these receptor expressions were also evaluated. In the entire patient cohort, nuclear AR and cytoplasmic GR-β were negatively associated with vimentin expression whereas negative association among vimentin expression and MR was only detected in the TNBC group. In the TNBC group MR was also shown to be positively associated with SIP1 (Jääskeläinen et al., 2019).

Survival analysis of the patients with a median follow-up time of 100 months were also evaluated in regard to their expression status. High cytoplasmic MR expression

was associated with better overall survival outcome, breast-cancer-specific survival and distant disease-free survival in TNBC patients. On the other hand, the non-TNBC group (ER/PR+HER2-) were exhibiting an opposite effect wherein low cytoplasmic MR expression being associated with relapse-free survival. This outcome highlights the possibility of crosstalk among nuclear receptor e.g., ER, PR and MR in breast cancer (Jääskeläinen et al., 2019).

Functional studies evaluating the role of aldosterone signaling and MR in breast, although in very few numbers, still exist. In one of such studies, effect of MR, GR, HSD11β2 agonists and/or antagonists were used for testing 11- hydroxysteroid dehydrogenase activity and proliferation in breast cancer cells, PMC42, *in vitro* (Koyama et al., 2001). Herein, initially effects of cortisol (GR ligand) and glycyrrhetinic acid, an 11βHSD inhibitor, were tested on the cells. Cortisol, at physiological levels, increased 11βBSD activity which was then diminished by addition of the glycyrrhetinic acid. In addition, although cortisol did not exert any effect on cellular proliferation, glycyrrhetinic acid addition lead to antiproliferative behavior of cells. In order to identify the molecular mechanism behind the anti-proliferative activity of the 11βHSD inhibitor, studies on MR and GR signaling were pursued. Initially, ligand binding assays revealed binding constants of aldosterone and dexamethasone as well as the number of binding sites for MR and GR, respectively. Glycyrrhetinic acid was then shown to inhibit ligand binding of MR and GR. Then the effects of MR and GR agonists and/or antagonists were tested by means of their effect on 11βHSD activity and proliferation. GR agonist cortisol and GR/PR antagonist RU38486 and MR antagonist spironolactone was shown to induce 11βHSD activity yet aldosterone, did not exhibit any alterations on the 11βHSD activity. Both of the agonist ligands, aldosterone and cortisol, when applied solely, did not exhibit any alteration in cell proliferation yet the antagonists (RU38486 and spironolactone) regardless of the presence of their ligands, have been shown to reduce cell numbers. Overall, these findings highlighted the presence of 11βHSD2 activity in breast cancer cells and indicated a potential role for steroid receptors in proliferation (Koyama et al., 2001).

Another study has also contributed to identification of downstream effectors of aldosterone signaling in breast cancer. Herein, possible effects of aldosterone exerted through GPER and/or MR had been examined in breast cancer disease; SkBr3 (HER2+) cell line and breast tumor derived endothelial cells (BTEC). Initially, aldosterone was shown to be activating EGFR and ERK1/2 transduction pathways through GPER and MR. Aldosterone stimulation results in upregulation of the NHE-1, regulator of the cell pH and volume, in SkBr3 and BTECs in the presence of both receptors. Aldosterone exerted proliferative effects on SkBr3 cells which was reverted by silencing either one of the MR or GPER. Addition of NHE-1 inhibitor also reverted the effect of proliferative effect of aldosterone on naïve SkBr3 cells. The same trend was also observed for migration assay performed on BTEC cells wherein aldosterone was resulting in migration which was reverted by NHE-1 inhibitor or MR/GPER silencing. These findings reveal the importance of aldosterone signaling both at cytoplasmic and nuclear levels and it also reveals the possibility of cross-talk among MR and growth factor receptors in breast cancer and also validates cell-type specific actions of aldosterone by the means of tumorigenesis.

1.2.5. MR overexpression studies

Successful cloning of human MR (hMR) in 1987 had been a scientific breakthrough for the scientific community focusing on the corticosteroids and MR (Arriza et al., 1987). Gene functionality studies upon gene silencing and/or overexpression studies then became more feasible in practice. Initially, hMR was overexpressed in *Spodoptera frugiperda* (Sf9) insect cells and was further characterized by immunoblotting and ligand binding assessments (Alnemri et al., 1991). Numerous studies harbor MR overexpression model established in African Green Monkey SV40-transformed kidney fibroblast (COS-7) cells which do not possess endogenous MR expression (Hernández-Díaz et al., 2010; Hubert et al., 2011; Shibata et al., 2013; Sonoyama et al., 2017).

In vitro MR overexpression models have been used to decipher wide-range of questions raised for identifying molecular function of MR in different experimental settings including disease-specific mutation assessments, e.g., pseudohypoaldosteronism 1 (Balsamo et al., 2007; Riepe et al., 2006), mutation assessments for identifying effects of different post-translational modifications on MR

(Faresse et al., 2012; Shibata et al., 2013), immunology-based studies (Haas et al., 2018) and cancer research (Nie et al., 2015; Tiberio et al., 2013; C. Yang et al., 2019).

1.3. Aims and rationale

Zebrafish has become a model of choice in cancer, stem cell and patient derived xenografting however there is no database to collect and analyze methodology and content of these ever-increasing xenograft studies. In addition, there are many molecular modifications, e.g, overexpression of oncogenes/tumor-suppressors in cell lines, which can benefit from *in vivo* validation. There are understudied molecules such as Mineralocorticoid Receptor (MR) whose overexpression has not been addressed in breast cancer in cell lines or in zebrafish yet, providing excellent opportunities to test in zebrafish. Mouse has been the gold-standard model to date, yet zebrafish offers many advantages as a xenograft model. Furthermore, there is a need to develop high throughput methodologies in quantification of xenografts in zebrafish as has been done more frequently at the molecular level as in mouse. It is important also to make use of zebrafish host to demonstrate that xenograft studies can take advantage of mutant/modified zebrafish to address the interaction between microenvironment and xenografted tumor. Accordingly, in the present study:

1) I aimed to review plethora of xenograft (primary, stem or cancer cell line as well as patient-derived tumor) studies particularly those possessing molecular modifications including overexpression, knock out and knock in and transgenics along with those using modified hosts to understand the state-of-the art and to provide a foundation for a searchable and updatable database that will provide leads for upcoming studies and researchers in the zebrafish field;

2) As a case study, I aimed to help develop a quantitative method for xenograft tumor size measurements *in vivo* in a high throughput manner using a modified ALU quantification method from mouse model and apply this technique in *ache* null zebrafish microenvironment using liver cancer cell xenografts;

3) As a case study, I aimed to apply xenograft technologies to better understand MR signaling in breast cancer and hence a) to study role of MR *in vitro* in breast cancer cells and *ex vivo* in patient tumor diagnosis and prognosis; b) develop an overexpression model in MCF7 and ZR-75-1 cells, which inherently do not express (or negligibly express) MR and test whether MR overexpression is oncogenic or tumor-suppressing; c) apply MR-overexpressing cells as xenografts in zebrafish to

understand the tumor forming ability of MCF7 cells with or without modification and MR's role in carcinogenesis.

CHAPTER 2

MATERIALS AND METHODS

2.1. Development of ZenoFishDb v1.1 zebrafish xenotransplantation database

2.1.1. Manual data curation guidelines

The current literature on zebrafish xenograft studies were identified, reviewed and subjected to manual curation based on four major aspects: presence of molecularly modified cell injections, presence of stem cell featured cell injections, patient-derived xenograft models and any kind of injections applied onto the modified zebrafish stains. Once these criteria were met, the data were sorted out based on the attributes for precise categorization of cumulative data present on each and every research article for the generalized data as well as PDX-associated data display purposes. The database was organized to deliver the data through four modules; *Data Table*, *Visualization*, *PDX-Details* and *PDX Charts*. The *Data Table* and *PDX Details* were designed to deliver the data in table format as stated in **Table 2.1** whereas the *Visualization* page and *PDX Charts to* graphically and statistically represent the curated data.

Table 2. 1 The name of the attributes and their explanations are presented for the *Data Table* and *PDX Details* modules.

Attribute	**Specification**
Data Table	
Cancer type/tissue of origin	Cancer type nomenclature was sorted based on the nominated cell line/s and PDXs. Tissue types were named after the original statements of tissue origins on the original articles.
Abbreviations	Cancer and tissue type abbreviations were nominated after the original nomenclature of cancer type/tissue of

	origins. These names were specific use of ZenoFishDb v1.1.
Cell line species	Cell line species were designated to classify the species of cell lines and or PDXs incorporated onto the ZenoFishDb v1.1.
Cell lines	Selected articles for incorporation were screened for also naïve cell line injections in parallel to modified-cell injections, herein all xenografts injections were recorded onto cell lines attribute.
Modified cell lines	Modified cell lines aimed to display the data on only injections of molecularly modified cell lines and PDXs.
Molecular modifications	Molecular modifications attribute was established to accommodate any type of molecular modification applied to cells or PDXs prior to injections.
Modified genes	Gene subjected to modifications were recorded with their names as appeared on the original articles.
PDX	Absence and presence of PDXs were re-called as 'PDX' or 'n/a'.
Stem cell properties	Injections harboring stem cells, cancer stem cells or any stem-cell associated features were displayed through this attribute.
Treatment	Treatments incorporated onto the ZenoFishDb v1.1 were initially sorted based on three criteria; any treatments applied to fish water; any treatments introduced through direct injection

	and/or oral gavage; any treatments applied to *in vitro* cell cultures or PDX material upon engraftment.
Injection site	Injection site or transplantation site of cells and/or tissues were stated in this attribute.
Injected cell numbers (Exact)	Injected cell numbers and/or formulas were incorporated onto the ZenoFishDb v1.1 as appeared on the original article.
Injected cell numbers (Categorized)	Injected cell numbers were categorized into four intervals; and displayed for ease of statistical analysis and data presentation.
Developmental stage	Developmental stage of fish e.g., adult, juvenile or embryo were stated through this attribute.
Injection time (hpf)	Injection time as of hours post fertilization (hpf) were recorded onto this attribute.
Tumor assessment (hpi)	Tumor assessment as of hours post injection (hpi) was aimed to represent the final point of assessment time for any kind of assessment applied on the xenograft models.
Zebrafish lines	Zebrafish lines attribute was generated to display all the zebrafish strains used for injection. A communized language was used for all synonyms of the same fish strains.
Host modifications	Host modifications attribute was designed to categorize fish strain modifications as mutants, morphants and transgenic strains. N/a were either

	symbolizing wild-type or non-informative studies.
Host modification details	Host modification details attribute delivered explanatory information about the host modifications.
Cell tracking sources	Cell tracking sources used for visualization and analysis were available through this attribute.
Analyses	Analyses attribute was designed to deliver type of analyses used in each study. More than one analyses were recorded where applicable.
References	References were listed in the author-date format.
PubMed hyperlink	PubMed hyperlinks were added for easy access to the main articles.
PDX Details	
Mentioned PDX-ID/Name	PDX name and/or any kind of identification were recorded as mentioned in the original article.
ZenoFishDb PDX-ID	ZenoFishDb also attributed a specific PDX ID as follows ZenoFishDb_PMID ID_NUMBER OF PDX.
Age	Age of the patients were recorded.
Sex	Sex of the patients were recorded.
Ethnicity	Ethnicity of the patients were recorded.
Detailed nature of disease	The disease nature, as detailed in the original article, were recorded.
Primary site	Primary site displayed the primary site of the tumor.
Collection site	Collection site displayed the location where the tumor sample was collected.

Primary/Metastatic/Recurrent	The tumor was specified as primary, metastatic or recurrent if stated in the main article.
Patient treatment (if received before specimen prep.)	Any kind of treatment applied before specimen preparation was recorded to the database.
Clinical information	Clinical information such as grade, stage, size, hormone receptor presence, and TNM were recorded.
Mutations/Rearrangements	Any mutations and/or rearrangements present in the PDX stated in the original articles were incorporated into the database.
Cytogenetics analysis	Originals articles mentioning cytogenetics analyses for PDXs such as translocations, deletions etc. were sorted and data were incorporated into this attribute.
Karyotype	Originals articles mentioning karyotype analyses for PDXs were sorted and stated in this attribute.
Other relevant data	Not properly classified and/or mentioned PDX-associated details were incorporated to this attribute.
Zebrafish line	PDX injected zebrafish lines were recorded.
PDX-tissue/PDX-cell line	PDX transplantation method were distinguished as direct tissue transplantation (PDX-tissue) or patient-derived primary cell culture transplantation (PDX-cell line). The type of transplantation method was reported.

Cell number (if available)	Injected cell numbers were recorded for PDX-cell line injections.
Injection site	Injection site were displaying PDX injection sites.
Injection period	Injection period of the PDX transplantations were states as 'adult' for adult fish and 'hpf' were stated for the fish embryos.
PubMed link	PudMed hyperlinks were stated for feasible access to the original articles.
Study-Author date; PMID:	Study author-date and PMID numbers were stated.
Mouse xenograft	Mouse xenografts of the same PDX used in the original article were stated as 'present' in this attribute.

2.1.2. ZenoFishDb v1.1 was developed using R Shiny

The interactive web page of ZenoFishDb v1.1 database was developed using Shiny application in the R environment. The data tables, *Data Table* and *PDX Details,* were generated using the DT package, an R interface of JavaScript library *DataTables*. Further data fine-tuning and focused search enabled through the subselection filtering by the application of dplyr package. The graphical representation pages, *Visualization* and *PDX-Charts* were generated employing an R graphing library*, Plotly*. The webpage and Shiny app were developed by Tuğberk Kaya.

2.2 *In vitro* and *in vivo* studies

2.2.1. Materials

2.2.1.2. List of laboratory solutions, reagents and kits

Table 2. 2 Laboratory materials, reagents and kits for used cell culture studies.

Product Name	**Producer**	**Catalogue Number**
PBS-1X w/o Ca, Mg	Lonza, Switzerland	BE17-516F
DMEM w/1.0 g/L glucose w/o L-Glut	Lonza, Switzerland	BE12-707F
RPMI 1640, with L-Glutamine	Lonza, Switzerland	BE12-702F
DMEM, low glucose, w/pvruvate, w/o L-Glut, w/o phenol red	Thermo Fisher Scientific, USA	11880-28
RPMI 1640, without L-Glutamine and phenol red	Lonza, Switzerland	BE12-918F
Opti-MEM® I Reduced Serum Medium	Thermo Fisher Scientific, USA	31985-070
FBS South America, Gamma Irradiated	Biowest, France	S181G-500
Fetal Bovine Serum (FBS) South America, Charcoal Stripped	Biowest, France	S181F-100
Lipofectamine® 2000	Thermo Fisher Scientific, USA	11668027
Aldosterone	Sigma, Germany	A9477
Spironolactone	Sigma, Germany	S3378

Table 2. 3 Laboratory materials, reagents and kits for RNA, protein and immunohistochemistry studies are listed.

Product Name	**Producer**	**Catalogue Number**
QIAZOL lysis reagent	Qiagen, Germany	79306
iScript cDNA Synthesis Kit	BIO-RAD	1708891

DNA-free™ DNA Removal Kit	Thermo Fisher Scientific, USA	AM1906
LightCycler® 480 SYBR Green I Master	Roche, Switzerland	4887352001
LightCycler 480 Multiwell Plate 96, White	Roche, Switzerland	04729692001
TissueScan™ Breast Cancer cDNA Array I BCRT101	Origene, USA	BCRT101
TissueScan™, Breast Cancer cDNA Array I BCRT102	Origene, USA	BCRT102

2.2.1.2. Primer lists

Table 2. 4 List of primers used, their sequences and annealing temperatures**.**

Gene ID	**Band size**	**Amplified Variants**	**Forward Primer Sequence**	**Reverse Primer Sequence**	**Tm**
TPT1 (reference)	100bp	1, 2	*GATCGCGGACGGGTTGT*	*TTCAGCGGAGGCATTTCC*	60°C
MR (NR3C2) QIAGEN	n/a	1, 2	*N/A*	*N/A*	60°C
MR (NR3C2)	175bp	1	*AGTGGAAGGGCAACACAACT*	*CTGCTCCTCGTGAATCCCTTT*	60°C
GR (NR3C1)	160bp	1 ,2 ,3 ,4 ,5, 6 , 7 ,8, 9, 10, 11, 12, 13, 14, X2, X3, X7	*CTGGGGTGGAGATCATATAGACA*	*CATAAGATACCTGAAGCCTGTGT*	60°C
SGK1	118bp	1, 3, 4, 5, X1	*AACCCTTCTCCTCCACCAAG*	*TTCCAAAACTGCCCTTTCCG*	60°C
ZBTB16	107bp	1, 2, 3, 4, 5, X1	*AGACGTACCTCTACCTGTGCTATGTGT*	*TGTCATAGTCCTTCCTTCATCTCACT*	60°C
PER1	103bp	PER1mRNA, X1, X2, X3,	*TCCATTCGGGTTACGAAGCT*	*GCAGCCCTTTCATCCACATC*	58°C
ACHE	200bp	-	*ACACGTGCCATATTGCAGAG*	*CTGCTCCAGGGAAGAACTTG*	62°C
ALU	-	-	*CGAGGCGGGTGGATCATGAGGT*	*TCTGTCGCCCAGGCCGGACT*	62°C

2.2.1.3. DNA constructs

MR-STAG-pcDNA3.1 plasmid was a kind gift from Dr. Nourdine Faresse, University of Zurich Switzerland and pcDNA3.1 plasmid was a kind gift from Dr. Ebru Erbay lab, Bilkent University.

2.2.2. Methods

2.2.2.1. Cell culture studies

MCF7, MDA-MB-231, MDA-MB-453, BT-20, HEK-293, Hep3B and SKHep1 cell lines were maintained in DMEM supplemented with 10% fetal bovine serum, 1% non-essential amino acid, 2% sodium pyruvate and 2% L-Glutamine. ZR-75-1, T47D and HCC-1937 cell lines were maintained in in RPMI with glutamine supplemented with 10% fetal bovine serum, 1% non-essential amino acid, 2% sodium pyruvate. Cells were regularly grown in T75 flasks and passaged when confluency reached 80% and were maintained at 5% CO_2 37°C incubator.

2.2.2.2. Transfection protocol for overexpression studies on six-well plates

Transfection protocol was initially optimized according to Lipofectamine 2000 manufacturers' protocols. For 6 well plate forward transfection protocol, initially 200.000 MCF7 or ZR-75-1 cells were seeded onto the 6-well plates. The following day, the transfection complex was prepared for the MR/NR3C2-Stag-pcDNA3.1 vector (test) and pcDNA3.1 vector (control). Initially, 1 μg of each plasmid (either MR-Stag-pcDNA3.1 vector or pcDNA3.1 vector) was mixed with 250 μl of serum-reduced OPTI-MEM I and 2 μl of lipofectamine was mixed to 250 μl serum-reduced OPTI-MEM I in separate Eppendorf tubes and let to stand for 5 minutes at room temperature. Next, ingredients of two tubes were collected in one tube, for forming MR-Stag-pcDNA3.1 and lipofectamine complex and pcDNA3.1 and lipofectamine complex for test and control samples, respectively. The ingredients in each tube were then mixed by vortexing or pipetting up and down and let stand for additional 20 minutes (at least) at the room temperature. While waiting, the media on top of the six well plates were removed and replaced with 1500 μl of standard pen-strep free media. Next, 500 μl of the transfection complex was added on the plates in a drop-wise manner and incubated for 4-6 hours before replenishing the media.

2.2.2.3. Transfection protocol for overexpression studies on ninety-six well plates

For 96 well plate forward transfection protocol, different protocols were followed for optimizing the cell seeding density and transfection efficiency in MCF7 and ZR-75-1 cells. Initially, 5.000 cells or 10.000 cells were seeded onto 96 well plates in 100ul culture media with phenol red and the following day 25 ng or 50 ng of plasmid-transfection complex (either MR-Stag-pcDNA3.1 vector or pcDNA3.1 vector or no vector control (lipofectamine control)) were administered to cells, respectively. Each plasmid was calculated to be diluted in 12.5 μl of serum-reduced OPTI-MEM I and 0.2 μl of lipofectamine for each well were calculated to be diluted with 12.5 μl serum-reduced OPTI-MEM I in separate Eppendorf tubes. For the feasibility, this ratio was calculated and multiplied with the number of wells to be transfected for each vector as well as for the only lipofectamine control. Once the master mixes were prepared, the Eppendorf tubes were let stand for 5 minutes at room temperature and then mixed and, let stand for another 20 minutes (at least). In the meanwhile, the media on 96-well plate were aspirated and replaced with 75 μl penicillin streptomycin-free media. Once the incubation period was over, the mixture for each treatment (25 μl) were added onto the wells. The media were then removed after 4-6 hours and replaced with fresh media.

2.2.2.4. Hormone treatment conditions

Aldosterone steroid hormone was diluted in molecular grade EtOH to yield 10 mM stock concentration and were stored at -20°C or -80°C. Spironolactone, a synthetic steroid, was diluted with molecular grade EtOH to yield 50mM stock concentration and kept at 20°C for storage.

Aldosterone and spironolactone treatments were applied to naïve cells or transfected cells at different experimental settings. Once the cell seeding and/or transfection protocols were successfully established, the wells were washed with PBS for two times and 5% charcoal stripped FBS phenol red-free media was added on top of the wells, 2000 μl and 100 μl for 6-well and 96-well treatments, respectively. The wells were then incubated for 24 hours in order to remove masking effects of aldosterone on the

cells. Next, 5 μM and 50 μM working solutions were prepared in 5% charcoal stripped FBS phenol red-free media using 10 mM aldosterone and 50 mM spironolactone stocks, respectively. Then, the working solutions were further diluted to final concentration of the drugs and aldosterone and/or spironolactone and ethanol control treatments were administered to cells. Initially, cells were treated with spironolactone for 1-1.5 hours and then aldosterone treatment administered to wells and the plates were then incubated for 24 hours for assessing long-term genomic effects of aldosterone.

2.2.2.5. RNA extraction

QIAZOL lysis reagent was used for total RNA isolation according to manufacturer's protocol under the chemical hood. Cell pellets collected from 6-well plates were kept in 15ml Falcons at -80°C and were thawed on ice prior to total RNA extraction. For each pellet tube 700 μl of QIAZOL lysis reagent was added and mixed by thorough pipetting then transferred to Eppendorf tubes. Next, 140 μl of chloroform was added and the tubes were inverted up and down up to 15 times and let stand for 10 minutes at room temperature. Later on, the tubes were centrifuged for 20 min at 13.000 rpm at 4°C. Upon successful lysis, lower organic phase, middle phase containing white strains of DNA and an aqueous phase containing RNA material became visible. Next, the aqueous phase (~350 μl) were removed carefully without intervening any other phase and transferred into newly labelled Eppendorf tubes. Then the same volume of isopropanol (~350 μl) were added on the aqueous phase and the solutions were mixed by inverting the tubes up and down for 5-10 times. The tubes were then let stand for 10 minutes at the room temperature and were then centrifuged at 13.000 rpm for 12 minutes at 4°C. The RNA pellets were formed (if visible) at the bottom of the tubes and the supernatants were removed without disturbing the pellet. Next, the pellets were washed with 1ml 75% EtOH, centrifuged at 8.000 rpm at 4°C for 8 minutes. After this step, the pellets became more visible. Then the pellets were washed with 1ml 100% EtOH, again centrifuged at 8.000 rpm at 4°C for 8 minutes. After removing the 100% EtOH with care, the pellets were air dried under the chemical hood and were then solubilized in 20 to 50 μl of nuclease-free H_20 based on pellet size.

2.2.2.6. DNAseI treatment

DNA-free™ kit DNase treatment and removal reagents by Ambion Life Technologies were purchased for DNAseI treatment for RNA-seq sample treatments. Initially, the RNA concentration was measured and was diluted to 200 ng in 44 µl of RNase DNase free water as the starting material. The RNA sample was prepared accordingly in a 200 µl PCR tube and then, 5 µl of the DNAse Buffer and 1 µl of DNase were added into same tube. Then the tube was quickly span down. The sample was then placed onto the previously heated thermal cycler (37°C) and incubated for 30 minutes. Next, the tube was taken from the thermal cycler and at the room temperature, 5 µl of DNAse inactivation buffer was directly pipetted down into the mixture and mixed well. It was crucial to mix the ingredients well in this step to visualize the cloudy appearance. Then the tube was incubated for 2 minutes at room temperature and transferred to Eppendorf tubes. The tube was than span down at 13.000 for 2 minutes and here, two layers of phases were visualized. Then the 41 µl of supernatant (RNA) was carefully removed without entering to the bottom of the tube.

2.2.2.7. cDNA synthesis

iScript™ cDNA synthesis kit was purchased for cDNA synthesis reactions. The kit was composed of three components; 5x iScript reaction mix, nuclease-free water and iScript reverse transcriptase. The total volume of each reaction was set to be 20 µl and a constant volume of 5x iScript reaction mix (4 µl) and iScript reverse transcriptase (1 µl) adding up to a total volume of 5 µl. The remaining 15 µl were to be composed of RNA and nuclease free water. As a standard of our laboratory protocol, 1 microgram RNA was used in each reaction, hence the volume of RNA (X µl) and the remaining amount of nuclease free water (15-X µl) to be added were calculated for each sample and added accordingly. iScript reverse transcriptase lacking samples were also run in parallel as negative controls for each experiment set up. The thermocycler was then adjusted to run the reaction protocols as follow; 5 minutes at 25°C, 30 minutes at 42°C, 5 minutes at 85°C. Then this protocol was further optimized by the company and changed to 5 minutes at 25°C, 20 minutes at 46°C, 1 minutes at 95°C. Once the cDNAs were ready, they were diluted in 1/10 and stored at -20°C for further use.

2.2.2.8. *Ex vivo* cDNA array dilution

TissueScan™ ORIGENE Breast cancer cDNA Arrays, namely BCRT101 and BCRT102, were received in lyophilized form embedded on a 96 well plate and covered with a seal. The seal was cut and removed for each well in order, diluted with 20 µl of nuclease free water and transferred into PCR tubes for further use.

2.2.2.9. RNA quality assessment

RNA quality assessment was purchased as a service procurement from Ankara University. RNA 6000 Nano Assay Kit (Cat No:5067-1511) was used for assessing the RNA quality and integrity. RNA integrity values (RIN) of RNA samples to be sent for RNA Sequencing are recorded as recorded in the table below.

Table 2. 5 The RNA integrity (RIN) values of RNA samples submitted for RNA-Seq.

SAMPLE NAME	RIN
MCF7-EV-ETOH-25	7.70
MCF7-EV-ALDO-42	9.70
MCF7-EV-ALDOSPIRO-44	8.10
MCF7-MR-OVEX-ETOH-21	7.70
MCF7-OVEX-ALDO-31	6.20
MCF7-OVEX-ALDO-46	8.10
MCF7-OVEX-ALDOSPIRO-41	9.10
MCF7-OVEX-ALDOSPIRO-36	8.70
ZR-75-1-EV-ETOH-23	10
ZR-75-1-EV-ALDO-32	9.70
ZR-75-1-OV-ETOH-24	10
ZR-75-1-OV-ALDO-22	10

2.2.2.10. RNA sequencing protocol and normalization

RNA Sequencing assessment was purchased as a service procurement from Genomics Core Facility EMBL, Germany. The samples were run on the Illumina NextSeq500 platform using 75bp long single end pairing and the sequence were identified using hg19 (Human) genome as reference genome. RNAseq analysis pipeline included

sequence alignment and sorting from retrieved from provided BAM files, alignment quality control by using Alignment Metric QC (Seven Bridges Cancer Genomics Cloud), obtaining raw count data by using HT-Sew Count (Seven Bridges Cancer Genomics Cloud), performing differential gene expression analysis by using DESeq2 R package from Bioconductor. The RNAseq pipeline was established and performed by the help of Ayse G. Keskus, Fatma B. Dincaslan, and Ronaldo Leka from Konu Lab.

2.2.2.11. Quantitative real time polymerase chain reaction (qRT-PCR)

2.2.2.11.1. Mammalian cell culture qRT-PCR conditions

LightCycler® 480 SYBR Green I Master mix was purchased for performing qRT-PCR experiments. The kit consisted of SYBR Green I Master mix and nuclease free water. The protocol was standardized to the total volume of 10 µl. In each reaction, 5 µl of SYBR Green I Master mix, 1 µl of 10 µM forward primer of interest, 1 µl of 10 µM reverse primer of interest, 1 µl of nuclease free water and 2 µl of cDNAs were present. For ease of the distribution on to the 96 well plates, the number of samples, negative controls and pipetting error were calculated and a master mix of gene of interest were prepared in each experiment. Following the preparation of master mix, the master mix was spun down, then mixed by pipetting up and down and distributed as 8 µl onto each well. Then 2 µl of cDNAs were added onto the side of the wells. The plate was then covered, sealed and centrifuged for 2 minutes at 2000 rpm at room temperature. The plate was then inserted onto the Light Cycler 480 I Cycler and were run at the conditions as follows: initial denaturation at 95°C for 5 minutes; 45 cycles of amplification (95°C 10 seconds, X°C 20 seconds, 72°C 20 seconds); melting curve analysis at 95°C for 5 seconds, 55°C for 1 minute, 95°C continuous; cooling at 40°C for 40 seconds, X symbolizing the Tm for each primer set used.

2.2.2.11.2. *Ex vivo* cDNA array qRT-PCR conditions

Quantitative real time polymerase chain reactions were performed using LightCycler® 480 SYBR Green I Master mix (5 µl), nuclease free water (2 µl), 10 µM forward primer of interest (1µl), 10 µM forward primer of interest (1µl) and cDNA (2 µl). The master mix was prepared for the gene of interest considering the total number

of samples, negative controls and pipetting error. 8 µl of master mix was distributed onto each well of the 96 well plates and 2 µl of cDNAs were added to the sides of the wells. The plate was then sealed and centrifuged at 2000 rpm for 2 minutes. Then the reaction was run on the Light Cycler 480 I at the following cycling conditions: initial denaturation at 95°C for 5 minutes; 50 cycles of amplification (95°C 10 seconds, 60°C 20 seconds, 72°C 20 seconds); melting curve analysis at 95°C for 5 seconds, 55°C for 1 minute, 95°C continuous; cooling at 40°C for 40 seconds. The DDCT were calculated.

2.2.2.12. *In silico* gene expression analysis

In silico analysis of MR and GR mRNA co-expression were studied across 994 breast invasive carcinoma complete case set samples of the Cancer Genome Atlas (TCGA)-PanCancer Atlas dataset on cBioPortal platform (Cerami et al., 2012).

2.2.2.13. Survival analysis by GEPIA 2 and KM Plotter

Gene Expression Profiling Interactive Analysis 2 (GEPIA 2), formerly known as GEPIA, uses RNA-Seq data derived from TCGA and GTEx projects for expression analyses of tumor and normal subjects (Z. Tang et al., 2017, 2019). Herein, GEPIA was used to generate survival plots for establishing association of median-defined high or low MR and/or GR mRNA expressions with overall survival (OS) and disease-free survival (RFS) plots in breast cancer patients.

KM Plotter is another well-established platform enabling survival analysis across different cancer types based upon both microarray and RNA-Seq data (Lánczky et al., 2016). For breast cancer survival analysis, the microarray-based analysis enables generation of relapse-free survival (RFS), overall survival (OS), distant-metastasis free survival (DMFS) and post-progression survival (PPS) along with enabling the choice of hormone status (ER, PR and HER2) as well as intrinsic subtype, lymph node status, grade, TP53 status and pietonpol subtype. Herein, MR and GR expression were studied with 205259_at and 216321_s_at IDs, respectively.

2.2.2.14. MTT cell viability assay

MTT (3-(4,5-dimethylthiazol-2-yl)-2,5-diphenyltetrazolium bromide) cell viability assay was performed according to manufacturer's protocol. For a 96 well plate, 0.001 g of MTT powder was measured, solubilized in 1ml of PBS and sterile filtered freshly. Then 1 ml of the MTT solution was mixed with 10 ml phenol-red free complete DMEM, next 110 μl of MTT was replaced with the media covering top of the cells and plate was incubated at 37°C, 5% CO_2 incubator for exactly 4 hours. Next, 12 mM SDS-HCL solution was prepared by mixing 1g of SDS with 0.01 M 10ml HCL freshly. Once prepared, incubated at 37°C water bath for 5 minutes for dissolving the SDS in HCL homogenously. Upon completion of 4-hour MTT incubation 100 μl of the SDS-HCL mix were added on top of the MTT solution bearing wells. Different than the manufacturers protocol, the context of the wells was not pipetted up and down as this was causing loss of the cells and bearing error-prone results. Negative controls, wells with no cells seeded, were also treated in the same manner. Once the SDS-HCL mixture was added the plate was incubated for 12-16 hours and the absorbance were then read at 570 n.m. microplate reader.

2.2.2.15. Zebrafish xenotransplantation studies

2.2.2.15.1. Xenografting MR-overexpressing breast cancer cells and liver cancer cells

Zebrafish experiments were performed with permission from Bilkent University Animal Ethics Committee according to regulations (Protocol no: 176, Decree no: 2013/48 for ache study; 2017/17 for MR study). Zebrafish were maintained in 14-hour light and 10-hour dark cycles. *casper*, wild type (AB Strain), and *ache*^{sb55} null mutant zebrafish embryos were used for xenotransplantation at different experimental settings. Zebrafish embryos 48 hours post fertilization (hpf) were used for injection. Transiently MR-overexpressing (MR/NR3C2-Stag), control vector expressing (pcDNA3.1) and/or lipofectamine treated MCF7 cells were injected yolk sacs of these embryos. The cell numbers in volume of nanolitres to be injected were determined using 0.01mm Olympus objective micrometre, AX0001 OB-M 1/100, varied among different setups. The cells were injected into the mineral oil dropped on the objective

micrometre and the radius of the sphere formed was used in $4\pi r^3$ formula to correctly determine the number of injected cells. The formula used was as follow where d symbolizes sphere diameter in micrometers (μm), V symbolizes volume of injection in nanoliters (nl) and symbolizes the *pi* value, 3.14. (Hadzhiev et al., 2016).

For Hep3B and SKHep1 cells, approximately 300 cells were injected to 2 dpf *ache*^{sb55} homozygous mutant embryos, *ache*^{sb55} heterozygous embryos and wild-type embryo yolks and the fish were grown until 3 dpi and sacrificed using Tricaine. Each fish embryo was frozen in liquid nitrogen and stored at -80°C for further use.

For MCF-7 breast cancer cells, at the first experimental setting, approximately 600 transiently MR-overexpressing cells were injected to 2 dpf *casper* zebrafish embryo yolks and fluorescent microscopy images were obtained at 3 dpi (5dpf) and each fish embryo were frozen in liquid nitrogen and stored at -80°C for further use. At the second experimental setting, approximately 300 cells were injected to 2 dpf wild type zebrafish embryo yolks and fluorescent microscopy images were obtained at 3 dpi injection (5 dpf) and embryo were using Tricaine, then each fish embryo was frozen in liquid nitrogen and stored at -80°C for further use.

2.2.2.16. Zebrafish DNA extraction

Every single zebrafish embryo was used for DNA extraction and registered as an individual sample for further experimental analysis. The defrosted embryos were transferred to 1.5ml Eppendorf tubes and the E3 media was removed. Next, 200 μl of DNA extraction buffer (100 mM Tris pH 8.2, 10 mM EDTA, 200 mM NaCl and 0.5% SDS) and 2-3 μl of proteinase K (200 μg/ml) were added onto each tube and the tubes were incubated at 55°C overnight. Next, the tubes were placed onto the pre-heated 95°C heat block for 20 minutes. The samples were then centrifuged at 13.000 rpm for 20 minutes at room temperature and the supernatant was carefully removed (~175 μl) and placed into newly labelled Eppendorf tube. Then the same volume of isopropanol was added, and tubes were inverted up and down several times for efficient mixing. The tubes were then centrifuged at 13.000 rpm at 4°C for 25 minutes. No pellet formation was observed due to small sample size. The supernatants were then carefully removed without touching the walls of the Eppendorf tubes and the invisible pellets

were washed with 500-700 µl of 70% EtOH. The samples were then centrifuged at 13.000 rpm at 4°C for 20 minutes. Then the supernatant was discarded very carefully and let for airdry. The invisible pellets were then resuspended with 20 µl of nuclease-free water by washing the sides of the Eppendorf tubes for precise resuspension of the invisible DNA pellet which was qualified and quantified before use.

2.2.2.17. ALU repeat-based human DNA quantification in zebrafish xenografts

ALU repeat-based DNA quantification method was based on the quantification of extracted human cell injected zebrafish DNA by quantifying human DNA and total zebrafish embryo DNA using human-DNA specific ALU primers and a zebrafish housekeeping primer employing qRT-PCR, respectively (Avci et al., 2018). For these experimental setups, ALU primers ALU-F-5'-3' and ALU-R-5'-3- were used for human DNA quantification and *ache* zebrafish primers *ache*-F-5'-3' and *ache*-R-5'-3' were used for zebrafish DNA quantification as a reference model. For each standard DNA qRT-PCR reaction, 5 µl of LightCycler® 480 SYBR Green I Master mix, 2 µl of nuclease free water, 1 µl of 10 µM forward primer of interest, 1 µl of 10 µM forward primer of interest and 1 µl of extracted zebrafish DNA. Mastermix for ALU-primer bearing samples and ache-primer bearing samples were then distributed onto 96 well plates, centrifuges at 2000 rpm for 2 minutes, sealed and run on the Roche 480 I cycler. The samples were then subjected to Tm and Ct analysis. The tm of ache primers was as tm:84 and the tm of ALU primers were accepted as Tm1: 84, Tm2: 90. Initially, the tm analysis was performed and a tm of 89 (+/-1) were taken into consideration as the actual amplicon, the amplicon with a double tm was also taken into consideration wherein the tm was (84+/-2). The Tm of 84(+/-2) alone were not taken into consideration as it was reflecting presence of a dimer. Following the initial tm analysis and elimination of not suitable samples, the –Delta Ct (*ache* Ct- ALU Ct) were then calculated for each registered sample and used for statistical analysis.

2.2.2.18. Use of Image J as an alternative tumor growth quantification method in *casper* zebrafish xenografts

Proliferation assessment on the MR-overexpressing MCF7 bearing zebrafish xenografts were performed by image-based Image J software analysis. The images

taken by the fluorescent microscope DsRed channel and bright field channels were opened using Image J software, the images were converted to 8-bit gray-scale images, the tumor area were selected by using the manual selection and the intensity density, raw intensity value, mean gray value, max gray value and area were recorded. The corrected cell total fluorescence was calculated as CTCT = Integrated density (3 replicates) – (Area of the selection point (3 replicates) x mean fluorescence of background selections (3 replicates)).

2.2.2.19. Statistical analysis

GraphPad Prism 6 was used for statistical software analysis of all the assessment in this thesis. *In vitro* MR expression analysis among ER+ and TNBC breast cancer cell lines was performed by 'unpaired t test with equal SD' selection. Pearson correlation analysis between MR and GR was calculated for entire set of the breast cancer cell lines. *Ex vivo* cDNA array qRT-PCR results was performed using Two-Way ANOVA statistics followed with Sidak's multiple comparisons test comparing each cell mean with the other cell mean of the row where raw was representing either log2 DDCT of ARRAY I or ARRAY II. Normalized MR and GR (-Delta Ct) expressions were used for computing Pearson correlation among their expressions in both arrays. RNA sequencing confirmation qRT-PCR results were statistically analyzed were performed using One-Way ANOVA statistics followed with Tukey's multiple comparison test. *In vitro* MTT cell viability assessments and *in vivo* xenotransplantation experiments were statistically tested using One-Way ANOVA statistics followed with Tukey's multiple comparison test. *In vivo* xenotransplantation correlation analyses were performed by using Pearson correlation.

CHAPTER 3

RESULTS

3.1. Overview of ZenoFishDb v1.1 database

ZenoFishDb v1.1 database, https://konulab.shinyapps.io/zenofishdb/, is designed to house xenotransplantation studies performed in zebrafish (Targen et al., 2020). To our knowledge, ZenoFishDb v1.1 database project is the first-ever database housing intriguing details of xenotransplantation studies in zebrafish. The current version of ZenoFishDb v1.1 specifically houses expertly curated data on the transplantation studies harboring molecularly modified cell injections, stem cell and cancer stem cell injections, patient-derived xenograft models as well as distinguished modified hosts used for engraftment as highlighted in the welcoming page of the ZenoFishDbv1.1 (**Figure 3. 1**).

In the light of this research question, the literature was mined for several keyword searches including 'zebrafish xenograft', 'zebrafish xenotransplant', 'zebrafish xenotransplantation', 'zebrafish xenograft primary cell', 'zebrafish patient derived xenograft', 'zebrafish morpholino', 'zebrafish crispr', 'zebrafish microenvironment' and similar words through NCBI PubMed. This research was performed until November 2019 and the total number of studies with relevant information were summing up to a total number 211 publications and were implemented onto the database.

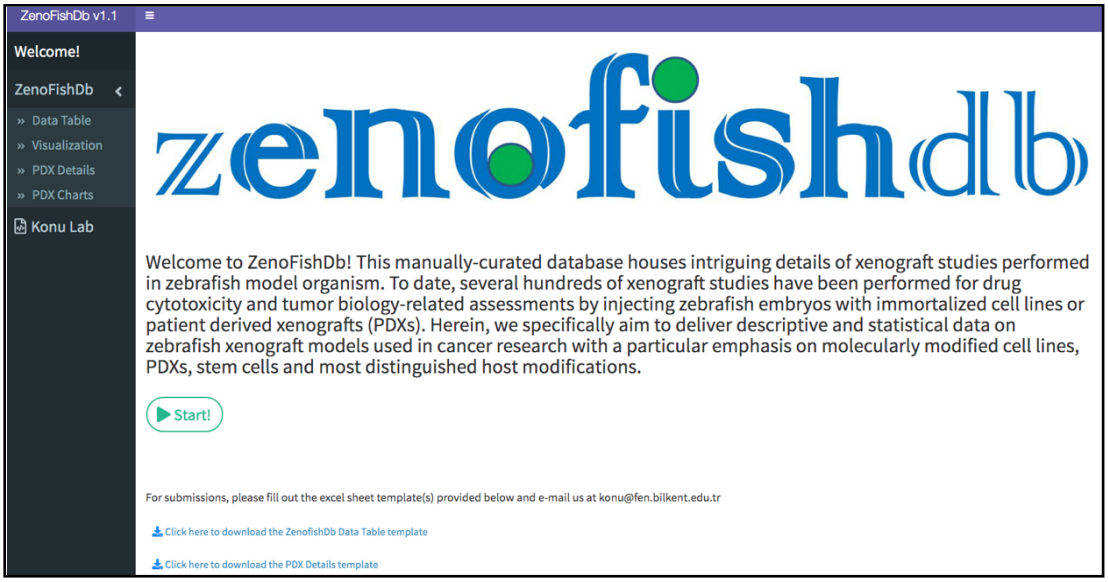

Figure 3. 1 ZenoFishDbv1.1 Homepage. The welcome page highlights the key features of the database and informs the user. On the left, access for Data Table, Visualization, PDX Details and PDX Charts modules are provided. Forms for data submission are also provided on the welcoming page.

(This screenshot image was retrieved from https://konulab.shinyapps.io/zenofishdb/ , (ZenoFishDb v1.1) published as Targen, S., Kaya, T., Avci, M. E., Gunes, D., Keskus, A. G., & Konu, O. (2020). ZenoFishDb v1.1: A Database for Xenotransplantation Studies in Zebrafish. *Zebrafish*. https://doi.org/10.1089/zeb.2020.1869).

3.2. Structure of the ZenoFishDb v1.1.

ZenoFishDb v1.1 database was then organized to deliver and display the mined data through a user-friendly interface that enables data search and visualization through four modules, i.e., *Data Table, Visualization, PDX Details* and *PDX Charts*, as described in methods.

The *Data Table* module was organized to display the implemented data in a table format for all possible 23 attributes as mentioned in the methods in which the publications were initially screened for. The *Data Table* itself enables search through two the attributes selection box (top left) or search box (top right) as depicted below (**Figure 3. 2**). The attributes selection option enables selection of any of the above-mentioned attribute and further refines the search with availability of defined sub-selections. Hence, all the required information can be accessed through *Data Table* search for these attributes.

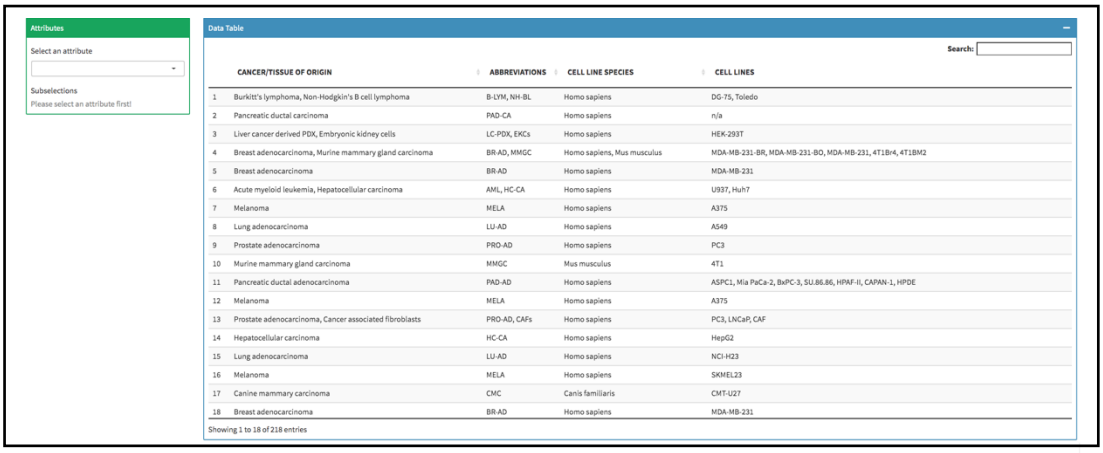

Figure 3. 2 ZenoFishDb v1.1 database displaying the *Data Table* module. The *Data Table* module presents the attributes of the database in the table format, enables search through the attribute search box with possible sub-selections (top left) and the search box (top right).

(This image was adapted from Targen, S., Kaya, T., Avci, M. E., Gunes, D., Keskus, A. G., & Konu, O. (2020). ZenoFishDb v1.1: A Database for Xenotransplantation Studies in Zebrafish. *Zebrafish*. https://doi.org/10.1089/zeb.2020.1869).

The *Visualization* module was designed to exhibit graphical representation as well as statistical information of the implemented data using bar or pie charts . Herein, limited number of attributes (19) were designed to fit in this format as they would also mirror statistical information about the implemented data together with its presence frequencies and percentages. The charts were also designed to be displayed in downloadable table format for clearer representation of the relevant statistical information for the users. Below, the screenshot of the *Visualization* page was used to exemplify the graphical representation of 'cancer type/tissue of origin' attribute using bar chart and 77 unique variables were totally displayed through this whereas a total number of 218 variables were present for this attribute (**Figure 3. 3**). Additionally, the graphical representation could be manually adjusted through the 'Chart height', 'Legend font size (pie chart only)', 'Inside text font size (pie chart only)' and 'Bar plot label size' and users' for optimized visualization of one's interest.

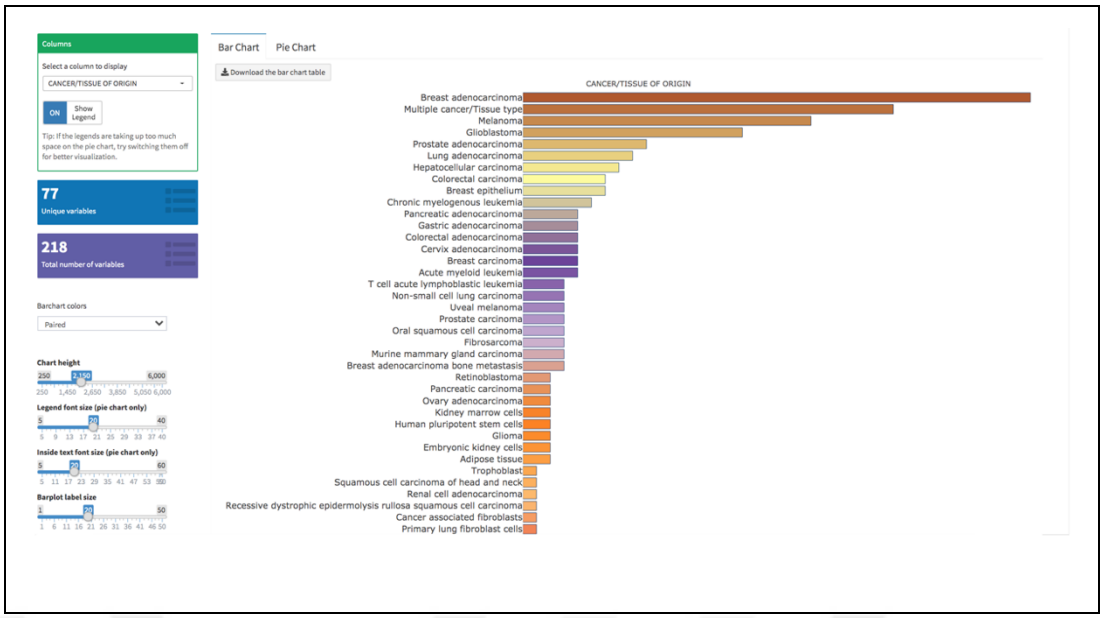

Figure 3. 3 Screenshot of the ZenoFishDb v1.1 *Visualisation* page. The graphical and statistical representation of 'cancer/tissue of origin' attribute is displayed through the *Visualization* page.

(This image was adapted from Targen, S., Kaya, T., Avci, M. E., Gunes, D., Keskus, A. G., & Konu, O. (2020). ZenoFishDb v1.1: A Database for Xenotransplantation Studies in Zebrafish. *Zebrafish*. https://doi.org/10.1089/zeb.2020.1869).

The *PDX Details* and *PDX Charts* modules were established in order to accommodate PDX-associated information of the PDX studies implemented to this database. In fact, *PDX Details page* was used for displaying both patient- tumor- and zebrafish-associated information of zebrafish PDX models in a table format as in the *Data Table* module. A total of 115 patient-derived xenograft models of zebrafish were implemented and the data were displayed through attributes as described in **section 2.1.1**. Herein, attribute-specific search was enabled through attributes selection box (top left) or search box (top right) (**Figure 3. 4**). Furthermore, presence of subselection option enabled further search through individual attribute option of prior choice. PDX Details page, therefore, serves as the first database to identify and accommodate patient-derived xenograft applications in zebrafish model organism.

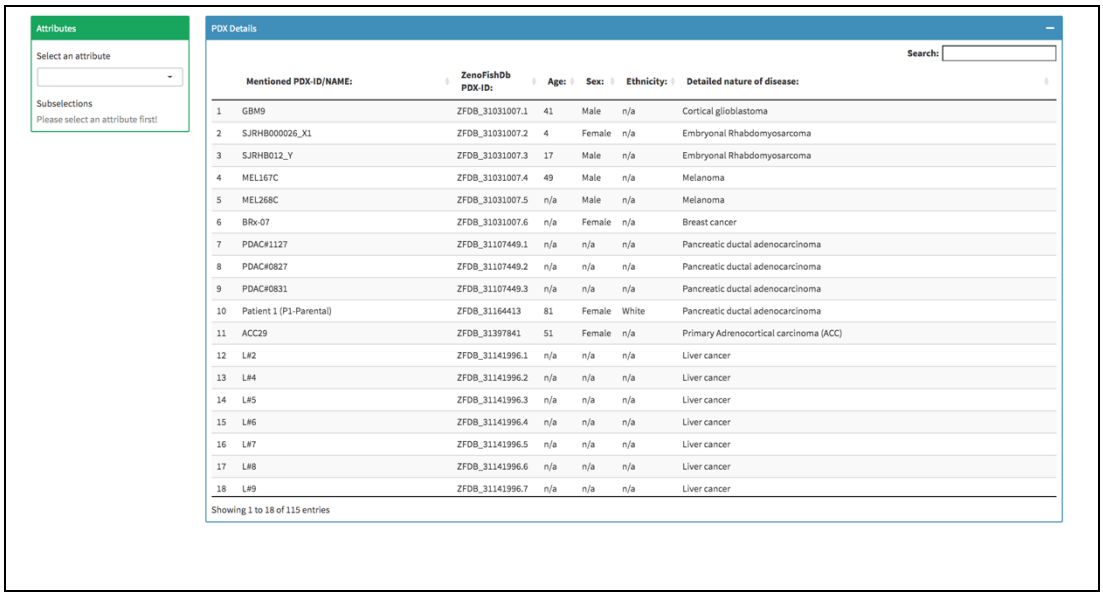

Figure 3. 4 *PDX Details* module displays patient data, tumor data and zebrafish injection details of patient-derived xenografts listed on ZenoFishDb v1.1. The data table format enables search of PDX-associated attributes through attributes option (top left) and search box (top right).

(This image was adapted from Targen, S., Kaya, T., Avci, M. E., Gunes, D., Keskus, A. G., & Konu, O. (2020). ZenoFishDb v1.1: A Database for Xenotransplantation Studies in Zebrafish. *Zebrafish*. https://doi.org/10.1089/zeb.2020.1869).

The *PDX Charts* module was designed to graphically represent and statistically inform the users displaying the data in bar chart format for selected attributes. The attributes available are implemented according to their statistical informativeness and therefore 'Sex', 'Detained nature of disease', 'Primary/Metastatic/Recurrent', 'Zebrafish line', 'PDX-tissue/PDX-cell line', 'Cell number (if available)' and 'Study Author-Date, PMID'. Regarding to these implementation methods, the screenshot of *PDX Charts* with selection of 'Detained nature of disease' was used for exemplification (**Figure 3. 5**). Accordingly, glioblastoma followed by liver and colon cancer were among the most tested PDXs in zebrafish.

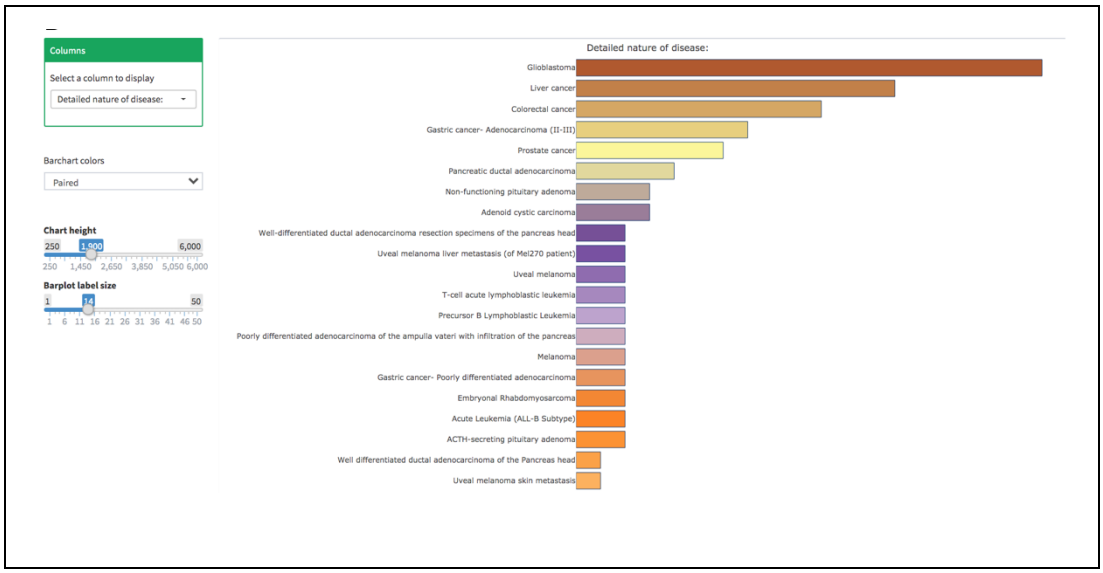

Figure 3. 5 Screenshot of the *PDX Charts* module on ZenoFishDb v1.1. PDX Charts module exhibits graphical and statistical representation of frequently registered attribute, 'Detailed nature of disease'.

(This image was adapted from Targen, S., Kaya, T., Avci, M. E., Gunes, D., Keskus, A. G., & Konu, O. (2020). ZenoFishDb v1.1: A Database for Xenotransplantation Studies in Zebrafish. *Zebrafish*. https://doi.org/10.1089/zeb.2020.1869).

3.3. The cancer and tissue types, cell lines and cell species incorporated onto ZenoFishDb v1.1

ZenoFishDb v1.1 database, accommodating a total number of 211 studies, specifically focuses on the application of molecularly modified cell injections, stem cell injections, cancer stem cell injections and patient-derived primary cell and/or tissue injections as well as the injection applications performed on modified hosts regardless of the injection material. In this database, all these injection materials were initially classified based on their type, i.e. cancer and/or tissue of origin, to illustrate the statistical data based on these implementations. In fact, as shown in **Figure 3. 6** breast adenocarcinoma (BR-AD) (14.74 %) accounted for the majorly studied cancer type and was then followed by multiple cancer/tissue types (MULTIPLE) (10.76%), melanoma (MELA) (8.37%), and glioblastoma (GLIO-B) (6.38%). In line with this finding, MDA-MB-231 breast adenocarcinoma cell line (8.71%) ranked as the top injected cell line which was then followed by another breast adenocarcinoma cell line MCF7 (3.73%), glioblastoma cell line U-87 MG (2.49%) and K562 (2.24%) leukemia cell lines. The cell lines which were categorized by their species revealed that most of

the injection materials, i.e., cells and/or tissues, belonged to human (80.51%), and other species included mouse (14.41%), zebrafish (2.97%), rat (1.27%), goldfish (0.42%) and dog (0.42%)**.**

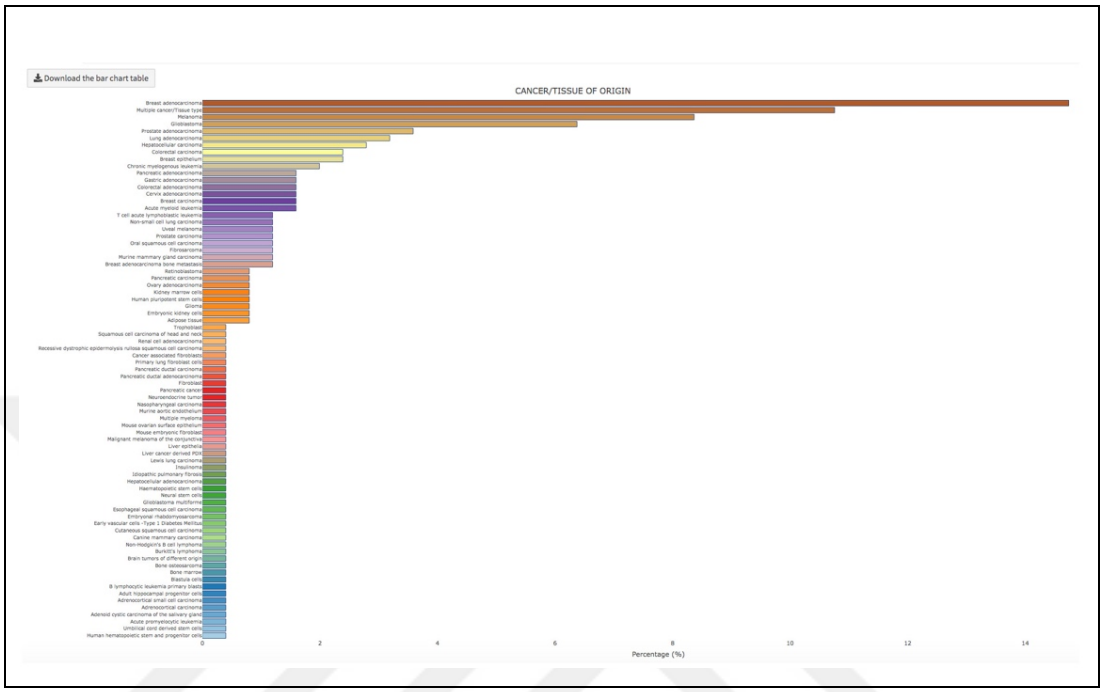

Figure 3. 6 Graphical representation of registered cancer and tissue types on ZenoFishDb v.1.1. The screenshot of the 'cancer/tissue of origin' attribute obtained through the visualization page lists 77 unique variables with their corresponding percentages. The 'download the bar chart table' provides a link for downloadable form for the number of each unique variable as frequency and percentages for this attribute.

(This image was retrieved from https://konulab.shinyapps.io/zenofishdb/ (ZenoFishDbv1.1) published as Targen, S., Kaya, T., Avci, M. E., Gunes, D., Keskus, A. G., & Konu, O. (2020). ZenoFishDb v1.1: A Database for Xenotransplantation Studies in Zebrafish. *Zebrafish*. https://doi.org/10.1089/zeb.2020.1869).

3.4. ZenoFishDb v1.1 houses molecularly-modified cells, stem cells and PDXs as injection materials

Understanding and classifying the nature of zebrafish transplantation materials are of importance for mirroring all types of possible injection procedures to be undertaken for the research community. The current version of ZenoFishDb was established to accommodate zebrafish xenograft models of molecularly modified-cells, stem cells, cancer stem cells and patient-derived xenografts. The molecularly modified cells were

approximately of 76 % of all the incorporated studies. In total, 12 number of different molecular modifications were registered onto the database and among these tag expression vectors accounted for 37.36 %, overexpression vectors accounted for 12.45 %, shRNA accounted for 10.94 %, siRNA accounted for 9.81 %, mutations accounted for 1.13 %, morpholino accounted for 0.76 % and Crispr/Cas9 accounted for 0.38% (**Figure 3. 7**).

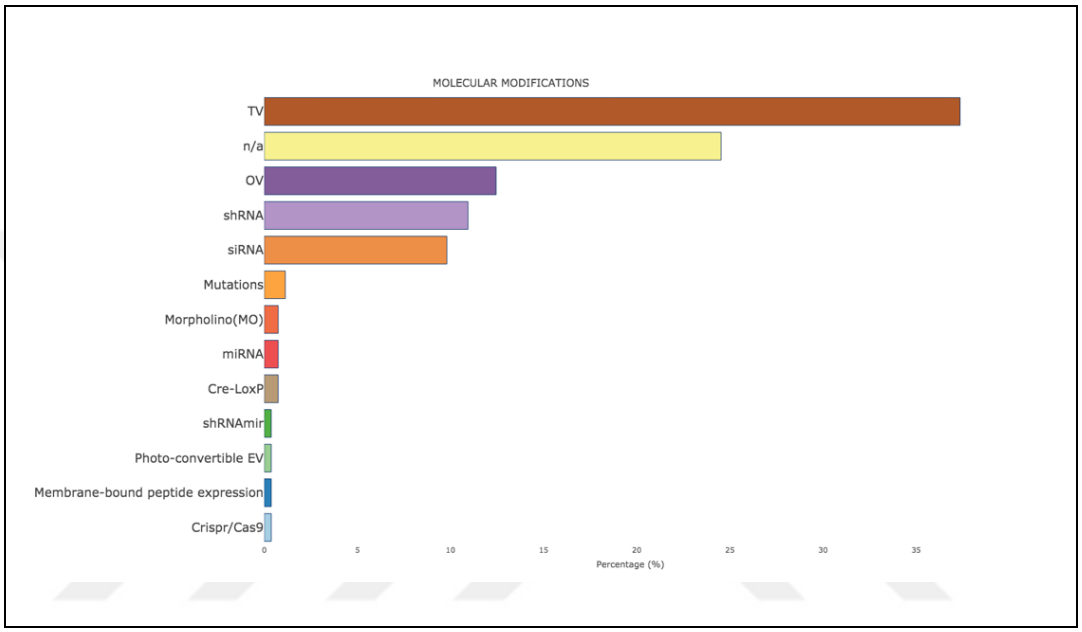

Figure 3. 7 Molecular modifications represented on ZenoFishDb v1.1. A total number of 13 molecular modifications were incorporated onto ZenoFishDb as TV (Tag expression vectors), OV (Overexpression vectors), shRNA (short hairpin RNA), siRNA (silencing RNA), Mutations, Morpholino (MO), miRNA (microRNA), Cre-LoxP, shRNAmir, Photo-convertible expression vector, membrane-bound peptine expression and Crirspr/Cas9.

(This image was adapted from Targen, S., Kaya, T., Avci, M. E., Gunes, D., Keskus, A. G., & Konu, O. (2020). ZenoFishDb v1.1: A Database for Xenotransplantation Studies in Zebrafish. *Zebrafish*. https://doi.org/10.1089/zeb.2020.1869).

PDX studies were also registered onto the current version of the database namely as PDX where patient-derived primary cell lines or patient-derived tissue transplantations were present, and these studies accounted for 13.74 % of all incorporated studies onto ZenoFishDb v1.1

Stem cell (SC) and cancer stem cell (CSC) zebrafish xenografts are signature characteristics of ZenoFishDb v1.1 enabling detailed search of stem-cell specific transplantations and associated bioassessments through the database as well as technical details of xenotransplantation procedures required for stem cell xenograft models. Stem cell and cancer stem cell injections accounted for 16.4 % of all studies and fine tuning of stem cell properties based on their characteristics were also incorporated under the name of stem cell properties. Cancer stem cell injections (5.61%) ranked the top which were followed by leukemia stem cells (LSCs) (1.87%) and neuronal stem cells (NSCs) (1.40%). Yet, injections of hematopoietic stem and progenitor cells, induced pluripotent stem cell injections and mesenchymal stem cells were also among stem-cell featured zebrafish xenograft models listed on ZenoFishDb v1.1 (**Figure 3. 8**).

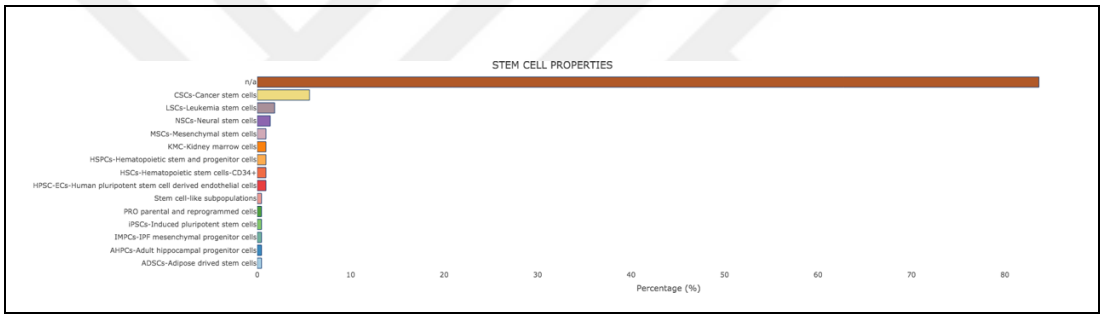

Figure 3. 8 Stem cell properties of stem cell (SC) and cancer stem cell (CSC) xenograft models displayed on ZenoFishDb v1.1. Diverse application of stem cell of any origin was reflected by total number of 14 different zebrafish xenograft model. Yet among all this diversity, cancer stem cell, leukemia stem cell and neuronal stem cell injections accounted for majority zebrafish xenotransplantation studies.

(This image was retrieved from https://konulab.shinyapps.io/zenofishdb/ published as Targen, S., Kaya, T., Avci, M. E., Gunes, D., Keskus, A. G., & Konu, O. (2020). ZenoFishDb v1.1: A Database for Xenotransplantation Studies in Zebrafish. *Zebrafish*. https://doi.org/10.1089/zeb.2020.1869).

3.5. Biological pathway analysis of molecularly modified genes accessible through ZenoFishDb v1.1

ZenoFishDb v1.1 was designed to accommodate molecularly-modified immortalized cell line names and PDXs through the 'molecularly modified cells' as displayed both through the *Data Table* and *Visualization* pages. Additionally, manipulated gene

names were also stated through the 'modified genes' attribute easing the search for users. All the gene names listed on the *Data Table* were, copied and pasted to excel, searched for their human orthologs (when applicable) and run for biological pathway analysis and protein-protein interaction analysis employing GO PANTHER (Mi et al., 2009; P. D. Thomas et al., 2003) and STRING (Szklarczyk et al., 2015, 2019), respectively.

A total of 94 genes were run on GO PANTHER platform and the pathway analysis revealed 202 pathway hits whereas CCKR signaling, inflammation mediated by chemokine and cytokine signaling, integrin signaling, gonadotrophin-releasing hormone receptor, angiogenesis and Ras pathways were among most highlighted pathways (**Figure 3. 9**).

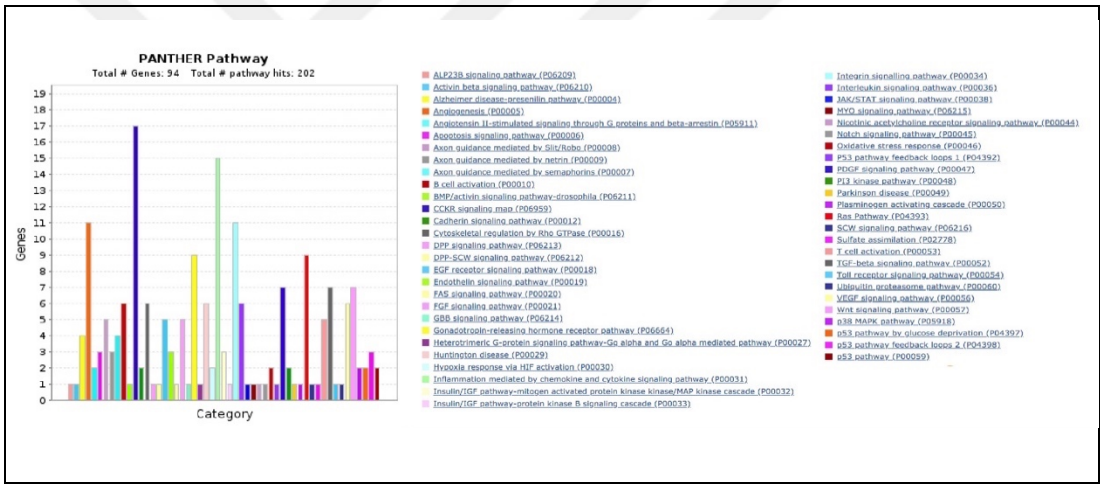

Figure 3. 9 GO PANTHER Pathway analysis of molecularly modified genes. GO PANTHER pathway analysis search for a total of 94 genes reveals 202 pathway hits and displayed the matched number of genes for each categorized pathway.

(This image was adapted from Targen, S., Kaya, T., Avci, M. E., Gunes, D., Keskus, A. G., & Konu, O. (2020). ZenoFishDb v1.1: A Database for Xenotransplantation Studies in Zebrafish. *Zebrafish*. https://doi.org/10.1089/zeb.2020.1869).

The same gene list was then run on the STRING platform in order to illustrate the protein-protein interactions among these proteins for functional enrichment analysis (**Figure 3. 10**) and herein, KEGG Pathways and Reactome Pathways analyses were used as default for pathway identification. KEGG Pathways analysis revealed 106 significant pathway hits; 'pathways in cancer', 'colorectal cancer', 'pancreatic cancer',

'proteoglycans in cancer', 'Kaposi's sarcoma-associated herpesvirus infection' ranking the top five. The Reactome Pathways analyses identified 144 significant hits wherein 'signal transduction', 'interleukin-4 and interleukin-13 signaling', 'developmental biology', 'signaling by receptor kinases' and 'signaling by interleukins' pathways were sitting at the top five.

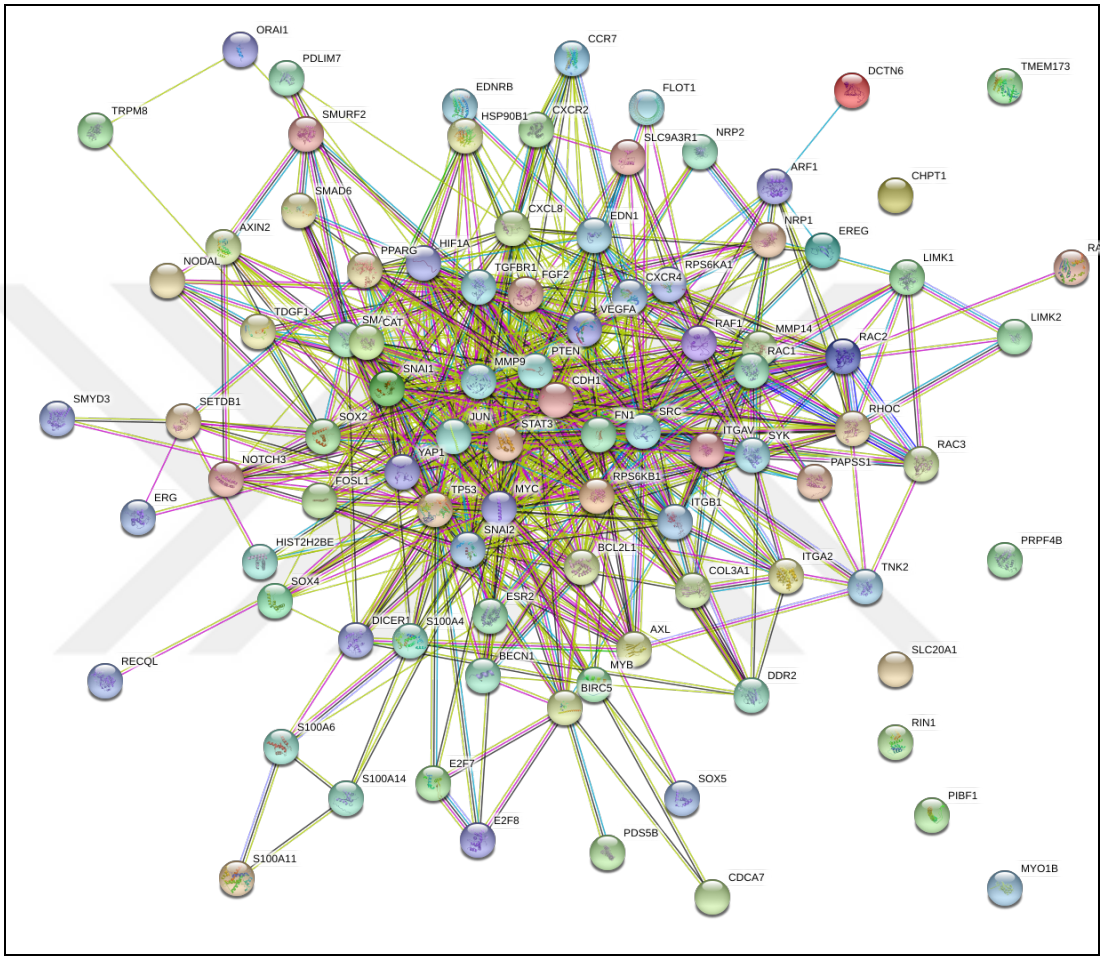

Figure 3. 10 STRING analyses of molecularly-modified genes.

3.6. ZenoFishDb v1.1 reveals biological assessments performed on zebrafish xenograft models

Successful implementation of cell transplantation into zebrafish opened new avenues for feasible biological assessment for cancer research community. From now and then zebrafish xenografts enabled biological assessment of wide range of biological questions. ZenoFishDb v1.1 served as a platform to exhibit all range of assessments performed on engrafted fish through the 'Analyses' attribute that is searchable through both *Data Table* and *Visualization* pages. A search through the *Visualization* page revealed 71 unique variables reflecting the number of 71 different biological assessments incorporated onto the database. Metastasis ranked the highest among all analyses listed and was assessed in 67 different studies representing 15.80% of all biological analyses (**Figure 3. 11**). This finding was followed by tumor growth (11.32%) proliferation (10.61%), invasion (9.67%), angiogenesis (8.73%), migration (7.55%) and dissemination (5.19%) analyses accounting mostly for tumor establishment and metastasis associated analyses. Drug screening and associated analyses were also among many studies presented on the analyses page and these included drug screening (0.47%), drug efficacy (0.47%), drug resistance (0.24%), clinical outcome prediction, exosome drug delivery efficacy (0.24%) and drug delivery (0.24%). In addition, although sparser, analyses such as gene expression, F-actin synthesis, fibrogenicity, regeneration, stemness, stem cell plasticity, differentiation, nitric oxide production were also among many presented through the analysis platform.

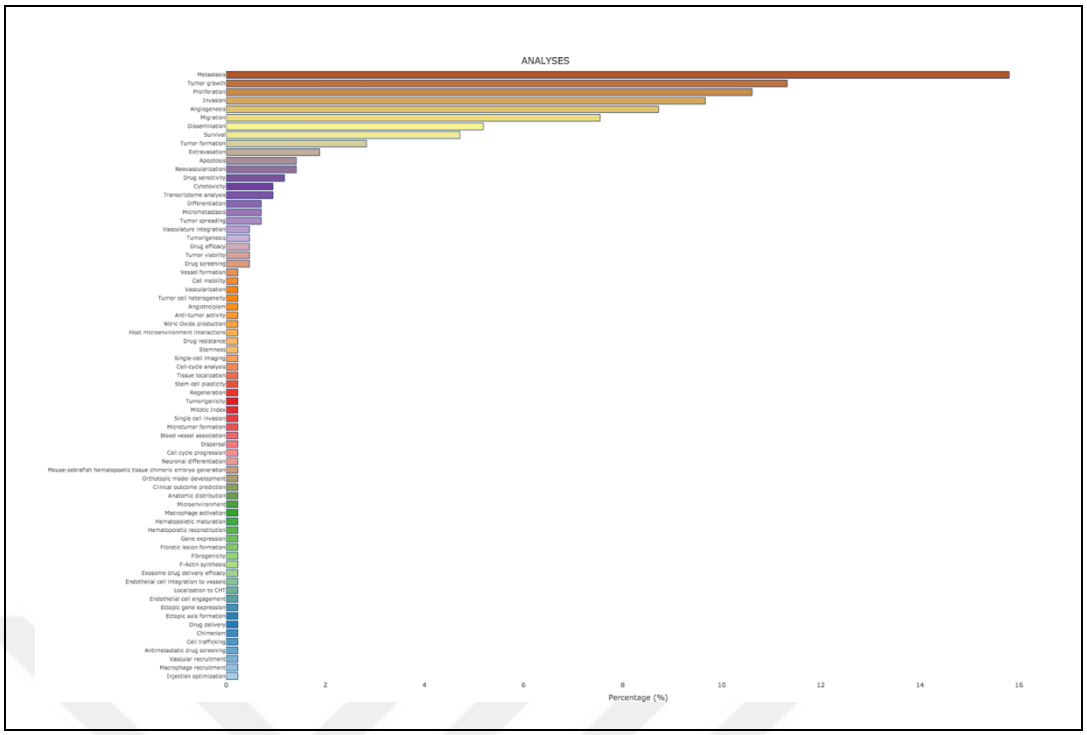

Figure 3. 11 List of biological assessments performed on zebrafish xenograft studies incorporated onto ZenoFishDb v1.1. Seventy-one different biological assessments and their percentages are displayed through the 'analyses' attribute of the *Visualization* page.

(This image was adapted from Targen, S., Kaya, T., Avci, M. E., Gunes, D., Keskus, A. G., & Konu, O. (2020). ZenoFishDb v1.1: A Database for Xenotransplantation Studies in Zebrafish. *Zebrafish*. https://doi.org/10.1089/zeb.2020.1869).

3.7. ZenoFishDb v1.1 identifies most distinguished modified hosts for xenotransplantation studies.

One major criterion of ZenoFishDb v1.1 data implementation was to integrate all the zebrafish xenotransplantation studies with distinguished host modifications. Hence, transgenic zebrafish strains, mutant's zebrafish strains and morphant zebrafish stains were of great interest for the purposes of data delivery to the scientific community. All the host relevant data were gathered and illustrated by two different attributes of the database; 'host modifications' and 'host modification details'. All the host relevant date on the original article were fitted into a common language, by choosing a common name for all available synonyms, and were recorded and explained where applicable by the 'host modification details' attribute. The 'host modifications' attribute then was designed to further refine this information into four categories; 'transgenic', 'mutant',

'morphant' and 'n/a' where n/a was either symbolizing wild-type fish or unavailability of this information. Overall, transgenic fish ranked the highest with a percentage, 55.74%, and was followed by n/a (21.72%), mutant (20.08%), and morphant (2.46%) fish strains (**Figure 3. 12**). Graphical and statistical visualization of host modification details was disabled due to the complex nature of the integrated data on the ZenoFishDb v1.1, however, this data were made accessible through the 'host modifications detail' attribute available through the *Data Table* (**Figure 3. 12**).

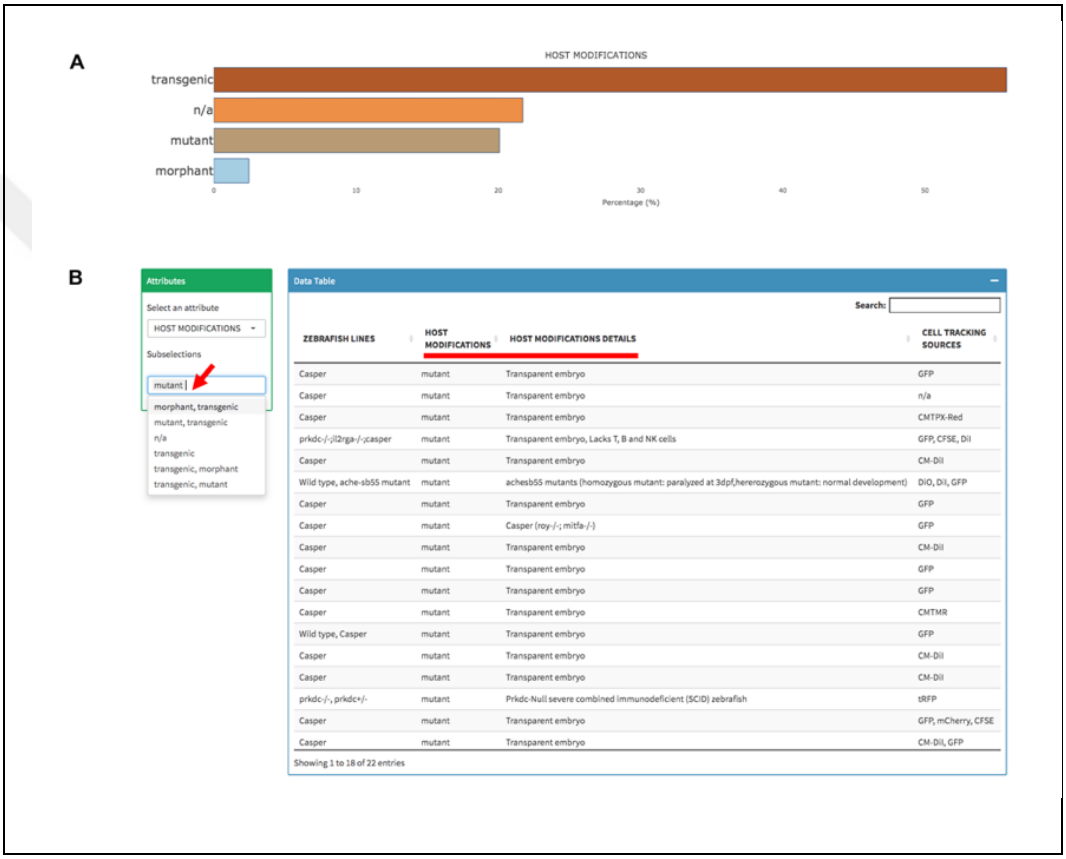

Figure 3. 12 Host modifications and host modification details search through the *Visualization* and *Data Table* modules.

(This image was adapted from Targen, S., Kaya, T., Avci, M. E., Gunes, D., Keskus, A. G., & Konu, O. (2020). ZenoFishDb v1.1: A Database for Xenotransplantation Studies in Zebrafish. *Zebrafish*. https://doi.org/10.1089/zeb.2020.1869).

3.8. ZenoFishDb v1.1 delivers technical details of xenotransplantation procedures

Zebrafish xenotransplantation study design and application requires precision when considering the technical aspects of transplantation procedure. Injection site, location, injected cell numbers and cell tracking sources were of the four attributes to be considered as the technical aspects of engraftment models in fish. These attributes were individually mined and curated for each and every study listed on the ZenoFishDb v1.1. Injection site of fish is often decided by the nature of the biological assessment to be undertaken. For instance, yolk injections are often preferred for assessing proliferation and tumor growth, whereas injections made to duct to Cuvier (J. Cao et al., 2018; Tulotta et al., 2019) or directly to the circulation (Fu et al., 2018; Qinjie Wu et al., 2013) often aims to assess for metastasis-related events. A search through ZenoFishDb v1.1 revealed number of different injection sites for embryo or adult fish transplantations. Yolk sac (37.10%), duct of Cuvier (13.31%) and perivitelline space (20.97%) ranked as the most preferred injection sites among all studies (**Figure 3. 13**).

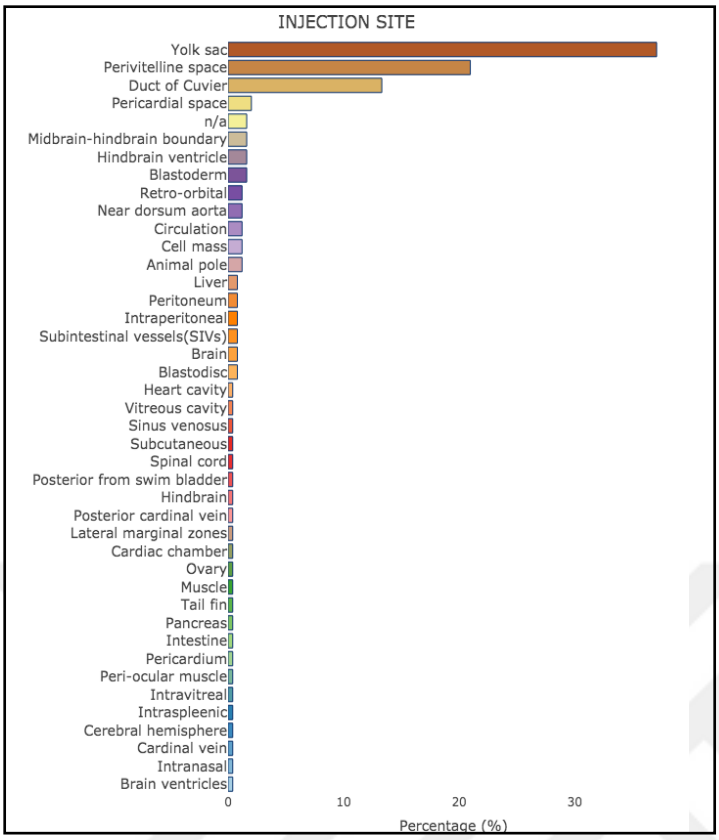

Figure 3. 13 ZenoFishDb v1.1 reveals the injection sites of all zebrafish xenotransplantation studies.

(This image was adapted from Targen, S., Kaya, T., Avci, M. E., Gunes, D., Keskus, A. G., & Konu, O. (2020). ZenoFishDb v1.1: A Database for Xenotransplantation Studies in Zebrafish. *Zebrafish*. https://doi.org/10.1089/zeb.2020.1869).

Injected cell numbers were considered to be another technical aspect to be carefully illustrated through the database. Therefore, the database was designed to implement two attributes labelled as 'injected cell numbers (exact)' and injected cell numbers (categorized)'. The exact injected cell numbers illustrated the exact number of cells and/or formulas as appeared in the original articles and can be visualized through the *Data Table.* The categorized cell numbers, on the other hand, was designed to classify these data among different intervals wherein each cell number was assigned to an appropriate interval for reflecting a statistical value for injected cell numbers. The cell number (n) intervals were as follows ≤ 50, $50<n\leq 200$, $200<n\leq 500$, $500<n<1000$ and ≥ 1000. Majority of the studies had cell injections of $50<n\leq 200$ (39.57%) and $200<n\leq 500$ (28.51%) intervals (**Figure 3. 14**).

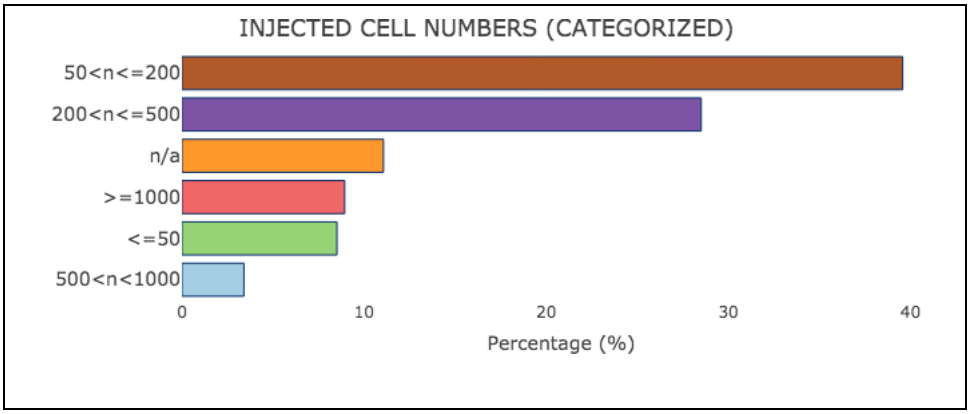

Figure 3. 14 ZenoFishDb v1.1 reveals the categorized injection cell numbers of all zebrafish xenotransplantation studies.

(This image was adapted from Targen, S., Kaya, T., Avci, M. E., Gunes, D., Keskus, A. G., & Konu, O. (2020). ZenoFishDb v1.1: A Database for Xenotransplantation Studies in Zebrafish. *Zebrafish*. https://doi.org/10.1089/zeb.2020.1869).

Time of injection, another technical perspective incorporated to the database, was also of great importance as was highlighting that the majority of the studies injected the fish at 48 hpf (76.85%).

Another technical aspect considered for incorporation onto the database was the cell tracking sources used for visualization and analyses purposes of the injected material. Tag vector expressing, e.g., GFP, RFP or live-dye possessing cells were the kind of applications used for cell tracking purposes in the cells. In fact, majority of the studies used CM-DiI (21.61%) dye for visualization purposes.

3.9. ALU quantification of liver cancer xenografts in zebrafish *ache* mutants is advantageous over imaging

ZenoFishDb v.1.1 indicated that tumor growth is an important parameter to test proliferation of cancer cells in zebrafish (**Figure 3. 11**). However, imaging is cumbersome, takes time and effort and may not be as precise in tumor quantification. Therefore, there is a need for assessing tumor size in a more unbiased manner. Liver cancer cell lines were used in this part of the thesis and human ALU DNA was quantified of cells implanted in ache null mutant (*ache*^{sb55}) and wild-type (wt) siblings. Initially, we have performed an ALU-detection assessment (AluYb8 qPCR) for human

DNA detection ranging from 0.01pg to 10.000pg in the presence of 100ng of zebrafish DNA. Based on the retrieved data points, a dilution curve was generated to test the linearity of the measurement scale (**Figure 3. 15**). Next, a qPCR using primer pairs specific to ALU as well as mutant *ache* and wt alleles was performed. This novel methodology allowed to genotype the fish while quantifying the human DNA in the fish. The data were represented through -DeltaCt plot (**Figure 3. 16**). The findings were in accord with those obtained by fluorescent imaging and quantification yet allowed for testing the heterozygote fish which was not possible by imaging studies since genotyping could not be performed at the same time for recessive phenotypes. Accordingly, mutant fish (*ache* null) had larger tumors when compared with wildtype homozygous or heterozygous siblings suggesting that *ache* depleted hence, acetylcholinesterase accumulated microenvironment could be oncogenic for liver cancer (Avci et al. 2018).

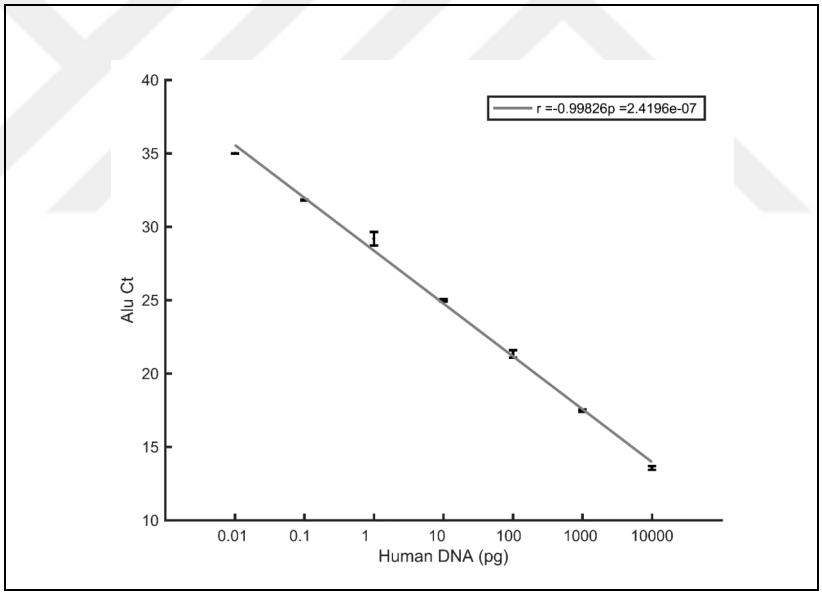

Figure 3. 15 Correlation of Alu Ct and Human DNA (pg) injected in zebrafish model organism. A negative correlation exists among the increased amount of Alu Ct and injected human DNA as stated in picograms (r=-0.99826, p-value=2.4196e-07).

(The image is retrieved from Avci, M. E., Keskus, A. G., Targen, S., Isilak, M. E., Ozturk, M., Atalay, R. C., Adams, M. M., & Konu, O. (2018). Development of a novel zebrafish xenograft model in ache mutants using liver cancer cell lines. *Scientific Reports*, *8*(1), 1570. https://doi.org/10.1038/s41598-018-19817-w).

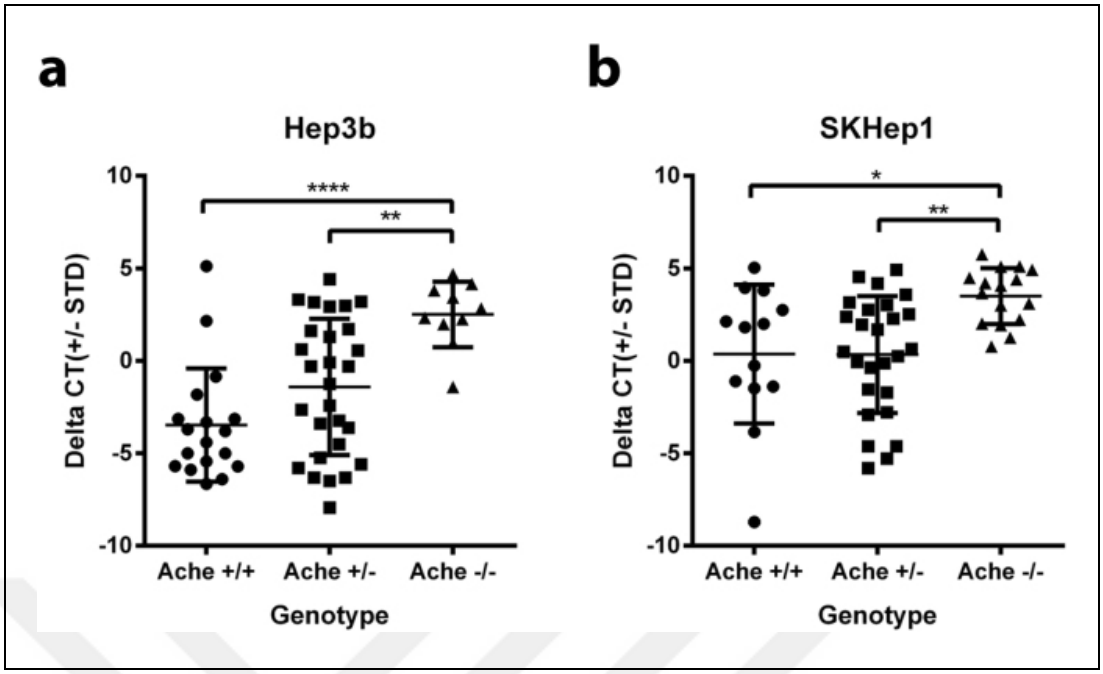

Figure 3. 16 ALU-based tumor proliferation comparison among ache mutant and wildtype fish injected with liver cancer cell lines. **A)** Hep3b cell line-injected fish were genotyped to classify *ache*+/+ (wt) (n=18), *ache*+/- (n=28) and *ache*-/- (n=10). ALU Ct normalized to *ache* Ct, lead classification of tumor DNA presence among these groups exhibiting increased tumor proliferation in *ache*-/- with regard to *ache*+/+ (p=0.0001) and *ache*+/- (p=0.005). **B)** SK-Hep1 cell line-injected fish were genotyped to classify *ache*+/+ (wt) (n=13), *ache*+/- (n=26) and *ache*-/- (n=16). ALU Ct normalized to *ache* Ct, lead classification of tumor DNA presence among these groups exhibiting increased tumor proliferation in *ache*-/- with regard to *ache*+/+ (p=0.017) and *ache*+/- (p=0.004).

(The image is retrieved from Avci, M. E., Keskus, A. G., Targen, S., Isilak, M. E., Ozturk, M., Atalay, R. C., Adams, M. M., & Konu, O. (2018). Development of a novel zebrafish xenograft model in ache mutants using liver cancer cell lines. *Scientific Reports*, *8*(1), 1570. https://doi.org/10.1038/s41598-018-19817-w).

3.10. CASE STUDY: Analysis of MR signaling in breast cancer using *in vitro*, *ex vivo* and *in vivo* models

3.1.1. MR and GR expression in breast cancer cell lines

MR and GR expression were studied across eight breast cancer cell lines covering different molecular subtypes: ZR-75-1, MCF7, T47D (Estrogen positive (ER+) cell lines); BT20, HCC1937, MDA-MB-231, CAL-51 (Triple Negative Breast Cancer (TNBC) cell lines); MDA-MB-453 (HER2 positive (HER2+) (**Figure 3. 17**). At the mRNA level, *MR* was highly expressed in TNBC cell lines based on -Delta Ct values normalized to *TPT1* (-6.610, -9.040, -9.400, -8,265, for MDA-MB-231, HCC1937, BT20 and CAL-51 cell lines, respectively) when compared to ER+ cell lines (-Delta Ct normalized to *TPT1*; -12.345, -11.785, -12.490 for ZR-75-1, MCF7 and T47D cell lines, respectively) (P-Value: 0.0037; Figure not shown). *GR mRNA* exhibited a strongly correlation pattern to MR mRNA among six cell lines (Pearson correlation r:0.9250, P-Value:0.0082 of ZR-75-1, T47D, BT20, HCC1937, MDA-MB-231, MDA-MB-453) with two distinctively dysregulated cell lines MCF7 and CAL-51 (**Figure 3. 17**). At the protein level (Bircan Coban MS Thesis, 2016) (Coban, 2016), high levels of MR protein were detected in mesenchymal-like triple negative cell lines such as CAL-51 and MDA-MB-231. GR, on the other hand, exhibited variable protein levels across, MCF7, T47D BT20, HCC1937, MDA-MB-231, MDA-MB-453 cell lines whereas in CAL-51 and ZR-75-1 cell lines its expression was minute. These findings suggested expression levels of MR and GR resembled each other in differentially classified molecular subtyped breast cancer cell lines. However, there were exceptions suggesting possible dysregulation of receptor expression. Expression profiling of MR in breast cancer cell lines enabled us also to select cell lines with low/no MR levels to be used in overexpression studies.

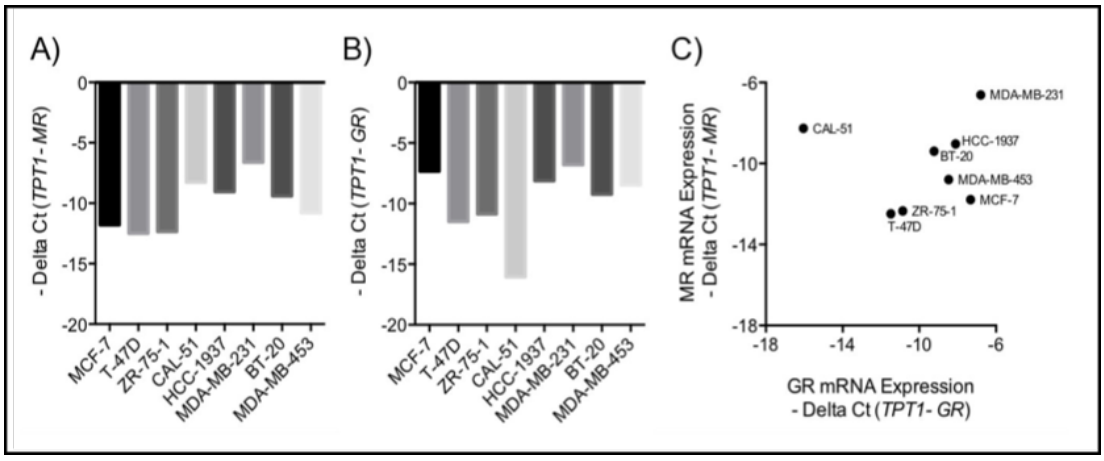

Figure 3. 17 Mineralocorticoid and glucocorticoid expression across breast cancer cell lines. A) MR and **B)** GR mRNA expressions were studied across ZR-75-1, MCF7, T47D (Estrogen positive (ER+) cell lines); BT20, HCC1937, MDA-MB-231, CAL-51 (Triple Negative Breast Cancer (TNBC) cell lines); MDA-MB-453 (HER2 positive (HER2+). **C)** Pearson correlation of MR and GR has been studied across these eight cell lines correspond to r:0.05646, P-value:0.8944 yet when this finding reverted to significant (P-value: 0.0082) with an r of 0.9250 when dysregulated cell lines (MCF7 and CAL-51) were excluded.

3.1.2. MR and GR expression in breast cancer tissue on *ex vivo* cDNA panel

MR and GR expression were also studied in normal breast- and breast cancer tissue-derived cDNA embedded *ex vivo* arrays; TissueScan™ ORIGENE Array I-BCRT101 and Array II-BCRT102. Array I- BCRT101 harboring 7 normal and 41 diseased-breast and 5 normal and 40 diseased-breast working samples, respectively. In fact, Array I and Array II differed among each other by the number of patient samples belonging to different molecular subtype groups. Array I and Array II have been individually analyzed for revealing relative MR and GR expressions and statistical analysis were performed on log2 MR and GR relative expression fold change performing repeated-measures Two-Way ANOVA statistics followed by Sidak's multiple comparisons test. Statistics for MR expression data among normal and tumor-derived cDNAs of Array I and Array II did not exhibit any difference among the two arrays yet, a significant difference was detected among normal and tumor samples in Array II, MR being downregulated in tumor samples (Interaction P-value:0.3570, Row factor P-value:0.3570 and Column factor:0.0011) (**Figure 3. 18**). Glucocorticoid receptor expression data statistics however, revealed no significant differences among the two

arrays or among the test groups of each array although normal vs. tumor difference approached significance (Interaction P-value:0.4145, Row factor P-value:0.4145 and Column factor:0.0677) (**Figure 3. 18**). Additionally, correlation of MR and GR was also studied across these arrays. Accordingly, MR and GR expressions normalized to the reference gene results, were reflected as -delta Ct, were used for Pearson correlation analysis in both Array I and II for a total number of 88 matching samples out of which 12 were normal breast-derived and 76 were cancer tissue derived cDNA samples. MR and GR expressions, hence, depicted a significantly positive correlation among these samples (r:0.3269, P-value:0.0019).

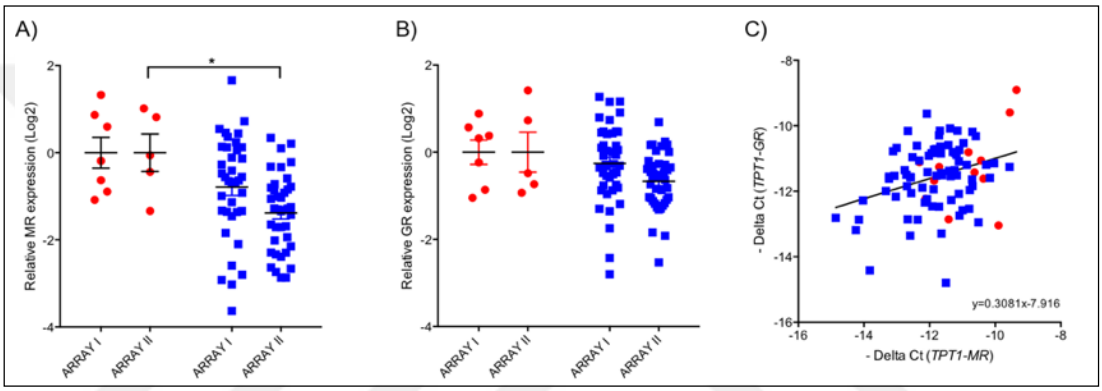

Figure 3. 18 MR and GR mRNA expression in *ex vivo* breast cancer cDNA arrays. **A)** MR expression is significantly downregulated in breast tumors of Array II. **B)** GR expression did not exhibit any difference among normal and tumor samples. **C)** MR and GR expression significantly correlates in breast cancer tumors and normal breast samples (r:0.3269, P-value:0.0019).

3.1.3. *In silico* analysis of MR and GR expression

The Cancer Genome Atlas (TCGA) platform provides vast number of patient gene expression data and enables gene expression analysis of any gene of interest based on inquiry. Cbioportal.org (Cerami et al., 2012) plot function was used to assess the correlation of expression between MR and GR (n =994) based on RNAseq-Illumina_HiSeq platforms of TCGA PanCan dataset with complete case set samples option; and MR(NR3C2) and GR(NR3C1) exhibited a moderate yet highly significant correlation in a cohort of invasive breast carcinoma samples (Spearman correlation, r: 0.46, P-value:1.49e-52; Pearson correlation, r:0.42, P-value:2.13e-44).

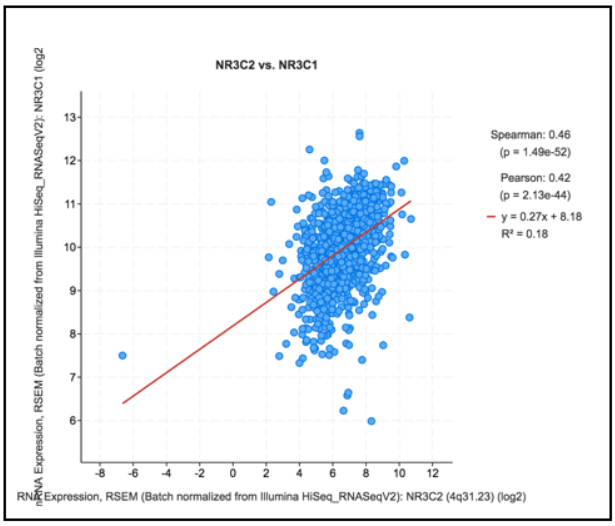

Figure 3. 19 MR and GR are co-expressed in breast cancer tissue. MR and GR mRNA expressions are significantly correlated aa cohort of 994 TCGA invasive breast carcinoma complete dataset (Spearman correlation, r: 0.46, P-value:1.49e-52; Pearson correlation, r:0.42, P-value:2.13e-44).

3.1.4. Survival analysis based on MR and GR expressions on two different platforms: GEPIA and KM-Plotter

3.1.4.1. Survival analysis of MR and GR expression by GEPIA

MR expression in breast cancer patients and their association with overall survival (OS) were identified using GEPIA (Konu & Targen, 2019). Herein, the study was expanded to test the association of both MR and GR expressions with OS and disease-free survival (RFS) in breast cancer. Mineralocorticoid receptor expression was classified as high MR expressing patients (n=533) and low MR expressing patients (n=535) by median and high MR expression was shown to be associated with better overall survival (Log-rank test p=0.027, HR=0.69, pHR=0.028) (**Figure 3. 20**). The RFS and MR expression stratification, by these parameters, did not reveal any significant association (Log-rank test p=0.1, HR=0.73, pHR=0.11). GR expression was also classified as high GR expressing patients (n=535) and low GR expressing patients (n=535) by median. No association was found neither with overall survival (Log-rank test p=0.93, HR=0.99, pHR=0.93) nor disease free survival (Log-rank test p=0.13, HR=0.75, pHR=0.13) based on these parameters (**Figure 3. 20).**

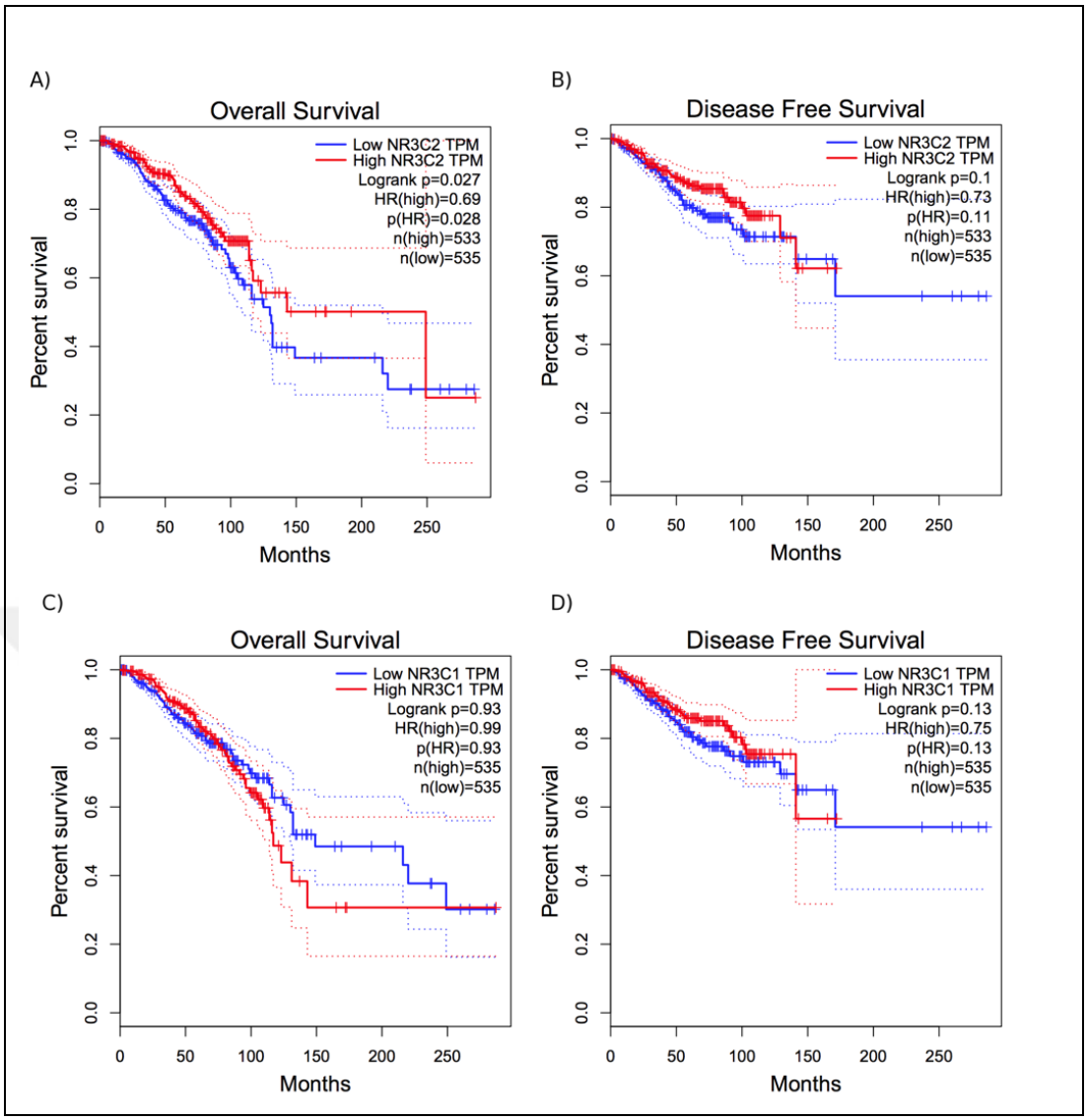

Figure 3. 20 Kaplan-Meier plots illustrating survival graphs of MR and GR in breast cancer. A) MR-Overall survival **B)** MR-Disease free survival **C)** GR-Overall survival **D)** GR-Disease free survival.

(The image was adapted from 2019 Konu, O., & Targen, S. Investigating the Role of Mineralocorticoid Receptor Signaling in Cancer Biology in the Genomic Era. In *Aldosterone-Mineralocorticoid Receptor - Cell Biology to Translational Medicine*. Licence: CC BY-NC 4.0 license for Monograph. https://doi.org/10.5772/intechopen.87233).

3.1.4.2. Survival analysis of MR and GR receptor expressions using KM Plotter

For the interest of this thesis, intrinsic subtypes classified as basal, luminal A, luminal B and HER2+, and their association with stratified MR and GR expression in regard to overall survival (OS) and relapse free survival (RFS) were examined by the microarray platform option where applicable.

Initially, OS and RSF and MR expression was studied across all breast cancer data without any categorization of the data. Stratification of MR expression did not reveal any significant association with OS yet, high MR expression was found to be associated with better RFS (HR=0.77 (0.69-0.86), logrank P=1.7e-06 (**Figure 3. 21**). Intrinsic subtype-based RFS analysis of MR revealed significant association among high MR expression and better relapse free survival in luminal A subtype (HR=0.66 (0.56-0.79), logrank P=3e-06) wherein in luminal B subtype, although approaching significance, this profile was no longer detected (HR=0.85, (0.7-1.03), logrank P=0.098). MR expression was not found to be associated with RFS in basal and HER2+ intrinsic subtypes.

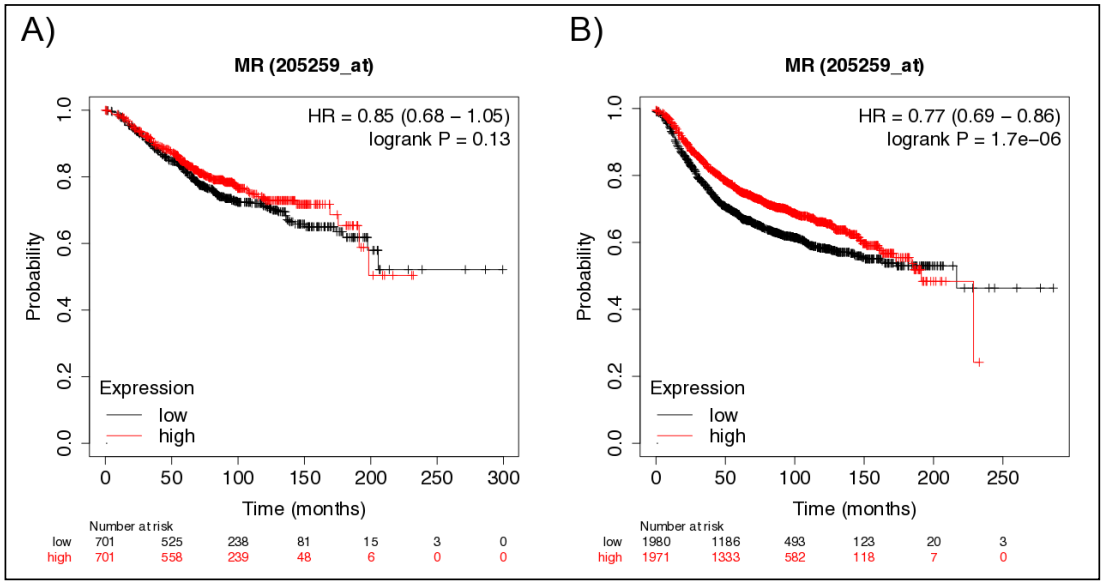

Figure 3. 21 KM Plotter microarray-based overall survival (OS) and relapse free survival (RFS) analysis for MR in breast cancer patients. A) MR - Overall survival **B)** MR- Relapse free survival.

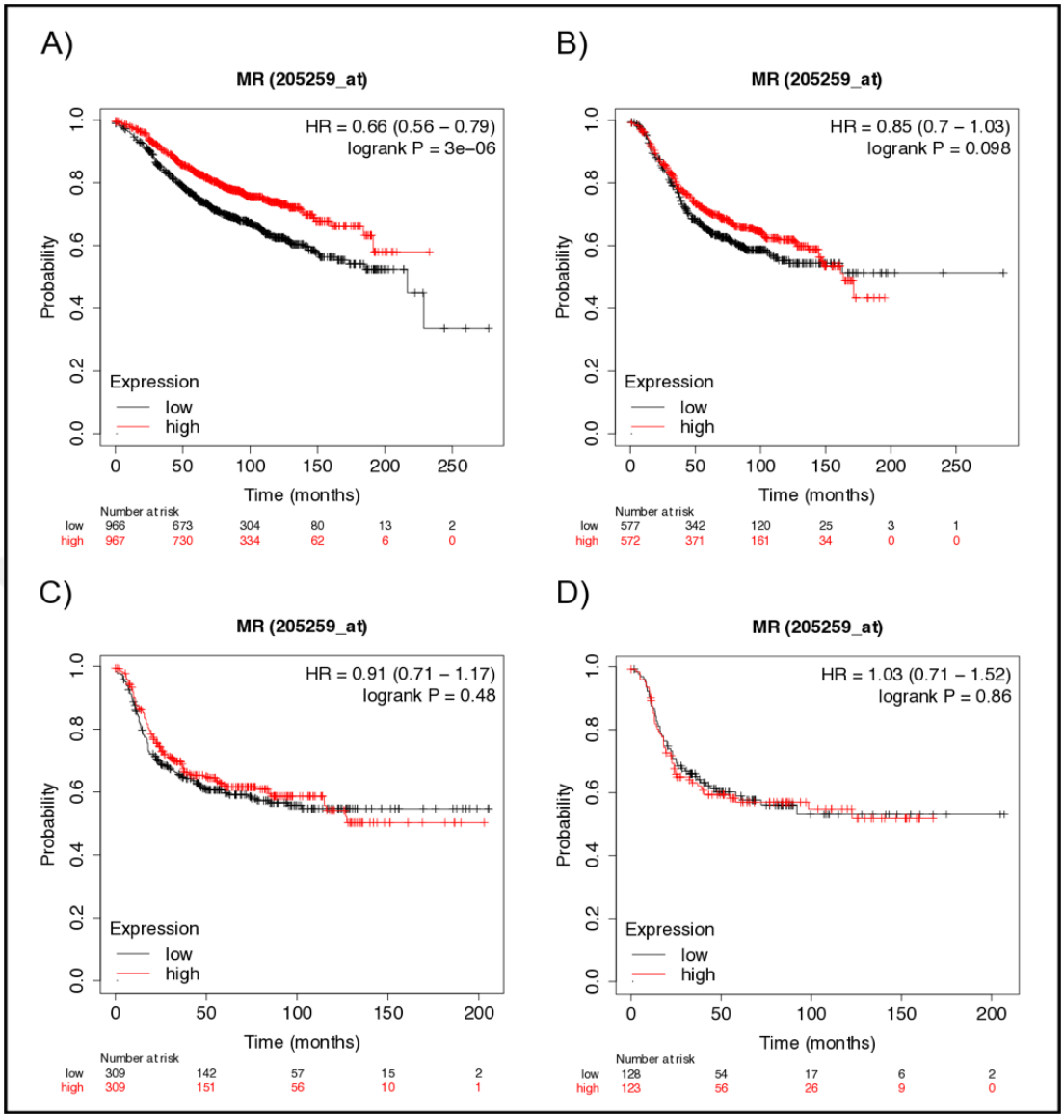

Figure 3. 22 Association of stratified MR expression and RFS across intrinsic subtypes of breast cancer. **A)** Luminal A subtype **B)** Luminal B subtype **C)** Basal subtype **D)** HER2+ subtype

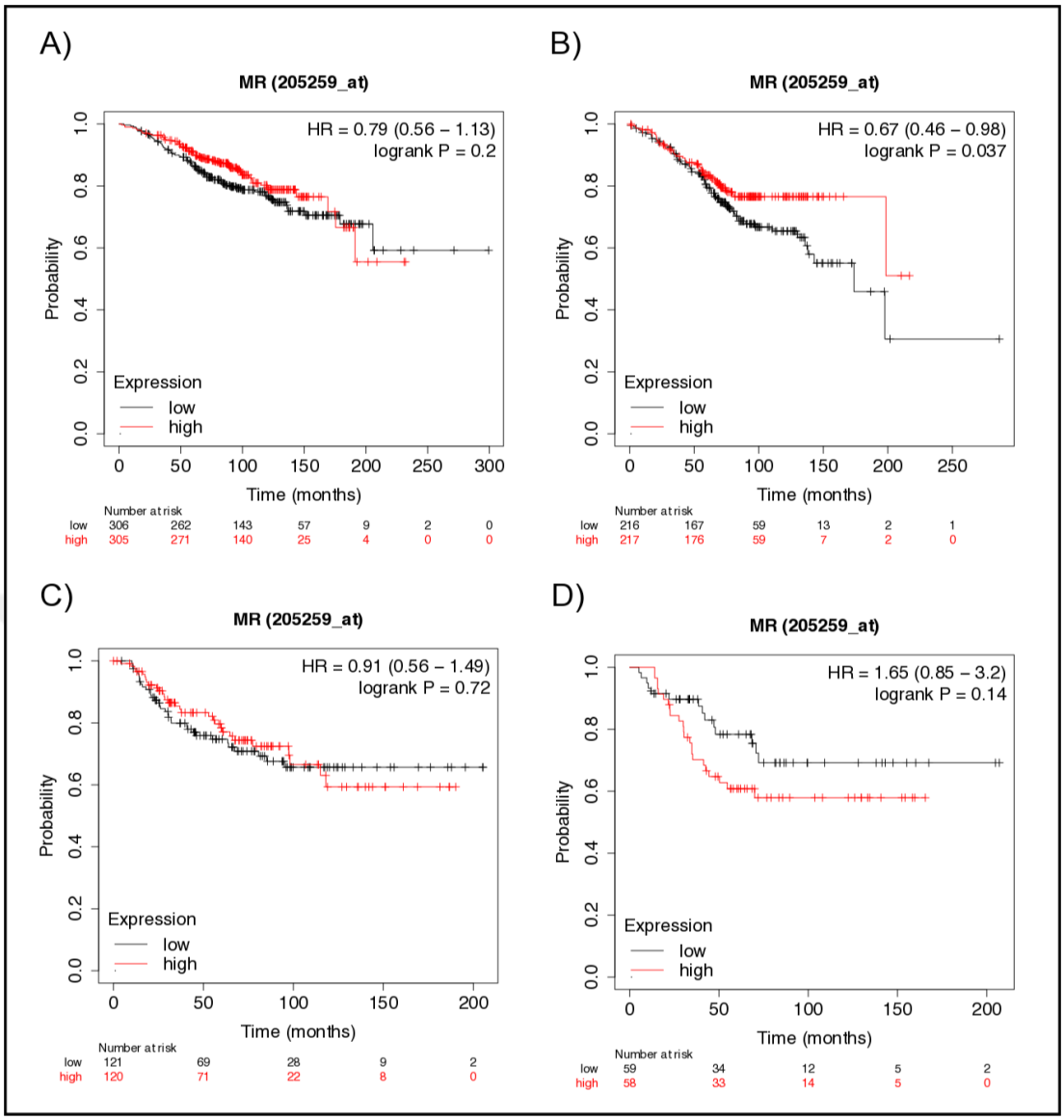

Figure 3. 23 Association of stratified MR expression and OS across intrinsic subtypes of breast cancer. A) Luminal A subtype **B)** Luminal B subtype **C)** Basal subtype **D)** HER2+ subtype.

GR, when expressed high, was associated with better overall survival in breast cancer patients (HR= 0.78(0.63-0.96), logrank P=0.02). Yet, assessment of association among RFS and GR expression, however, was not significant (**Figure 3. 24).** Assessment of intrinsic subtypes showed that low GR expression was associated with better RFS in basal subtype (HR=1.35(1.04-1.73), logrank P=0.021) yet no other significant association were detected among GR expression and RFS in luminal A, luminal B, and HER2+ subtypes. Assessment of intrinsic subtypes by terms of OS, revealed that high GR expression was associated with better overall survival in luminal B subtype and also, low expression was associated with better overall survival in basal subtype. No association among GR expression stratification and luminal A or HER2+ and overall survival prediction was identified.

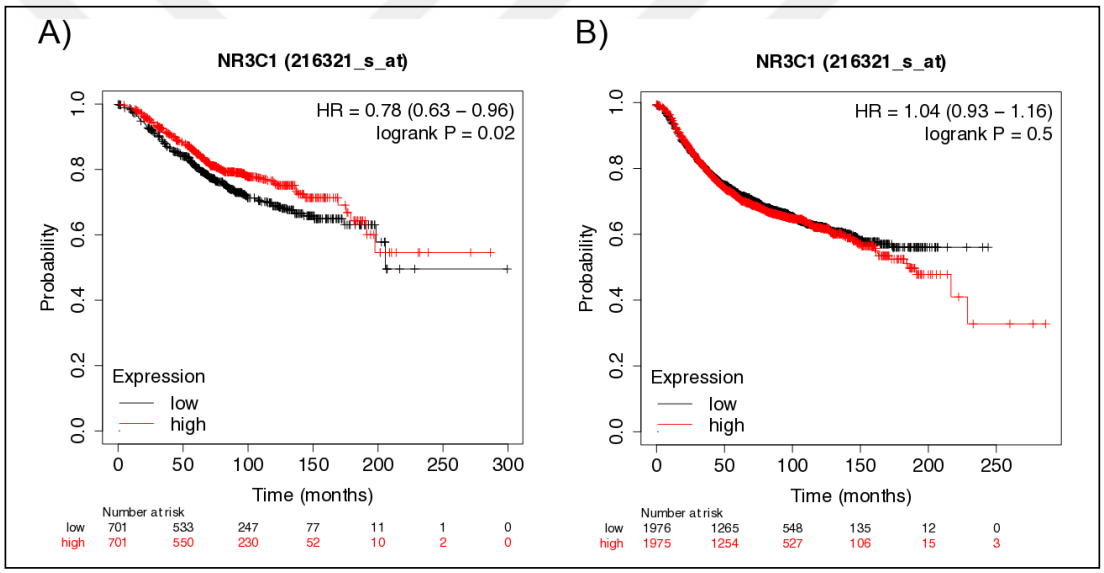

Figure 3. 24 KM-Plotter microarray-based overall survival (OS) and relapse free survival (RFS) analysis for GR in breast cancer patients. A) GR - Overall survival **B)** GR- Relapse free survival.

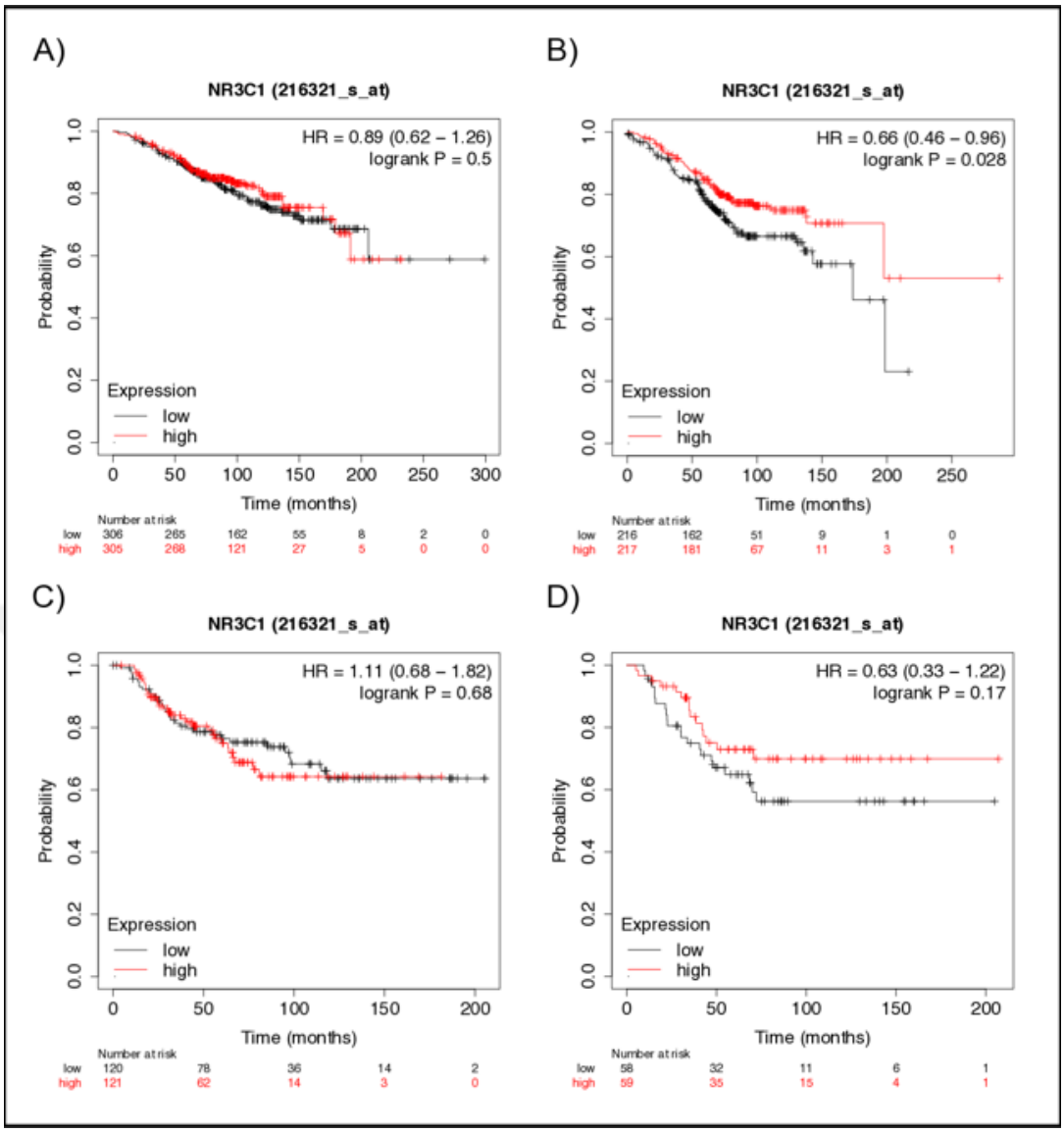

Figure 3. 25 Association of stratified GR expression and OS across intrinsic subtypes of breast cancer. A) Luminal A subtype **B)** Luminal B subtype **C)** Basal subtype **D)** HER2+ subtype

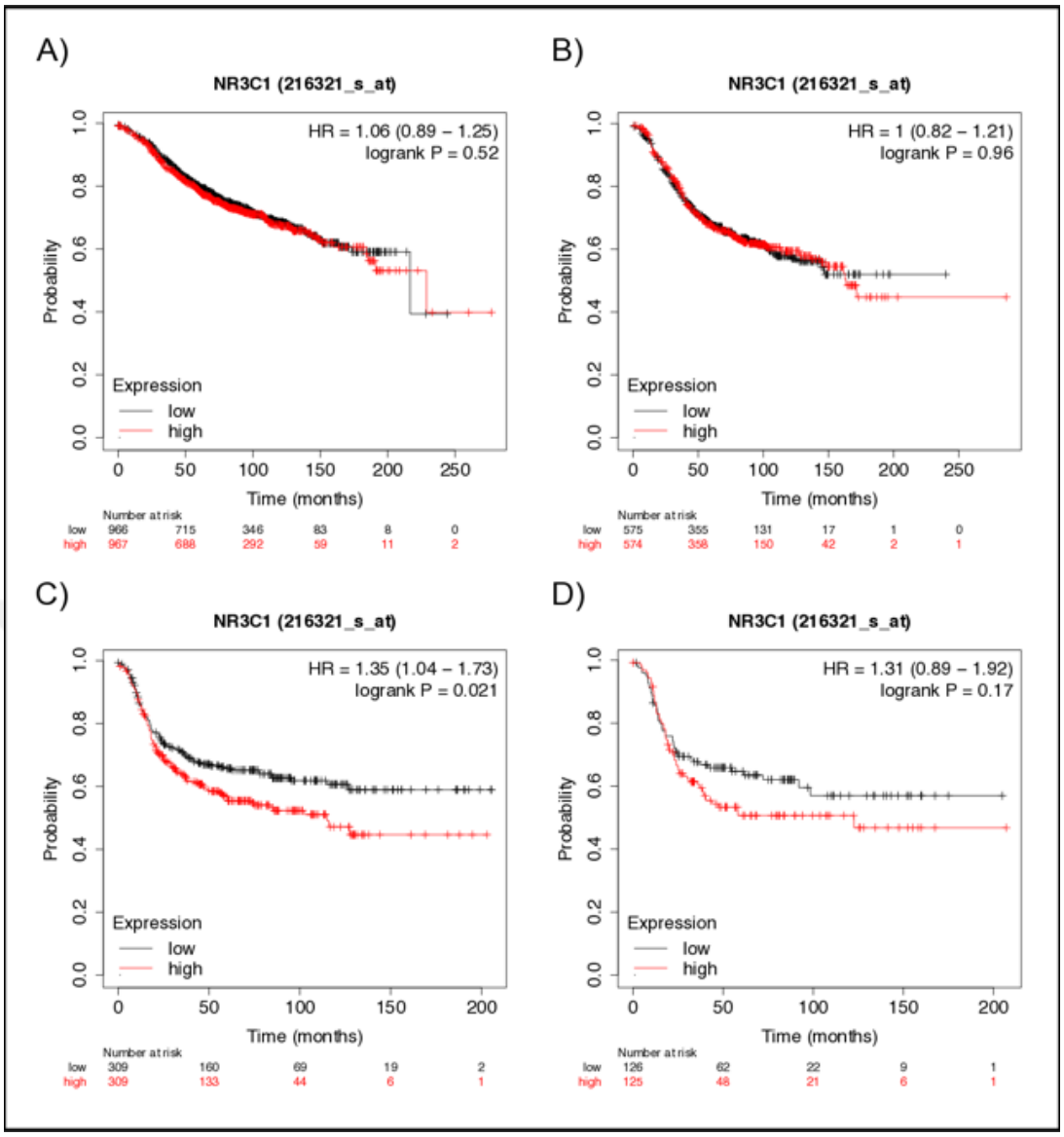

Figure 3. 26 Association of stratified GR expression and RFS across intrinsic subtypes of breast cancer. A) Luminal A subtype **B)** Luminal B subtype **C)** Basal subtype **D)** HER2+ subtype.

3.1.5. Establishment and whole transcriptome analysis of MR-overexpressing ZR-75-1 and MCF7 cell lines in the presence or absence of Aldosterone and/or Spironolactone

MR expression in MCF-7 and ZR-75-1 cell lines are very minute at protein level (Coban, 2016). I have found that mRNA expression was also at the lower end across the cancer cell line panel we used. In order to decipher how presence of MR in the absence/presence of its well-established agonist, aldosterone (ALDO) and/or antagonist, spironolactone (SPIRO) affects entire transcriptome in breast cancer cell lines, an MR-overexpression mimicking approach was adopted in both of these cell lines. Hence, MR was successfully overexpressed in MCF-7 and ZR-75-1 cell lines and the transiently MR-overexpressing MCF-7 and ZR-75-1 cells were treated with ALDO and/or SPIRO for 24 h for deciphering the late response genes and/or activated pathways in the transcriptome. In this experimental setting, initially, overexpression of MR of both MCF-7 and ZR-75-1 cell lines were confirmed at mRNA levels (**Figure 3. 27**).

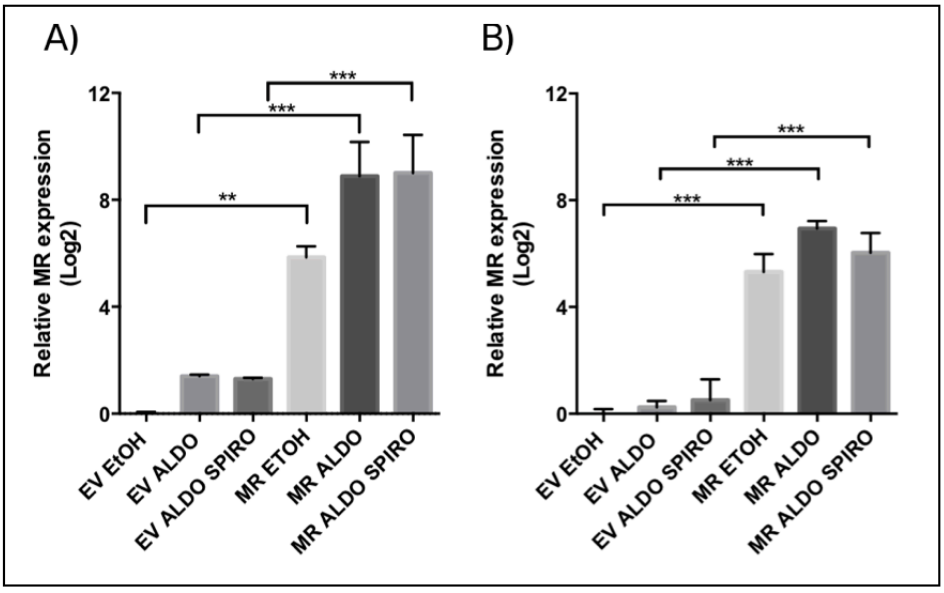

Figure 3. 27 MR overexpression model in breast cancer cell lines. A) In MCF-7 cell line, MR is significantly overexpressed in MR-Stag-pcDNA3.1 (MR) vector treated groups when compared to pcDNA3.1 (EV) vector treated groups regardless of presence of ALDO and/or SPIRO. **B)** In ZR-75-1 cell line, MR is significantly over expressed in MR-Stag-pcDNA3.1 (MR) vector treated groups when compared to pcDNA3.1 (EV) vector treated groups regardless of presence of ALDO and/or SPIRO (**: $p<0.01$, ***: $p<0.001$, ****: $p<0.0001$; data was shown as the mean ± standard deviation (SD).

3.1.6. RNAseq expression profiling and Principal Component Analysis show MR overexpression with or without ALDO alter cell transcriptome

RNA sequencing of the aforementioned experimental groups was performed and PCA analysis were performed for both cell lines showing the association among the treatments within the same experimental group shown solely for the MCF7 experimental set up as well as between the different experimental groups, e.g., MCF7 and ZR-75-1 experimental set up treatment samples. PCA performed for MR-overexpressing MCF7 cell lines in the presence of ALDO and/or SPIRO was shown (**Figure 3. 28**). In order to compare, the association among the MR-overexpressing and ALDO treated cell lines as well as control treated cell lines another PCA was performed between the MCF7 and ZR-75-1 cell lines subjected to the treatments. Herein, as ZR-75-1 only had the MR-overexpression (OV) and MR-overexpression ALDO (OVAL) group (treatment groups) as well as Empty vector (EV) and Empty vector ALDO group (control groups). PCA analysis were only performed among these two groups, separately for reflecting a more detailed picture of variance among variables. Graphical representation of the PCA analysis were shown (**Figure 3. 29**) for the treatment groups (A) and control groups (B).

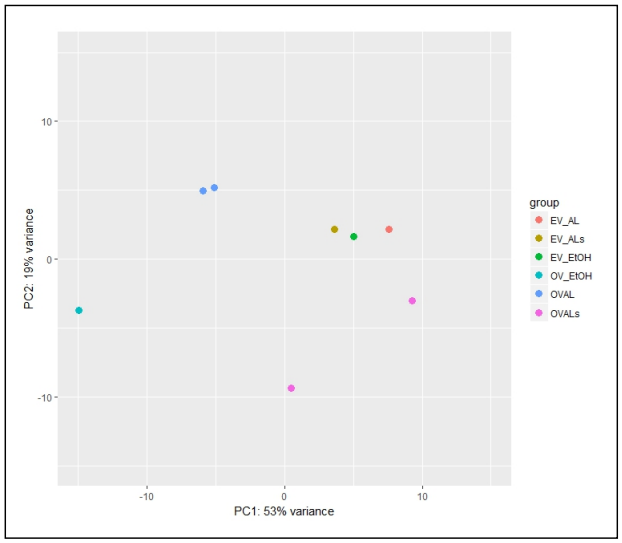

Figure 3. 28 Principal component analysis of MR-overexpressing MFC7 cell lines in the presence of aldosterone and/or spironolactone. The groups represented in the PCA graph and the number of the studies samples were as follows; MCF7-MR-Ovex (OV_ETOH) (n=1), MCF7-MR-Ovex-ALDO (OVAL) (n=2), MCF7-Ovex-ALDOSPIRO (OVALs) (n=2), MCF7-EV (EV_ETOH) (n=1) and MCF7-EV-ALDO (EV_AL) (n=1), MCF7-EV-ALDOSPIRO (EV_ALs) (n=1).

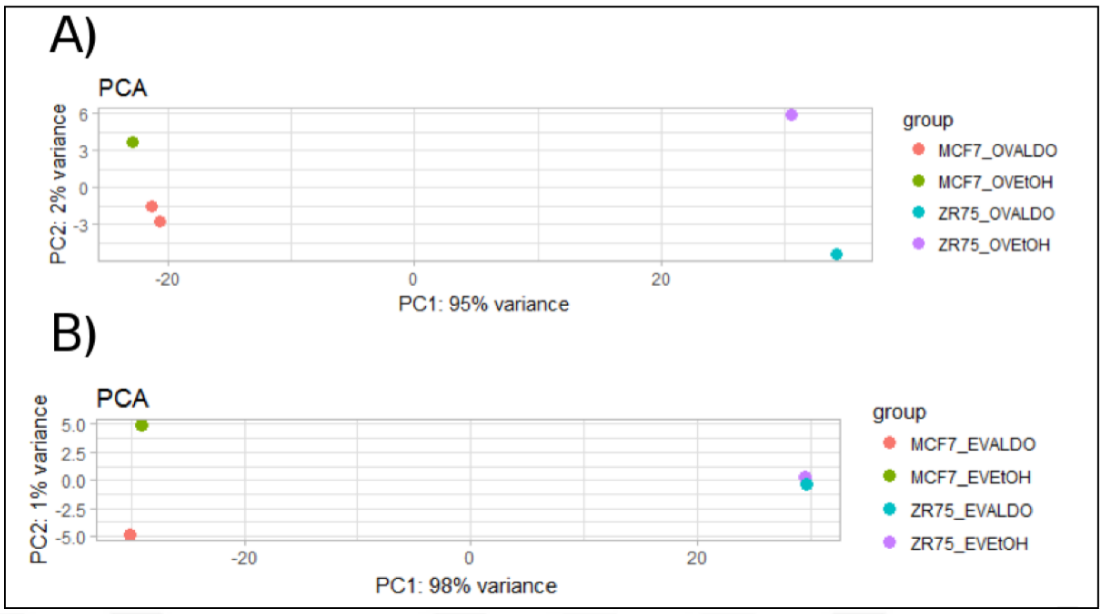

Figure 3. 29 Principal component analysis of MR-overexpressing MFC7 and ZR-75-1 cell lines in the presence and absence of aldosterone. **A)** The groups represented in the PCA graph includes MCF7-MR-Ovex (MCF7_OVETOH) (n=1), MCF7-MR-Ovex-ALDO (MCF7_OVALO) (n=2), ZR-75-1-MR-Ovex (ZR75_OVETOH) (n=1), ZR-75-1-MR-Ovex-ALDO (ZR75_OVALDO) (n=1). **B)** The groups represented in the PCA graph includes ZR-75-1-EV (ZR75_EVETOH) (n=1), ZR-75-1-EV-ALDO (ZR75_ALDO) (n=1), MCF7-EV (MCF7_EVETOH) (n=1), and MCF7-EV-ALDO (MCF7_EVALDO) (n=1).

In **Figure 3. 29**, PCA showed that in both MCF7 and ZR-75-1, the effect of ALDO on MR-overexpressing cells could be seen across PC2 where 2 percent of the variation was explained while these two cell lines were rather distinct in their expression. Interestingly, the direction of change from OVEtOH to OVALDO was the same for MCF7 and ZR-75-1 suggesting that they were affected similarly by the same treatment. On the other hand, PCA for EVEtOH vs. EVALDO showed differences; ALDO had no effect in ZR-75-1 when MR was not overexpressed while MCF7 exhibited a modulation although less in magnitude when compared with that in OV plot (1% vs 2% of variation on PC). This suggested that overexpression of MR alone and in the absence of ALDO, resulted in significant modulation of expression in both cell lines when compared with naïve ones.

Following PCA, known target genes of MR, e.g., ZBTB16, PER1 and SGK1 genes were tested on the treatment groups in MCF7 and ZR-75-1 cell lines for assessing their

alterations and validation of RNAseq results by qRT-PCR (**Figure 3. 30** and **Figure 3. 31**). The results showed that in MCF7 cells, ALDO increased SGK1, PER1 and ZBTB16 expression regardless of MR expression while for PER1 was not responsive to ALDO in the presence of MR overexpression. SPIRO acted to inhibit/reduce the ALDO driven transcriptional regulation of the targets as expected. However, MR independence of these targets to ALDO suggested that GR expression could also be responsible for these actions; and novel and only MR dependent actions of ALDO can be studied only in comparison with ZR-75-1 expression profiles and needed further research. Interestingly in **Figure 3. 31** where the same target genes were studied in ZR-75-1 in which GR cannot be detected at protein level, SGK1 and PER1 was not affected significantly by ALDO or SPIRO but ZBTB16 was increased by ALDO regardless of MR level and SPIRO was not affective suggesting that this increase was in collaboration with other receptors or targets of ALDO and not possibly the MR.

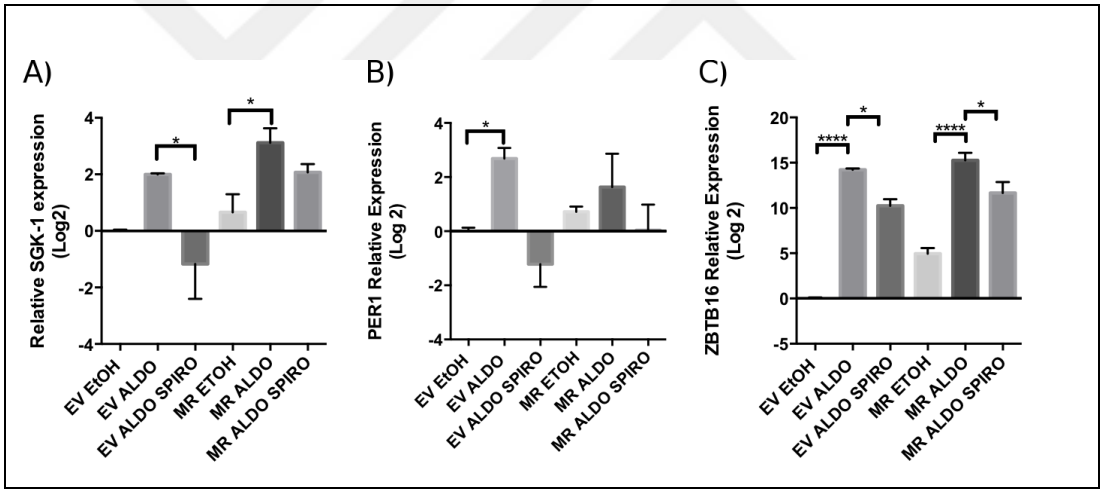

Figure 3. 30 Confirmation of MR downstream target genes in MR-Overexpressing MCF7 cells in the presence of 24-hour aldosterone and/or spironolactone treatment. **A)** SGK-1 expression was shown. **B)** PER1 expression was shown. **C)** ZBTB16 expression was shown. One-way Anova with Tukey's multiple comparison test was performed for statistical analysis of the data (*: $p<0.05$, **: $p<0.01$, ***: $p<0.001$, ****: $p<0.0001$; data was shown as the mean ± standard deviation (SD).

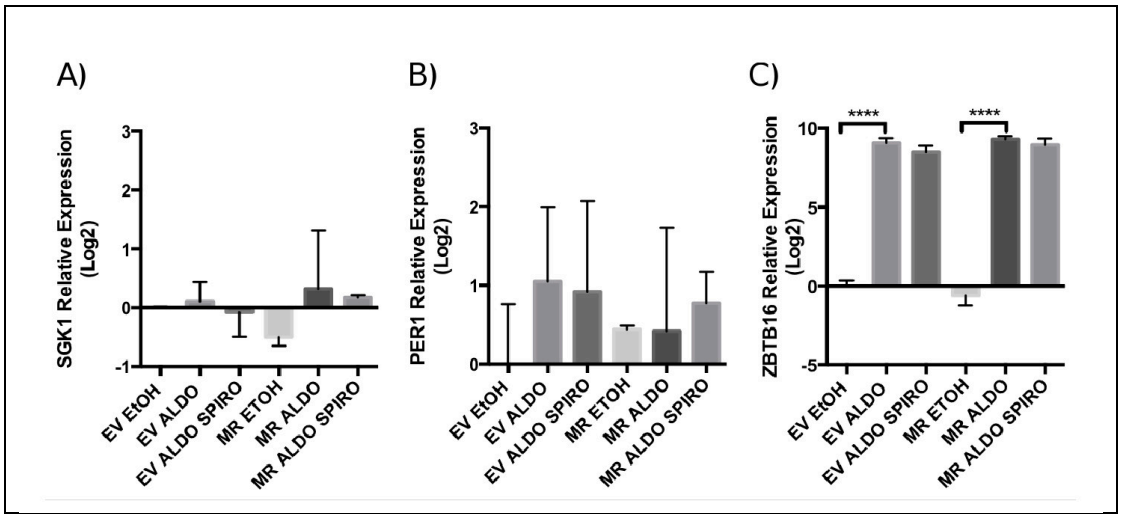

Figure 3. 31 Confirmation of MR downstream target genes in MR-overexpressing ZR-75-1 cells in the presence of 24-hour aldosterone and/or spironolactone treatment. A) SGK-1 expression was shown. **B)** PER1 expression was shown. **C)** ZBTB16 expression was shown. One-way Anova with Tukey's multiple comparison test was performed for statistical analysis of the data (*: $p<0.05$, **: $p<0.01$, ***: $p<0.001$, ****: $p<0.0001$; data was shown as the mean ± standard deviation (SD).

3.1.7. Pathways modulated by overexpression of MR in MCF7 cells without ALDO and/or SPIRO

Herein the context of this dissertation, the biological pathways affected in accord with the overexpression MR without ALDO were of our main interest to further test MR overexpressing cells in the xenograft model. The differentially expressed genes among OV_ETOH and EV_ETOH groups in MCF7 were filtered for fold change greater and equal to 2 with a P-value of smaller than 0.1. P-value was determined based on DESeq2. Herein, a total number of 244 genes were identified and then run in the GO PANTHER gene enrichment analysis tool for identifying modulated molecular functions, biological processes, cellular components protein class and pathways on this platform. Findings showed that pathways involving cell structure and signaling pathways were modulated yet cell proliferation was not among them suggesting that MR overexpression without its ligand ALDO may not be altering cell viability drastically although has a significant modulation of signaling.

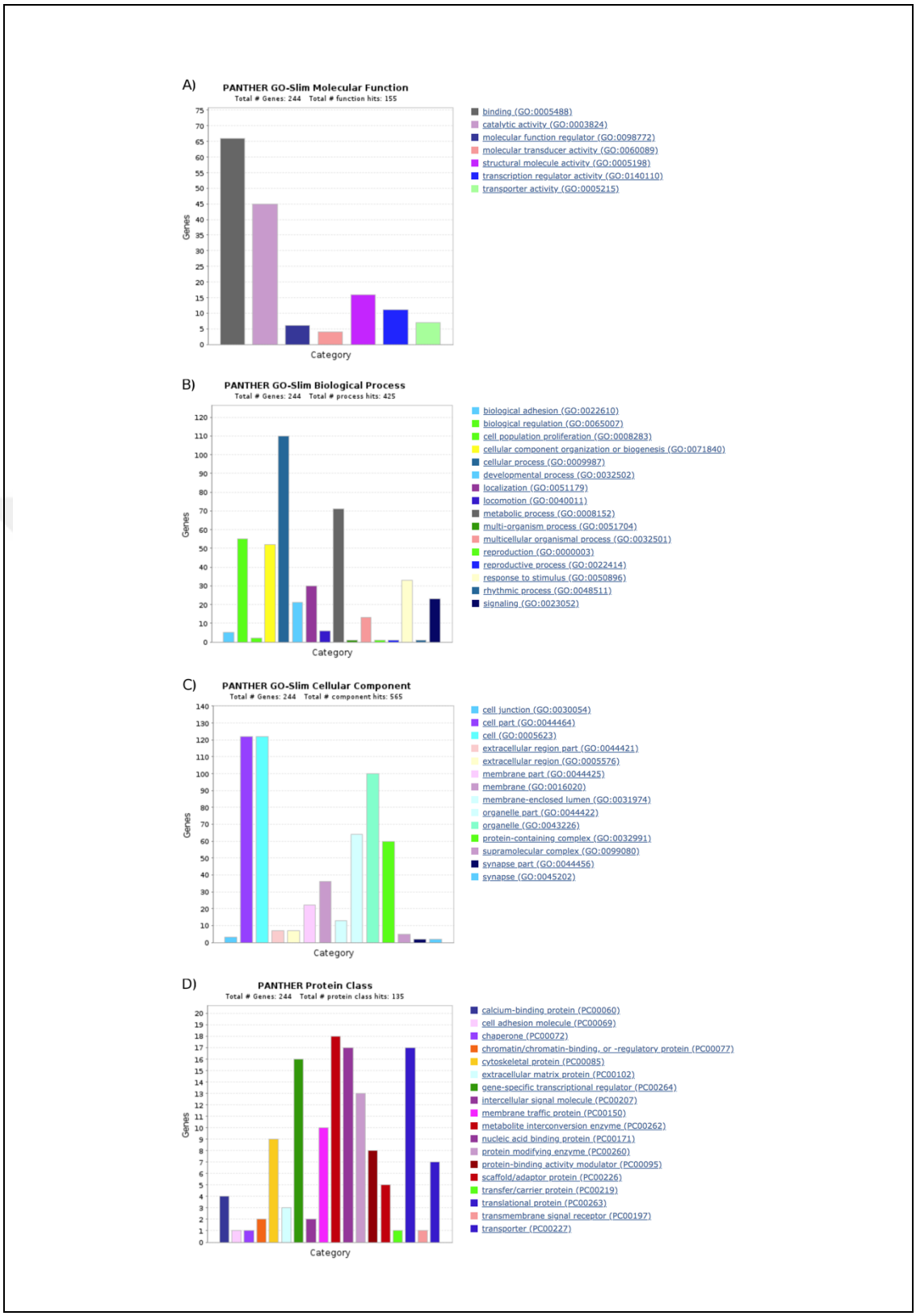

Figure 3. 32 GO Slim and PANTHER analysis of MR-induced upregulated genes in MCF7 cell line. A) Molecular function **B)** Biological processes **C)** Cellular components and **D)** Protein class.

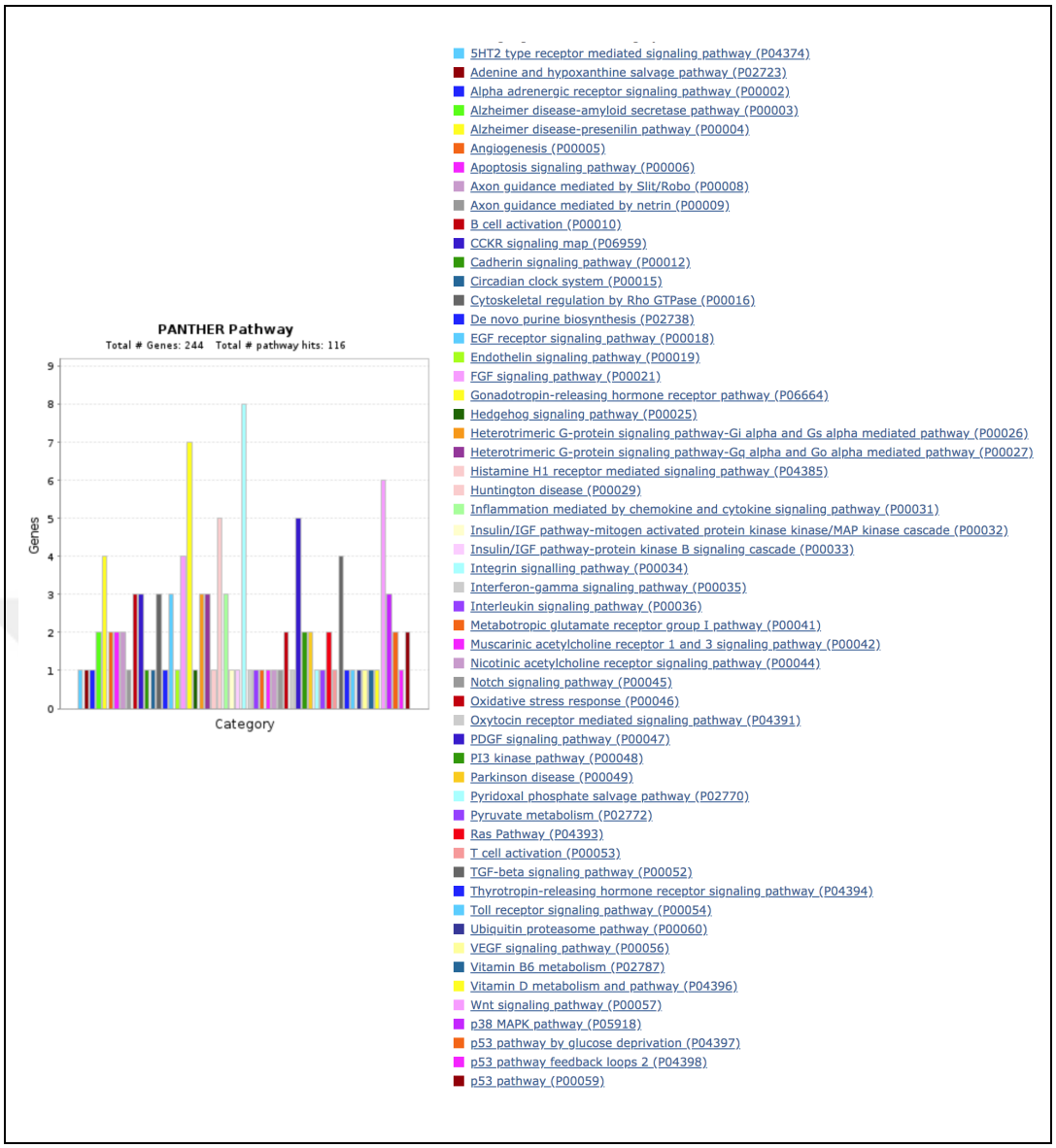

Figure 3. 33 GO Panther pathway analysis of upregulated genes in the presence of MR overexpression in MCF7 cells.

3.1.8. Cell viability assessment of naïve and MR-overexpressing MCF7 cell lines in the presence or absence of ALDO

The cytotoxic effect of different doses of aldosterone ranging from physiologic (0.1-1nM) to supra-physiologic (100nM) on naive MCF-7 cells employing two differential experimental setups wherein in one setting aldosterone administration was at once and in the other, ALDO treatment was replenished every other day and the final assessment was performed 120 hours from the initial aldosterone administration in both experimental settings. Herein, no significant alteration was detected among any treatment groups at 120 hours when aldosterone was only administered at once (**Figure 3. 34**). Additionally, administration of aldosterone every other day also did not yield any significant changes on 120 hours' time point. Overall, aldosterone did not exhibit significant cytotoxic effect on naïve MCF7 cells although a trend of increased cell proliferation was there it was not found significant.

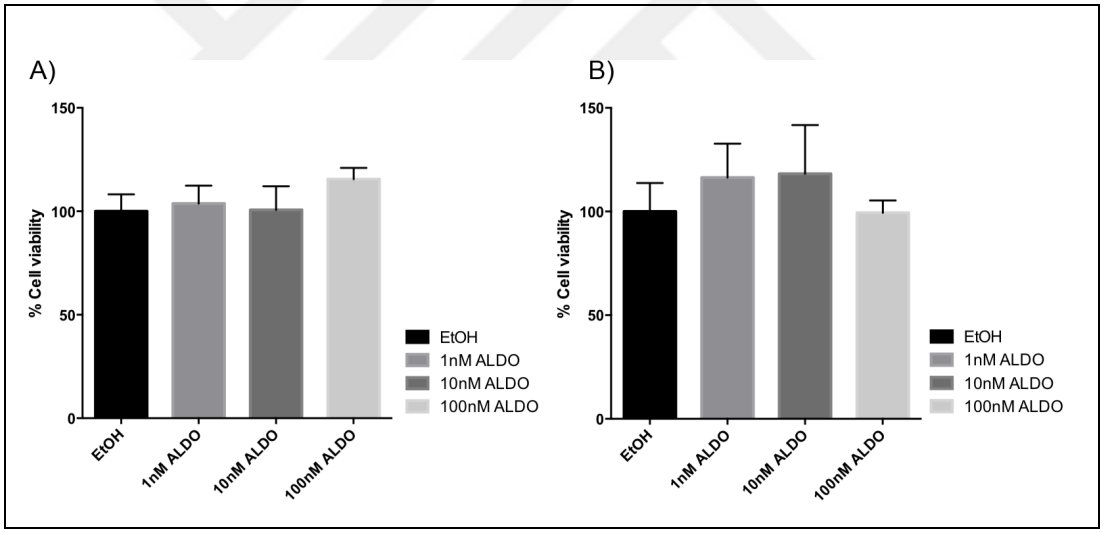

Figure 3. 34 Effect of five-day aldosterone exposure on naïve MCF7 cell viability. A) 5-day exposure of aldosterone on naïve MCF7 cells with no treatment replenishment (P-value:0.0423)**. B)** 5-day exposure of aldosterone on naïve MCF7 cells with treatment media replenishment every other day (P-value:0.1562)**.** One-way ANOVA with Tukey's multiple comparisons test was used for statistical analysis of A) and B). Data was shown as the mean ± standard deviation (SD). Each treatment group had 5 biological replicates in both experimental setups.

The cytotoxic effect of MR expression was further tested by overexpressing MR in MCF7 cells. Herein, 5.000 cells were seeded and the next day transfected with 25ng

of MR overexpression vector (MR-S-Tag-pcDNA3.1) or the control vector EV (pcDNA3.1) and media were replenished after 4-6 hours, the following day the media was switched to 5% charcoal stripped FBS supplemented phenol-red free media in order to remove any masking effects of ALDO present in the standard FBS supplemented media. The cells were then assessed for cell viability after four days being exposed to both expression vectors. For each treatment group 15 biological replicates were used in order to minimize standard deviation. The results showed that mainly EV treatment was cytotoxic at the concentration used. Yet, MR exerted a mild yet further significant cytotoxicity suggesting that MR overexpression in naïve cells without ALDO could decrease cell survival (**Figure 3. 35**).

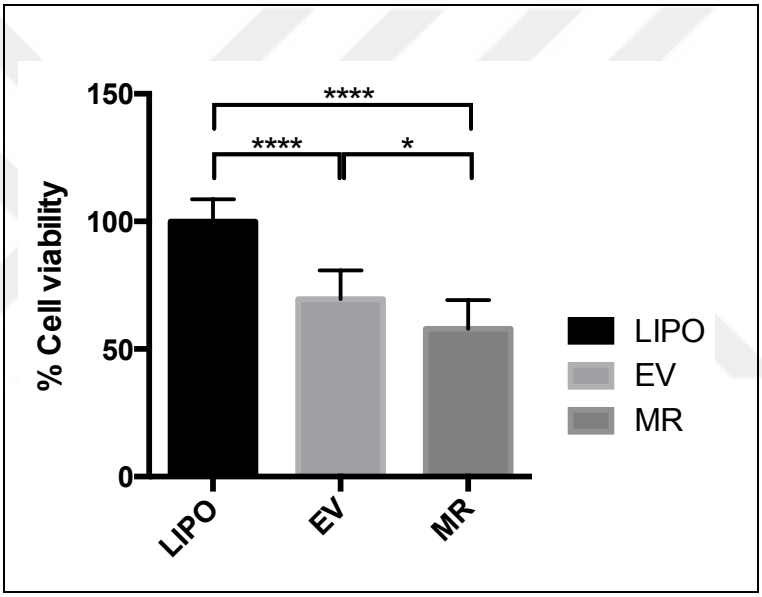

Figure 3. 35 Viability effect of transiently MR-overexpressing cells on MCF7 supplemented with 5% charcoal-striped FBS-supplemented media. MCF7 cells subjected to four-day MR-overexpression vector had significantly diminished cell viability when compared to control vector transfected cells**.** One-way ANOVA with Tukey's multiple comparisons test was used for statistical analysis (*: $p<0.05$, **: $p<0.01$, ***: $p<0.001$, ****: $p<0.0001$). Data was shown as the mean ± standard deviation (SD). Each treatment group had 15 biological replicates.

The cytotoxic effect of MR expression was further tested by overexpressing MR in MCF7 cells in standard FBS (10%)-supplemented media. Herein, 10.000 cells were seeded and the next day transfected with 50ng of MR overexpression vector (MR-S-Tag-pcDNA3.1) or the control vector (pcDNA3.1) and media were replenished after

4-6 hours with normal FBS supplemented phenol-red bearing media. The cells were then assessed for cell viability after four days being exposed to both expression vectors. For each treatment group 5 biological replicates. As expected cytotoxic effect of EV increased with respect to 25ng concentration when 50ng was used and there was a trend for MR overexpression being more cytotoxic than EV group yet not significant (**Figure 3. 36**).

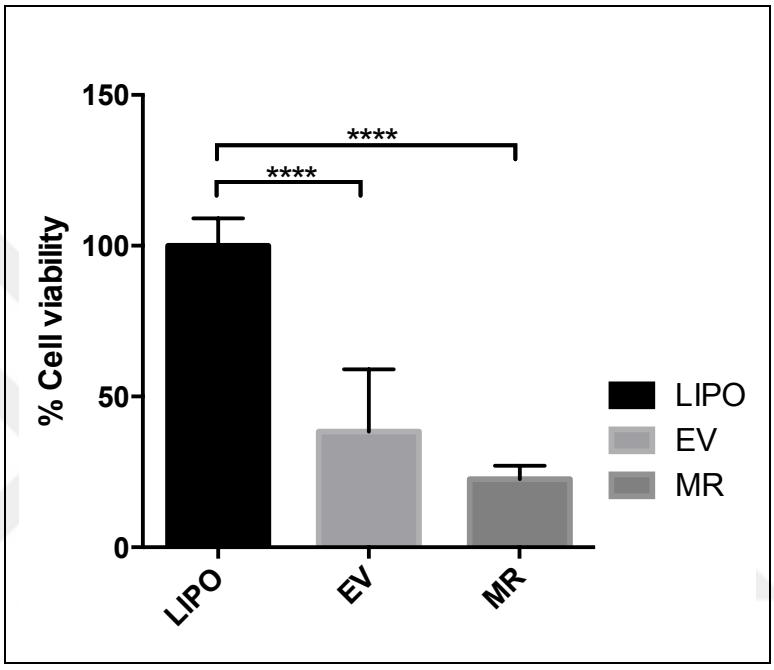

Figure 3. 36 Viability effect of transiently MR-overexpressing cells on MCF7 cells supplemented with standard-FBS supplemented media. MCF7 cells subjected to four-day MR-overexpression vector in the presence of standard DMEM supplemented with 10% FBS and no significant alteration was detected among EV- and MR-transfected groups**.** One-way ANOVA with Tukey's multiple comparisons test was used for statistical analysis (****: $p<0.0001$). Data was shown as the mean ± standard deviation (SD). Each treatment group had 5 biological replicates.

Another cytotoxicity test performed in parallel with the above-stated experiment (**Figure 3. 35**), aimed to investigate the effects of aldosterone on MR-overexpressing cells. In the experimental set up, wherein 5.000 cells seeded, transfected with 25 ng of vector, subjected to charcoal stripped 5% FBS-supplemented phenol red-free DMEM for 24 hours prior to aldosterone administration. Upon aldosterone administration, the cells were kept for further 24 hours before ending the experiment. Each treatment

group had 6 biological replicates. Although, the experiment was run in parallel, with 6 biological replicates no difference was observed among EV and MR groups and aldosterone (10nM) did not affect cell proliferation regardless of MR presence.

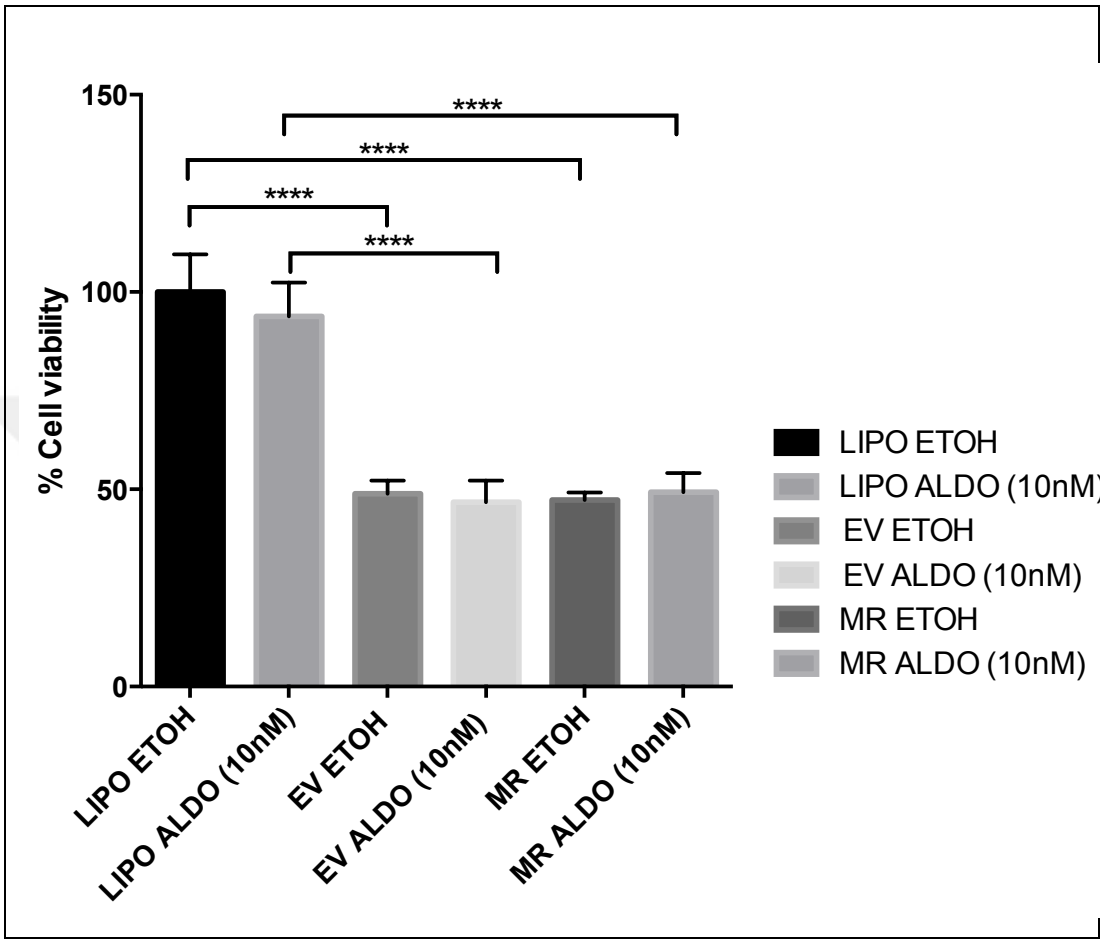

Figure 3. 37 Effect of aldosterone exposure on transiently MR-overexpressing cells on MCF7 cell viability. MCF7 cells subjected to four-day MR-overexpression vector and two-day aldosterone (10nM) exposure**.** One-way ANOVA with Tukey's multiple comparisons test was used for statistical analysis (****: $p<0.0001$). Data was shown as the mean ± standard deviation (SD). Each treatment group had 6 biological replicates.

3.1.9. Establishing zebrafish xenograft model of MR-overexpressing MCF7 cell line

3.1.9.1. Comparison of fluorescence image-based and ALU-based tumor proliferation assessment methods in MR-overexpressing MCF7 cell line transplanted *casper* fish

Transiently MR-overexpressing MCF7 cell lines were injected to yolk sacs of fourteen 48 hpf *casper* zebrafish and establishment of successful tumor transplantation was observed at 24 hpi and fish were kept alive until the scheduled tumor viability assessment end-point, 72 hpi. The tumor proliferation of the fish set was assessed by employing fluorescence-based as well as ALU-based quantification methods.

For the image-based analyses; the bright field and fluorescent images were captured both at 24 hpi and 72 hpi. The fluorescent images obtained at the two time points were processed on Image J to 8-bit and then the tumor area was selected on the area of yolk where fluorescence was emitted. Herein, we aimed to quantify the tumor presence at 24 and 72 hpi by using corrected total cell fluorescence (CTCF) (CTCF=Integrated density-(area of selected cell x mean fluoresce of background readings). The results were then recorded as CTCF log2 for 24 hpi and 72 hpi fish (**Figure 3. 38**, **Figure 3. 39**). The log2 of CTCF values were then transformed into a box plot and the change in tumor growth was statistically analyzed with parametric paired t-test (**Figure 3. 40**).

Tumor DNA-based quantification was then pursued on the same set of fish on 72 hpi. Initially the extracted fish DNA was measured and recorded. Then, the ALU-based tumor quantification was pursued where presence of the human DNA was detected by ALU repeat primers which were normalized against the zebrafish housekeeping gene, *ache* (-Delta CT= *ache* Ct- ALU Ct). The ALU Ct and *ache* Ct reads were obtained and – Delta Ct was calculated for each fish. Next, Pearson correlation was performed to compute the r between the log2 CTCF and – Delta Ct for each fish (r:0.4990, P-value:0.0693) (**Figure 3. 41**) showing the two methods behaved similar. Another normalization was also used to check the correlation among *ache* Ct and DNA concentration (ng/µl) (r:-0.3603, P-value:0.2057) (**Figure 3. 42**). Furthermore, transfected MR DNA was amplified using a human specific cDNA primer pair and the

correlation analysis among raw MR Ct and normalized ALU Ct exerted a negative significant correlation (**Figure 3. 43**). In addition, correlation among raw MR Ct and log2 CTCF differences of 72hpi and 24hpi fish images were studied yet no significant correlation was detected among these parameters (**Figure 3. 44**).

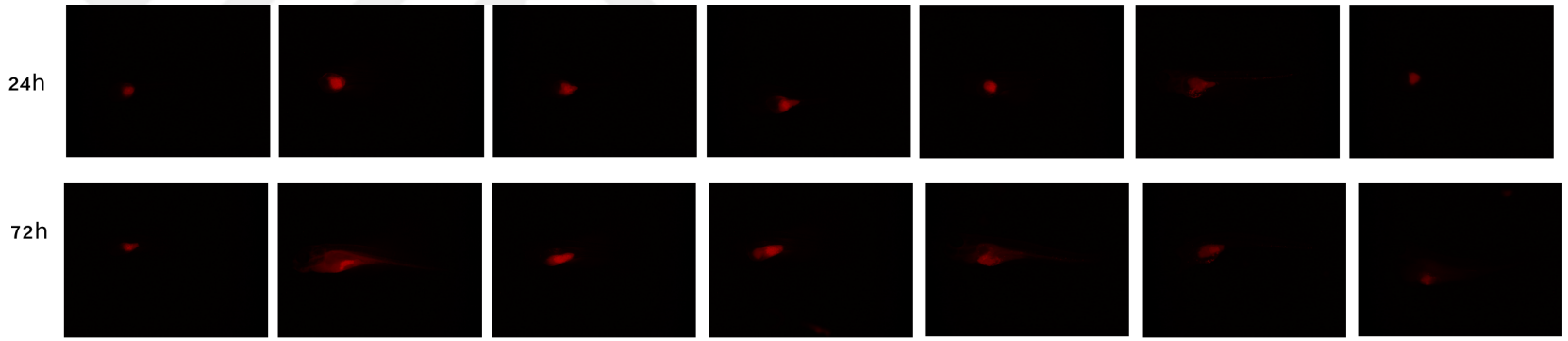

	FISH1	FISH2	FISH3	FISH4	FISH5	FISH6	FISH7
DNA Conc.	145.785 ng/ul	155.14 ng/ul	151.362 ng/ul	136.764 ng/ul	122.232 ng/ul	136.416 ng/ul	147.303 ng/ul
Raw ache Ct	20.5	20.28	20.06	20.14	20.745	20.565	20.655
ALU Ct	19.545	18.6725	18.2575	17.93	18.705	19.1725	22.0475
- Delta Ct (ache-ALU)	0.955	1.6075	1.8025	2.21	2.04	1.3925	-1.3925
MR Ct	20.39	19.825	19.8	18.95	20.87	20.81	21.585
CTCF (Log 2):72h	21.65	24.35	23.25	23.43	23.37	22.50	21.36
CTCF (Log2): 24h	21.86	23.15	22.54	22.74	22.51	22.63	21.66

Figure 3. 38 Fluorescent microscope images of zebrafish xenograft model of MR-overexpressing MCF7 cells (FISH1-FISH7). Image J has been used for generation of the pictures from merged fish and tumor images with split image function. The DNA Concentration of the extracted is recorded in ng/µl, Raw Ct value of *ache* amplicon, Ct of the ALU amplicon, Ct of the MR amplicon, corrected total cell fluorescence (CTCF) in log2 format was recorded under each fish label.

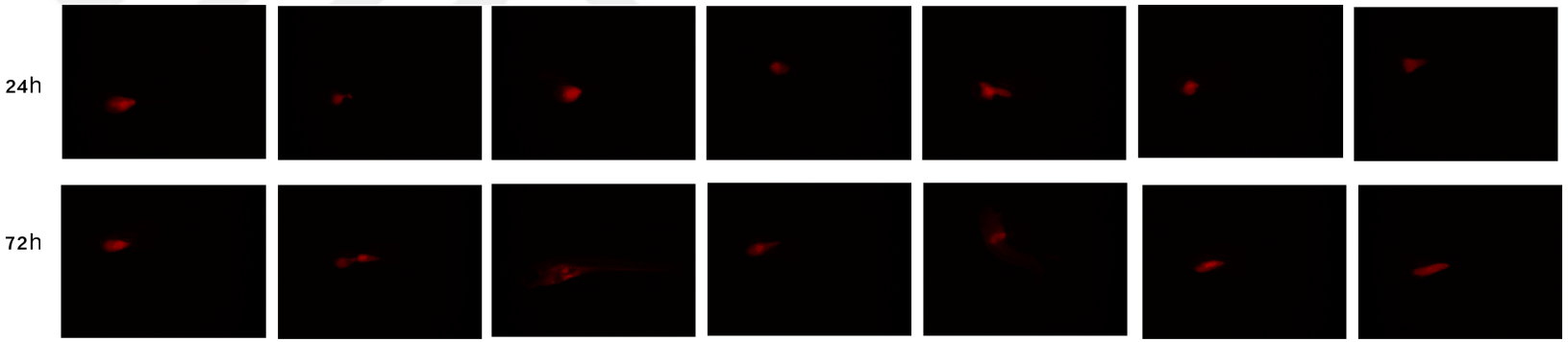

	FISH8	FISH9	FISH10	FISH11	FISH12	FISH13	FISH14
DNA Conc.	176.708 ng/ul	141.238 ng/ul	139.762 ng/ul	155.086 ng/ul	97.268 ng/ul	163.215 ng/ul	150.414 ng/ul
Raw ache Ct	20.26	21.99	19.93	19.815	20.89	20.325	20.4
ALU Ct	16.5925	23.0475	19.86	18.185	19.9775	18.6375	18.4175
- Delta Ct (ache-ALU)	3.6675	-1.0575	0.07	1.63	0.9125	1.6875	1.9825
MR Ct	18.28	20.72	23.505	19.395	20.045	19.705	19.225
CTCF (Log 2):72h	23.09	22.79	23.27	22.60	22.44	22.87	23.09
CTCF (Log2): 24h	23.28	21.57	23.33	22.00	23.28	22.45	22.39

Figure 3. 39 Fluorescent microscope images of zebrafish xenograft model of MR-overexpressing MCF7 cells (FISH8-FISH14). Image J has been used for generation of the pictures from merged fish and tumor images with split image function. The DNA Concentration of the extracted is recorded in ng/µl, Raw Ct value of *ache* amplicon, Ct of the ALU amplicon, Ct of the MR amplicon, corrected total cell fluorescence (CTCF) in log2 format was recorded under each fish label.

A)

	CTCF 72 HPI	CTCF 72 HPI LOG2	CTCF 24 HPI	CTCF 24 HPI LOG2
FISH1	3294008.09	21.6514127	3806061.51	21.8598674
FISH2	21321817.8	24.3458271	9303552.93	23.1493503
FISH3	9976061.9	23.250039	6113022.79	22.5434545
FISH4	11278850.5	23.4271167	7006878.18	22.7403404
FISH5	10834952.4	23.3691895	5982820.2	22.5123943
FISH6	5934990.08	22.5008142	6480543.24	22.6276833
FISH7	2698072.04	21.3634974	3318612.09	21.6621486
FISH8	8916800.03	23.0880946	10181683.6	23.2794728
FISH9	7238071.53	22.7871739	3103845.43	21.5656253
FISH10	10090231.1	23.2664559	10538206.6	23.329126
FISH11	6343664.5	22.596885	4196648.17	22.0008061
FISH12	5709473.02	22.4449262	10190147.4	23.2806716
FISH13	7680573.74	22.8727827	5714319.61	22.4461503
FISH14	8921586.81	23.0888689	5490914.76	22.3886151

B)

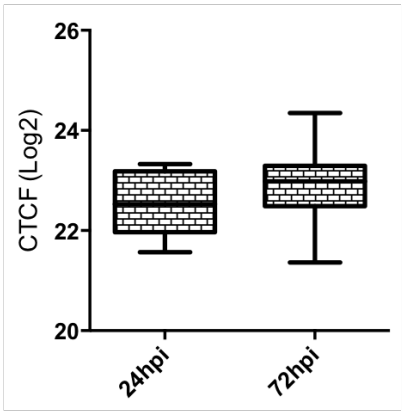

Figure 3. 40 Assessment of tumor growth at 24 hpi and 72 hpi by measuring CTCF. A) CTCF for each was calculated and transformed into log for 24 hpi and 72 hpi CTCF values. **B)** Statistical analysis was performed by using parametric paired t-test (P-value:0.0652).

A)

	- DELTA CT (ACHE-ALU)	CTCF 72 HPI	CTCF 72 HPI LOG2
FISH1	0.955	3294008.09	21.6514127
FISH2	1.6075	21321817.8	24.3458271
FISH3	1.8025	9976061.9	23.250039
FISH4	2.21	11278850.5	23.4271167
FISH5	2.04	10834952.4	23.3691895
FISH6	1.3925	5934990.08	22.5008142
FISH7	-1.3925	2698072.04	21.3634974
FISH8	3.6675	8916800.03	23.0880946
FISH9	-1.0575	7238071.53	22.7871739
FISH10	0.07	10090231.1	23.2664559
FISH11	1.63	6343664.5	22.596885
FISH12	0.9125	5709473.02	22.4449262
FISH13	1.6875	7680573.74	22.8727827
FISH14	1.9825	8921586.81	23.0888689

B)

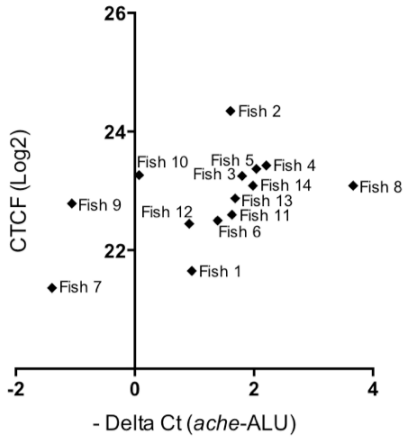

Figure 3. 41 Comparison of ALU-based tumor quantification and corrected total cell fluorescence-based tumor quantification in 3 dpi MR-Overexpressing *casper* zebrafish strain. Total number of 14 fish were used for the comparison and the correlation was calculated by Pearson r analysis (r:0.4990 P-value:0.0693).

A)

	CT (ACHE)	DNA CONC. (NG/UL)	DNA CONC. (LOG2)
FISH1	20.5	145.785	7.18769848
FISH2	20.28	155.14	7.2774269
FISH3	20.06	151.362	7.24185925
FISH4	20.14	136.764	7.09554471
FISH5	20.745	122.232	6.93347822
FISH6	20.565	136.416	7.09186906
FISH7	20.655	147.303	7.202643
FISH8	20.26	176.708	7.46522355
FISH9	21.99	141.238	7.14198449
FISH10	19.93	139.762	7.12682835
FISH11	19.815	155.086	7.27692465
FISH12	20.89	97.268	6.60389335
FISH13	20.325	163.215	7.35062984
FISH14	20.4	150.414	7.23279504

B)

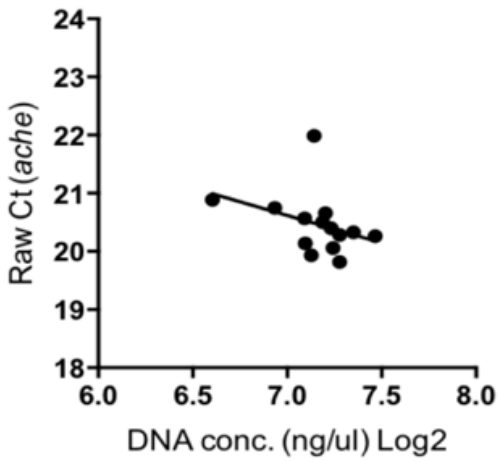

Figure 3. 42 Correlation analysis of raw *ache* Ct and DNA concentration (log2) in 3 dpi MR-overexpressing *casper* zebrafish strain. Total number of 14 fish were used for the comparison and the correlation was calculated by Pearson r analysis (r:-0.3603, P-value:0.2057).

A)

	CT (MR)	- DELTA CT (ACHE-ALU)
FISH1	20.39	0.955
FISH2	19.825	1.6075
FISH3	19.8	1.8025
FISH4	18.95	2.21
FISH5	20.87	2.04
FISH6	20.81	1.3925
FISH7	21.585	-1.3925
FISH8	18.28	3.6675
FISH9	20.72	-1.0575
FISH10	23.505	0.07
FISH11	19.395	1.63
FISH12	20.045	0.9125
FISH13	19.705	1.6875
FISH14	19.225	1.9825

B)

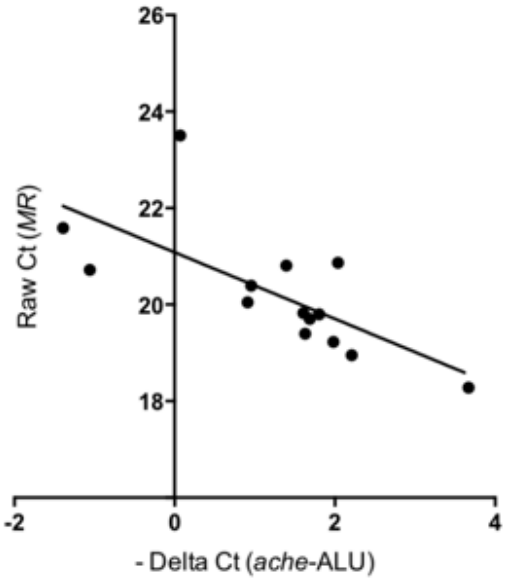

Figure 3. 43 Correlation analysis of raw MR Ct and *ache* normalized ALU DNA in 3 dpi MR-overexpressing *casper* zebrafish strain. A) MR Ct values and -Delta Ct was recorded. **B)** Correlation among MR Ct and normalized ALU Ct was calculated by Pearson r analysis (r:-0.7086, P-value:0.0046).

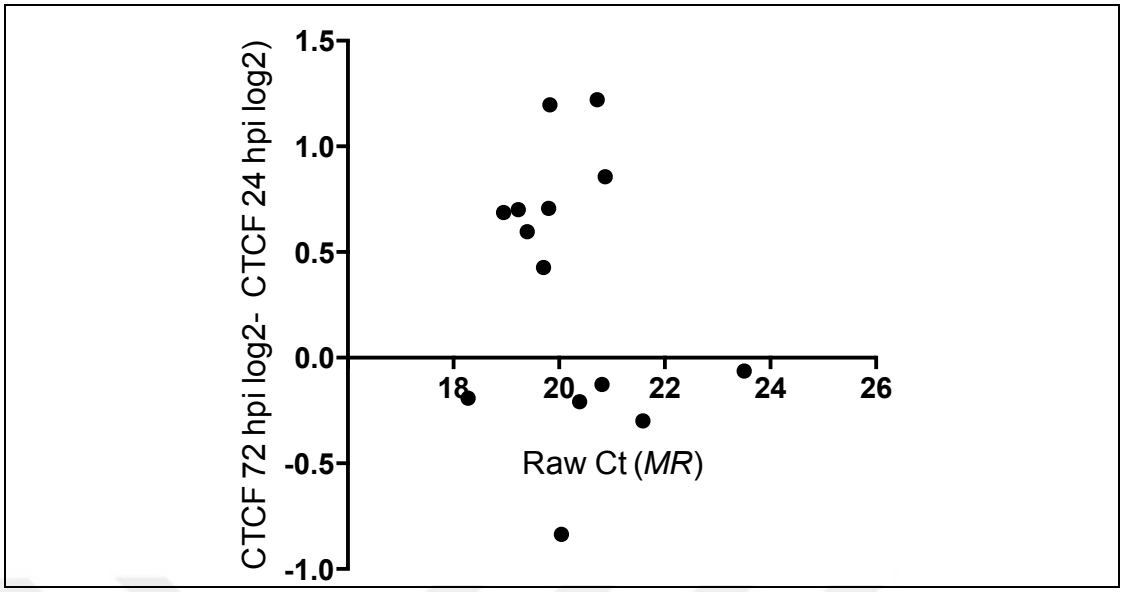

Figure 3. 44 Correlation analysis of raw MR Ct and CTCF difference among 72hpi and 24hpi. MR Ct did not exhibit any significant correlation with the CTCF difference of 72hpi and 24hpi-imaged fish (r: -0.2030, P-Value:0.4863).

3.1.9.2. ALU-based tumor quantification assessment of zebrafish xenograft model of MR-overexpressing MCF7 cell lines

Proliferative capacity of MR-overexpressing MCF7 cells were aimed to be further investigated using zebrafish model organism. Herein, 48 hpf wild-type (AB Strain) zebrafish were injected with approximately 300 MCF7 cells of three different groups lipofectamine treated MCF7 cells, empty vector transfected MCF7 cells and MR-vector transfected MCF7 cells. Next day, the tumor presence was checked under the light microscope the DsRed channel, fish emitting any kind of tumor specific fluorescence were then separated and kept at 32-33°C until three days post injection (72hpi). No fluorescence image was captured as pigmentation would interfere with the imaging analysis. The fish were then sacrificed and subjected to DNA extraction. Total number of nine lipofectamine-group fish (LIPO), ten empty vector-group fish (EV) and eight MR-overexpressing vector-fish (MR) were run for tumor DNA quantification assessment. The obtained data points (raw Ct) were exhibiting high variation among within groups especially in the MR-overexpressing group and when run through GraphPad outlier analysis, one data point was found to be an outlier significantly and was removed from the quantification analysis. The remaining analysis were performed for the samples that exhibit a Ct for both ache and ALU

amplicons. Initially, *ache* Ct normalized ALU Ct values (*ache* Ct-ALU Ct) were calculated among each group yet this assessment revealed no difference among any test groups and high variability was detected within each group (**Figure 3. 45**). Next, the correlation between the extracted DNA concentration in ng/µl and raw *ache* Ct were tested. Herein, a significant negative correlation (r:-0.6567, P-value:0.0002) was detected among total DNA concentration and raw *ache* Ct values (**Figure 3. 46**). MR DNA amount was also quantified using human MR cDNA-specific primers and as expectedly it could not be detected in the LIPO and EV groups since no MR was overexpressed yet also in a few of the fish (5 out of 9) housing MR-transfected MCF7 cells. This showed that number of injected MCF7 cells might be a factor since this set of experiments 300 cells per fish were used.

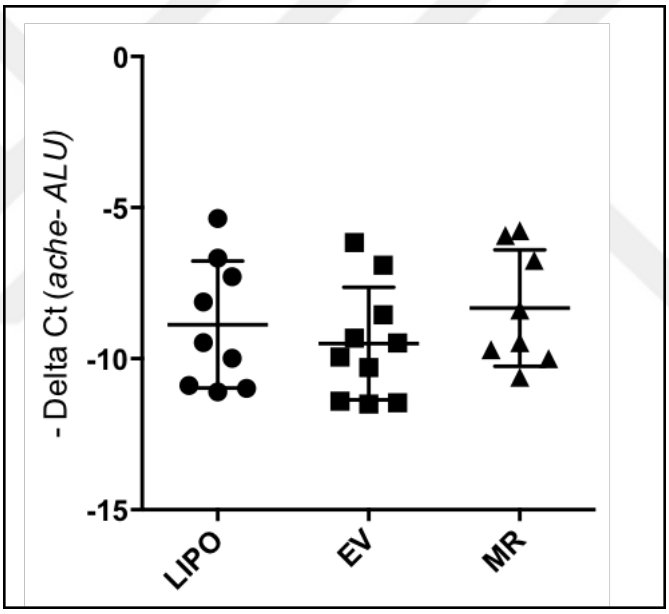

Figure 3. 45 ALU-based tumor quantification in MR-overexpressing MCF7 cell line experimental setup. Lipofectamine treated cell injections (n=9), empty vector transfected cell injections (n=10) and MR-overexpression vector transfected cell injections(n=8) did not reveal any significant difference in tumor quantification, hence in proliferation, *in vivo* (P-value:0.4582*)*.

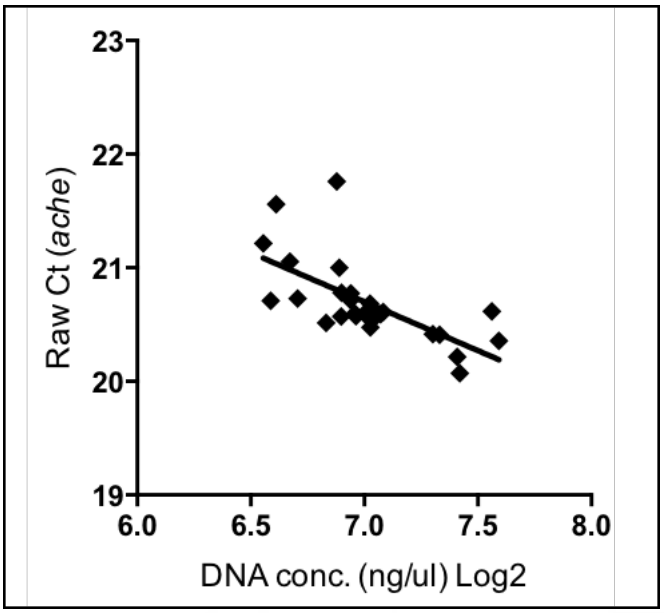

Figure 3. 46 Correlation analysis of ache Ct values and total DNA extracted from zebrafish. *ache* Ct and the DNA concentration exhibits significant negative correlation (n=27) (r:-0.6567, P-Value:0.0002).

CHAPTER 4

CONCLUSIONS, DISCUSSION AND FUTURE PERSPECTIVES

4.1. ZenoFishDb v1.1

In the present thesis a database specifically focusing on cataloguing xenograft studies that incorporate molecularly-modified cells, stem cells, cancer stem cells, patient-derived xenografts and distinguished hosts has been developed. Stringent manual curation has been performed in order to accommodate and categorize the curated data in Microsoft Excel file format which was then transformed into an online database called ZenoFishDb v1.1. To our knowledge, this has been the first -ever xenotransplantation database of zebrafish model organism while many was already present for mouse xenografts as indicated in the introduction section. ZenoFishDb v.1.1 also provides details of the PDXs studies in zebrafish and in the future, it is possible to connect the zebrafish data with those of the mouse (Bult et al., 2015; Conte et al., 2018; Krupke et al., 2008) since a similar structure about the clinical and demographic parameters of the tumors stored in ZenoFishDb v1.1. Finally, it is very important that ZenoFishDb is modular and updatable so that it becomes a "live review" and can expand to include new studies as well as new concepts. Based on these ZenoFishDb v1.1 provides a structured database through which the users can obtain the necessary background that is relevant to their studies while the database content and visualization tools help user plan experiments and decide on the endpoint parameters, such as time to injection, time to assessment, the number of cells to be injected and where to inject, and what type of cell tracker to use.

In addition, ZenoFishDb v1.1 resulted in identification of which genes and pathways have been studied most with xenografts in zebrafish host and future studies can focus on how this compares to the mouse studies. Zebrafish is a fast-developing organism in comparison to rodents and most zebrafish studies are conducted in embryos and early larva due to transparency of tissues and lack of immune response to transplanted materials. These characteristics make zebrafish amenable for high throughput studies and many genes/pathways can be studied in the future. At the moment these remain restricted in number yet most of them are connected via a STRING protein-protein interaction analysis since many xenograft studies are cancer cell line based and involve

assessment of tumor size and migration hence pathways such as ‘pathways in cancer’, ‘VEGF signaling pathway’, ‘Ras signaling pathway’, ‘Cell cycle’, ‘Apoptosis’ ‘PI3K-Akt signaling pathway’, ‘MAPK signaling pathway’ are frequently studied according to ZenoFishDb v1.1.

Platforms accommodating details of mouse xenotransplantation studies when compared to ZenoFishDb v1.1, often appear to accommodate data attributes in common. One such example is the Mouse Models of Human Cancer Database (formerly known as the Mouse Tumor Biology Database) (Bult et al., 2015). This database allows advanced search by enabling selection of multiple attributes simultaneously for maximizing the fine-tuning and delivering to-the-point results. These two databases share several attributes in common including search of tumor type, strain related information, human tissue transplant and references. The Mouse Models of Human Cancer Database additionally accommodates information about tumor frequency and tumor inducing agent details which are not applicable to fish studies for this kind of data mining. Yet, study size which has not been incorporated to ZenoFishDbv1.1 has been incorporated into this mouse database and could be a future add-on attribute also informing the users about the statistical power of the studies performed in the literature.

PDX-Finder is the most-comprehensive xenotransplantation database harboring 4031 PDX models in its reservoir only applied on rodents (Conte et al., 2018). The advanced search option allows search through five main attributes, namely, PDX models, molecular data, treatment/drug dosing data, patient/tumor data. When we compare ZenoFishDb v1.1 to PDX-Finder, initially it is important to mention that ZenoFishDb v1.1 only houses 115 PDX studies as zebrafish xenotransplantation studies are considered relatively new when compared mouse xenotransplantation studies. Although on the smaller-scale, PDX Details module of the ZenoFishDb v1.1 also delivers patient and tumor data, such as data about patient treatment and molecular data if appeared on the original article. However, the delivered information could differ from one study to another as we could only incorporate the PDX-associated data as appeared on the articles. For generating a more comprehensive PDX database in zebrafish, the PDX study authors could be individually contacted and all details could be gathered for this purpose.

Overall, ZenoFishDb v1.1 focuses mainly on xenografts studies in zebrafish if they accommodate use of molecular modification, such as transgene, shRNA/siRNA, etc. in the cells transplanted, stem cells, cancer stem cells, PDXs and modified hosts used for xenotransplantation. Future versions of this database are required for implementing all of the xenotransplantation studies regardless of presence/absence of cell and/or host modifications as this would better reflect the current status of the zebrafish xenograft studies literature as well as incorporating more comprehensive collection of data on the database. In regard to this issue as well as vastly accumulating data on zebrafish xenograft studies, the ZenoFishDbv1.1 will be updated bi-annually. More details are provided in the Future Perspectives section.

4.2. Development of a high throughput tumor size estimation methodology using ALU quantification in zebrafish

In this dissertation, an ALU-repeat based tumor DNA detection previously applied for tumor DNA quantification in mouse and rat xenografts (Prigent et al., 2015) was modified to be applied in zebrafish xenograft models. Herein, an ALU-based tumor DNA quantification had been applied to zebrafish xenografts for the first time paving the way for high throughput tumor cell number/tumor DNA quantification. Initially, this method was applied for testing tumor proliferation in an altered tumor microenvironment wherein liver cancer cells were transplanted to yolk sac of *ache* null mutant fish that had excess acetylcholine accumulation. Hence, this application was becoming of importance due to establishing two novelties in the fish xenografts; successful application of ALU-based tumor DNA quantification and successful testing of tumor-microenvironment interactions on proliferation in mutant fish. *ache* mutant and wildtype siblings from the same breeding pairs were used making comparisons between genotypes possible in terms of how much tumor growth the host genotype contributed however this type of analysis requires genotyping the fish with the tumor and most imaging studies just use the images obtained from the fixed animal. The novelty of ALU method in zebrafish is that it allows both human DNA detection through ALU quantification and zebrafish DNA variation detection for mutation analysis; and when combined, this allows for testing whether the host genotype has impact on tumor growth. In our case, *ache* mutants, leading to accumulation of excess

acetylcholine, provided a microenvironment which can be oncogenic. The reasons for this could be indirect such that that lack of acetylcholinesterase (achE) results in paralysis and potentially cardiac problems and affect circulation and potentially resulting in inflammation (Behra et al., 2002). However, it is also possible that achE results in changes in the metabolism and affect growth of tumor cells (Y. Zhao et al., 2011). Future experiments are needed to address these direct or indirect effects.

When ZenoFishDb v1.1 is searched for analyses methods applied on tumor cell engrafted fish, it becomes clear that tumor size/volume assessments are done using mostly imaging techniques that allow for tracing fluorescent dyes or fluorescent protein expressing cells. ZenoFishDb estimates 10.6 % of the curated studies assess tumor proliferation and more than 30 % of them uses fluorescently labeled cells and 16.5 % uses GFP expressing cells. None of them reported an ALU-based tumor DNA quantification like method which makes this study highly novel and also impactful.

ALU-based tumor DNA quantification has its challenges and future studies should focus on improving the quantification. Additional primers can be used to detect the ALU copies in addition to the one used in the present study which were obtained from existing mouse studies (Prigent et al., 2015). Moreover, ALUs can be variable so a more thorough quantification of different types of ALUs can also be used in the future (Abellaneda et al., 2015). Furthermore, in order to refine use of this method, different types of DNA extraction method could be assessed as this was suggested to be a parameter for yielding best results in mouse and rat xenografts (Prigent et al., 2015). Additionally, ALU-based DNA applications in fish could be also further tested on adult fish xenografts for standardizing the use of method for fish at any developmental stage.

In addition, there is a need to confirm that ALU-DNA levels correlate with dye intensity obtained from the corresponding image of the tumors. I have addressed this question in the next section where xenografts obtained MR-overexpressing MCF7 cells were compared using both ALU and images to estimate the correlation between these two methodologies (see below sections).

4.3. MR and GR expression and breast cancer

In the context of TUBITAK 1001 project 114S226, we initially tested MR expression levels both at mRNA and protein levels across different breast cancer cell lines. Upon revealing the expression profile among these cell lines, cells with no to negligible amounts of MR expression were used to establish an MR overexpression model in order to decipher the role of aldosterone and MR signaling in breast cancer disease by the terms of transcriptomics studies and cell proliferation assessments. Herein, MR and GR, expression levels across different breast cancer cell lines were quantified by qRT-PCR for the first time in literature. This has allowed us to determine cell lines which highly and lowly express MR along with its close relative GR. In fact, although MR and GR were highly correlative in most of the studied cell lines dysregulated cell lines were also present highlighting also possible routes of unshared regulatory networks between the two receptors in disease of breast.

Ex vivo MR and GR expression in normal breast and breast cancer tissue- derived cDNA arrays also revealed a moderate correlation among the two receptors. *In silico* analyses of MR and GR expression across 994 breast cancer patient sample data (TCGA PanCan complete case dataset) performed through cBioPortal.org (Cerami et al., 2012) also exhibited significant moderate correlation between the two receptors. The *ex vivo* correlation analysis which was much smaller in number was therefore tested in a larger scale and a similar pattern was detected in much larger cohort of breast cancer patients. This finding again highlighted the presence of MR and GR co-expression in patient data. This is to our knowledge is the first confirmatory real-time qRT-PCR study for the correlation of expression between MR and GR at the mRNA level *ex vivo*.

If to consider GR, MR and their genomic actions; both receptors are well-characterized transcription factors and act through binding to hormone response elements (HREs). Until recently, MR and GR was known to bind to GREs or negative GREs for gene transactivation or repression, respectively. MREs, mineralocorticoid receptor elements, have been only recently discovered. Moreover, MR and GR have been shown to bind the HREs also as heterodimers (Ou et al., 2001). Altogether, the availability of different HREs, different dimer complexes formation and ligand

availability, may possibly influence the regulation of shared and unshared networks among MR and GR in breast tissue.

Survival analysis, OS and RFS, were performed using GEPIA and KM-Plotter tools for stratification of MR and GR expression. The reason for employing two different tools were that GEPIA tool was using RNA-Seq data and was used to study overall OS and RFS across approximately 1000 patients. KM-Plotter microarray data option allowed studying OS and RFS across approximately 1400 and 4000 patients, respectively. KM-Plotter microarray data option further allowed classification of data based on their intrinsic subtypes e.g., Luminal A, Luminal B, Basal and HER2+.

GEPIA analysis revealed high MR expression to be associated with better overall survival and marked MR as a good prognostic factor. In KM-Plotter analyses, however, although approaching significant this could not be detected for MR in the case of OS yet, herein high MR expression was shown to be highly significant with better RFS outcome. These results were suggesting a tumor suppressive role for MR in breast cancer. Yet, as due to the complex nature of cancer disease and breast cancer heterogeneity, the intrinsic subtypes and MR expression stratification was further studied in this set. Herein, high MR expression was found to be a good prognostic indicator of RFS in luminal A patients. These findings suggest that high MR expression to be an indicator of better prognosis in hormone receptor, i.e., ER and PR, positive subtypes. Although MR has not been widely studied in breast cancer yet, possible interaction of ER and MR gained attention as cardiovascular disease (Barrett Mueller et al., 2014). Within this concept, E2-induced ER activity was shown to be inhibiting transcriptional activity of MR and moreover, immunoprecipitation studies revealed MR and ERα being part of a protein complex. Yet, effects of ER and MR co-ordination as well as MR-PR co-ordination remains to be elucidated in breast cancer signaling. In fact, recently, Leo and colleagues have shown that MR and GR crosstalk with PR leads to induction of focal adhesion and inhibits growth of breast cancer cells (Leo et al., 2004). This finding further encourages for further research deciphering possible crosstalk among MR, ER and PR in normal and diseased breast tissue.

GR, on the other hand, when expressed in high levels, it exerted better overall survival. When studied across intrinsic subtypes, high GR expression was associated with better

OS in luminal B patients. By terms of RFS and GR analysis, low GR expression was shown to be associated with better RFS in basal subtype. GR, although has been extensively studied in breast cancer, yet, MR and GR co-expression and co-ordination needs to be further addressed in breast cancer signaling. Although MR and GR were found to be correlated in their expression patterns the correlation value was only moderate suggesting that divergence in paired expression and hence differences in survival impact could also emerge.

4.4. Aldosterone and MR signaling in breast cancer

In addition, effects of ALDO were studied using MTT assay on cell viability and showing ALDO did not have a significant effect on naïve MCF7 cells over 5 days of treatment. The indifference between different doses of aldosterone, ranging from physiologic (0.1-1nM) to supraphysiologic (100nM) as well as ethanol control could be due to absence of MR in the naïve MCF7 cells which has led us to overexpress MR in MCF7 cells. Only one study was identified in literature to test proliferative effects of aldosterone along with vasopressin and angiotensin on MCF7 cells by trypan blue staining and manual counting. The cells were seeded in standard media and 24 hours later the drugs were administered with media without serum. No significant difference were detected in the proliferative activity of ALDO induced cells of various concentrations ranging from 10^{-6} M to 10^{-14} M for 48 hours and 72 hours (De Azevedo Delou et al., 2014). However, another study performed on MR expressing PMC42 cells also did not present any significant alteration in cell proliferation upon 72 hour ALDO exposure (Koyama et al., 2001). However, ALDO exerted proliferative effect on an HER2+ cell line, SkBr3 cell line after 5-day exposure (Rigiracciolo et al., 2016). These findings imply cell-line dependent effects of ALDO on cell proliferation, furthermore, the molecular subtype, e.g., the hormone status could also possibly affect the anti- and/or pro- proliferative effects of ALDO due to possible crosstalk among MR and other steroid receptors(Leo et al., 2004; Rigiracciolo et al., 2016).

Using MCF7 cells transfected with empty- (EV-) or MR-containing overexpression vectors, I have further tested the effect of MR-overexpression on cell viability. Although the cytotoxicity of EV when compared to LIPO treatment was not neglectable, MR was showing mild but significant further cytotoxicity over EV in

MCF7 cells yet not in all sets to the same degree. It is possible that since EV had cytotoxic effects already and reduced cell viability when compared with control treatment (Lipofectamine only). MR's effects were not prominent and was partially masked.

RNAseq analysis of MCF7 and ZR-75-1 cells expressing MR at no or very low levels were also tested when transfected with EV or MR in the presence of ALDO or EtOH to confirm that the decrease we observed in MR overexpressing cells were due to cell cycle inhibition. Pathway analysis of the differentially expressed genes when MR was overexpressed in MCF7 cells revealed modulation of integrin, Wnt, and TGF-β signaling pathways as majorly upregulated pathways implying possible association of MR signaling with regulation of stemness in breast cancer cells, some of which were previously shown in the literature (Cai et al., 2013; Lamb et al., 2013; Park et al., 2016; Shackleton et al., 2006; Shipitsin et al., 2007; Stingl et al., 2006; Y. Wang et al., 2011). Recently, role of MR signaling has been studied in the context of stem cell biology. For instance, silencing of MR was shown to be increasing survival of mesenchymal stem cells (MSCs) and improving their effects on myocardial infarction therapy (X. Xie et al., 2019). Another study highlighted the anti-proliferative effect of aldosterone on progenitor cells in the adult hippocampus of adrenalectomized rats (E. Y. H. Wong & Herbert, 2005). In the light of the RNA-Seq data analysis and current literature, MR and aldosterone signaling could be also studied in breast cancer stem cells. Wnt signaling, another upregulated pathway in MR-overexpressing MCF7 cell, has not been widely studied in the context of aldosterone and MR signaling. Yet, a study performed by Zhu and colleagues has shown inhibition of mesangial cell apoptosis by SPIRO through the Wnt signaling pathway (Zhu et al., 2013). Hence, Wnt signaling pathway members could be further studied in MR-overexpressing MCF7 cell samples alone as well as in the ALDO and/or SPIRO treated samples. If to consider the genes upregulated upon MR-overexpression in the above-mentioned pathways; *MAPK13, JUND, PRKCD* genes were among many.

Cell cycle inhibition was not detected in pathway analyses predominantly, and this could be due to the fact that MR alone without ALDO treatment may not exhibit the same effects. Future studies testing the effect of stable transfection of EV and MR on cells to test the effects of MR on cell viability and RNA expression.

4.5. Assessing role of MR overexpression on growth of MCF7 cells *in vivo* using zebrafish xenografts

Since I have identified a mild decrease *in vitro* in cell viability when MR was overexpressed in comparison with respect to EV, I wanted to test if this holds in the *in vivo* setting using zebrafish xenografts. As a case study, I have transplanted MR-transfected MCF7 cells into the zebrafish *casper* embryos, which are widely used in xenotransplantation since they are transparent and make possible to obtain a clear fluorescent signal carried by the xenografts. Then, I have transplanted both EV- and MR-transfected MCF7 cells into the AB zebrafish embryos and my aim was to test if MR reduces cell viability *in vivo*. This is the first time for showing the correlation between image based and ALU repeat-based quantification tumor growth assays in zebrafish.

In *casper* fish xenografts, I have compared the signal obtained from the images with the ALU quantification results. This is very important to state for ALU method to become a more mainstream as in the case of imaging quantification. The results revealing that there was a positive correlation approaching significance among the tumor quantification obtained by ALU-DNA and corrected total cell fluorescence (CTCF) is highly promising for this former method to be used more frequently in the literature. This was further supporting the idea of ALU-DNA quantification being more sensitive method for quantifying as the background signal emitted from the image profiles appear to interfere with the outcomes in image analyses. Herein, I have also studied the correlation among the extracted fish DNA (ng/ul) and the Raw *ache* Ct value representative of the fish DNA, solely, although this has been a valid approach with larger sample size as in *ache* experimental set up, herein the correlation among these values did not exhibit significant correlation. Increasing the sample size would be a possible solution to overcome this issue. In fact, for the injections performed in AB wild-type fish with three experimental groups with a total number 27 fishes, the negative correlation among the extracted fish DNA and the raw *ache* Ct value were highly significant. This suggested that using *ache* Ct as a normalization factor in ALU DNA incorporates the differences in assayed zebrafish DNA as also shown in liver cancer cells xenografts of *ache* mutants (Avci et al., 2018). In the future,

other measurements on different genes or zebrafish specific transposable elements can be used to compare with *ache* DNA. These different normalization methodologies are novel contributions from this thesis to the literature and can help ease adopting this methodology to different settings. In addition, quantification of the overexpressed gene, herein MR, was successfully performed.

When I compared the normalized ALU concentrations between the three groups of the xenograft experiment (i.e., LIPO (Lipofectamine treated only), EV or MR overexpressing cells transfected with lipofectamine) I have not observed a significant difference among any of the groups. Yet, I expected to observe at least LIPO treated fish to have larger tumors when compared with EV or MR as in the case of the *in vitro* MTT experiment. This could be due to the difference between *in vitro* and *in vivo* microenvironment. We grow MCF7 cells in 10% FBS- supplemented DMEM without insulin as also practiced in the literature (Ciccarone et al., 2020). Presence of insulin alters how the MCF7 cell responds to estrogen or anti-estrogens. Yet, we do not know how presence or absence of insulin might affect to the stress caused by exogenous plasmid DNA. Igoucheva and colleagues' studies effects of exogenous DNA one of which was a plasmid DNA transfected to mammalian cells and upon 6 hours of transfection the gene expression profile of the mammalian cell culture was studied and ATM/ATR, apoptosis, cell cycle arrest and genome stability/repair pathways were up-regulated compared to controls and this was regardless of the plasmid sequence as it was also tested in this study (Igoucheva et al., 2006). *In vivo*, however, this phenomenon was no longer present as there were no significant alterations among EV-bearing cell injections or lipofectamine treated cell injections. Also, *in vitro*, the effects of EV with or without MR expression was independent of charcoal-stripped serum suggesting that this may not be the case since regular serum has many growth factors, yet the dosage might still be important. *In vivo*, in zebrafish the microenvironment is not modulate while the cancer cells were (EV, MR, unmodified) and might provide an environment in which growth factors are abundant and hence tumors grow similarly and no reduction by EV is observed. Not finding a significant difference between EV and MR test groups suggest that the effect might also depend on presence/absence of ALDO and should be tested further upon treatment of zebrafish embryos with ALDO upon xenotransplantation.

Overall, I have helped increase access to literature on xenograft studies in zebrafish through manual curation of the literature focusing on molecular modifications and host modifications. Analysis through ZenoFishDb v1.1 has revealed many different aspects of the state of xenotransplantation in zebrafish and will help researchers design their experiments. For instance, screening through the ZenoFishDb v1.1revaled total of 15 studies harboring MCF7 cell line injections with injected cell numbers mostly ranging from 50 to 500 cells and for other cell lines injections as small as 10 cells exist as projected on the ZenoFishDbv1.1 *Data Table* (Targen et al., 2020). Hence ZenoFishDb v1.1 help researchers access the data, interpret it, and use it effectively for their own interest I also have helped develop a high-throughput assay for human xenografted tumor size estimation using ALU DNA and made possible to detect human DNA while genotyping the host which can be useful in future zebrafish xenograft studies. Finally, I have compared the performance of ALU-based quantification with that of image-based intensity measurements and found a significant correlation between these two methods further validating the accuracy of the method. In addition, I showed that ALU-based method can be used to test effects of microenvironment in tumor cell line growth by comparing *in vitro* and *in vivo* findings and identifying discrepancies in the context of effects of MR overexpression between cell culture and zebrafish environments in breast cancer. These show the importance of testing molecular modifications and potential treatments in the *in vivo* context in addition to the cell culture. In addition, I have for the first time tested the importance of MR signaling using a cancer cell line panel, an *ex vivo* expression panel and an overexpression model in which effects of ALDO and SPIRO could be tested. My findings which also have led to identification of several different upregulated pathways in MR expression through use of RNA-seq and which require further validations.

4.6. Future perspectives

- ZenoFishDb v1.1 would be further expanded to accommodate all of the immortalized-cell injected fish details regardless of their filters such as molecular-modification status and/or host modifications.
- ZenoFishDb v1.1 upcoming versions will be designed to deliver drug dosing details of the zebrafish xenotransplantation studies to be more compatible with the current databases on the rodent xenotransplantation models and this would further increase

the impact of the current study by providing intriguing details about the drug delivery routes, study plan, and drug doses and associated-assessments as a separate module linked to each study.

- ALU-based DNA tumor quantification and fluorescent imaging-based tumor quantification will be further assessed with several other conditions to further support our findings. Two essential parameters should be tested to further support these findings; 1) *in vitro* setting: different number of cells ranging from 20-1000 cells, covering all possible injection ranges performed in fish xenotransplantation studies, should be counted, their DNA should be extracted, ALU Ct's should be tested in the presence of a constant amount of zebrafish DNA; 2) *in vivo* setting: the same number of cells ranging from 20-1000 cells should be injected to transparent fish; the fluorescence imaging should be obtained and then the DNA extraction should be performed and ALU and an internal zebrafish control gene should be quantified. The findings will then reveal the correlation among ALU Ct's *in vitro* and *in vivo* and reflect the success of the xenotransplantation. Different number of injected cells ranging from 20-1000 cells and quantifying both with ALU-based and fluorescent imaging-based system will better reflect the reliability of the systems with regard to injected cell numbers providing a better in sight for the use of both systems in a comparative manner at once.
- Successful establishment of the transiently MR-overexpressing MCF7 cell xenotransplantation and assessment by ALU-based quantification and lastly, by human MR quantification further highlighted the need of 'molecular-modification specific' assessments to be performed in the xenografted fish. In the case of transient overexpression models, the efficiency rate of each transfection in the transplanted fish could be determined by quantifying gene of interest, e.g., along with the ALU-based DNA quantification. Further optimizations should be pursued such as; injecting the cells that has been transfected with different amounts of vectors and/or transfected with different amounts of vectors which has been also marked with fluorescent tags.
- RNASeq data on both MCF7 and ZR-75-1 cell lines should be comprehensively validated on the entire set up at mRNA levels employing qRT-PCR. The same experimental design should be repeated also for pursing protein studies and checking altered genes also at the protein levels.

- RNASeq data pathway analysis should be pursued for the entire experimental set-up on both MCF7 and ZR-75-1 cell lines, therefore effect of ALDO and/or ALDO-SPIRO would better reflect the ALDO-mediated MR signaling in breast cancer cells.

REFERENCES

Abellaneda, J. M., Martínez-Alarcón, L., Quereda, J. J., Herrero-Medrano, J. M., Mendonça, L., Mrowiec, A., García-Nicolás, O., Pallarés, F. J., Ríos, A., Muñoz, A., Ramírez, P., & Ramis, G. (2015). Validation of a quantitative polymerase chain reaction method for human alu gene detection in microchimeric pigs used as donors for xenotransplantation. *Transplantation Proceedings*. https://doi.org/10.1016/j.transproceed.2014.11.016

Agarwal, M. K., Mirshahi, F., Mirshahi, M., & Rostene, W. (1993). Immunochemical detection of the mineralocorticoid receptor in rat brain. *Neuroendocrinology*. https://doi.org/10.1159/000126593

Alnemri, E. S., Maksymowych, A. B., Robertson, N. M., & Litwack, G. (1991). Overexpression and characterization of the human mineralocorticoid receptor. *Journal of Biological Chemistry*.

Annila, T., Lihavainen, E., Marques, I. J., Williams, D. R., Yli-Harja, O., & Ribeiro, A. (2013). ZebIAT, an image analysis tool for registering zebrafish embryos and quantifying cancer metastasis. *BMC Bioinformatics*. https://doi.org/10.1186/1471-2105-14-S10-S5

Antelmi, E., Cardone, R. A., Greco, M. R., Rubino, R., Di Sole, F., Martino, N. A., Casavola, V., Carcangiu, M. L., Moro, L., & Reshkin, S. J. (2013). ß1 Integrin Binding Phosphorylates Ezrin at T567 to Activate a Lipid Raft Signalsome Driving Invadopodia Activity and Invasion. *PLoS ONE*. https://doi.org/10.1371/journal.pone.0075113

Arriza, J. L., Weinberger, C., Cerelli, G., Glaser, T. M., Handelin, B. L., Housman, D. E., & Evans, R. M. (1987). Cloning of human mineralocorticoid receptor complementary DNA: Structural and functional kinship with the glucocorticoid receptor. *Science*. https://doi.org/10.1126/science.3037703

Arroyo, J. P., Lagnaz, D., Ronzaud, C., Vázquez, N., Ko, B. S., Moddes, L., Ruffieux-Daidié, D., Hausel, P., Koesters, R., Yang, B., Stokes, J. B., Hoover, R. S., Gamba, G., & Staub, O. (2011). Nedd4-2 modulates renal Na+-Cl- cotransporter via the aldosterone-SGK1-Nedd4-2 pathway. *Journal of the American Society of Nephrology*. https://doi.org/10.1681/ASN.2011020132

Avci, M. E., Keskus, A. G., Targen, S., Isilak, M. E., Ozturk, M., Atalay, R. C., Adams, M. M., & Konu, O. (2018). Development of a novel zebrafish xenograft model in ache mutants using liver cancer cell lines. *Scientific Reports*, *8*(1), 1570. https://doi.org/10.1038/s41598-018-19817-w

Balsamo, A., Cicognani, A., Gennari, M., Sippell, W. G., Menabò, S., Baronio, F., & Riepe, F. G. (2007). Functional characterization of naturally occurring NR3C2 gene mutations in Italian patients suffering from pseudohypoaldosteronism type 1. *European Journal of Endocrinology*. https://doi.org/10.1530/eje.1.02330

Banasavadi-Siddegowda, Y. K., Welker, A. M., An, M., Yang, X., Zhou, W., Shi, G., Imitola, J., Li, C., Hsu, S., Wang, J., Phelps, M., Zhang, J., Beattie, C. E., Baiocchi, R., & Kaur, B. (2018). PRMT5 as a druggable target for glioblastoma therapy. *Neuro-Oncology*. https://doi.org/10.1093/neuonc/nox206

Bansal, N., Davis, S., Tereshchenko, I., Budak-Alpdogan, T., Zhong, H., Stein, M. N., Kim, I. Y., Dipaola, R. S., Bertino, J. R., & Sabaawy, H. E. (2014). Enrichment of human prostate cancer cells with tumor initiating properties in mouse and zebrafish xenografts by differential adhesion. *Prostate*, *74*(2), 187–

200. https://doi.org/10.1002/pros.22740
Bar, J., Ding, K., Zhao, H., Han, L., Laurie, S. A., Seymour, L., Addison, C. L., Shepherd, F. A., Goss, G. D., Dimitroulakos, J., & Bradbury, P. A. (2015). Angiotensin-converting enzyme and aldosterone serum levels as prognostic and predictive biomarkers for cediranib in NCIC Clinical Trials Group Study BR.24. *Clinical Lung Cancer*, *16*(6), e189–e201. https://doi.org/10.1016/j.cllc.2015.05.002
Barrett Mueller, K., Lu, Q., Mohammad, N. N., Luu, V., McCurley, A., Williams, G. H., Adler, G. K., Karas, R. H., & Jaffe, I. Z. (2014). Estrogen receptor inhibits mineralocorticoid receptor transcriptional regulatory function. *Endocrinology*. https://doi.org/10.1210/en.2014-1270
Behra, M., Cousin, X., Bertrand, C., Vonesch, J. L., Biellmann, D., Chatonnet, A., & Strähle, U. (2002). Acetylcholinesterase is required for neuronal and muscular development in the zebrafish embryo. *Nature Neuroscience*. https://doi.org/10.1038/nn788
Bledsoe, R. K., Madauss, K. P., Holt, J. A., Apolito, C. J., Lambert, M. H., Pearce, K. H., Stanley, T. B., Stewart, E. L., Trump, R. P., Willson, T. H., & Williams, S. P. (2005). A ligand-mediated hydrogen bond network required for the activation of the mineralocorticoid receptor. *Journal of Biological Chemistry*. https://doi.org/10.1074/jbc.M504098200
Bosma, G. C., Custer, R. P., & Bosma, M. J. (1983). A severe combined immunodeficiency mutation in the mouse. *Nature*. https://doi.org/10.1038/301527a0
Bosma, M. J., & Carroll, A. M. (1991). The scid mouse mutant: Definition, characterization, and potential uses. In *Annual Review of Immunology*. https://doi.org/10.1146/annurev.iy.09.040191.001543
Brennan, F. E., & Fuller, P. J. (2000). Rapid upregulation of serum and glucocorticoid-regulated kinase (sgk) gene expression by corticosteroids in vivo. *Molecular and Cellular Endocrinology*. https://doi.org/10.1016/S0303-7207(00)00274-4
Britto, D. D., Wyroba, B., Chen, W., Lockwood, R. A., Tran, K. B., Shepherd, P. R., Hall, C. J., Crosier, K. E., Crosier, P. S., & Astin, J. W. (2018). Macrophages enhance Vegfa-driven angiogenesis in an embryonic zebrafish tumour xenograft model. *DMM Disease Models and Mechanisms*. https://doi.org/10.1242/dmm.035998
Bult, C. J., Krupke, D. M., Begley, D. A., Richardson, J. E., Neuhauser, S. B., Sundberg, J. P., & Eppig, J. T. (2015). Mouse Tumor Biology (MTB): A database of mouse models for human cancer. *Nucleic Acids Research*. https://doi.org/10.1093/nar/gku987
Bult, C. J., Krupke, D. M., & Eppig, J. T. (1999). Electronic access to mouse tumor data: The Mouse Tumor Biology Database (MTB) project. In *Nucleic Acids Research*. https://doi.org/10.1093/nar/27.1.99
Cabezas-Sainz, P., Guerra-Varela, J., Carreira, M. J., Mariscal, J., Roel, M., Rubiolo, J. A., Sciara, A. A., Abal, M., Botana, L. M., López, R., & Sánchez, L. (2018). Improving zebrafish embryo xenotransplantation conditions by increasing incubation temperature and establishing a proliferation index with ZFtool. *BMC Cancer*. https://doi.org/10.1186/s12885-017-3919-8
Cai, W. Y., Wei, T. Z., Luo, Q. C., Wu, Q. W., Liu, Q. F., Yang, M., Ye, G. D., Wu, J. F., Chen, Y. Y., Sun, G. Bin, Liu, Y. J., Zhao, W. X., Zhang, Z. M., & Li, B. A. (2013). The wnt-β-catenin pathway represses let-7 microrna expression

through transactivation of Lin28 to augment breast cancer stem cell expansion. *Journal of Cell Science*. https://doi.org/10.1242/jcs.123810

Cao, J., Pontes, K. C. S., Heijkants, R. C., Brouwer, N. J., Groenewoud, A., Jordanova, E. S., Marinkovic, M., van Duinen, S., Teunisse, A. F. A. S., Verdijk, R. M., Snaar-Jagalska, E., Jochemsen, A. G., & Jager, M. J. (2018). Overexpression of EZH2 in conjunctival melanoma offers a new therapeutic target. *Journal of Pathology*. https://doi.org/10.1002/path.5094

Cao, Y., Hoeppner, L. H., Bach, S., Guangqi, E., Guo, Y., Wang, E., Wu, J., Cowley, M. J., Chang, D. K., Waddell, N., Grimmond, S. M., Biankin, A. V., Daly, R. J., Zhang, X., & Mukhopadhyay, D. (2013). Neuropilin-2 promotes extravasation and metastasis by interacting with endothelial α5 integrin. *Cancer Research*, *73*(14), 4579–4590. https://doi.org/10.1158/0008-5472.CAN-13-0529

Cerami, E., Gao, J., Dogrusoz, U., Gross, B. E., Sumer, S. O., Aksoy, B. A., Jacobsen, A., Byrne, C. J., Heuer, M. L., Larsson, E., Antipin, Y., Reva, B., Goldberg, A. P., Sander, C., & Schultz, N. (2012). The cBio Cancer Genomics Portal: An open platform for exploring multidimensional cancer genomics data. *Cancer Discovery*. https://doi.org/10.1158/2159-8290.CD-12-0095

Chan, X. Y., Black, R., Dickerman, K., Federico, J., Levesque, M., Mumm, J., & Gerecht, S. (2015). Three-Dimensional Vascular Network Assembly from Diabetic Patient-Derived Induced Pluripotent Stem Cells. *Arteriosclerosis, Thrombosis, and Vascular Biology*. https://doi.org/10.1161/ATVBAHA.115.306362

Chapman, K., Holmes, M., & Seckl, J. (2013). 11β-hydroxysteroid dehydrogenases intracellular gate-keepers of tissue glucocorticoid action. *Physiological Reviews*. https://doi.org/10.1152/physrev.00020.2012

Chen, S. Y., Bhargava, A., Mastroberardino, L., Meijer, O. C., Wang, J., Buse, P., Firestone, G. L., Verrey, F., & Pearce, D. (1999). Epithelial sodium channel regulated by aldosterone-induced protein sgk. *Proceedings of the National Academy of Sciences of the United States of America*. https://doi.org/10.1073/pnas.96.5.2514

Cheng, J., Gu, Y. J., Wang, Y., Cheng, S. H., & Wong, W. T. (2011). Nanotherapeutics in angiogenesis: synthesis and in vivo assessment of drug efficacy and biocompatibility in zebrafish embryos. *International Journal of Nanomedicine*. https://doi.org/10.2147/ijn.s20145

Ciccarone, F., De Falco, P., & Rosa Ciriolo, M. (2020). Aconitase 2 sensitizes MCF-7 cells to cisplatin eliciting p53-mediated apoptosis in a ROS-dependent manner. *Biochemical Pharmacology*. https://doi.org/10.1016/j.bcp.2020.114202

Coban, B. (2016). *REGULATION OF MINERALOCORTICOID RECEPTOR AND ITS DOWNSTREAM TARGETS BY ESTROGEN AND ALDOSTERONE IN BREAST CANCER*. Bilkent University.

Conde, I., Paniagua, R., Fraile, B., Lucio, J., & Arenas, M. I. (2008). Glucocorticoid receptor changes its cellular location with breast cancer development. *Histol Histopathol*, *23*(1), 77–85. http://www.ncbi.nlm.nih.gov/entrez/query.fcgi?cmd=Retrieve&db=PubMed&dopt=Citation&list_uids=17952860

Conte, N., Mason, J., Halmagyi, C., Neuhauser, S. B., Mosaku, A., Begley, D. A., Krupke, D. M., Parkinson, H., Meehan, T., & Bult, C. J. (2018). PDX Finder: A Portal for Patient-Derived tumor Xenograft Model Discovery. *BioRxiv*. https://doi.org/10.1101/291443

Corkery, D. P., Clarke, L. E., Gebremeskel, S., Salsman, J., Pinder, J., Le Page, C.,

Meunier, L., Xu, Z., Mes-Masson, A. M., Berman, J. N., Johnston, B., & Dellaire, G. (2018). Loss of PRP4K drives anoikis resistance in part by dysregulation of epidermal growth factor receptor endosomal trafficking. *Oncogene*, *37*(2), 174–184. https://doi.org/10.1038/onc.2017.318

Corkery, Dale P., Dellaire, G., & Berman, J. N. (2011). Leukaemia xenotransplantation in zebrafish - chemotherapy response assay in vivo. In *British Journal of Haematology* (Vol. 153, Issue 6, pp. 786–789). https://doi.org/10.1111/j.1365-2141.2011.08661.x

De Azevedo Delou, J. M., Lopes, A. G., & Capella, M. A. M. (2014). Effects of angiotensin, vasopressin and aldosterone on proliferation of MCF-7 cells and their sensitivity to doxorubicin. *Anticancer Research*.

De Boeck, M., Cui, C., Mulder, A. A., Jost, C. R., Ikeno, S., & Dijke, P. Ten. (2016). Smad6 determines BMP-regulated invasive behaviour of breast cancer cells in a zebrafish xenograft model. *Scientific Reports*. https://doi.org/10.1038/srep24968

Debonneville, C., Flores, S. Y., Kamynina, E., Plant, P. J., Tauxe, C., Thomas, M. A., Münster, C., Chraïbi, A., Pratt, J. H., Horisberger, J. D., Pearce, D., Loffing, J., & Staub, O. (2001). Phosphorylation of Nedd4-2 by Sgk1 regulates epithelial Na+ channel cell surface expression. *EMBO Journal*. https://doi.org/10.1093/emboj/20.24.7052

Di Fabio, F., Alvarado, C., Majdan, A., Gologan, A., Voda, L., Mitmaker, E., Beitel, L. K., Gordon, P. H., & Trifiro, M. (2007). Underexpression of mineralocorticoid receptor in colorectal carcinomas and association with VEGFR-2 overexpression. *J Gastrointest Surg*, *11*(11), 1521–1528. http://www.ncbi.nlm.nih.gov/entrez/query.fcgi?cmd=Retrieve&db=PubMed&dopt=Citation&list_uids=17703341

Eden, C. J., Ju, B., Murugesan, M., Phoenix, T. N., Nimmervoll, B., Tong, Y., Ellison, D. W., Finkelstein, D., Wright, K., Boulos, N., Dapper, J., Thiruvenkatam, R., Lessman, C. A., Taylor, M. R., & Gilbertson, R. J. (2015). Orthotopic models of pediatric brain tumors in zebrafish. *Oncogene*. https://doi.org/10.1038/onc.2014.107

Eguiara, A., Holgado, O., Beloqui, I., Abalde, L., Sanchez, Y., Callol, C., & Martin, A. G. (2011). Xenografts in zebrafish embryos as a rapid functional assay for breast cancer stem-like cell identification. *Cell Cycle*, *10*(21), 3751–3757. https://doi.org/10.4161/cc.10.21.17921

Fan, Y., Xue, W., Schachner, M., & Zhao, W. (2019). Honokiol eliminates glioma/glioblastoma stem cell-like cells via JAK-STAT3 signaling and inhibits tumor progression by targeting epidermal growth factor receptor. *Cancers*. https://doi.org/10.3390/cancers11010022

Faresse, N., Vitagliano, J. J., & Staub, O. (2012). Differential ubiquitylation of the mineralocorticoid receptor is regulated by phosphorylation. *FASEB Journal*. https://doi.org/10.1096/fj.12-209924

Feldman, R. D., Ding, Q., Hussain, Y., Limbird, L. E., Pickering, J. G., & Gros, R. (2016). Aldosterone mediates metastatic spread of renal cancer via the G protein-coupled estrogen receptor (GPER). *FASEB Journal*, *30*(6), 2086–2096. https://doi.org/10.1096/fj.15-275552

Fior, R., Póvoa, V., Mendes, R. V., Carvalho, T., Gomes, A., Figueiredo, N., & Ferreira, F. R. (2017). Single-cell functional and chemosensitive profiling of combinatorial colorectal therapy in zebrafish xenografts. *Proceedings of the National Academy of Sciences of the United States of America*. https://doi.org/10.1073/pnas.1618389114

Flanagan, S. P. (1966). 'Nude', a new hairless gene with pleiotropic effects in the mouse. *Genetical Research*. https://doi.org/10.1017/S0016672300010168

Fu, A., Peh, Y. M., Ngan, W., Wei, N., & Luo, K. Q. (2018). Rapid identification of antimicrometastases drugs using integrated model systems with two dimensional monolayer, three dimensional spheroids, and zebrafish xenotransplantation tumors. *Biotechnology and Bioengineering*. https://doi.org/10.1002/bit.26816

Fukushima, K., Sasano, H., Sasaki, I., Nagura, H., Funayama, Y., & Matsuno, S. (1994). Increased expression of mineralocorticoid receptor in human ileum after total colectomy: Immunohistochemical and immunoblotting studies. *Tohoku Journal of Experimental Medicine*. https://doi.org/10.1620/tjem.173.383

Fuller, P. J., & Funder, J. W. (1976). Mineralocorticoid and glucocorticoid receptors in human kidney. *Kidney International*, *10*(2), 154–157.

Fuller, P. J., & Young, M. J. (2005). Mechanisms of mineralocorticoid action. In *Hypertension*. https://doi.org/10.116110.1161/01.HYP.0000193502.77417.17

Funder, J. W., Feldman, D., & Edelman, I. S. (1972). Specific aldosterone binding in rat kidney and parotid. *Journal of Steroid Biochemistry*. https://doi.org/10.1016/0022-4731(72)90052-0

Gacha-Garay, M. J., Niño-Joya, A. F., Bolaños, N. I., Abenoza, L., Quintero, G., Ibarra, H., Gonzalez, J. M., Akle, V., & Garavito-Aguilar, Z. V. (2019). Pilot study of an integrative new tool for studying clinical outcome discrimination in acute leukemia. *Frontiers in Oncology*. https://doi.org/10.3389/fonc.2019.00245

Gamble, J. T., Reed-Harris, Y., Barton, C. L., La Du, J., Tanguay, R., & Greenwood, J. A. (2018). Quantification of glioblastoma progression in zebrafish xenografts: Adhesion to laminin alpha 5 promotes glioblastoma microtumor formation and inhibits cell invasion. *Biochemical and Biophysical Research Communications*. https://doi.org/10.1016/j.bbrc.2018.10.076

Gaytan-Cervantes, J., Gonzalez-Torres, C., Maldonado, V., Zampedri, C., Ceballos-Cancino, G., & Melendez-Zajgla, J. (2017). Protein Sam68 regulates the alternative splicing of survivin DEx3. *Journal of Biological Chemistry*. https://doi.org/10.1074/jbc.M117.800318

Ghotra, V. P. S., He, S., de Bont, H., van der Ent, W., Spaink, H. P., van de Water, B., Snaar-Jagalska, B. E., & Danen, E. H. J. (2012). Automated whole animal bio-imaging assay for human cancer dissemination. *PloS One*, *7*(2), e31281. https://doi.org/10.1371/journal.pone.0031281

Gianoncelli, A., Guarienti, M., Fragni, M., Bertuzzi, M., Rossini, E., Abate, A., Basnet, R. M., Zizioli, D., Bono, F., Terzolo, M., Memo, M., Berruti, A., & Sigala, S. (2019). Adrenocortical Carcinoma Xenograft in Zebrafish Embryos as a Model To Study the In Vivo Cytotoxicity of Abiraterone Acetate. *Endocrinology*. https://doi.org/10.1210/en.2019-00152

Greco, M. R., Bon, E., Rubino, R., Guerra, L., Bernabe-Garcia, M., Cannone, S., Cayuela, M. L., Ciaccia, L., Marionneau-Lambot, S., Oullier, T., Fromont, G., Guibon, R., Roger, S., Reshkin, S. J., & Cardone, R. A. (2019). Phosphorylation of NHERF1 S279 and S301 differentially regulates breast cancer cell phenotype and metastatic organotropism. *Biochimica et Biophysica Acta - Molecular Basis of Disease*. https://doi.org/10.1016/j.bbadis.2018.10.017

Grossmann, C., Husse, B., Mildenberger, S., Schreier, B., Schuman, K., & Gekle, M. (2010). Colocalization of mineralocorticoid and EGF receptor at the plasma membrane. *Biochimica et Biophysica Acta - Molecular Cell Research*. https://doi.org/10.1016/j.bbamcr.2010.02.008

Haas, J. G., Weber, J., Gonzalez, O., Zimmer, R., & Griffiths, S. J. (2018). Antiviral activity of the mineralocorticoid receptor NR3C2 against Herpes simplex virus Type 1 (HSV-1) infection. *Scientific Reports*. https://doi.org/10.1038/s41598-018-34241-w

Hadzhiev, Y., Miguel-Escalada, I., Balciunas, D., & Müller, F. (2016). Testing of Cis-regulatory elements by targeted transgene integration in Zebrafish using PhiC31 integrase. In *Methods in Molecular Biology*. https://doi.org/10.1007/978-1-4939-3771-4_6

Halasz, M., Polgar, B., Berta, G., Czimbalek, L., & Szekeres-Bartho, J. (2013). Progesterone-induced blocking factor differentially regulates trophoblast and tumor invasion by altering matrix metalloproteinase activity. *Cellular and Molecular Life Sciences*. https://doi.org/10.1007/s00018-013-1404-3

Hamilton, N., Sabroe, I., & Renshaw, S. A. (2018). A method for transplantation of human HSCs into zebrafish, to replace humanised murine transplantation models [version 1; referees: 2 approved]. *F1000Research*. https://doi.org/10.12688/f1000research.14507.1

Han, H. W., & Hsu, S. hui. (2016). Chitosan-hyaluronan based 3D co-culture platform for studying the crosstalk of lung cancer cells and mesenchymal stem cells. *Acta Biomaterialia*. https://doi.org/10.1016/j.actbio.2016.06.014

He, Sheng, Hu, B., Li, C., Lin, P., Tang, W. G., Sun, Y. F., Feng, F. Y. M., Guo, W., Li, J., Xu, Y., Yao, Q. L., Zhang, X., Qiu, S. J., Zhou, J., Fan, J., Li, Y. X., Li, H., & Yang, X. R. (2018). PDXliver: A database of liver cancer patient derived xenograft mouse models. *BMC Cancer*. https://doi.org/10.1186/s12885-018-4459-6

He, Shuning, Lamers, G. E. M., Beenakker, J. W. M., Cui, C., Ghotra, V. P. S., Danen, E. H. J., Meijer, A. H., Spaink, H. P., & Snaar-Jagalska, B. E. (2012). Neutrophil-mediated experimental metastasis is enhanced by VEGFR inhibition in a zebrafish xenograft model. *Journal of Pathology*. https://doi.org/10.1002/path.4013

Helsen, C., & Claessens, F. (2014). Looking at nuclear receptors from a new angle. *Molecular and Cellular Endocrinology*, *382*(1), 97–106. https://doi.org/10.1016/j.mce.2013.09.009

Hernández-Díaz, I., Giraldez, T., Arnau, M. R., Smits, V. A. J., Jaisser, F., Farman, N., & Alvarez De La Rosa, D. (2010). The mineralocorticoid receptor is a constitutive nuclear factor in cardiomyocytes due to hyperactive nuclear localization signals. *Endocrinology*. https://doi.org/10.1210/en.2010-0099

Hollenbach, M., Stoll, S. J., Jörgens, K., Seufferlein, T., & Kroll, J. (2013). Different Regulation of Physiological and Tumor Angiogenesis in Zebrafish by Protein Kinase D1 (PKD1). *PLoS ONE*. https://doi.org/10.1371/journal.pone.0068033

Hubert, E. L., Teissier, R., Fernandes-Rosa, F. L., Fay, M., Rafestin-Oblin, M. E., Jeunemaitre, X., Metz, C., Escoubet, B., & Zennaro, M. C. (2011). Mineralocorticoid receptor mutations and a severe recessive pseudohypoaldosteronism type 1. *Journal of the American Society of Nephrology*. https://doi.org/10.1681/ASN.2011030245

Igoucheva, O., Alexeev, V., & Yoon, K. (2006). Differential cellular responses to exogenous DNA in mammalian cells and its effect on oligonucleotide-directed gene modification. *Gene Therapy*. https://doi.org/10.1038/sj.gt.3302643

Jääskeläinen, A., Jukkola, A., Haapasaari, K. M., Auvinen, P., Soini, Y., & Karihtala, P. (2019). Cytoplasmic Mineralocorticoid Receptor Expression Predicts Dismal Local Relapse-free Survival in Non-triple-negative Breast

Cancer. *Anticancer Research*. https://doi.org/10.21873/anticanres.13792
Jensen, E. C. (2012). Use of Fluorescent Probes: Their Effect on Cell Biology and Limitations. In *Anatomical Record*. https://doi.org/10.1002/ar.22602
Jeong, Y., Xie, Y., Xiao, G., Behrens, C., Girard, L., Wistuba II, Minna, J. D., & Mangelsdorf, D. J. (2010). Nuclear receptor expression defines a set of prognostic biomarkers for lung cancer. *PLoS Med*, *7*(12), e1000378. https://doi.org/10.1371/journal.pmed.1000378
Jerónimo, A., Rodrigues, G., Vilas-Boas, F., Martins, G. G., Bagulho, A., & Real, C. (2017). Hydrogen peroxide regulates angiogenesis-related factors in tumor cells. *Biochemistry and Cell Biology*. https://doi.org/10.1139/bcb-2017-0083
Jin, S. W., Beis, D., Mitchell, T., Chen, J. N., & Stainier, D. Y. R. (2005). Cellular and molecular analyses of vascular tube and lumen formation in zebrafish. *Development*. https://doi.org/10.1242/dev.02087
Jung, I. H., Chung, Y. Y., Jung, D. E., Kim, Y. J., Kim, D. H., Kim, K. S., & Park, S. W. (2016). Impaired Lymphocytes Development and Xenotransplantation of Gastrointestinal Tumor Cells in Prkdc-Null SCID Zebrafish Model. *Neoplasia (United States)*, *18*(8), 468–479. https://doi.org/10.1016/j.neo.2016.06.007
Jung, J., Seol, H. S., & Chang, S. (2018). The generation and application of patient-derived xenograft model for cancer research. In *Cancer Research and Treatment*. https://doi.org/10.4143/crt.2017.307
Karkampouna, S., van der Helm, D., Gray, P. C., Chen, L., Klima, I., Grosjean, J., Burgmans, M. C., Farina-Sarasqueta, A., Snaar-Jagalska, E. B., Stroka, D. M., Terracciano, L., van Hoek, B., Schaapherder, A. F., Osanto, S., Thalmann, G. N., Verspaget, H. W., Coenraad, M. J., & Kruithof-de Julio, M. (2018). CRIPTO promotes an aggressive tumour phenotype and resistance to treatment in hepatocellular carcinoma. *Journal of Pathology*. https://doi.org/10.1002/path.5083
Kenouch, S., Lombes, M., Delahaye, F., Eugene, E., Bonvalet, J. P., & Farman, N. (1994). Human skin as target for aldosterone: coexpression of mineralocorticoid receptors and 11 beta-hydroxysteroid dehydrogenase. *The Journal of Clinical Endocrinology & Metabolism*. https://doi.org/10.1210/jcem.79.5.7962326
Khan, N., Mahajan, N. K., Sinha, P., & Jayandharan, G. R. (2019). An efficient method to generate xenograft tumor models of acute myeloid leukemia and hepatocellular carcinoma in adult zebrafish. *Blood Cells, Molecules, and Diseases*. https://doi.org/10.1016/j.bcmd.2018.12.007
King, S., Bray, S., Galbraith, S., Christie, L., & Fleming, S. (2014). Evidence for aldosterone-dependent growth of renal cell carcinoma. *International Journal of Experimental Pathology*, *95*(4), 244–250. https://doi.org/10.1111/iep.12074
Kolla, V., & Litwack, G. (2000). Inhibition of mineralocorticoid-mediated transcription by NF-κB. *Archives of Biochemistry and Biophysics*. https://doi.org/10.1006/abbi.2000.2045
Konu, O., & Targen, S. (2019). Investigating the Role of Mineralocorticoid Receptor Signaling in Cancer Biology in the Genomic Era. In *Aldosterone-Mineralocorticoid Receptor - Cell Biology to Translational Medicine*. https://doi.org/10.5772/intechopen.87233
Koyama, K., Myles, K., Smith, R., & Krozowski, Z. (2001). Expression of the 11??-hydroxysteroid dehydrogenase type II enzyme in breast tumors and modulation of activity and cell growth in PMC42 cells. *Journal of Steroid Biochemistry and Molecular Biology*, *76*(1–5), 153–159. https://doi.org/10.1016/S0960-0760(00)00157-6

Krupke, D. M., Begley, D. A., Sundberg, J. P., Bult, C. J., & Eppig, J. T. (2008). The mouse tumor biology database. In *Nature Reviews Cancer*. https://doi.org/10.1038/nrc2390

Lai, Y. J., Tsai, J. C., Tseng, Y. T., Wu, M. S., Liu, W. S., Lam, H. I., Yu, J. H., Nozell, S. E., & Benveniste, E. N. (2017). Small G protein Rac GTPases regulate the maintenance of glioblastoma stem-like cells in vitro and in vivo. *Oncotarget*. https://doi.org/10.18632/oncotarget.14949

Lam, S. H., Chua, H. L., Gong, Z., Lam, T. J., & Sin, Y. M. (2004). Development and maturation of the immune system in zebrafish, Danio rerio: A gene expression profiling, in situ hybridization and immunological study. *Developmental and Comparative Immunology*. https://doi.org/10.1016/S0145-305X(03)00103-4

Lamb, R., Ablett, M. P., Spence, K., Landberg, G., Sims, A. H., & Clarke, R. B. (2013). Wnt Pathway Activity in Breast Cancer Sub-Types and Stem-Like Cells. *PLoS ONE*. https://doi.org/10.1371/journal.pone.0067811

Lánczky, A., Nagy, Á., Bottai, G., Munkácsy, G., Szabó, A., Santarpia, L., & Győrffy, B. (2016). miRpower: a web-tool to validate survival-associated miRNAs utilizing expression data from 2178 breast cancer patients. *Breast Cancer Research and Treatment*. https://doi.org/10.1007/s10549-016-4013-7

Lara, R., Mauri, F. A., Taylor, H., Derua, R., Shia, A., Gray, C., Nicols, A., Shiner, R. J., Schofield, E., Bates, P. A., Waelkens, E., Dallman, M., Lamb, J., Zicha, D., Downward, J., Seckl, M. J., & Pardo, O. E. (2011). An siRNA screen identifies RSK1 as a key modulator of lung cancer metastasis. *Oncogene*. https://doi.org/10.1038/onc.2011.61

Lawson, N. D., & Weinstein, B. M. (2002). In vivo imaging of embryonic vascular development using transgenic zebrafish. *Developmental Biology*. https://doi.org/10.1006/dbio.2002.0711

Leali, D., Bianchi, R., Bugatti, A., Nicoli, S., Mitola, S., Ragona, L., Tomaselli, S., Gallo, G., Catello, S., Rivieccio, V., Zetta, L., & Presta, M. (2010). Fibroblast growth factor 2-antagonist activity of a long-pentraxin 3-derived anti-angiogenic pentapeptide. *Journal of Cellular and Molecular Medicine*. https://doi.org/10.1111/j.1582-4934.2009.00855.x

Lee, L. M. J., Seftor, E. a, Bonde, G., Cornell, R. a, & Hendrix, M. J. C. (2005). The fate of human malignant melanoma cells transplanted into zebrafish embryos: assessment of migration and cell division in the absence of tumor formation. *Developmental Dynamics : An Official Publication of the American Association of Anatomists*, *233*(4), 1560–1570. https://doi.org/10.1002/dvdy.20471

Leo, J. C., Guo, C., Woon, C. T., Aw, S. E., & Lin, V. C. (2004). Glucocorticoid and mineralocorticoid cross-talk with progesterone receptor to induce focal adhesion and growth inhibition in breast cancer cells. *Endocrinology*, *145*(3), 1314–1321. http://www.ncbi.nlm.nih.gov/entrez/query.fcgi?cmd=Retrieve&db=PubMed&dopt=Citation&list_uids=14617569

Leung, A. W. Y., Veinotte, C. J., Melong, N., Oh, M. H., Chen, K., Enfield, K. S. S., Backstrom, I., Warburton, C., Yapp, D., Berman, J. N., Bally, M. B., & Lockwood, W. W. (2017). In vivo validation of PAPSS1(3′-phosphoadenosine 5′-phosphosulfate synthase 1) as a cisplatin-sensitizing therapeutic target. *Clinical Cancer Research*. https://doi.org/10.1158/1078-0432.CCR-17-0700

Li, J., Zeng, G., Qi, Y., Tang, X., Zhang, J., Wu, Z., Liang, J., Shi, L., Liu, H., & Zhang, P. (2015). Xenotransplantation of human adipose-derived stem cells in zebrafish embryos. *PLoS ONE*. https://doi.org/10.1371/journal.pone.0123264

Liekens, S., Noppen, S., Gijsbers, S., Sienaert, R., Ronca, R., Tobia, C., & Presta, M. (2015). The broad-spectrum anti-DNA virus agent cidofovir inhibits lung metastasis of virus-independent, FGF2-driven tumors. *Oncotarget*. https://doi.org/10.18632/oncotarget.3079

Lin, H. S., Huang, Y. L., Wang, Y. R., Hsiao, E., Hsu, T. A., Shiao, H. Y., Jiaang, W. T., Sampurna, B. P., Lin, K. H., Wu, M. S., Lai, G. M., & Yuh, C. H. (2019). Identification of novel anti-liver cancer small molecules with better therapeutic index than sorafenib via zebrafish drug screening platform. *Cancers*. https://doi.org/10.3390/cancers11060739

Liu, W., Lo, Y. L., Hsu, C., Wu, Y. T., Liao, Z. X., Wu, W. J., Chen, Y. J., Kao, C., Chiu, C. C., & Wang, L. F. (2019). CS-PEI/Beclin-siRNA Downregulate Multidrug Resistance Proteins and Increase Paclitaxel Therapeutic Efficacy against NSCLC. *Molecular Therapy - Nucleic Acids*. https://doi.org/10.1016/j.omtn.2019.06.017

Loffing, J., Zecevic, M., Féraille, E., Kaissling, B., Asher, C., Rossier, B. C., Firestone, G. L., Pearce, D., & Verrey, F. (2001). Aldosterone induces rapid apical translocation of ENaC in early portion of renal collecting system: Possible role of SGK. *American Journal of Physiology - Renal Physiology*. https://doi.org/10.1152/ajprenal.2001.280.4.f675

Lombès, M., Oblin, M. E., Gasc, J. M., Baulieu, E. E., Farman, N., & Bonvalet, J. P. (1992). Immunohistochemical and biochemical evidence for a cardiovascular mineralocorticoid receptor. *Circulation Research*. https://doi.org/10.1161/01.res.71.3.503

Marques, I. J., Weiss, F. U., Vlecken, D. H., Nitsche, C., Bakkers, J., Lagendijk, A. K., Partecke, L. I., Heidecke, C. D., Lerch, M. M., & Bagowski, C. P. (2009). Metastatic behaviour of primary human tumours in a zebrafish xenotransplantation model. *BMC Cancer*. https://doi.org/10.1186/1471-2407-9-128

Marranci, A., D'Aurizio, R., Vencken, S., Mero, S., Guzzolino, E., Rizzo, M., Pitto, L., Pellegrini, M., Chiorino, G., Greene, C. M., & Poliseno, L. (2019). Systematic evaluation of the microRNAome through miR-CATCHv2.0 identifies positive and negative regulators of BRAF-X1 mRNA. *RNA Biology*. https://doi.org/10.1080/15476286.2019.1600934

Martinez-Ordoñez, A., Seoane, S., Cabezas, P., Eiro, N., Sendon-Lago, J., MacIa, M., Garcia-Caballero, T., Gonzalez, L. O., Sanchez, L., Vizoso, F., & Perez-Fernandez, R. (2018). Breast cancer metastasis to liver and lung is facilitated by Pit-1-CXCL12-CXCR4 axis. *Oncogene*, *37*(11), 1430–1444. https://doi.org/10.1038/s41388-017-0036-8

Matulich, D. T., Spindler, B. J., Schambelan, M., & Baxter, J. D. (1976). Mineralocorticoid receptors in human kidney. *J Clin Endocrinol Metab*, *43*(5), 1170–1174.

Mazumder, A., Lee, J. Y., Talhi, O., Cerella, C., Chateauvieux, S., Gaigneaux, A., Hong, C. R., Kang, H. J., Lee, Y., Kim, K. W., Kim, D. W., Shin, H. Y., Dicato, M., Bachari, K., Silva, A. M. S., Orlikova-Boyer, B., & Diederich, M. (2018). Hydroxycoumarin OT-55 kills CML cells alone or in synergy with imatinib or Synribo: Involvement of ER stress and DAMP release. *Cancer Letters*. https://doi.org/10.1016/j.canlet.2018.07.041

McBride, C., Gaupp, D., & Phinney, D. G. (2003). Quantifying levels of transplanted murine and human mesenchymal stem cells in vivo by realtime PCR. *Cytotherapy*. https://doi.org/10.1080/14653240310000038

Meehan, T. F., Conte, N., Goldstein, T., Inghirami, G., Murakami, M. A., Brabetz, S., Gu, Z., Wiser, J. A., Dunn, P., Begley, D. A., Krupke, D. M., Bertotti, A., Bruna, A., Brush, M. H., Byrne, A. T., Caldas, C., Christie, A. L., Clark, D. A., Dowst, H., … Bult, C. J. (2017). PDX-MI: Minimal information for patient-derived tumor xenograft models. *Cancer Research*. https://doi.org/10.1158/0008-5472.CAN-17-0582

Mercatali, L., La Manna, F., Groenewoud, A., Casadei, R., Recine, F., Miserocchi, G., Pieri, F., Liverani, C., Bongiovanni, A., Spadazzi, C., de Vita, A., van der Pluijm, G., Giorgini, A., Biagini, R., Amadori, D., Ibrahim, T., & Snaar-Jagalska, E. (2016). Development of a patient-derived xenograft (PDX) of breast cancer bone metastasis in a Zebrafish model. *International Journal of Molecular Sciences*, *17*(8). https://doi.org/10.3390/ijms17081375

Mi, H., Dong, Q., Muruganujan, A., Gaudet, P., Lewis, S., & Thomas, P. D. (2009). PANTHER version 7: Improved phylogenetic trees, orthologs and collaboration with the Gene Ontology Consortium. *Nucleic Acids Research*. https://doi.org/10.1093/nar/gkp1019

Mira, E., Lacalle, R. A., Gómez-Moutón, C., Leonardo, E., & Mañes, S. (2002). Quantitative determination of tumor cell intravasation in a real-time polymerase chain reaction-based assay. *Clinical and Experimental Metastasis*. https://doi.org/10.1023/A:1015563031769

Mizgirev, I. V., & Revskoy, S. (2010). A new zebrafish model for experimental leukemia therapy. *Cancer Biology and Therapy*. https://doi.org/10.4161/cbt.9.11.11667

Moore, J. C., Tang, Q., Yordán, N. T., Moore, F. E., Garcia, E. G., Lobbardi, R., Ramakrishnan, A., Marvin, D. L., Anselmo, A., Sadreyev, R. I., & Langenau, D. M. (2016). Single-cell imaging of normal and malignant cell engraftment into optically clear prkdc-null scid zebrafish. *Journal of Experimental Medicine*. https://doi.org/10.1084/jem.20160378

Moshal, K. S., Ferri-Lagneau, K. F., Haider, J., Pardhanani, P., & Leung, T. C. (2011). Discriminating different cancer cells using a zebrafish in vivo assay. *Cancers*. https://doi.org/10.3390/cancers3044102

Myles, K., & Funder, J. W. (1996). Progesterone binding to mineralocorticoid receptors: In vitro and in vivo studies. *American Journal of Physiology - Endocrinology and Metabolism*. https://doi.org/10.1152/ajpendo.1996.270.4.e601

Naber, H. P. H., Drabsch, Y., Snaar-Jagalska, B. E., ten Dijke, P., & van Laar, T. (2013). Snail and Slug, key regulators of TGF-β-induced EMT, are sufficient for the induction of single-cell invasion. *Biochemical and Biophysical Research Communications*. https://doi.org/10.1016/j.bbrc.2013.04.037

Nehmann, N., Wicklein, D., Schumacher, U., & Müller, R. (2010). Comparison of two techniques for the screening of human tumor cells in mouse blood: Quantitative real-time polymerase chain reaction (qRT-PCR) versus laser scanning cytometry (LSC). *Acta Histochemica*. https://doi.org/10.1016/j.acthis.2009.05.004

Nicoli, S., & Presta, M. (2007). The zebrafish/tumor xenograft angiogenesis assay. *Nature Protocols*. https://doi.org/10.1038/nprot.2007.412

Nicoli, S., Ribatti, D., Cotelli, F., & Presta, M. (2007). Mammalian tumor xenografts induce neovascularization in zebrafish embryos. *Cancer Research*, *67*(7), 2927–2931. https://doi.org/10.1158/0008-5472.CAN-06-4268

Nie, H., Li, J., Yang, X. M., Cao, Q. Z., Feng, M. X., Xue, F., Wei, L., Qin, W., Gu,

J., Xia, Q., & Zhang, Z. G. (2015). Mineralocorticoid receptor suppresses cancer progression and the Warburg effect by modulating the miR-338-3p-PKLR axis in hepatocellular carcinoma. *Hepatology*, *62*(4), 1145–1159. https://doi.org/10.1002/hep.27940

Nouri, M., Caradec, J., Lubik, A. A., Li, N., Hollier, B. G., Takhar, M., Altimirano-Dimas, M., Chen, M., Roshan-Moniri, M., Butler, M., Lehman, M., Bishop, J., Truong, S., Huang, S. C., Cochrane, D., Cox, M., Collins, C., Gleave, M., Erho, N., … Buttyan, R. (2017). Therapy-induced developmental reprogramming of prostate cancer cells and acquired therapy resistance. *Oncotarget*. https://doi.org/10.18632/oncotarget.14850

Olszewski, M. B., Pruszko, M., Snaar-Jagalska, E., Zylicz, A., & Zylicz, M. (2019). Diverse and cancer type-specific roles of the p53 R248Q gain-of-function mutation in cancer migration and invasiveness. *International Journal of Oncology*. https://doi.org/10.3892/ijo.2019.4723

Orlova, V. V., Van Den Hil, F. E., Petrus-Reurer, S., Drabsch, Y., Ten Dijke, P., & Mummery, C. L. (2014). Generation, expansion and functional analysis of endothelial cells and pericytes derived from human pluripotent stem cells. *Nature Protocols*, *9*(6), 1514–1531. https://doi.org/10.1038/nprot.2014.102

Ou, X. M., Storring, J. M., Kushwaha, N., & Albert, P. R. (2001). Heterodimerization of Mineralocorticoid and Glucocorticoid Receptors at a Novel Negative Response Element of the 5-HT1A Receptor Gene. *Journal of Biological Chemistry*. https://doi.org/10.1074/jbc.M005363200

Pantelouris, E. M. (1968). Absence of thymus in a mouse mutant. In *Nature*. https://doi.org/10.1038/217370a0

Park, S. J., Kim, J. G., Kim, N. D., Yang, K., Shim, J. W., & Heo, K. (2016). Estradiol, TGF-β1 and hypoxia promote breast cancer stemness and EMT-mediated breast cancer migration. *Oncology Letters*. https://doi.org/10.3892/ol.2016.4115

Patel, N., Klassert, T. E., Greco, S. J., Patel, S. A., Munoz, J. L., Reddy, B. Y., Bryan, M., Campbell, N., Kokorina, N., Sabaawy, H. E., & Rameshwar, P. (2012). Developmental regulation of TAC1 in peptidergic-induced human mesenchymal stem cells: Implication for spinal cord injury in zebrafish. *Stem Cells and Development*. https://doi.org/10.1089/scd.2011.0179

Pressley, L., & Funder, J. W. (1975). Glucocorticoid and mineralocorticoid receptors in gut mucosa. *Endocrinology*, *97*(3), 588–596. https://doi.org/10.1210/endo-97-3-588

Prigent, J., Herrero, A., Ambroise, J., Smets, F., Deblandre, G. A., & Sokal, E. M. (2015). Human progenitor cell quantification after xenotransplantation in rat and mouse models by a sensitive qPCR assay. *Cell Transplantation*, *24*(8), 1639–1652. https://doi.org/10.3727/096368914X681955

Prochazka, M., Gaskins, H. R., Shultz, L. D., & Leiter, E. H. (1992). The nonobese diabetic scid mouse: Model for spontaneous thymomagenesis associated with immunodeficiency. *Proceedings of the National Academy of Sciences of the United States of America*. https://doi.org/10.1073/pnas.89.8.3290

Rajan, V., Melong, N., Wong, W. H., King, B., Tong, R. S., Mahajan, N., Gaston, D., Lund, T., Rittenberg, D., Dellaire, G., Campbell, C. J. V., Druley, T., & Berman, J. N. (2019). Humanized zebrafish enhance human hematopoietic stem cell survival and promote acute myeloid leukemia clonal diversity. *Haematologica*. https://doi.org/10.3324/haematol.2019.223040

Riepe, F. G., Finkeldei, J., De Sanctis, L., Einaudi, S., Testa, A., Karges, B., Peter,

M., Viemann, M., Grötzinger, J., Sippell, W. G., Fejes-Toth, G., & Krone, N. (2006). Elucidating the underlying molecular pathogenesis of NR3C2 mutants causing autosomal dominant pseudohypoaldosteronism type 1. *Journal of Clinical Endocrinology and Metabolism*. https://doi.org/10.1210/jc.2006-1161

Rigiracciolo, D. C., Scarpelli, A., Lappano, R., Pisano, A., Santolla, M. F., Avino, S., De Marco, P., Bussolati, B., Maggiolini, M., & De Francesco, E. M. (2016). GPER is involved in the stimulatory effects of aldosterone in breast cancer cells and breast tumor-derived endothelial cells. *Oncotarget*. https://doi.org/10.18632/oncotarget.6475

Robinson-Rechavi, M., Garcia, H. E., & Laudet, V. (2003). The nuclear receptor superfamily. In *Journal of Cell Science*. https://doi.org/10.1242/jcs.00247

Rodriguez, G. V., Abrahamsson, A., Jensen, L. D. E., & Dabrosin, C. (2017). Estradiol promotes breast cancer cell migration via recruitment and activation of neutrophils. *Cancer Immunology Research*. https://doi.org/10.1158/2326-6066.CIR-16-0150

Rousseau, G., Baxter, J. D., Funder, J. W., Edelman, I. S., & Tomkins, G. M. (1972). Glucocorticoid and mineralocorticoid receptors for aldosterone. *Journal of Steroid Biochemistry*. https://doi.org/10.1016/0022-4731(72)90053-2

Rupprecht, R., Arriza, J. L., Spengler, D., Reul, J. M. H. M., Evans, R. M., Holsboer, F., & Damm, K. (1993). Transactivation and synergistic properties of the mineralocorticoid receptor: Relationship to the glucocorticoid receptor. *Molecular Endocrinology*. https://doi.org/10.1210/mend.7.4.8388999

Sandquist, E. J., Essner, J. J., & Sakaguchi, D. S. (2018). Xenotransplantation of adult hippocampal neural progenitors into the developing zebrafish for assessment of stem cell plasticity. *PLoS ONE*. https://doi.org/10.1371/journal.pone.0198025

Sasano, H., Fukushima, K., Sasaki, I., Matsuno, S., Nagura, H., & Krozowski, Z. S. (1992). Immunolocalization of mineralocorticoid receptor in human kidney, pancreas, salivary, mammary and sweat glands: A light and electron microscopic immunohistochemical study. *Journal of Endocrinology*. https://doi.org/10.1677/joe.0.1320305

Sasano, Hironobu, Frost, A. R., Saitohi, R., Matsunaga, G., Nagura, H., Krozowski, Z. S., & Silverberg, S. G. (1997). Localization of mineralocorticoid receptor and 11 beta-hydroxysteroid dehydrogenase type II in human breast and its disorders. *Anticancer Research*.

Shackleton, M., Vaillant, F., Simpson, K. J., Stingl, J., Smyth, G. K., Asselin-Labat, M. L., Wu, L., Lindeman, G. J., & Visvader, J. E. (2006). Generation of a functional mammary gland from a single stem cell. *Nature*. https://doi.org/10.1038/nature04372

Shi, L., Sheng, J., Wang, M., Luo, H., Zhu, J., Zhang, B., Liu, Z., & Yang, X. (2019). Combination Therapy of TGF-β Blockade and Commensal-derived Probiotics Provides Enhanced Antitumor Immune Response and Tumor Suppression. *Theranostics*. https://doi.org/10.7150/thno.35131

Shibata, S., Rinehart, J., Zhang, J., Moeckel, G., Castañeda-Bueno, M., Stiegler, A. L., Boggon, T. J., Gamba, G., & Lifton, R. P. (2013). Mineralocorticoid receptor phosphorylation regulates ligand binding and renal response to volume depletion and hyperkalemia. *Cell Metabolism*. https://doi.org/10.1016/j.cmet.2013.10.005

Shinkai, Y., Rathbun, 0Gary, Lam, K. P., Oltz, E. M., Stewart, V., Mendelsohn, M., Charron, J., Datta, M., Young, F., Stall, A. M., & Alt, F. W. (1992). RAG-2-

deficient mice lack mature lymphocytes owing to inability to initiate V(D)J rearrangement. *Cell*. https://doi.org/10.1016/0092-8674(92)90029-C

Shipitsin, M., Campbell, L. L., Argani, P., Weremowicz, S., Bloushtain-Qimron, N., Yao, J., Nikolskaya, T., Serebryiskaya, T., Beroukhim, R., Hu, M., Halushka, M. K., Sukumar, S., Parker, L. M., Anderson, K. S., Harris, L. N., Garber, J. E., Richardson, A. L., Schnitt, S. J., Nikolsky, Y., … Polyak, K. (2007). Molecular Definition of Breast Tumor Heterogeneity. *Cancer Cell*. https://doi.org/10.1016/j.ccr.2007.01.013

Sonoyama, Y. K., Tajima, T., Fujimoto, M., Hasegawa, A., Miyahara, N., Nishimura, R., Hashida, Y., Hayashi, A., Hanaki, K., & Kanzaki, S. (2017). A novel frameshift mutation in NR3C2 leads to decreased expression of mineralocorticoid receptor: A family with renal pseudohypoaldosteronism type 1. *Endocrine Journal*. https://doi.org/10.1507/endocrj.EJ16-0280

Spender, L. C., Ferguson, G. J., Liu, S., Cui, C., Girotti, M. R., Sibbet, G., Higgs, E. B., Shuttleworth, M. K., Hamilton, T., Lorigan, P., Weller, M., Vincent, D. F., Sansom, O. J., Frame, M., Dijke, P. ten, Marais, R., & Inman, G. J. (2016). Mutational activation of BRAF confers sensitivity to transforming growth factor beta inhibitors in human cancer cells. *Oncotarget*. https://doi.org/10.18632/oncotarget.13226

Stingl, J., Eirew, P., Ricketson, I., Shackleton, M., Vaillant, F., Choi, D., Li, H. I., & Eaves, C. J. (2006). Purification and unique properties of mammary epithelial stem cells. *Nature*. https://doi.org/10.1038/nature04496

Stoletov, K., Montel, V., Lester, R. D., Gonias, S. L., & Klemke, R. (2007). High-resolution imaging of the dynamic tumor cell vascular interface in transparent zebrafish. *Proceedings of the National Academy of Sciences*, *104*(44), 17406–17411. https://doi.org/10.1073/pnas.0703446104

Sullivan, C., & Kim, C. H. (2008). Innate Immune System of the Zebrafish, Danio rerio. In H. Heine (Ed.), *Innate Immunity of Plants, Animals, and Humans* (pp. 113–133). Springer Berlin Heidelberg. https://doi.org/10.1007/978-3-540-73930-2_6

Sun, Y., Sheng, Z., Ma, C., Tang, K., Zhu, R., Wu, Z., Shen, R., Feng, J., Wu, D., Huang, D., Huang, D., Fei, J., Liu, Q., & Cao, Z. (2015). Combining genomic and network characteristics for extended capability in predicting synergistic drugs for cancer. *Nature Communications*. https://doi.org/10.1038/ncomms9481

Sutanto, W., & de Kloet, E. R. (1991). Mineralocorticoid receptor ligands: biochemical, pharmacological, and clinical aspects. *Med Res Rev*, *11*(6), 617–639. http://www.ncbi.nlm.nih.gov/entrez/query.fcgi?cmd=Retrieve&db=PubMed&dopt=Citation&list_uids=1662327

Suzuki, S., Suzuki, T., Tsubochi, H., Koike, K., Tateno, H., Krozowski, Z. S., & Sasano, H. (2000). Expression of 11β-hydroxysteroid dehydrogenase type 2 and mineralocorticoid receptor in primary lung carcinomas. *Anticancer Research*.

Szklarczyk, D., Franceschini, A., Wyder, S., Forslund, K., Heller, D., Huerta-Cepas, J., Simonovic, M., Roth, A., Santos, A., Tsafou, K. P., Kuhn, M., Bork, P., Jensen, L. J., & Von Mering, C. (2015). STRING v10: Protein-protein interaction networks, integrated over the tree of life. *Nucleic Acids Research*. https://doi.org/10.1093/nar/gku1003

Szklarczyk, D., Gable, A. L., Lyon, D., Junge, A., Wyder, S., Huerta-Cepas, J., Simonovic, M., Doncheva, N. T., Morris, J. H., Bork, P., Jensen, L. J., & Von Mering, C. (2019). STRING v11: Protein-protein association networks with

increased coverage, supporting functional discovery in genome-wide experimental datasets. *Nucleic Acids Research*. https://doi.org/10.1093/nar/gky1131

Tan, D. S. W., Haaland, B., Gan, J. M., Tham, S. C., Sinha, I., Tan, E. H., Lim, K. H., Takano, A., Krisna, S. S., Thu, M. M. M., Liew, H. P., Ullrich, A., Lim, W. T., & Chua, B. T. (2014). Bosutinib inhibits migration and invasion via ack1 in kras mutant non-small cell lung cancer. *Molecular Cancer*. https://doi.org/10.1186/1476-4598-13-13

Tang, Q., Abdelfattah, N. S., Blackburn, J. S., Moore, J. C., Martinez, S. A., Moore, F. E., Lobbardi, R., Tenente, I. M., Ignatius, M. S., Berman, J. N., Liwski, R. S., Houvras, Y., & Langenau, D. M. (2014). Optimized cell transplantation using adult rag2 mutant zebrafsh. *Nature Methods*. https://doi.org/10.1038/nmeth.3031

Tang, Z., Kang, B., Li, C., Chen, T., & Zhang, Z. (2019). GEPIA2: an enhanced web server for large-scale expression profiling and interactive analysis. *Nucleic Acids Research*. https://doi.org/10.1093/nar/gkz430

Tang, Z., Li, C., Kang, B., Gao, G., Li, C., & Zhang, Z. (2017). GEPIA: A web server for cancer and normal gene expression profiling and interactive analyses. *Nucleic Acids Research*. https://doi.org/10.1093/nar/gkx247

Targen, S., Kaya, T., Avci, M. E., Gunes, D., Keskus, A. G., & Konu, O. (2020). ZenoFishDb v1.1: A Database for Xenotransplantation Studies in Zebrafish. *Zebrafish*. https://doi.org/10.1089/zeb.2020.1869

Tenente, I. M., Tang, Q., Moore, J. C., & Langenau, D. M. (2014). Normal and malignant muscle cell transplantation into immune compromised adult zebrafish. *Journal of Visualized Experiments*. https://doi.org/10.3791/52597

Thomas, C., Rajapaksa, G., Nikolos, F., Hao, R., Katchy, A., McCollum, C. W., Bondesson, M., Quinlan, P., Thompson, A., Krishnamurthy, S., Esteva, F. J., & Gustafsson, J. Å. (2012). ERβ1 represses basal-like breast cancer epithelial to mesenchymal transition by destabilizing EGFR. *Breast Cancer Research*. https://doi.org/10.1186/bcr3358

Thomas, P. D., Campbell, M. J., Kejariwal, A., Mi, H., Karlak, B., Daverman, R., Diemer, K., Muruganujan, A., & Narechania, A. (2003). PANTHER: A library of protein families and subfamilies indexed by function. *Genome Research*. https://doi.org/10.1101/gr.772403

Tiberio, L., Nascimbeni, R., Villanacci, V., Casella, C., Fra, A., Vezzoli, V., Furlan, L., Meyer, G., Parrinello, G., Baroni, M. D., Salerni, B., & Schiaffonati, L. (2013). The decrease of mineralcorticoid receptor drives angiogenic pathways in colorectal cancer. *PLoS One*, *8*(3), e59410. https://doi.org/10.1371/journal.pone.0059410

Timmermans-Sprang, E. P. M., Mestemaker, H. M., Steenlage, R. R., & Mol, J. A. (2019). Dasatinib inhibition of cSRC prevents the migration and metastasis of canine mammary cancer cells with enhanced Wnt and HER signalling. *Veterinary and Comparative Oncology*. https://doi.org/10.1111/vco.12490

Topczewska, J. M., Postovit, L. M., Margaryan, N. V., Sam, A., Hess, A. R., Wheaton, W. W., Nickoloff, B. J., Topczewski, J., & Hendrix, M. J. C. (2006). Embryonic and tumorigenic pathways converge via Nodal signaling: Role in melanoma aggressiveness. *Nature Medicine*. https://doi.org/10.1038/nm1448

Tulotta, C., Groenewoud, A., Snaar-Jagalska, B. E., & Ottewell, P. (2019). Animal models of breast cancer bone metastasis. In *Methods in Molecular Biology*. https://doi.org/10.1007/978-1-4939-8997-3_17

van der Ent, W., Burrello, C., de Lange, M. J., van der Velden, P. A., Jochemsen, A. G., Jager, M. J., & Snaar-Jagalska, B. E. (2015). Embryonic Zebrafish: Different Phenotypes after Injection of Human Uveal Melanoma Cells. *Ocular Oncology and Pathology*. https://doi.org/10.1159/000370159

Vazquez Rodriguez, G., Abrahamsson, A., Jensen, L. D. E., & Dabrosin, C. (2018). Adipocytes Promote Early Steps of Breast Cancer Cell Dissemination via Interleukin-8. *Frontiers in Immunology*. https://doi.org/10.3389/fimmu.2018.01767

Veinotte, C. J., Dellaire, G., & Berman, J. N. (2014). Hooking the big one: The potential of zebrafish xenotransplantation to reform cancer drug screening in the genomic era. In *DMM Disease Models and Mechanisms*. https://doi.org/10.1242/dmm.015784

von Mässenhausen, A., Sanders, C., Brägelmann, J., Konantz, M., Queisser, A., Vogel, W., Kristiansen, G., Duensing, S., Schröck, A., Bootz, F., Brossart, P., Kirfel, J., Lengerke, C., & Perner, S. (2016). Targeting DDR2 in head and neck squamous cell carcinoma with dasatinib. *International Journal of Cancer*. https://doi.org/10.1002/ijc.30279

Wang, L., Chen, H., Fei, F., He, X., Sun, S., Lv, K., Yu, B., Long, J., & Wang, X. (2019). Patient-derived Heterogeneous Xenograft Model of Pancreatic Cancer Using Zebrafish Larvae as Hosts for Comparative Drug Assessment. *Journal of Visualized Experiments : JoVE*. https://doi.org/10.3791/59507

Wang, X. Q., Tang, Z. X., Yu, D., Cui, S. J., Jiang, Y. H., Zhang, Q., Wang, J., Yang, P. Y., & Liu, F. (2016). Epithelial but not stromal expression of collagen alpha-1(III) is a diagnostic and prognostic indicator of colorectal carcinoma. *Oncotarget*. https://doi.org/10.18632/oncotarget.6815

Wang, Y., Yu, Y., Tsuyada, A., Ren, X., Wu, X., Stubblefield, K., Rankin-Gee, E. K., & Wang, S. E. (2011). Transforming growth factor-B regulates the sphere-initiating stem cell-like feature in breast cancer through miRNA-181 and ATM. *Oncogene*. https://doi.org/10.1038/onc.2010.531

Weijts, B. G. M. W., Westendorp, B., Hien, B. T., Martínez-López, L. M., Zijp, M., Thurlings, I., Thomas, R. E., Schulte-Merker, S., Bakker, W. J., & De Bruin, A. (2018). Atypical E2Fs inhibit tumor angiogenesis. *Oncogene*. https://doi.org/10.1038/onc.2017.336

Weiss, F. U., Marques, I. J., Woltering, J. M., Vlecken, D. H., Aghdassi, A., Partecke, L. I., Heidecke, C. D., Lerch, M. M., & Bagowski, C. P. (2009). Retinoic Acid Receptor Antagonists Inhibit miR-10a Expression and Block Metastatic Behavior of Pancreatic Cancer. *Gastroenterology*. https://doi.org/10.1053/j.gastro.2009.08.065

Welker, A. M., Jaros, B. D., An, M., & Beattie, C. E. (2017). Changes in tumor cell heterogeneity after chemotherapy treatment in a xenograft model of glioblastoma. *Neuroscience*. https://doi.org/10.1016/j.neuroscience.2017.05.010

White, R. M., Sessa, A., Burke, C., Bowman, T., LeBlanc, J., Ceol, C., Bourque, C., Dovey, M., Goessling, W., Burns, C. E., & Zon, L. I. (2008). Transparent Adult Zebrafish as a Tool for In Vivo Transplantation Analysis. *Cell Stem Cell*. https://doi.org/10.1016/j.stem.2007.11.002

Willett, C. E., Zapata, A. G., Hopkins, N., & Steiner, L. A. (1997). Expression of zebrafish rag genes during early development identifies the thymus. *Developmental Biology*. https://doi.org/10.1006/dbio.1996.8446

Wong, C. W., Zhilenkov, A. V., Kraevaya, O. A., Mischenko, D. V., Troshin, P. A., & Hsu, S. H. (2019). Toward understanding the antitumor effects of water-

soluble fullerene derivatives on lung cancer cells: apoptosis or autophagy pathways? *Journal of Medicinal Chemistry*. https://doi.org/10.1021/acs.jmedchem.9b00652

Wong, E. Y. H., & Herbert, J. (2005). Roles of mineralocorticoid and glucocorticoid receptors in the regulation of progenitor proliferation in the adult hippocampus. *European Journal of Neuroscience*. https://doi.org/10.1111/j.1460-9568.2005.04277.x

Wu, J. Q., Zhai, J., Li, C. Y., Tan, A. M., Wei, P., Shen, L. Z., & He, M. F. (2017). Patient-derived xenograft in zebrafish embryos: A new platform for translational research in gastric cancer. *Journal of Experimental and Clinical Cancer Research*, *36*(1). https://doi.org/10.1186/s13046-017-0631-0

Wu, Qinjie, Deng, S., Li, L., Sun, L., Yang, X., Liu, X., Liu, L., Qian, Z., Wei, Y., & Gong, C. (2013). Biodegradable polymeric micelle-encapsulated quercetin suppresses tumor growth and metastasis in both transgenic zebrafish and mouse models. *Nanoscale*. https://doi.org/10.1039/c3nr04651f

Wu, Qiong, Zheng, K., Huang, X., Li, L., & Mei, W. (2018). Tanshinone-IIA-Based Analogues of Imidazole Alkaloid Act as Potent Inhibitors to Block Breast Cancer Invasion and Metastasis in Vivo. *Journal of Medicinal Chemistry*. https://doi.org/10.1021/acs.jmedchem.8b01018

Xia, H., Bodempudi, V., Benyumov, A., Hergert, P., Tank, D., Herrera, J., Braziunas, J., Larsson, O., Parker, M., Rossi, D., Smith, K., Peterson, M., Limper, A., Jessurun, J., Connett, J., Ingbar, D., Phan, S., Bitterman, P. B., & Henke, C. A. (2014). Identification of a cell-of-origin for fibroblasts comprising the fibrotic reticulum in idiopathic pulmonary fibrosis. *American Journal of Pathology*. https://doi.org/10.1016/j.ajpath.2014.01.012

Xie, X., Shen, Y., Chen, J., Huang, Z., & Ge, J. (2019). Mineralocorticoid receptor deficiency improves the therapeutic effects of mesenchymal stem cells for myocardial infarction via enhanced cell survival. *Journal of Cellular and Molecular Medicine*. https://doi.org/10.1111/jcmm.14026

Xie, Z., Guo, W., Guo, N., Huangfu, M., Liu, H., Lin, M., Xu, W. H., Chen, J., Wang, T. T., Wei, Q., Han, M., & Gao, J. (2018). Targeting tumor hypoxia with stimulus-responsive nanocarriers in overcoming drug resistance and monitoring anticancer efficacy. *Acta Biomaterialia*. https://doi.org/10.1016/j.actbio.2018.03.013

Yakirevich, E., Morris, D. J., Tavares, R., Meitner, P. A., Lechpammer, M., Noble, L., De Rodriguez, A. F., Gomez-Sanchez, C. E., Wang, L. J., Sabo, E., Delellis, R. A., & Resnick, M. B. (2008). Mineralocorticoid receptor and 11β-hydroxysteroid dehydrogenase type II expression in renal cell neoplasms: A tissue microarray and quantitative RT-PCR study. *American Journal of Surgical Pathology*, *32*(6). https://doi.org/10.1097/PAS.0b013e31815f2362

Yamamoto, D., Sato, D., Nakayama, H., Nakagawa, Y., & Shimada, Y. (2019). ZF-Mapper: Simple and Complete Freeware for Fluorescence Quantification in Zebrafish Images. *Zebrafish*. https://doi.org/10.1089/zeb.2018.1683

Yan, C., Brunson, D. C., Tang, Q., Do, D., Iftimia, N. A., Moore, J. C., Hayes, M. N., Welker, A. M., Garcia, E. G., Dubash, T. D., Hong, X., Drapkin, B. J., Myers, D. T., Phat, S., Volorio, A., Marvin, D. L., Ligorio, M., Dershowitz, L., McCarthy, K. M., … Langenau, D. M. (2019). Visualizing Engrafted Human Cancer and Therapy Responses in Immunodeficient Zebrafish. *Cell*. https://doi.org/10.1016/j.cell.2019.04.004

Yang, B., Wang, N., Wang, S., Li, X., Zheng, Y., Li, M., Song, J., Zhang, F., Mei,

W., Lin, Y., & Wang, Z. (2019). Network-pharmacology-based identification of caveolin-1 as a key target of Oldenlandia diffusa to suppress breast cancer metastasis. *Biomedicine and Pharmacotherapy*. https://doi.org/10.1016/j.biopha.2019.108607

Yang, C., Ma, X., Guan, G., Liu, H., Yang, Y., Niu, Q., Wu, Z., Jiang, Y., Bian, C., Zang, Y., & Zhuang, L. (2019). MicroRNA-766 promotes cancer progression by targeting NR3C2 in hepatocellular carcinoma. *FASEB Journal*. https://doi.org/10.1096/fj.201801151R

Yang, J., & Fuller, P. J. (2012). Interactions of the mineralocorticoid receptor - Within and without. In *Molecular and Cellular Endocrinology*. https://doi.org/10.1016/j.mce.2011.07.001

Yang, X. J., Chen, G. L., Yu, S. C., Xu, C., Xin, Y. H., Li, T. T., Shi, Y., Gu, A., Duan, J. J., Qian, C., Cui, Y. H., Zhang, X., & Bian, X. W. (2013). TGF-β1 enhances tumor-induced angiogenesis via JNK pathway and macrophage infiltration in an improved zebrafish embryo/xenograft glioma model. *International Immunopharmacology*. https://doi.org/10.1016/j.intimp.2012.12.002

Yang, X. jun, Cui, W., Gu, A., Xu, C., Yu, S. cang, Li, T. ting, Cui, Y. hong, Zhang, X., & Bian, X. wu. (2013). A Novel Zebrafish Xenotransplantation Model for Study of Glioma Stem Cell Invasion. *PLoS ONE*. https://doi.org/10.1371/journal.pone.0061801

Zhang, B., Shimada, Y., Hirota, T., Ariyoshi, M., Kuroyanagi, J., Nishimura, Y., & Tanaka, T. (2016). Novel immunologic tolerance of human cancer cell xenotransplants in zebrafish. *Translational Research*. https://doi.org/10.1016/j.trsl.2015.12.007

Zhang, B., Shimada, Y., Kuroyanagi, J., Ariyoshi, M., Nomoto, T., Shintou, T., Umemoto, N., Nishimura, Y., Miyazaki, T., & Tanaka, T. (2015). Invivo selective imaging and inhibition of leukemia stem-like cells using the fluorescent carbocyanine derivative, DiOC5(3). *Biomaterials*. https://doi.org/10.1016/j.biomaterials.2015.02.009

Zhang, B., Shimada, Y., Kuroyanagi, J., Nishimura, Y., Umemoto, N., Nomoto, T., Shintou, T., Miyazaki, T., & Tanaka, T. (2014). Zebrafish xenotransplantation model for cancer stem-like cell study and high-throughput screening of inhibitors. *Tumor Biology*. https://doi.org/10.1007/s13277-014-2417-8

Zhang, B., Shimada, Y., Kuroyanagi, J., Umemoto, N., Nishimura, Y., & Tanaka, T. (2014). Quantitative phenotyping-based in vivo chemical screening in a zebrafish model of leukemia stem cell xenotransplantation. *PLoS ONE*. https://doi.org/10.1371/journal.pone.0085439

Zhang, S., Cao, Z., Tian, H., Shen, G., Ma, Y., Xie, H., Liu, Y., Zhao, C., Deng, S., Yang, Y., Zheng, R., Li, W., Zhang, N., Liu, S., Wang, W., Dai, L., Shi, S., Cheng, L., Pan, Y., … Wei, Y. (2011). SKLB1002, a novel potent inhibitor of VEGF receptor 2 signaling, inhibits angiogenesis and tumor growth in vivo. *Clinical Cancer Research*. https://doi.org/10.1158/1078-0432.CCR-10-3109

Zhao, C., Zhang, W., Zhao, Y., Yang, Y., Luo, H., Ji, G., Dong, E., Deng, H., Lin, S., Wei, Y., & Yang, H. (2016). Endothelial Cords Promote Tumor Initial Growth prior to Vascular Function through a Paracrine Mechanism. *Scientific Reports*, *6*. https://doi.org/10.1038/srep19404

Zhao, X., Li, L., Yu, G., Zhang, S., Li, Y., Wu, Q., Huang, X., & Mei, W. (2019). Nucleus-enriched Ruthenium Polypyridine Complex Acts as a Potent Inhibitor to Suppress Triple-negative Breast Cancer Metastasis In vivo. *Computational*

and Structural Biotechnology Journal. https://doi.org/10.1016/j.csbj.2018.11.010

Zhao, Y., Wang, X., Wang, T., Hu, X., Hui, X., Yan, M., Gao, Q., Chen, T., Li, J., Yao, M., Wan, D., Gu, J., Fan, J., & He, X. (2011). Acetylcholinesterase, a key prognostic predictor for hepatocellular carcinoma, suppresses cell growth and induces chemosensitization. *Hepatology*. https://doi.org/10.1002/hep.24079

Zhu, D., Yu, H., He, H., Ding, J., Tang, J., Cao, D., & Hao, L. (2013). Spironolactone inhibits apoptosis in rat mesangial cells under hyperglycaemic conditions via the Wnt signalling pathway. *Molecular and Cellular Biochemistry*. https://doi.org/10.1007/s11010-013-1672-0

Zijlstra, A., Mellor, R., Panzarella, G., Aimes, R. T., Hooper, J. D., Marchenko, N. D., & Quigley, J. P. (2002). A quantitative analysis of rate-limiting steps in the metastatic cascade using human-specific real-time polymerase chain reaction. *Cancer Research*, *62*(23), 7083–7092. https://doi.org/10.1158/0008-5472.can-08-3612

COPY RIGHT PERMISSIONS

Figure 1.1 Schematic representation of a standard zebrafish xenotransplantation procedure applied on zebrafish embryos and adult fish' was manually created with BioRender.com (Basic account).

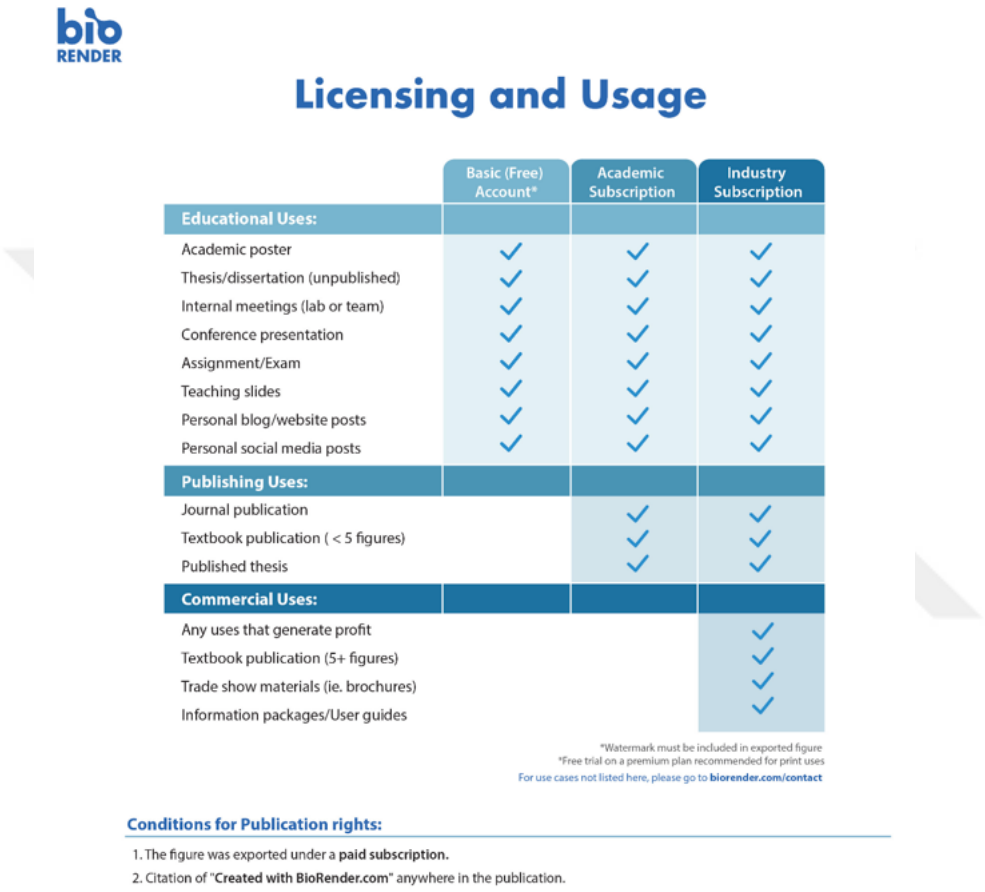

bio RENDER

Licensing and Usage

	Basic (Free) Account*	Academic Subscription	Industry Subscription
Educational Uses:			
Academic poster	✓	✓	✓
Thesis/dissertation (unpublished)	✓	✓	✓
Internal meetings (lab or team)	✓	✓	✓
Conference presentation	✓	✓	✓
Assignment/Exam	✓	✓	✓
Teaching slides	✓	✓	✓
Personal blog/website posts	✓	✓	✓
Personal social media posts	✓	✓	✓
Publishing Uses:			
Journal publication		✓	✓
Textbook publication (< 5 figures)		✓	✓
Published thesis		✓	✓
Commercial Uses:			
Any uses that generate profit			✓
Textbook publication (5+ figures)			✓
Trade show materials (ie. brochures)			✓
Information packages/User guides			✓

*Watermark must be included in exported figure
*Free trial on a premium plan recommended for print uses
For use cases not listed here, please go to **biorender.com/contact**

Conditions for Publication rights:

1. The figure was exported under a **paid subscription.**
2. Citation of "**Created with BioRender.com**" anywhere in the publication.

Figure 1.2 Comparison of ALU-based detection system and laser scanning cytometry system reflecting the number of cells present in colon cancer cell-spiked immune deficient mice blood.' and 'Table 1.1 Numerical representation and statistical analysis of recovered cells of ALU-based detection system and laser scanning cytometry method-based detection.

Images were obtained from N ehmann, N., Wicklein, D., Schumacher, U., & Müller, R. (2010). Comparison of two techniques for the screening of human tumor cells in mouse blood: Quantitative real-time polymerase chain reaction (qRT-PCR) versus laser scanning cytometry (LSC). *Acta Histochemica*. **https://doi.org/10.1016/j.acthis.2009.05.004**)

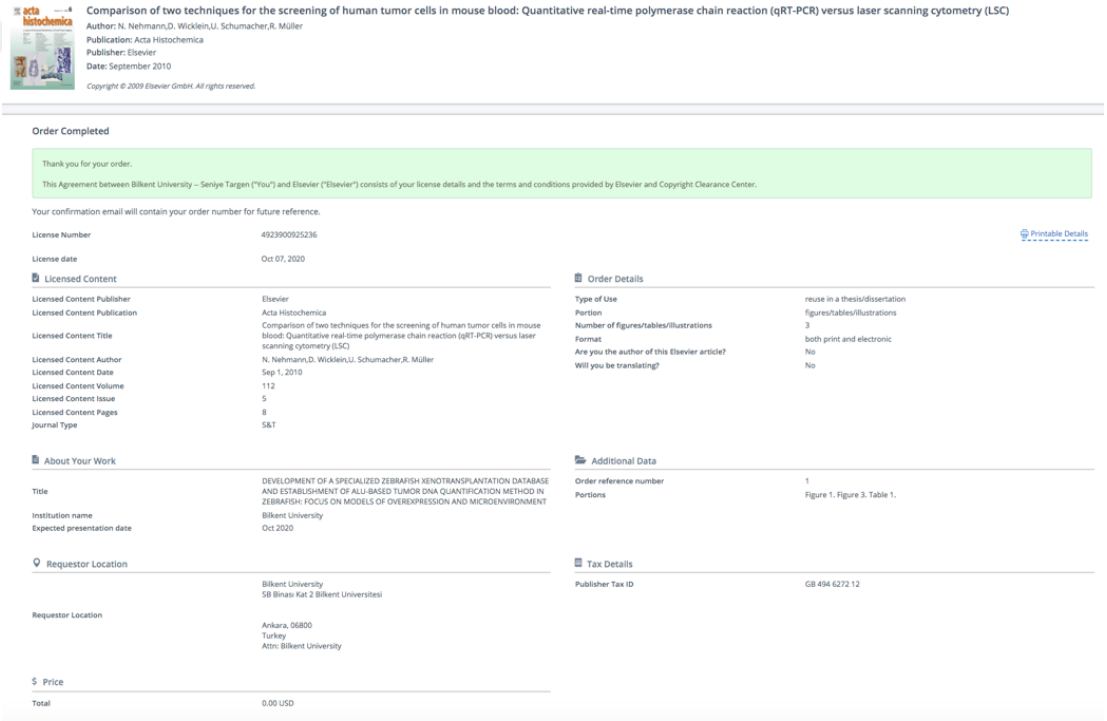

Comparison of two techniques for the screening of human tumor cells in mouse blood: Quantitative real-time polymerase chain reaction (qRT-PCR) versus laser scanning cytometry (LSC)
Author: N. Nehmann,D. Wicklein,U. Schumacher,R. Müller
Publication: Acta Histochemica
Publisher: Elsevier
Date: September 2010
Copyright © 2009 Elsevier GmbH. All rights reserved.

Order Completed

Thank you for your order.

This Agreement between Bilkent University – Seniye Targen ("You") and Elsevier ("Elsevier") consists of your license details and the terms and conditions provided by Elsevier and Copyright Clearance Center.

Your confirmation email will contain your order number for future reference.

Printable Details

License Number	4923900925236
License date	Oct 07, 2020

Licensed Content

Licensed Content Publisher	Elsevier
Licensed Content Publication	Acta Histochemica
Licensed Content Title	Comparison of two techniques for the screening of human tumor cells in mouse blood: Quantitative real-time polymerase chain reaction (qRT-PCR) versus laser scanning cytometry (LSC)
Licensed Content Author	N. Nehmann,D. Wicklein,U. Schumacher,R. Müller
Licensed Content Date	Sep 1, 2010
Licensed Content Volume	112
Licensed Content Issue	5
Licensed Content Pages	8
Journal Type	S&T

Order Details

Type of Use	reuse in a thesis/dissertation
Portion	figures/tables/illustrations
Number of figures/tables/illustrations	3
Format	both print and electronic
Are you the author of this Elsevier article?	No
Will you be translating?	No

About Your Work

Title	DEVELOPMENT OF A SPECIALIZED ZEBRAFISH XENOTRANSPLANTATION DATABASE AND ESTABLISHMENT OF ALU-BASED TUMOR DNA QUANTIFICATION METHOD IN ZEBRAFISH: FOCUS ON MODELS OF OVEREXPRESSION AND MICROENVIRONMENT
Institution name	Bilkent University
Expected presentation date	Oct 2020

Additional Data

Order reference number	1
Portions	Figure 1. Figure 3. Table 1.

Requestor Location

	Bilkent University SB Binası Kat 2 Bilkent Universitesi
Requestor Location	Ankara, 06800 Turkey Attn: Bilkent University

Tax Details

Publisher Tax ID	GB 494 6272 12

Price

Total	0.00 USD

Figure 1.3 Linear regression analysis of ALU-based detection method (AluYb8) performed across different species. A) Human DNA detection in water. B) Human DNA detection in 100ng mice DNA C) Human DNA detection in 200ng rat DNA.

(The copy right permission was taken and this imae was taken from Prigent, J., Herrero, A., Ambroise, J., Smets, F., Deblandre, G. A., & Sokal, E. M. (2015). Human progenitor cell quantification after xenotransplantation in rat and mouse models by a sensitive qPCR assay. *Cell Transplantation*, *24*(8), 1639–1652. https://doi.org/10.3727/096368914X681955).

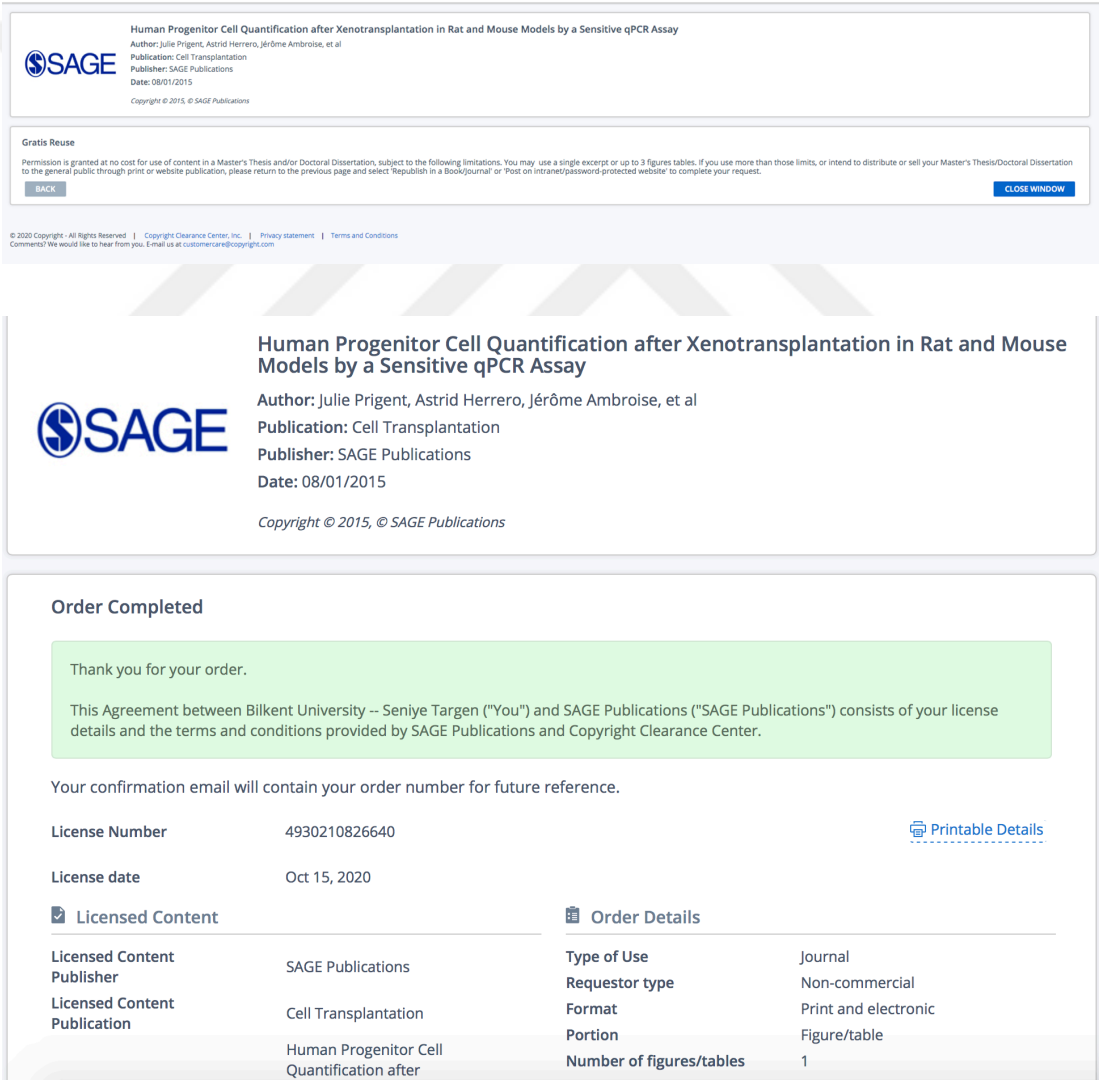

Publication	Cell Transplantation
Licensed Content Title	Human Progenitor Cell Quantification after Xenotransplantation in Rat and Mouse Models by a Sensitive qPCR Assay
Licensed Content Author	Julie Prigent, Astrid Herrero, Jérôme Ambroise, et al
Licensed Content Date	Aug 1, 2015
Licensed Content Volume	24
Licensed Content Issue	8
Licensed Content Pages	14
Portion	Figure/table
Number of figures/tables	1
Will you be translating?	No, only English
Circulation	4

About Your Work

Title of new article	DEVELOPMENT OF A SPECIALIZED ZEBRAFISH XENOTRANSPLANTATION DATABASE AND ESTABLISHMENT OF ALU-BASED TUMOR DNA QUANTIFICATION METHOD IN ZEBRAFISH: FOCUS ON MODELS OF OVEREXPRESSION AND MICROENVIRONMENT
Lead author	seniye targen
Title of targeted journal	not applicable
Publisher	not applicable
Expected publication date	Oct 2020

Additional Data

Order reference number	1
Portions	Figure 2. Linear regression analysis of the AluYb8 qPCR assay and comparison of standards for human cell quantification.

Requestor Location

Requestor Location	Bilkent University SB Binası Kat 2 Merkez Kampus Bilkent Universitesi Ankara Çankaya

Tax Details

Title of new article	DEVELOPMENT OF A SPECIALIZED ZEBRAFISH XENOTRANSPLANTATION DATABASE AND ESTABLISHMENT OF ALU-BASED TUMOR DNA QUANTIFICATION METHOD IN ZEBRAFISH: FOCUS ON MODELS OF OVEREXPRESSION AND MICROENVIRONMENT
Lead author	seniye targen
Title of targeted journal	not applicable
Publisher	not applicable
Expected publication date	Oct 2020
Portions	Figure 2. Linear regression analysis of the AluYb8 qPCR assay and comparison of standards for human cell quantification.

Requestor Location

Requestor Location	Bilkent University SB Binası Kat 2 Merkez Kampus Bilkent Universitesi Ankara Çankaya Ankara, 06800 Turkey Attn: Bilkent University

Tax Details

Billing Information

Billing Type	Credit Card
Credit card info	Master Card ending in 0013
Credit card expiration	02/2022

Price

Total	56.00 USD

Total: 56.00 USD

CLOSE WINDOW ORDER MORE

Human Progenitor Cell Quantification after Xenotransplantation in Rat and Mouse Models by a Sensitive qPCR Assay

Author: Julie Prigent, Astrid Herrero, Jérôme Ambroise, et al
Publication: Cell Transplantation
Publisher: SAGE Publications
Date: 08/01/2015

Order Completed

Thank you for your order.

This Agreement between Bilkent University -- Seniye Targen ("You") and SAGE Publications ("SAGE Publications") consists of your license details and the terms and conditions provided by SAGE Publications and Copyright Clearance Center.

Your confirmation email will contain your order number for future reference.

License Number	4930210826640
License date	Oct 15, 2020

Printable Details

Licensed Content

Licensed Content Publisher	SAGE Publications
Licensed Content Publication	Cell Transplantation
Licensed Content Title	Human Progenitor Cell Quantification after Xenotransplantation in Rat and Mouse Models by a Sensitive qPCR Assay

Order Details

Type of Use	Journal
Requestor type	Non-commercial
Format	Print and electronic
Portion	Figure/table
Number of figures/tables	1
Will you be translating?	No, only English

License date Oct 15, 2020

Licensed Content

Licensed Content Publisher	SAGE Publications
Licensed Content Publication	Cell Transplantation
Licensed Content Title	Human Progenitor Cell Quantification after Xenotransplantation in Rat and Mouse Models by a Sensitive qPCR Assay
Licensed Content Author	Julie Prigent, Astrid Herrero, Jérôme Ambroise, et al
Licensed Content Date	Aug 1, 2015
Licensed Content Volume	24
Licensed Content Issue	8
Licensed Content Pages	14

Order Details

Type of Use	Journal
Requestor type	Non-commercial
Format	Print and electronic
Portion	Figure/table
Number of figures/tables	1
Will you be translating?	No, only English
Circulation	4

About Your Work

Title of new article	DEVELOPMENT OF A SPECIALIZED ZEBRAFISH XENOTRANSPLANTATION DATABASE AND ESTABLISHMENT OF ALU-BASED TUMOR DNA QUANTIFICATION METHOD IN ZEBRAFISH: FOCUS ON MODELS OF OVEREXPRESSION AND MICROENVIRONMENT
Lead author	seniye targen
Title of targeted journal	not applicable
Publisher	not applicable
Expected publication date	Oct 2020

Additional Data

Order reference number	1
Portions	Figure 2. Linear regression analysis of the AluYb8 qPCR assay and comparison of standards for human cell quantification.

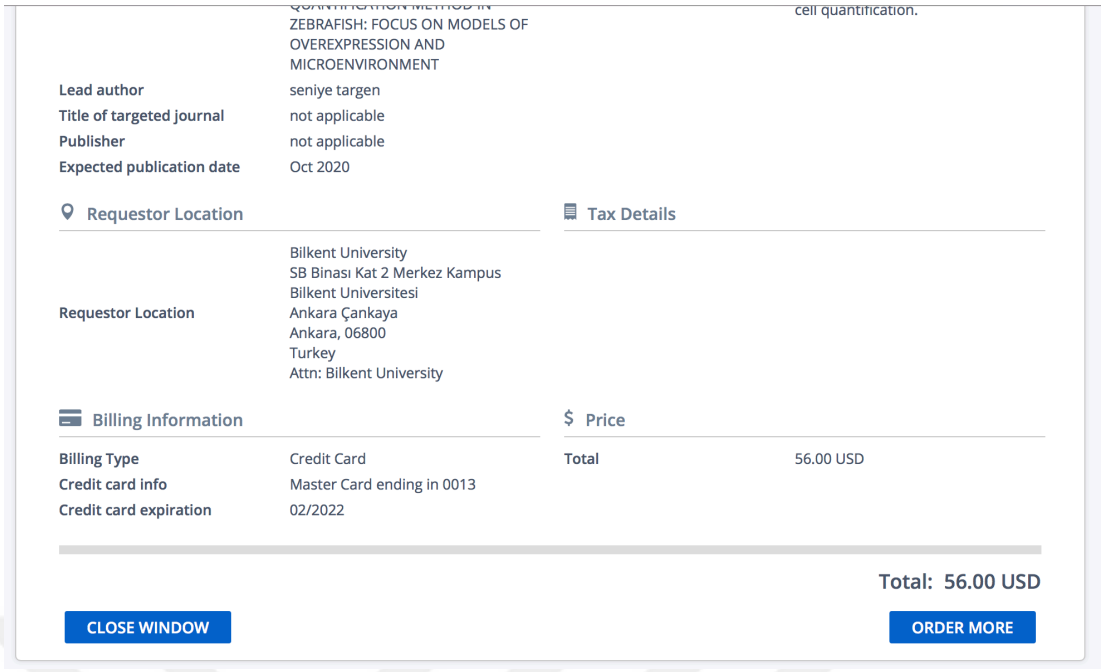
cell quantification.
ZEBRAFISH: FOCUS ON MODELS OF OVEREXPRESSION AND MICROENVIRONMENT
Lead author
seniye targen
Title of targeted journal
not applicable
Publisher
not applicable
Expected publication date
Oct 2020
Requestor Location
Tax Details
Requestor Location
Bilkent University
SB Binası Kat 2 Merkez Kampus
Bilkent Universitesi
Ankara Çankaya
Ankara, 06800
Turkey
Attn: Bilkent University
Billing Information
Price
Billing Type
Credit Card
Credit card info
Master Card ending in 0013
Credit card expiration
02/2022
Total
56.00 USD
Total: 56.00 USD
CLOSE WINDOW
ORDER MORE

Figure 1.4 Schematic representation of different injection sites for xenotransplantation studies in 48hpf fish.

(No copy right permission was required for this figure and the figure was was obtained from (Veinotte et al., 2014) and Veinotte, C. J., Dellaire, G., & Berman, J. N. (2014). Hooking the big one: The potential of zebrafish xenotransplantation to reform cancer drug screening in the genomic era. In *DMM Disease Models and Mechanisms*.)

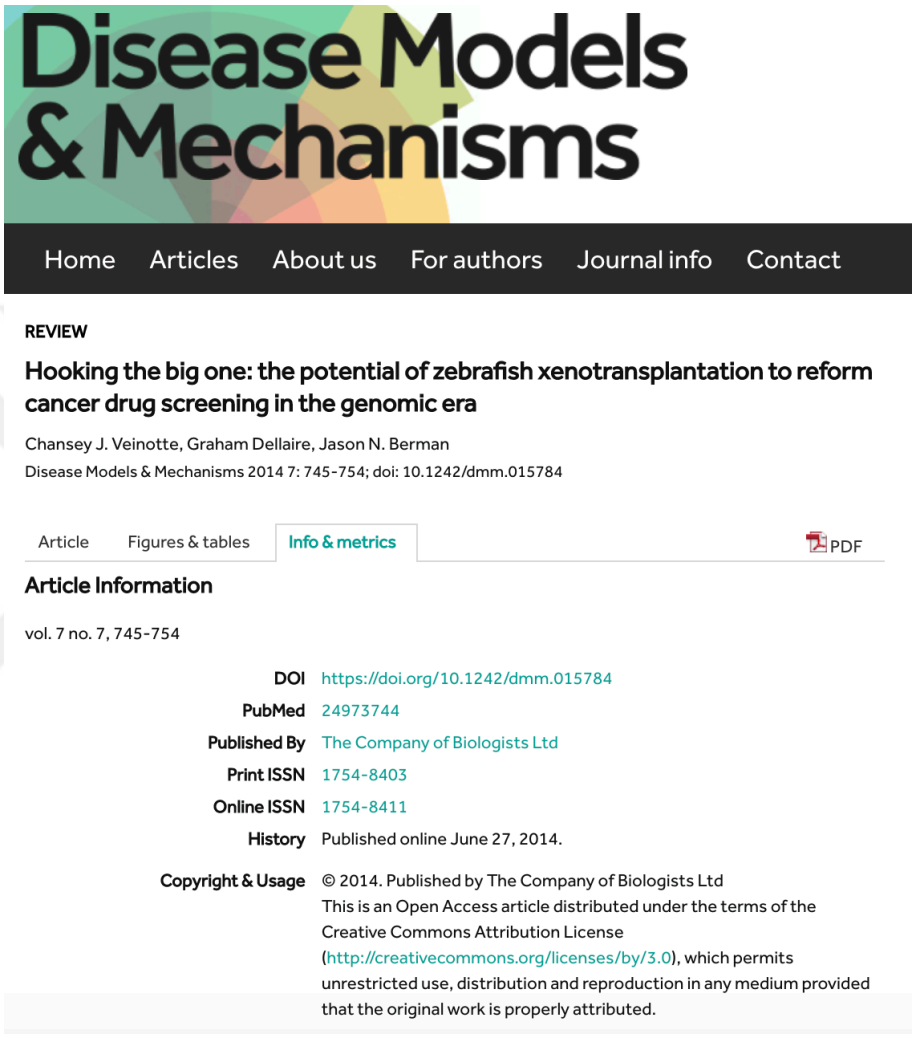

Figure 1.5 Screenshot of Mouse Tumor Biology database advanced search page.

(This image was retrieved from Krupke, D. M., Begley, D. A., Sundberg, J. P., Bult, C. J., & Eppig, J. T. (2008). The mouse tumor biology database. In *Nature Reviews Cancer*. https://doi.org/10.1038/nrc2390).

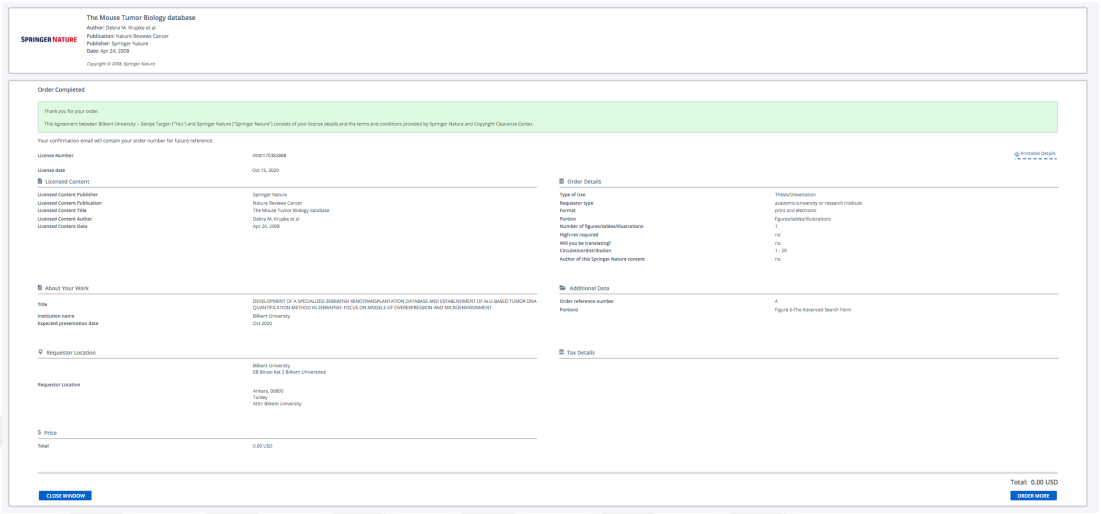

Figure 1. 6 Screenshots of PDX Finder homepage and search page.

(This image was retrieved from Conte, N., Mason, J., Halmagyi, C., Neuhauser, S. B., Mosaku, A., Begley, D. A., Krupke, D. M., Parkinson, H., Meehan, T., & Bult, C. J. (2018). PDX Finder: A Portal for Patient-Derived tumor Xenograft Model Discovery. *BioRxiv*. https://doi.org/10.1101/291443)

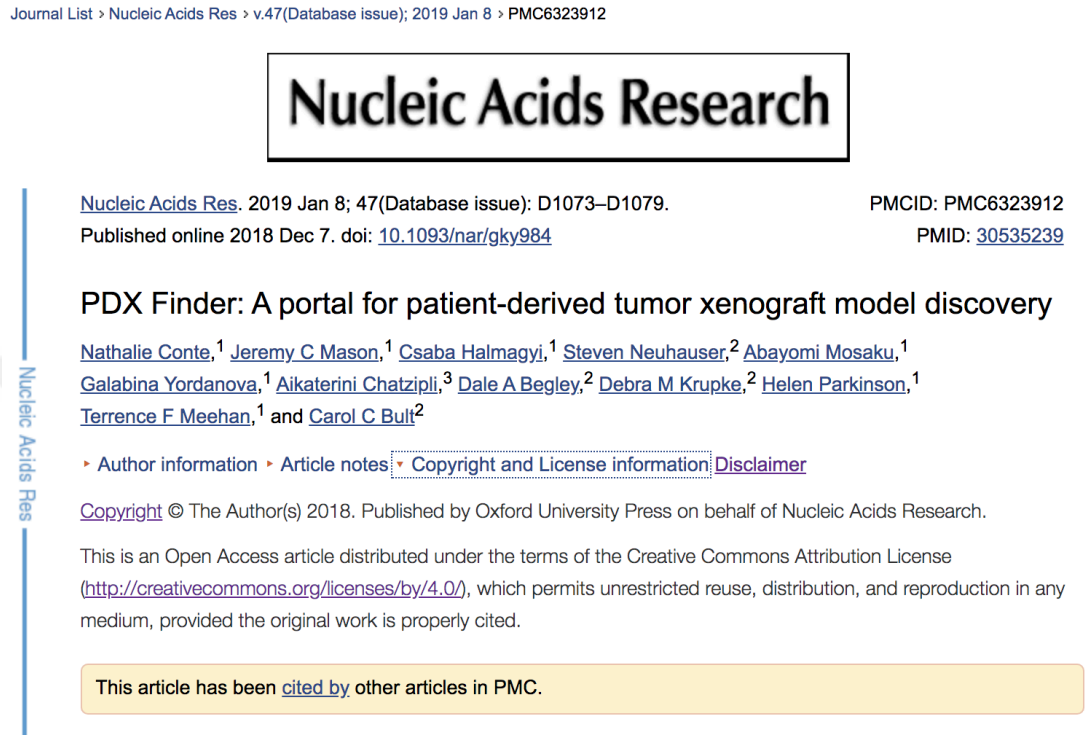

Journal List › Nucleic Acids Res › v.47(Database issue); 2019 Jan 8 › PMC6323912

Nucleic Acids Research

Nucleic Acids Res. 2019 Jan 8; 47(Database issue): D1073–D1079. PMCID: PMC6323912
Published online 2018 Dec 7. doi: 10.1093/nar/gky984 PMID: 30535239

PDX Finder: A portal for patient-derived tumor xenograft model discovery

Nathalie Conte,[1] Jeremy C Mason,[1] Csaba Halmagyi,[1] Steven Neuhauser,[2] Abayomi Mosaku,[1] Galabina Yordanova,[1] Aikaterini Chatzipli,[3] Dale A Begley,[2] Debra M Krupke,[2] Helen Parkinson,[1] Terrence F Meehan,[1] and Carol C Bult[2]

Author information Article notes Copyright and License information Disclaimer

Copyright © The Author(s) 2018. Published by Oxford University Press on behalf of Nucleic Acids Research.

This is an Open Access article distributed under the terms of the Creative Commons Attribution License (http://creativecommons.org/licenses/by/4.0/), which permits unrestricted reuse, distribution, and reproduction in any medium, provided the original work is properly cited.

This article has been cited by other articles in PMC.

Nucleic Acids Res

Figure 1.7 Screenshot of PDXliver browse and search page.

(These images were adapted/retrieved from He, Sheng, Hu, B., Li, C., Lin, P., Tang, W. G., Sun, Y. F., Feng, F. Y. M., Guo, W., Li, J., Xu, Y., Yao, Q. L., Zhang, X., Qiu, S. J., Zhou, J., Fan, J., Li, Y. X., Li, H., & Yang, X. R. (2018). PDXliver: A database of liver cancer patient derived xenograft mouse models. *BMC Cancer*. https://doi.org/10.1186/s12885-018-4459-6).

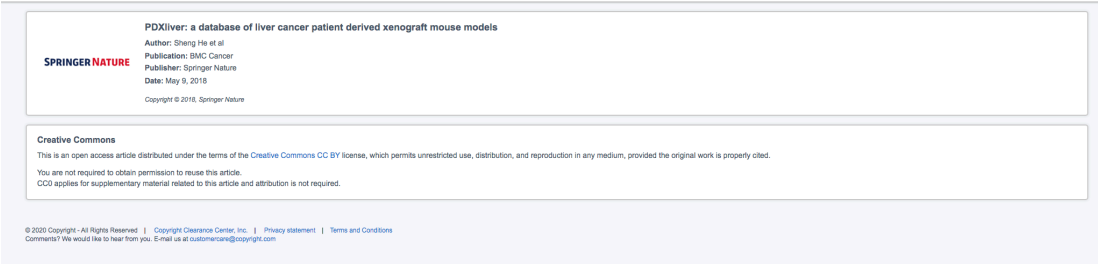

Figure 1. 8 Aldosterone-mediated transactivation of mineralocorticoid receptor.

(This figure was reproduced by copy right permission and was obtained from Yang, J., & Fuller, P. J. (2012). Interactions of the mineralocorticoid receptor - Within and without. In *Molecular and Cellular Endocrinology*. https://doi.org/10.1016/j.mce.2011.07.001 and its use is permitted with copy right permission from Elsevier Publications)

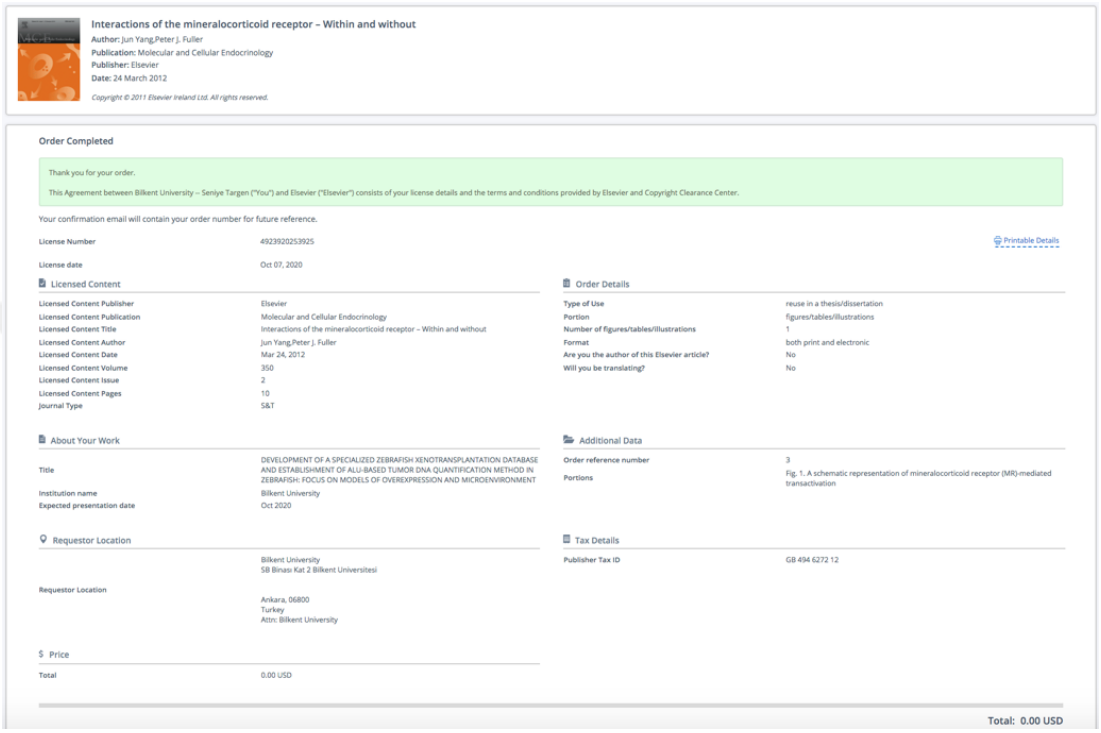

Interactions of the mineralocorticoid receptor – Within and without
Author: Jun Yang,Peter J. Fuller
Publication: Molecular and Cellular Endocrinology
Publisher: Elsevier
Date: 24 March 2012
Copyright © 2011 Elsevier Ireland Ltd. All rights reserved.

Order Completed

Thank you for your order.

This Agreement between Bilkent University – Seniye Targen ("You") and Elsevier ("Elsevier") consists of your license details and the terms and conditions provided by Elsevier and Copyright Clearance Center.

Your confirmation email will contain your order number for future reference.

Printable Details

License Number	4923920253925
License date	Oct 07, 2020

Licensed Content

Licensed Content Publisher	Elsevier
Licensed Content Publication	Molecular and Cellular Endocrinology
Licensed Content Title	Interactions of the mineralocorticoid receptor – Within and without
Licensed Content Author	Jun Yang,Peter J. Fuller
Licensed Content Date	Mar 24, 2012
Licensed Content Volume	350
Licensed Content Issue	2
Licensed Content Pages	10
Journal Type	S&T

Order Details

Type of Use	reuse in a thesis/dissertation
Portion	figures/tables/illustrations
Number of figures/tables/illustrations	1
Format	both print and electronic
Are you the author of this Elsevier article?	No
Will you be translating?	No

About Your Work

Title	DEVELOPMENT OF A SPECIALIZED ZEBRAFISH XENOTRANSPLANTATION DATABASE AND ESTABLISHMENT OF ALU-BASED TUMOR DNA QUANTIFICATION METHOD IN ZEBRAFISH: FOCUS ON MODELS OF OVEREXPRESSION AND MICROENVIRONMENT
Institution name	Bilkent University
Expected presentation date	Oct 2020

Additional Data

Order reference number	3
Portions	Fig. 1. A schematic representation of mineralocorticoid receptor (MR)-mediated transactivation

Requestor Location

	Bilkent University SB Binasi Kat 2 Bilkent Universitesi
Requestor Location	Ankara, 06800 Turkey Attn: Bilkent University

Tax Details

Publisher Tax ID	GB 494 6272 12

$ Price

Total	0.00 USD

Total: 0.00 USD

Figure 1. 9 Aldosterone and mineralocorticoid signaling in a polarized renal cell

(This image was reproducible without the need of copy right permission and required citation and it was obtained from Viengchareun, S., Le Menuet, D., Martinerie, L., Munier, M., Pascual-Le Tallec, L., & Lombes, M. (2007). The mineralocorticoid receptor: insights into its molecular and (patho)physiological biology. *Nucl Recept Signal*, *5*, e012. https://doi.org/10.1621/nrs.05012 .)

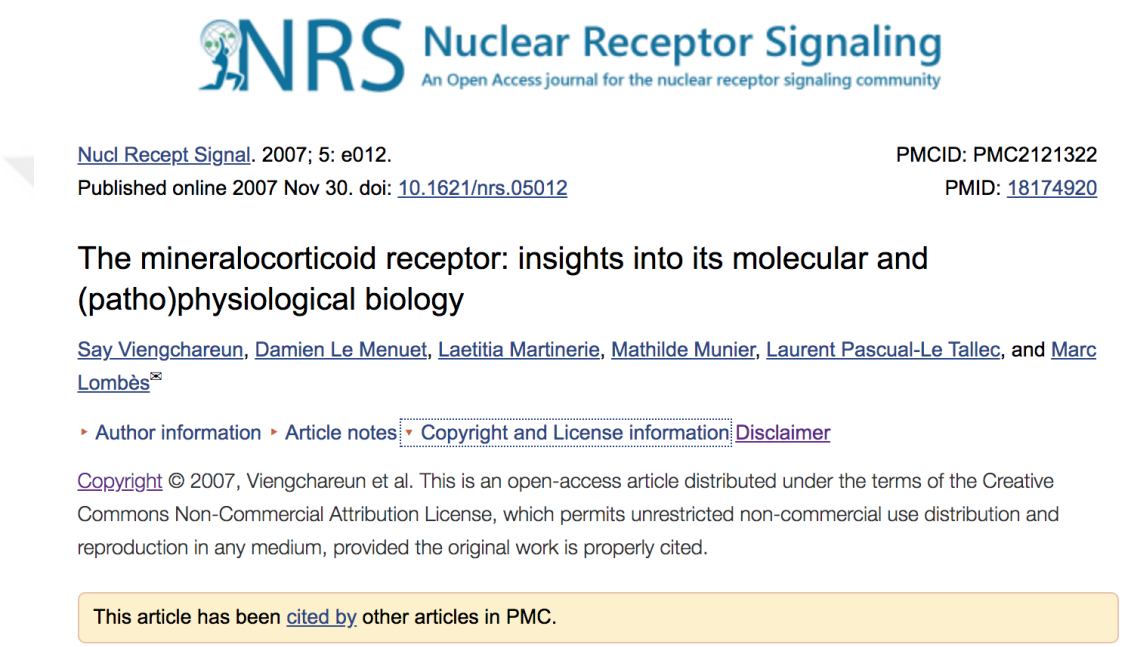

NRS Nuclear Receptor Signaling
An Open Access journal for the nuclear receptor signaling community

Nucl Recept Signal. 2007; 5: e012.
Published online 2007 Nov 30. doi: 10.1621/nrs.05012

PMCID: PMC2121322
PMID: 18174920

The mineralocorticoid receptor: insights into its molecular and (patho)physiological biology

Say Viengchareun, Damien Le Menuet, Laetitia Martinerie, Mathilde Munier, Laurent Pascual-Le Tallec, and Marc Lombès✉

▸ Author information ▸ Article notes ▾ Copyright and License information Disclaimer

Copyright © 2007, Viengchareun et al. This is an open-access article distributed under the terms of the Creative Commons Non-Commercial Attribution License, which permits unrestricted non-commercial use distribution and reproduction in any medium, provided the original work is properly cited.

This article has been cited by other articles in PMC.

Figure 3. 15Correlation of Alu Ct and Human DNA (pg) injected in zebrafish model organism. A negative correlation exists among the increased amount of Alu Ct and injected human DNA as stated in picograms (r=-0.99826, p-value=2.4196e-07).' and 'Figure 3. 16ALU-based tumor proliferation comparison among ache mutant and wildtype fish injected with liver cancer cell lines. A) Hep3b cell line-injected fish were genotyped to classify *ache*+/+ (wt) (n=18), *ache*+/- (n=28) and *ache*-/- (n=10). ALU Ct normalized to *ache* Ct, lead classification of tumor DNA presence among these groups exhibiting increased tumor proliferation in *ache*-/- with regard to *ache*+/+ (p=0.0001) and *ache*+/- (p=0.005). B) SK-Hep1 cell line-injected fish were genotyped to classify *ache*+/+ (wt) (n=13), *ache*+/- (n=26) and *ache*-/- (n=16). ALU Ct normalized to *ache* Ct, lead classification of tumor DNA presence among these groups exhibiting increased tumor proliferation in *ache*-/- with regard to *ache*+/+ (p=0.017) and *ache*+/- (p=0.004).

(The image is retrieved from Avci, M. E., Keskus, A. G., Targen, S., Isilak, M. E., Ozturk, M., Atalay, R. C., Adams, M. M., & Konu, O. (2018). Development of a novel zebrafish xenograft model in ache mutants using liver cancer cell lines. *Scientific Reports*, *8*(1), 1570. https://doi.org/10.1038/s41598-018-19817-w).

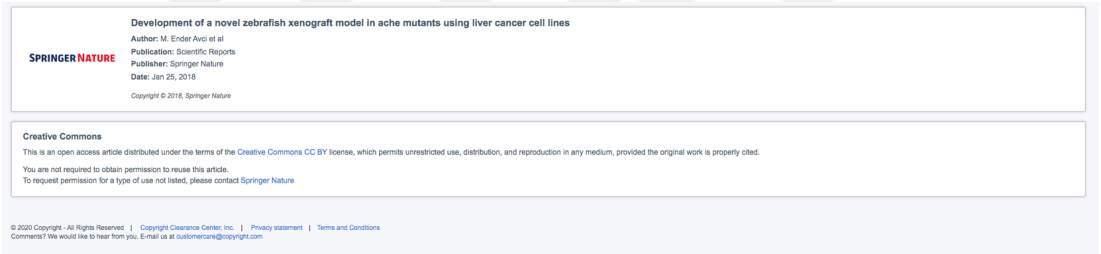

Figure 3. 20 47 Kaplan-Meier plots illustrating survival graphs of MR and GR in breast cancer. A) MR-Overall survival B) MR-Disease free survival C) GR-Overall survival D) GR-Disease free survival.

(The image was adapted from 2019 Konu, O., & Targen, S. Investigating the Role of Mineralocorticoid Receptor Signaling in Cancer Biology in the Genomic Era. In *Aldosterone-Mineralocorticoid Receptor - Cell Biology to Translational Medicine*. Licence: CC BY-NC 4.0 license for Monograph. https://doi.org/10.5772/intechopen.87233).

intechopen.com/page/copyright-policy

TERMS

All Works published on the IntechOpen platform and in print are licensed under a Creative Commons Attribution 3.0 Unported License, a license which allows for the broadest possible reuse of published material.

Copyright on the individual Works belongs to the specific Author, subject to an agreement with IntechOpen. The Creative Common license is granted to all others to:

- Share — copy and redistribute the material in any medium or format
- Adapt — remix, transform, and build upon the material

And for any purpose, provided the following conditions are met:

- An Attribution, giving appropriate credit and providing a link to the license, with an indication as to whether changes to the original were made
- A commitment not to add additional restrictions. In effect, this prohibits the application of legal conditions or technological measures that legally restrict others from doing anything that the license permits.

All Works are published under the CC BY 3.0 license. However, please note that book Chapters may fall under a different CC license, depending on their publication date as indicated in the table below:

LICENSE	USED FROM -	UP TO -
Creative Commons Attribution-NonCommercial-ShareAlike 3.0 Unported (CC BY-NC-SA 3.0)	1 July 2005 (2005-07-01)	3 October 2011 (2011-10-03)
Creative Commons Attribution 3.0 Unported (CC BY 3.0)	5 October 2011 (2011-10-05)	Currently

The CC BY 3.0 license permits Works to be freely shared in any medium or format, as well as the reuse and adaptation of the original contents of Works (e.g. figures and tables created by the Authors), as long as the source Work is cited and its Authors are acknowledged in the following manner:

From Figure 3.1 to 3.14 was used under the copy right permission of Zebrafish journal.

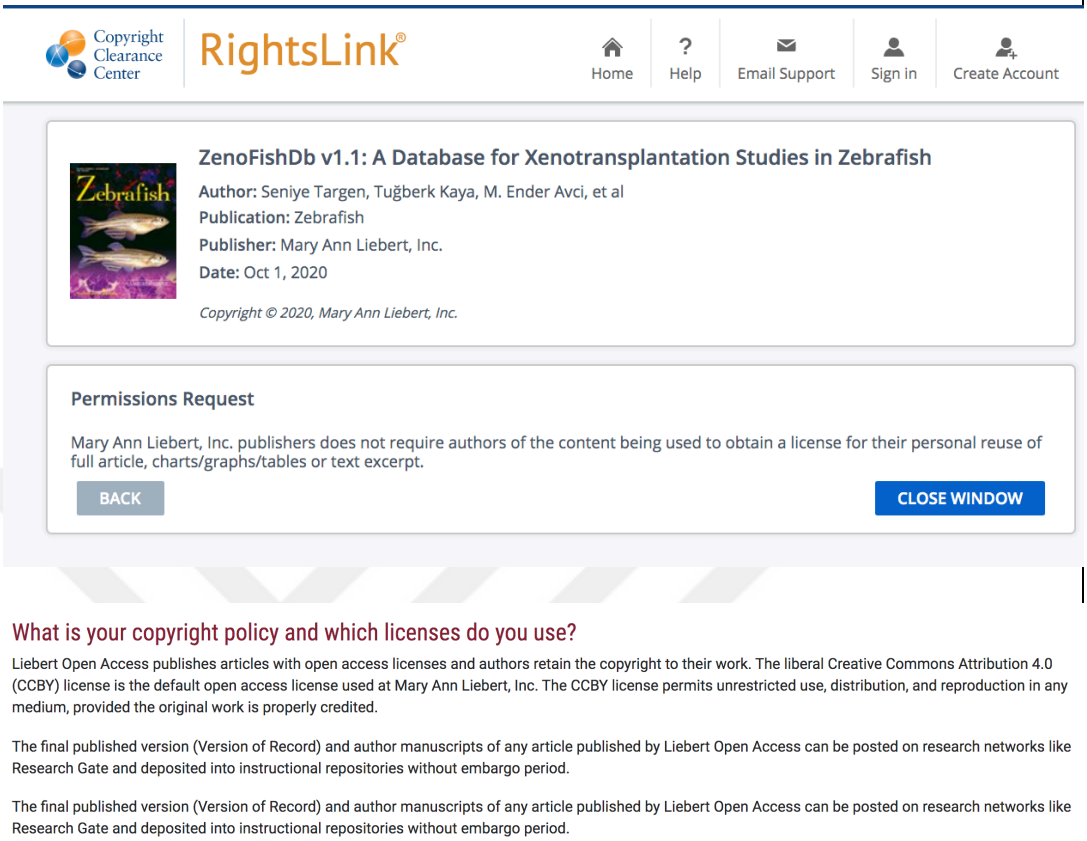

Figure 3. 1 ZenoFishDbv1.1 Homepage. The welcome page highlights the key features of the database and informs the user. On the left, access for Data Table, Visualization, PDX Details and PDX Charts modules are provided. Forms for data submission are also provided on the welcoming page.

(This screenshot image was retrieved from https://konulab.shinyapps.io/zenofishdb/ , (ZenoFishDb v1.1) published as Targen, S., Kaya, T., Avci, M. E., Gunes, D., Keskus, A. G., & Konu, O. (2020). ZenoFishDb v1.1: A Database for Xenotransplantation Studies in Zebrafish. *Zebrafish*. https://doi.org/10.1089/zeb.2020.1869).

Figure 3. 2 ZenoFishDb v1.1 database displaying the *Data Table* module. The *Data Table* module presents the attributes of the database in the table format, enables search through the attribute search box with possible sub-selections (top left) and the search box (top right).

(This image was adapted from Targen, S., Kaya, T., Avci, M. E., Gunes, D., Keskus, A. G., & Konu, O. (2020). ZenoFishDb v1.1: A Database for Xenotransplantation Studies in Zebrafish. *Zebrafish*. https://doi.org/10.1089/zeb.2020.1869).

Figure 3. 3 Screenshot of the ZenoFishDb v1.1 *Visualisation* page. The graphical and statistical representation of 'cancer/tissue of origin' attribute is displayed through the *Visualization* page.

(This image was adapted from Targen, S., Kaya, T., Avci, M. E., Gunes, D., Keskus, A. G., & Konu, O. (2020). ZenoFishDb v1.1: A Database for Xenotransplantation Studies in Zebrafish. *Zebrafish*. https://doi.org/10.1089/zeb.2020.1869).

Figure 3. 4 *PDX Details* module displays patient data, tumor data and zebrafish injection details of patient-derived xenografts listed on ZenoFishDb v1.1. The data table format enables search of PDX-associated attributes through attributes option (top left) and search box (top right).

(This image was adapted from Targen, S., Kaya, T., Avci, M. E., Gunes, D., Keskus, A. G., & Konu, O. (2020). ZenoFishDb v1.1: A Database for Xenotransplantation Studies in Zebrafish. *Zebrafish*. https://doi.org/10.1089/zeb.2020.1869).

Figure 3. 5 Screenshot of the *PDX Charts* module on ZenoFishDb v1.1. PDX Charts module exhibits graphical and statistical representation of frequently registered attribute, 'Detailed nature of disease'.

(This image was adapted from Targen, S., Kaya, T., Avci, M. E., Gunes, D., Keskus, A. G., & Konu, O. (2020). ZenoFishDb v1.1: A Database for Xenotransplantation Studies in Zebrafish. *Zebrafish*. https://doi.org/10.1089/zeb.2020.1869).

Figure 3. 6 Graphical representation of registered cancer and tissue types on ZenoFishDb v.1.1. The screenshot of the 'cancer/tissue of origin' attribute obtained through the visualization page lists 77 unique variables with their corresponding percentages. The 'download the bar chart table' provides a link for downloadable form for the number of each unique variable as frequency and percentages for this attribute.

(This image was retrieved from https://konulab.shinyapps.io/zenofishdb/ (ZenoFishDbv1.1) published as Targen, S., Kaya, T., Avci, M. E., Gunes, D., Keskus, A. G., & Konu, O. (2020). ZenoFishDb v1.1: A Database for Xenotransplantation Studies in Zebrafish. *Zebrafish*. https://doi.org/10.1089/zeb.2020.1869).

Figure 3. 7 Molecular modifications represented on ZenoFishDb v1.1. A total number of 13 molecular modifications were incorporated onto ZenoFishDb as TV (Tag expression vectors), OV (Overexpression vectors), shRNA (short hairpin RNA), siRNA (silencing RNA), Mutations, Morpholino (MO), miRNA (microRNA), Cre-LoxP, shRNAmir, Photo-convertible expression vector, membrane-bound peptine expression and Crirspr/Cas9.

(This image was adapted from Targen, S., Kaya, T., Avci, M. E., Gunes, D., Keskus, A. G., & Konu, O. (2020). ZenoFishDb v1.1: A Database for Xenotransplantation Studies in Zebrafish. *Zebrafish*. https://doi.org/10.1089/zeb.2020.1869).

Figure 3. 8Stem cell properties of stem cell (SC) and cancer stem cell (CSC) xenograft models displayed on ZenoFishDb v1.1. Diverse application of stem cell of any origin was reflected by total number of 14 different zebrafish xenograft model. Yet among all this diversity, cancer stem cell, leukemia stem cell and neuronal stem cell injections accounted for majority zebrafish xenotransplantation studies.

(This image was retrieved from https://konulab.shinyapps.io/zenofishdb/ published as Targen, S., Kaya, T., Avci, M. E., Gunes, D., Keskus, A. G., & Konu, O. (2020). ZenoFishDb v1.1: A Database

Figure 3. 9 GO PANTHER Pathway analysis of molecularly modified genes. GO PANTHER pathway analysis search for a total of 94 genes reveals 202 pathway hits and displayed the matched number of genes for each categorized pathway.

(This image was adapted from Targen, S., Kaya, T., Avci, M. E., Gunes, D., Keskus, A. G., & Konu, O. (2020). ZenoFishDb v1.1: A Database for Xenotransplantation Studies in Zebrafish. *Zebrafish*. https://doi.org/10.1089/zeb.2020.1869).

Figure 3. 11 List of biological assessments performed on zebrafish xenograft studies incorporated onto ZenoFishDb v1.1. Seventy-one different biological assessments and their percentages are displayed through the 'analyses' attribute of the *Visualization* page.

(This image was adapted from Targen, S., Kaya, T., Avci, M. E., Gunes, D., Keskus, A. G., & Konu, O. (2020). ZenoFishDb v1.1: A Database for Xenotransplantation Studies in Zebrafish. *Zebrafish*. https://doi.org/10.1089/zeb.2020.1869).

Figure 3. 12 Host modifications and host modification details search through the *Visualization* and *Data Table* modules.

(This image was adapted from Targen, S., Kaya, T., Avci, M. E., Gunes, D., Keskus, A. G., & Konu, O. (2020). ZenoFishDb v1.1: A Database for Xenotransplantation Studies in Zebrafish. *Zebrafish*. https://doi.org/10.1089/zeb.2020.1869).

Figure 3. 13 ZenoFishDb v1.1 reveals the injection sites of all zebrafish xenotransplantation studies.

(This image was adapted from Targen, S., Kaya, T., Avci, M. E., Gunes, D., Keskus,

A. G., & Konu, O. (2020). ZenoFishDb v1.1: A Database for Xenotransplantation Studies in Zebrafish. *Zebrafish*. https://doi.org/10.1089/zeb.2020.1869).

Figure 3.14 ZenoFishDb v1.1 reveals the categorized injection cell numbers of all zebrafish xenotransplantation studies.

(This image was adapted from Targen, S., Kaya, T., Avci, M. E., Gunes, D., Keskus, A. G., & Konu, O. (2020). ZenoFishDb v1.1: A Database for Xenotransplantation Studies in Zebrafish. *Zebrafish*. https://doi.org/10.1089/zeb.2020.1869).